UNIVERSITY OF SOUTHAMPTON

FACULTY OF PHYSICAL SCIENCES AND ENGINEERING

Physics and Astronomy

Aspects of Flavour and Entanglement in Gauge/Gravity Duality

by

Peter Anthony Ralph Jones

Thesis for the degree of Doctor of Philosophy

August 2017

UNIVERSITY OF SOUTHAMPTON

ABSTRACT

FACULTY OF PHYSICAL SCIENCES AND ENGINEERING

Physics and Astronomy

Thesis for the degree of Doctor of Philosophy

ASPECTS OF FLAVOUR AND ENTANGLEMENT IN GAUGE/GRAVITY DUALITY

by Peter Anthony Ralph Jones

This thesis investigates a number of topics relating to flavour physics and entanglement within gauge/gravity duality, or 'holography', which is a framework for studying equivalences between certain gravitational and non-gravitational theories. The field arose from generalisations of the original AdS/CFT correspondence, which postulated the equivalence between the $\mathcal{N} = 4$ super Yang-Mills gauge theory and type IIB superstring theory on $AdS_5 \times S^5$. The duality is such that the gauge theory is strongly-coupled when the string theory reduces to a classical supergravity theory, and consequently provides a new method of computation for strongly coupled physics such as QCD and many condensed matter systems. In this thesis we study applications of gauge/gravity duality to flavour physics, and both applications and fundamental issues of entanglement within the holographic framework. We study a holographic model of graphene in a cavity and find a new controlled example of mass gap generation, and a new phase in which a graphene sheet condenses with its mirror image. We then study a bottom-up model known as Dynamic AdS/QCD, and reproduce soft wall behaviour needed to obtain the known Regge behaviour for meson masses, discussing some inherent limitations in the approach. The discussion then moves onto the entanglement of flavour in AdS/CFT, and we compute the entanglement entropy in detail for the massive D3/D7 system, and present a new method for computing the entanglement entropy of any top-down brane probe system using Kaluza-Klein holography. Finally, we study the issue of entanglement entropy in generic top-down models, and provide strong evidence that it can be computed via a generalisation of the Ryu-Takayanagi formula, using codimension two minimal surfaces which asymptotically wrap the compact part of the geometry.

Table of Contents

List of Figures

Declaration of Authorship

I, Peter Anthony Ralph Jones, declare that the thesis entitled *Aspects of Flavour and Entanglement in Gauge/Gravity Duality* and the work presented in the thesis are both my own, and have been generated by me as the result of my own original research. I confirm that:

- this work was done wholly or mainly while in candidature for a research degree at this University;
- where any part of this thesis has previously been submitted for a degree or any other qualification at this University or any other institution, this has been clearly stated;
- where I have consulted the published work of others, this is always clearly attributed;
- where I have quoted form the work of others, the source is always given. With the exception of such quotations, this thesis is entirely my own work;
- I have acknowledged all main sources of help;
- where the thesis is based on work done by myself jointly with others, I have made clear exactly what was done by others and what I have contributed myself;
- parts of this work have been published as:
  - N. Evans, P. Jones, *Holographic Graphene in a Cavity*. Phys.Rev. D90 (2014) no.8, 086008. `arXiv:1407.3097 [hep-th]` [1]
  - P. Jones, M. Taylor, *Entanglement entropy and differential entropy for massive flavors*. JHEP 1508 (2015) 014. `arXiv:1505.07697 [hep-th]` [2]
  - N. Evans, P. Jones, M. Scott, *Soft walls in dynamic AdS/QCD and the technidilaton*. Phys.Rev. D92 (2015) no.10, 106003. `arXiv:1508.06540 [hep-th]` [3]
  - P. Jones, M. Taylor, *Entanglement Entropy in Top Down Models*. JHEP 1608 (2016) 158. `arXiv:1602.04825 [hep-th]` [4]

Signed: .....

Date: .....

Acknowledgements

I would like to thank my supervisors, Nick Evans and Marika Taylor, for all their guidance and support throughout my PhD, and for many enjoyable discussions often totally unrelated to physics. I would also like to thank Kostas Skenderis for useful discussions at the beginning of my time in Southampton. I would like to thank my physics friends from across the world over the past ten years for the friendly, enthusiastic and helpful atmosphere they have always provided, especially Nick Jones who has been there since the beginning. I would also especially like to thank Zoë Slade for all the support and countless laughs over the last four years, which have been invaluable to me during the PhD. Finally, I would like to thank my parents for all their love, support and encouragement throughout my life, without which I would surely not be where I am today.

CHAPTER 1

Prelude

Gauge/gravity duality or *holography* is a theoretical framework that studies equivalences between physical theories that initially appear very different - the structure of these equivalences is such that they always relate a d+1-dimensional gravitational theory to a d-dimensional non-gravitational theory. Over the past two decades a vast literature of research has arisen on the subject by virtue of the fact that its consequences are very far reaching - although its origins are rooted in string theory, it has provided insight into areas as varied as quantum gravity, particle physics, condensed matter, quantum information, hydrodynamics and more.

This thesis investigates two topics within the framework of gauge/gravity duality - *flavour* and *entanglement*. By 'flavour' we mean, formally, degrees of freedom that transform under the fundamental representation of a gauge group, but more intuitively this means degrees of freedom corresponding to matter, such as quarks. These can be introduced into gauge/gravity duality via the machinery of *probe branes* and related constructs which we introduce in detail and utilize in the following, and are frequently used in applications of gauge/gravity to the study of QCD and condensed matter theory.

Entanglement is one of the defining characteristics of quantum mechanics, and has been at the centre of discussions ranging from philosophical to computational in nature for nearly a century. Its relevance to gauge/gravity duality has arisen largely through consideration of a particular quantity, the *entanglement entropy*, which admits a particularly simple holographic description that we introduce and use many times in this thesis (its representation is in fact similar to the probe brane construction for introducing flavour, both involving extremal surfaces anchored to the boundary of anti-de Sitter space). Its

applications have again been diverse, including shedding light on the emergence of bulk spacetime in holography, providing an order parameter for phase transitions, and contributing to the study of renormalization group flows. In this thesis we will also study in detail the entanglement contribution of flavour degrees of freedom in the holographic framework, bringing these two topics together.

The structure of this thesis is as follows. Part I covers general background material on string theory, gauge theory, and gauge/gravity duality, that is relevant to both Parts II and III. Part II focuses on studies of flavour in gauge/gravity duality, with background on probe branes and QCD introduced in Chapter 4, and Chapters 5 and 6 comprising orginal research on applications of holography to graphene and QCD respectively. Part III then turns to the topic of entanglement, with Chapter 7 introducing further background material, and Chapters 8 and 9 comprising original research on the entanglement of flavour and other top-down holographic solutions. Parts II and III are largely independent of each other, though Chapter 8 does utilize the background of Chapter 4. We conclude with a brief outlook in Chapter 10.

Part I

Gauge/Gravity Duality

CHAPTER 2

String Theory and Gauge Theory

In this chapter we briefly introduce the main aspects of string theory and gauge theory needed in this thesis. String theory, as well as being a theory of 1-dimensional strings, is also a theory of higher-dimensional extended objects known as *branes*, which play a fundamental role in the following. The low-energy effective field theories living on the worldvolume of the branes are gauge theories, such as the maximally supersymmetric $\mathcal{N} = 4$ super Yang-Mills theory, and also play a crucial role in AdS/CFT. We follow closely here the treatments in [5] and [6].

2.1 Type IIB Supergravity and D-Branes

The gravitational framework within which the original AdS/CFT correspondence takes place, and within which we work for the majority of this thesis, is *type IIB string theory*. This is an $\mathcal{N} = 2$ supersymmetric theory of oriented closed strings in 10-dimensions. The low-energy effective action is of particular importance in AdS/CFT - it can be found by coupling strings to a background of the massless modes and requiring that the resulting theory is Weyl invariant. The resulting effective theory is *type IIB supergravity*, with the following (bosonic) action in string frame

$$S_{IIB} = S_{NS} + S_R + S_{CS} \tag{2.1.1}$$

where

$$\begin{aligned} S_{NS} &= \frac{1}{2\tilde{\kappa}_{10}^2}\int d^{10}x\sqrt{-g}e^{-2\Phi}\left(R + 4\partial_\mu\Phi\partial^\mu\Phi - \frac{1}{2}|H_3|^2\right) \\ S_R &= -\frac{1}{4\tilde{\kappa}_{10}^2}\int d^{10}x\sqrt{-g}\left(|F_1|^2 + |\tilde{F}_3|^2 + \frac{1}{2}|\tilde{F}_5|^2\right) \\ S_{CS} &= -\frac{1}{4\tilde{\kappa}_{10}^2}\int C_4 \wedge H_3 \wedge F_3 \end{aligned} \tag{2.1.2}$$

and the action must be supplemented with the self-duality condition $\tilde{F}_5 = \star\tilde{F}_5$. Here we have defined the field-strength tensors

$$\begin{gathered} F_p = dC_{p-1}, \qquad H_3 = dB_2, \qquad \tilde{F}_3 = F_3 - C_0 H_3 \\ \tilde{F}_5 = F_5 - \frac{1}{2}C_2 \wedge H_3 + \frac{1}{2}B_2 \wedge F_3 \end{gathered} \tag{2.1.3}$$

where B_2 is the NS-NS 2-form and C_p $(p = 0, 2, 4)$ are the R-R p-forms present in the massless spectrum of type IIB string theory. Φ is a scalar field known as the *dilaton* and its vacuum expectation value (VEV) is related to the string coupling constant as $g_s = e^{\langle\Phi\rangle}$. There are Majorana-Weyl fermions required for supersymmetry that we do not list here.

The coupling constant is the 10-dimensional gravitational constant:

$$2\tilde{\kappa}_{10}^2 = (2\pi)^7\alpha'^4 \tag{2.1.4}$$

where α' is related to the string length ($\alpha' = l_s^2$). This can be related to the 10-dimensional Newton constant by

$$2\kappa_{10}^2 \equiv 2\tilde{\kappa}_{10}^2 g_s^2 = 16\pi G_{10} \tag{2.1.5}$$

where g_s is the closed string coupling constant.[1] Note that via a Weyl rescaling the action (2.1.2) may be transformed such that the Einstein-Hilbert and dilaton kinetic terms are brought into canonical form - the resulting action with coupling $2\kappa_{10}^2$ is then said to be in *Einstein frame*, which will be of importance in Part III.

2.1.1 D-Branes

Of central importance to the AdS/CFT correspondence, and this thesis in particular, are certain non-perturbative objects in string theory known as *D-branes* [7]. These can be viewed as hyperplanes which the endpoints of open strings are confined to - an open string with Dirichlet boundary conditions in p spatial directions will require a Dp-brane, which has $p+1$ spacetime dimensions. Crucially, D-branes are not merely mathematical constructs, but physical objects with their own dynamics, as can be shown using T-duality [8] - in essence, they are required to be dynamical in order to restore momentum

[1] From string perturbation theory it is known that the closed string coupling constant g_s is related to the open string coupling constant as $g_s = g_{\text{open}}^2$.

conservation.

In a superstring theory, stable D-branes can exist by virtue of couplings to the R-R p-forms in the massless spectrum of the theory. In the same way that the worldline Σ_1 of a charged particle can couple to a gauge field 1-form,

$$S_0 = e\int_{\Sigma_1} P[A_1] = e\int_{\Sigma_1} d\tau\ A_\mu \frac{dx^\mu}{d\tau}, \tag{2.1.6}$$

the worldvolume Σ_{p+1} of a Dp-brane can couple to a $(p+1)$-form gauge field via the diffeomorphism invariant action,

$$S_p = \mu_p \int_{\Sigma_{p+1}} P[A_{p+1}] = \mu_p \int_{\Sigma_{p+1}} d^{p+1}\xi\ A_{\mu_1\ldots\mu_{p+1}} \frac{\partial x^{\mu_1}}{\partial \xi^0}\ldots\frac{\partial x^{\mu_{p+1}}}{\partial \xi^p}, \tag{2.1.7}$$

where P denotes the pullback from the bulk to the brane (ξ^α are the brane worldvolume coordinates), and μ_p denotes the brane charge. The brane can be understood to be electrically charged by virtue of Gauss's law $\mu_p = \int \star F_{p+2}$ where $F_{p+2} \equiv dA_{p+1}$, and the integral is over a sphere S^{D-p-2} as is required to surround a p-brane in D-dimensions. By analogy the charge of the magnetic dual brane will be given by $\int F_{p+2}$, where now the integral is over a surrounding S^{p+2} - in D-dimensions an S^{p+2} can surround a $(D-p-4)$-brane, and thus this is the magnetic dual of a p-brane.[2]

Given this, we now turn to the question of what stable D-branes exist in type IIB string theory. The type IIB spectrum includes the R-R forms C_p for $p = 0, 2, 4$, and we have seen from above that in 10-dimensions a p-form can couple electrically to a $(p-1)$-brane and magnetically to a $(7-p)$-brane. The conclusion is thus that one can introduce stable Dp-branes into type IIB theory for odd values of p - we shall be particularly interested in D3, D5, and D7-branes in this thesis.[3]

Note that adding D-branes to the type IIB vacuum gives a theory that includes both closed strings in the bulk and open strings ending on the branes. A consequence of this is that, in addition to breaking 10-dimensional Poincaré invariance as we will discuss below, introducing D-branes into type IIB breaks some of the supersymmetry of the Minkoswki vacuum.[4]

2.1.2 Brane Action (DBI)

We now wish to describe an action for the dynamics of D-branes, beginning with a single D-brane in Minkowski spacetime. These actions will be very important later when

[2] One can alternatively use the democratic formalism of [9].

[3] The D(-1)-brane and D1-brane are known as the D-instanton and D-string respectively, and the D9-brane is a spacetime-filling brane.

[4] Open string vector supermultiplets can only exist with at most 16 conserved supercharges, whereas the $\mathcal{N} = 2$ Minkowski vacuum has 32 conserved supercharges. At least half of the supersymmetries must thus be broken, and the stable D-branes discussed above are precisely those that preserve exactly half of the supersymmetry - they are known as *half-BPS* D-branes.

we consider probe branes in AdS/CFT. One might expect the action to incorporate a direct generalisation of the point particle and Nambu-Goto string actions as simply the worldvolume of the brane i.e.

$$S_p = -T_p \int d^{p+1}\xi \sqrt{-\text{det}G_{\alpha\beta}}, \tag{2.1.8}$$

where $G_{\alpha\beta} \equiv \eta_{\mu\nu}\partial_\alpha X^\mu \partial_\beta X^\nu$ is the induced metric on the brane, and T_p the brane tension. This is essentially correct, and the brane action will be used at times in this thesis in this simple form, but the full story is more involved as it includes additional fields living on the brane. Fermionic degrees of freedom must also be included as required by supersymmetry, but we will usually truncate to the bosonic sector throughout the following.

The main idea here is that, since the endpoints of open strings live on D-branes, the modes of the open string spectrum can be described by fields living on the brane worldvolume. If we wish to construct a low energy effective action (relative to the sting scale), then only the massless modes of the open string spectrum need to be taken into account - the latter form a vector supermultiplet, and thus the expectation is that the worldvolume theories of D-branes will be gauge theories. The relevant gauge field action takes the form of the Born-Infeld non-linear generalisation of the Maxwell action, and (2.1.8) becomes

$$S_{\text{DBI}} = -T_p \int d^{p+1}\xi \sqrt{-\text{det}\left(G_{\alpha\beta} + 2\pi\alpha' F_{\alpha\beta}\right)}, \tag{2.1.9}$$

where $F_{\alpha\beta}$ is the 1-form gauge field on the brane. This is known as the *DBI action*. The full action (see [5]) includes fermionic degrees of freedom through supersymmetric generalisations of $G_{\alpha\beta}$ and $F_{\alpha\beta}$ and a Chern-Simons term, but we focus here on the bosonic sector.

An important generalisation is to consider the D-brane in a non-trivial background consisting of the various (massless closed string) modes of type IIB supergravity. Again we truncate to the bosonic sector. The coupling to the NS-NS fields $g_{\mu\nu}$, $B_{\mu\nu}$ and Φ leads to the following generalisation of (2.1.9),

$$S_{\text{DBI}} = -T_p \int d^{p+1}\xi e^{-\Phi} \sqrt{-\text{det}\left(G_{\alpha\beta} + B_{\alpha\beta} + 2\pi\alpha' F_{\alpha\beta}\right)}, \tag{2.1.10}$$

where now $G_{\alpha\beta} \equiv g_{\mu\nu}\partial_\alpha X^\mu \partial_\beta X^\nu$, and analogously $B_{\alpha\beta} \equiv B_{\mu\nu}\partial_\alpha X^\mu \partial_\beta X^\nu$ is the pullback $P[B]$. Of course, couplings to background R-R fields C_p must also be considered - these do not contribute to the DBI action, but instead lead to a Chern-Simons term via couplings of the form (2.1.7). The full Chern-Simons term in a general background is in fact slightly more complicated, and given by

$$S_{\text{CS}} = \mu_p \int \left[\sum_q P[C_{q+1}] \wedge e^{P[B]+2\pi\alpha' F}\right]_{p+1} \tag{2.1.11}$$

where the subscript indicates that one should extract the $(p+1)$-form piece from the product in the integrand, as is appropriate for integration over a p-brane. The full bosonic action for a Dp-brane in the presence of background fields is then given by the combination of (2.1.10) and (2.1.11).

It remains to discuss the form of the brane tension T_p appearing in the DBI actions above. This can be found from expanding the DBI action in a weak-field expansion and identifying the Maxwell term and the relation $g_s \sim g_{\text{YM}}^2$ [5] - note that this is consistent with $g_{\text{YM}} \sim g_{\text{open}}$ which is understood since the gauge field arises from massless open string modes. The result is

$$T_p = (2\pi)^{-p} \alpha'^{-(p+1)/2} \frac{1}{g_s}. \tag{2.1.13}$$

where note in particular the factor of $1/g_s$ which shows that D-branes are in fact non-perturbative objects - in the weak coupling limit $g_s \to 0$ the D-branes become very heavy and can be treated as rigid objects with open strings as small perturbations.[6]

Note that D-brane actions are often simplified by fixing the diffeomorphism invariance using *static gauge* in which the first $p+1$ components of the brane embedding X^μ are set equal to the worldvolume coordinates ξ^α. The remaining $9-p$ embedding functions, X^i, are then left to remain as dynamical fields, and are scalars from the point of view of the worldvolume - they can be interpreted as Goldstone bosons associated with the broken translational symmetry due to the D-brane. The DBI action (2.1.10) then reduces to

$$S_{\text{DBI}} = -T_p \int d^{p+1}\xi e^{-\Phi} \sqrt{-\det\left(g_{\alpha\beta} + \partial_\alpha X^i \partial_\beta X^i + B_{\alpha\beta} + 2\pi\alpha' F_{\alpha\beta}\right)} \tag{2.1.14}$$

where $g_{\alpha\beta}$ corresponds to the components of the metric $g_{\mu\nu}$ in the worldvolume directions. We will use static gauge numerous times throughout this thesis.

2.1.3 Multiple D-branes - Non-Abelian Gauge Theory

In the previous section we saw that the worldvolume theory on a single Dp-brane is a gauge theory, which in a weak-field expansion is equivalent to a $U(1)$ gauge theory (i.e. supersymmetric Maxwell theory), and we described the action for such a system. Of particular importance to AdS/CFT however is the scenario in which there are multiple branes. It is possible, with some subtlety, to construct generalisations of the DBI and Chern-Simons brane actions in such cases, but we shall suffice here with a weak-field description of the relevant worldvolume theory, which is sufficient for AdS/CFT and our purposes.

[5] For later use we state this here fully as

$$g_{\text{YM}}^2 = (2\pi)^{p-2} \alpha'^{\frac{p-3}{2}} g_s. \tag{2.1.12}$$

[6] Note also that, since g_s already appears in T_p, the dilaton as appearing in (2.1.10) is technically shifted so that it has zero VEV.

In the case of multiple coincident D-branes, the endpoints of open strings have additional non-dynamical degrees of freedom known as *Chan-Paton factors* - these label which of the N coincident branes the endpoint lies on. For oriented string theories, such as type IIB, the endpoints of the string are distinguished and thus one identifies the fundamental ($\mathbf{N}$) and antifundamental ($\overline{\mathbf{N}}$) represensation with the two endpoints respectively - it is thus natural to associate such strings with adjoint degrees of freedom of a non-abelian symmetry group. We will use similar reasoning again in Chapter 4 (see, for example, Figure 4.1.1) when discussing probe branes as a means to introduce flavour degrees of freedom into AdS/CFT, and indeed similar global symmetry considerations were the original movitation for introducing such factors. Crucially however, when both string endpoints are on the stack of D-branes, it turns out that the worldvolume theory is a $U(N)$ gauge theory i.e. the symmetry is *local*. For a stack of N D3-branes, as will be relevant for AdS/CFT and this thesis, the worldvolume theory is the maximally supersymmetric gauge theory in 4-dimensions known as $\mathcal{N}=4$ *super Yang-Mills*, which we discuss in Section 2.2.

Note that separating M of the branes from the stack causes the connecting strings (i.e. gauge bosons) to become massive, and thus corresponds to breaking the gauge symmetry via a Higgs mechanism. Separating a stack of M from the original N breaks $U(N) \to U(N-M) \times U(M)$ for example. This is referred to as the *Coulomb Branch* of the gauge theory and is discussed further in Section 2.2 and Chapters 8 and 9.

2.1.4 D-brane Solutions of Type IIB Supergravity

We now take a different viewpoint in which the branes are viewed as sources of the type IIB fields, and discuss solutions of the low-energy supergravity theory that represent the D-branes we have just considered - these play an important role in AdS/CFT. The primary ingredients used here are symmetry considerations - a Dp-brane breaks 10-dimensional Poincaré invariance $\mathbb{R}^{1,9} \times SO(1,9) \to \mathbb{R}^{1,p} \times SO(1,p) \times SO(9-p)$, and also breaks half of the supersymmetries as mentioned previously. An appropriate solution to the type IIB supergravity equations is given by

$$\begin{aligned} ds^2 &= H(r)^{-1/2}\eta_{\mu\nu}dx^\mu dx^\nu + H(r)^{1/2}dy^i dy^i \\ e^\Phi &= g_s H(r)^{(3-p)/4} \\ C_{p+1} &= \left(H(r)^{-1}-1\right) dx^0 \wedge \cdots \wedge dx^p \end{aligned} \tag{2.1.15}$$

where $H(r)$ is a harmonic function, $\Box_y H(r) = 0$, and all other fields are set to zero. Here, x^μ represent the brane coordinates ($\mu = 0, \ldots, p$), y^i represent the transverse coordinates ($i = p+1, \ldots, 9$), and $r^2 \equiv y^i y^i$.

Of particular relevance to us in the following will be the solitonic case $p = 3$, for which

the dilaton is constant, and the harmonic function $H(r)$ can be written

$$H(r) = 1 + \left(\frac{L}{r}\right)^4 \tag{2.1.16}$$

where we have demanded that the solution becomes flat as $r \to \infty$. The constant L can be determined by integrating the 5-form flux $F_5 \equiv dC_4$ through an S^5 at infinity and using Gauss's law as in Section 2.1.1.[7] The result is

$$L^4 = 4\pi g_s N \alpha'^2 \tag{2.1.17}$$

which will be relevant for AdS/CFT later. Note that for the supergravity approximation to be valid the spacetime curvature must be weak (relative to the string scale) and thus the dimensionless ratio $L/\sqrt{\alpha'} \gg 1$, which from above corresponds to $g_s N \gg 1$. We will see from Section 2.2 and Chapter 3 that this corresponds to the strong coupling limit $\lambda \gg 1$ of the gauge theory.

Also note crucially that in the limit $r \ll L$, referred to as the *near-horizon* region, this solution becomes

$$ds^2 = \left(\frac{L^2}{r^2}dr^2 + \frac{r^2}{L^2}\eta_{\mu\nu}dx^\mu dx^\nu\right) + L^2 ds^2_{S^5} \tag{2.1.18}$$

which is the metric for $AdS_5 \times S^5$ with radius L in both components (frequently set to unity in the following). This near-horizon region of a stack of D3-branes is how the product space $AdS_5 \times S^5$ arises in the context of the AdS/CFT correspondence discussed in Section 3.1. Note that the boundary of the AdS_5 is at $r \to \infty$ (see Section 3.2).

2.2 $\mathcal{N} = 4$ Super Yang-Mills

A pure gauge theory in 4-dimensions has maximal supersymmetry when $\mathcal{N} = 4$, since above this gravity is necessarily included in the supermultiplet. The relevant massless vector supermultiplet contains a gauge field A_μ, four Weyl fermions λ^a_α, and six real scalars X^i, all of which are in the adjoint representation of the gauge group $SU(N)$ (since supersymmetry and the gauge symmetry commute). There is also an R-symmetry group $SU(4) \simeq SO(6)$ under which the fields A, λ and X transform in the singlet (**1**), fundamental (**4**) and antisymmetric (**6**) representations respectively.[8]

The action for the corresponding $d = 4$ field theory, known as $\mathcal{N} = 4$ *super Yang-Mills (SYM)*, can be constructed either using superspace formalism or via dimensional reduc-

[7] It is clear that the flux will encode the number of D3-branes enclosed N since the total charge Q will be given by $Q = N\mu_3$.

[8] Note that the same notation X^i used for the scalars here and those in the DBI action (2.1.14) is not an accident - the 6 scalars in the gauge theory (now adjoint fields) are precisely the 6 transverse embedding functions in the D3-brane picture.

tion of the 10-dimensional $\mathcal{N}=1$ SYM theory, and results in [10]

$$\mathcal{L}_{\text{SYM}} = \text{Tr}\Big(-\frac{1}{2g_{\text{YM}}^2}F_{\mu\nu}F^{\mu\nu} + \frac{\theta}{16\pi^2}F_{\mu\nu}\tilde{F}^{\mu\nu} - i\sum_a \bar{\lambda}^a\bar{\sigma}^\mu D_\mu\lambda_a \tag{2.2.1}$$
$$-\sum_i D_\mu X^i D^\mu X^i + g_{\text{YM}}\sum_{a,b,i}\Big(C_i^{ab}\lambda_a[X^i,\lambda_b] + \bar{C}_{iab}\bar{\lambda}^a[X^i,\bar{\lambda}^b]\Big) + \frac{g_{\text{YM}}^2}{2}\sum_{i,j}[X^i,X^j]^2\Big)$$

where g_{YM} is the gauge coupling, C_i are 4×4 matrices given in terms of Pauli matrices, and $\tilde{F}_{\mu\nu}$ here is the hodge dual of $F_{\mu\nu}$. The most remarkable property of this theory is that, as well as being classically conformal, the theory is believed to be UV finite with a vanishing β function - the quantised theory is thus fully conformal. In fact, it possesses a larger *superconformal* $SU(2,2|4)$ symmetry as a result of combining supersymmetry and conformal symmetry.

Of particular relevance is the scalar potential term in (2.2.1) which goes as $\sum_{i,j}[X^i,X^j]^2$. This must vanish in a supersymmetric vacuum state, and since all terms are non-negative, each term must independently vanish. In the case where all of the scalar VEVs vanish the ground state maintains superconformal invariance; if one or more of the scalars has a non-zero VEV however, $\langle X^i\rangle \neq 0$, then the theory is said to be on the Coulomb branch. In this case, the scale $\langle X^i\rangle$ breaks conformal invariance, and the gauge symmetry is also broken in the manner discussed in Section 2.1.3 in the context of multiple branes. We will study the entanglement entropy of such solutions in Part III.

The spectrum of the theory is organised into representations of the underlying $SU(2,2|4)$ symmetry group, analogous to the case of theories with simple Poincaré or conformal invariance - one first finds the *primary operators*, and the representations are then constructed by acting with generators of the algebra to construct the tower of *descendants*. The primary operators in $\mathcal{N}=4$ SYM are local gauge-invariant composite operators of the elementary fields. Of central importance to the AdS/CFT correspondence are certain *single-trace operators*,

$$\mathcal{O}_k \equiv N^{(1-k)/2}\text{Tr}\left(X^{(i_1}X^{i_2}\dots X^{i_k)}\right) - \dots, \tag{2.2.2}$$

where the $\dots$ denote the subtraction of all contractions of the $SO(6)$ indices - these operators are thus symmetric and traceless. They are in fact *chiral primary operators* i.e. BPS operators that generate short irreducible representations with protected dimensions Δ. These particular operators are 1/2-BPS operators, and are in the representation $[k,0,0]$ with $k=\Delta$ [9] - a representation is thus labelled by the dimension of its primary. Importantly, they are the leading operators in the large N limit discussed in the following section - they were consequently very important in early studies of the AdS/CFT correspondence when the mapping between $\mathcal{N}=4$ operators and bulk modes was performed in the large N limit, as we will discuss in Chapter 3.

[9] Equivalently this is the $[0,k,0]$ representation of $SU(4)$.

2.2.1 Large N Expansion of Gauge Theories

To conclude this chapter we briefly mention an important concept in AdS/CFT, namely the large N or $1/N$ expansion of non-abelian gauge theories. It was first noted by 't Hooft [11] that the perturbative expansion of gauge theories greatly simplifies in the large N limit, and the diagrammatic expansion organises itself into the form of a string perturbation series with coupling $1/N$ - this was one of the earliest hints at the duality between string theory and non-abelian gauge theory, at least at large N.

There exists a non-trivial large N limit for gauge theories such as $\mathcal{N} = 4$ SYM if one keeps $\lambda \equiv g^2_{\text{YM}} N$ fixed as the limit $N \to \infty$ is taken, which is known as the *'t Hooft limit*. The 't Hooft parameter λ then becomes the effective coupling for the gauge theory, and the strong coupling limit corresponds to $\lambda \to \infty$. This is also referred to as the *planar* limit as planar diagrams, i.e. those with Euler number $\chi = 2$, dominate the perturbation series in this regime - diagrams with more complex topologies are then included in a series in $1/N^2$. This is a very important limit in the AdS/CFT correspondence and will be used throughout this thesis, as we will discuss in Section 3.1.

CHAPTER 3

The AdS/CFT Correspondence and Holography

In this chapter we introduce the AdS/CFT correspondence and the main features of the holographic dictionary required throughout this thesis. The AdS/CFT correspondence is a set of dualities relating gravitational theories on asymptotically (locally) anti-de Sitter spaces (AAdS) to conformal field theories. The gravitational theory is usually a string theory (or M-theory), which in the most well-studied example is the type IIB string theory introduced in Chapter 2. The correspondence has been generalised in a number of ways as we will discuss, including relaxing the condition of conformality in the gauge theory - the more general term *gauge/gravity duality* has thus been adopted to refer to dualities between gravitational theories and gauge theories.

The AdS/CFT correspondence is a concrete realisation of the *holographic principle* [12–14], which states that in a theory of quantum gravity the information stored in a volume of spacetime V_{d+1} is encoded in degrees of freedom living on the boundary of the region A_d - this was originally motivated by the Bekenstein-Hawking black hole entropy formula [15, 16]

$$S_{\text{BH}} = \frac{A}{4G_N} \tag{3.0.1}$$

relating the entropy of a black hole to the surface area of its event horizon in units of Planck area. In AdS/CFT dualities the gauge theory can be considered to live on the d-dimensional conformal boundary of the d+1-dimensional AAdS space, and in this manner the holographic principle is realised - the gravitational theory is referred to as the *bulk* theory and the gauge theory is referred to as the *boundary* theory.

3.1 The AdS_5/CFT_4 Conjecture

The original and best understood example of the AdS/CFT correspondence [17] relates the type IIB string theory and $\mathcal{N} = 4$ SYM theory dicussed in Chapter 2. It can be motivated by studying a stack of N D3-branes from both open ($g_sN \ll 1$) and closed ($g_sN \gg 1$) string perspectives discussed previously and taking the *near-horizon* or *Maldacena limit* $\alpha' \to 0$ with r/α' fixed. We do not repeat here the details of this decoupling argument but simply state the celebrated AdS_5/CFT_4 conjecture that results:

$\mathcal{N} = 4$ SYM with gauge group $SU(N)$ is equivalent to type IIB string theory on $AdS_5 \times S^5$ with radius L and N units of F_5 flux.

Furthermore the two free parameters on either side map as

$$g^2_{\text{YM}} = 2\pi g_s \qquad\qquad 2g^2_{\text{YM}}N = \frac{L^4}{\alpha'^2} \tag{3.1.1}$$

The first of these can be understood from the discussion in Section 2.1.2, and the second can then be understood from equation (2.1.17). Note in particular that the second of these relates the dimensionless parameter $L/\sqrt{\alpha'}$ to the t'Hooft coupling λ.

The above equivalence is believed to hold for all values of the free parameters. However, progress in understanding the duality can be made by taking certain limits which simplify one of the theories. For example, it is common to take the limit $g_s \to 0$ whilst keeping λ fixed, which requires $N \to \infty$ - the duality then relates a *classical* string theory to a gauge theory in the t'Hooft limit discussed in 2.2.1. Futher progress can be made by then taking the limit $\lambda \to \infty$ which corresponds to $L/\sqrt{\alpha'} \to \infty$ - the duality then relates a classical supergravity theory to a strongly coupled gauge theory. This latter form is extremely useful and highlights the *strong/weak duality* nature of the AdS/CFT correspondence - one can study strongly coupled quantum field theories (for which traditional perturbative methods fail) by studying classical gravity theories. We will use this form of the duality throughout the remainder of this thesis.

The first immediate check of the duality that one can perform is to check that the global symmetries agree on both sides of the correspondence. Indeed, one finds that the full superconformal group $SU(2,2|4)$ is found on both sides - the bosonic subgroup $SO(4,2) \times SO(6)$, for example, corresponds to the conformal group and R-symmetry group in the boundary theory, and the isometries of the AdS_5 and S^5 factors respectively in the bulk theory. These field theory symmetries can thus be partially broken by perturbing the corresponding bulk geometry. More detailed mappings between the theories are given in the form of the holographic dictionary discussed in Section 3.2.

Many other cases of the AdS/CFT correspondence exist, and can be obtained in similar ways but with different types of branes in different backgrounds, within either 10-

dimensional string theory or 11-dimensional M-theory. For example, many other dualities of the form $\text{AdS}_{d+1}/\text{CFT}_d$ can be obtained in this manner, with different gauge theories (such as ABJM [18] or the $\mathcal{N} = (2,0)$ theory [19, 20]) on the field theory side and different compact space factors appearing on the gravity side. The duality can also be extended to *non-conformal field theories* in many ways, for example explicitly as in [21–23] where the near-horizon limit of the relevant stack of branes no longer contains an AdS factor (and correspondingly the gauge coupling in the dual field theory runs with energy scale), but also spontaneously as we will see at times in the following. We will for the majority of this thesis focus on the $\text{AdS}_5/\text{CFT}_4$ case and extensions thereof, though many aspects of the discussions do generalise to other settings.

3.1.1 Top-Down and Bottom-Up Holography

Stated in its current form, the holographic nature of the AdS/CFT duality is obscure, since the duality relates a gravitational theory in 10-dimensions to a gauge theory in 4-dimensions. It becomes manifest however after *Kaluza-Klein (KK) compactification* on the S^5 - the resulting 5-dimensional supergravity theory on AdS_5 is then equivalent to the 4-dimensional gauge theory living on the conformal boundary of AdS_5, in accordance with the holographic principle. Such constructions, where one begins with a full solution of string theory/supergravity and compactifies on the internal space to make the holographic identification, are referred to as *top-down*. Probe brane models, which we will study at numerous times throughout this thesis, are concrete examples of top-down constructions. The full procedure of obtaining 4-dimensional QFT data from a 10-dimensional supergravity solution uses the involved machinery of *Kaluza-Klein holography* [24, 25], which we will discuss in detail in Part III. The structure for the $\text{AdS}_5/\text{CFT}_4$ correspondence is illustrated schematically in Figure 3.1.1.

For certain purposes however, one in practice often uses a *bottom-up* approach - rather than working within the full framework of string theory or supergravity, one works with an effective 5-dimensional gravitational theory with a small field content, the details of which depend on the particular problem being studied. The actions of such 5-dimensional models are essentially ad-hoc or phenomenological, but are argued to capture the essential physics of the system under study and to exhibit some univeral features. The exact dual field theory is not known in such cases, but the payoff is that the resulting holographic analysis is significantly easier, and insight into a range of physical problems can be gained. Common applications of this approach range from studying strongly-coupled condensed matter systems and hydrodynamics, to QCD as we will see in Part II.

More rigorous simplifications can also exist in some cases however - for example, $\mathcal{N} = 8$ *gauged supergravity* in 5-dimensions [26, 27] with gauge group $SO(6)$ is believed to be a *consistent truncation* of type IIB supergravity on $AdS_5 \times S^5$, with a recent proof based on generalised geometry given in [28]. Here, the tower of KK modes is truncated and

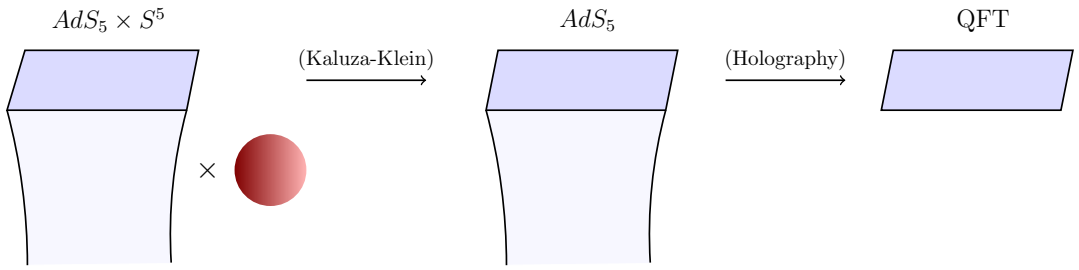

Figure 3.1.1: A schematic illustration of the AdS_5/CFT_4 correspondence and the nature of the holographic identification.

one is left with just the massless 5-dimensional gravity multiplet, but this truncation is consistent with the equations of motion i.e. the KK compactification produces no terms in the action that are linear in massive KK modes, and so these modes can be set to zero without contradiction. We will discuss consistent truncations more in Chapter 9 in the context of entanglement entropy.

To ensure that all quantities are consistent, one should use top-down constructions where possible. Whichever way the lower-dimensional gravitational theory is obtained however, it is within this AAdS setting (i.e. without the internal space) that the holographic dictionary is constructed, as described in the following section. It is also within this setting that the holographic entanglement entropy is described as we will discuss in Chapter 7 - indeed, the subject matter of Chapter 9 is whether the holographic entanglement entropy can equally well be computed directly from the top-down picture.

3.2 Holographic Dictionary

The statement that the two theories are equivalent is expanded upon via the precise *holographic dictionary* [29, 30] that relates quantities in the bulk and boundary theories. We review the necessary ingredients for the case of Euclidean signature here, mostly following the treatment of [31].[1]

3.2.1 Asymptotically Anti-de Sitter Space

A fundamental part of the correspondence is the identification of the AdS radial coordinate with the *renormalization group (RG) scale* of the dual field theory.[2] The scale invariance of the field theory implies that the transformation $x^\mu \to a x^\mu$ and $E \to E/a$ is a symmetry, where E is the energy scale. From the AdS_5 metric in (2.1.18),

$$ds^2 = \frac{L^2}{r^2} dr^2 + \frac{r^2}{L^2} \eta_{\mu\nu} dx^\mu dx^\nu, \tag{3.2.1}$$

[1] The real-time case was developed in [32–34].

[2] In the Wilsonian sense this means that modes with energy above this scale have been integrated out.

we see that the radial coordinate r plays an analogous role here, with the transformation $x^\mu \to ax^\mu$ and $r \to r/a$ a symmetry of the metric. Whilst the bulk coordinates x^μ are simply identified with the field theory directions x^μ, it is thus natural to identify the RG scale $E \sim r$.

Anti-de Sitter space also has a *conformal boundary* due to the second order pole in the metric at $r = \infty$ - a metric can be defined on the boundary via a defining function, but this procedure really only defines a conformal structure since the defining factor is ambiguous up to a scale factor. The boundary $r \to \infty$ thus corresponds to the ultravoilet (UV) of the dual field theory, and expected UV divergences in the QFT translate into near-boundary infrared (IR) divergences on the gravity side as we will discuss in Section 3.2.3. The fundamental gauge theory with $E \to \infty$ (i.e. with no degrees of freedom integrated out) can thus be considered to live at the conformal boundary $r \to \infty$, and high momenta modes are integrated out as one moves into the bulk radially.

It is often common to write the AdS metric using the inverse radial coordinate $z = L^2/r$ which takes the form

$$ds^2 = \frac{L^2}{z^2}\left(dz^2 + \eta_{\mu\nu}dx^\mu dx^\nu\right) \tag{3.2.2}$$

and is said to be in *Poincaré coordinates*.[3] More generally, an AAdS space may be written in *Fefferman-Graham gauge* [35] using the coordinate $\rho = z^2$,

$$ds^2 = L^2\left(\frac{d\rho^2}{4\rho^2} + \frac{1}{\rho}g_{\mu\nu}dx^\mu dx^\nu\right), \tag{3.2.3}$$

which is convenient for the field/operator map and holographic renormalisation as we will discuss in the following section. In these coordinates the conformal boundary corresponds to $\rho = 0$.

3.2.2 Field/Operator Map and Correlation Functions

The matching of the symmetries on the two sides of the AdS/CFT correspondence means that the spectrum of type IIB string theory on $AdS_5 \times S^5$ can be mapped to gauge-invariant operators of $\mathcal{N} = 4$ SYM in the same representation. Indeed, the analysis in the supergravity limit was performed in the early days of AdS/CFT [17, 36–39] - one finds the important result that there is a one-to-one mapping between the bulk modes obtained from KK reduction on the S^5, and the primary and descendant operators of the short representations discussed in Section 2.2. For example, the lowest multiplet is the short representation of $\mathcal{O}_2$ and contains the various symmetry currents of the QFT (energy-momentum tensor, R-symmetry currents and supercurrents) as descendants, and these map to the various gauge fields in the AdS_5 theory (metric, vector gauge fields and gravitinos), with the number of on-shell components exactly matching - this is the supergravity multiplet. Each of the fields in this multiplet form the base of a tower

[3] These coordinates only strictly cover half of the full AdS space.

of KK supergravity modes. The chiral primary operators $\mathcal{O}_k$ themselves map to AdS_5 scalars that are a mixture of the S^5 parts of the trace of the graviton and the 5-form field strength.[4]

Note that the bulk solution is really dual to a particular *state* in the boundary QFT - the pure $AdS_5 \times S^5$ bulk solution is dual to the vacuum of $\mathcal{N} = 4$ SYM for example. Finite temperature in the field theory is associated with a black hole solution in the bulk [40], and finite charge density can also be considered by introducing a bulk gauge field with particular asymptotics. We discuss these features further in Section 8.5.

The relevant KK analysis also leads to a relation between the masses of bulk modes and dimensions of boundary operators, which for the scalar case is

$$m^2 L^2 = \Delta(\Delta - d) \tag{3.2.4}$$

and is easily generalised to higher spins.[5] This is obtained by identifying field theory operators with KK modes associated with spherical harmonics in the same representations of $SO(6)$ - for example, the chiral primary operators and their associated bulk scalars mentioned above. It can also more simply be motivated by studying the asymptotics of a massive scalar in AdS_{d+1} (see Appendix 3.A).

In a general holographic setting, the core idea of this *field/operator map* [29, 30] is that every fundamental field Φ in the bulk theory has a corresponding gauge invariant boundary operator $\mathcal{O}_\Phi$. As alluded to in Appendix 3.A, the correspondence is in fact more precise - for every bulk field one can perform an asymptotic expansion near the conformal boundary in Fefferman-Graham form,

$$\Phi = \rho^m(\phi_{(0)} + \rho\phi_{(2)} + \cdots + \rho^n(\phi_{(2n)} + \tilde{\phi}_{(2n)} \log \rho) + \cdots). \tag{3.2.6}$$

The leading term $\phi_{(0)}$ can then be interpreted as the source for the dual operator $\mathcal{O}_\Phi$, and $\phi_{(2n)}$, although undetermined by the near-boundary analysis, is related to the VEV or 1-point function $\langle \mathcal{O}_\Phi \rangle$ as we will discuss in Section 3.2.3. The VEV can often be read off, with some subtlety, as the subleading term in the asymptotic expansion for a given solution to the equations of motion

$$\Phi \sim \rho^m \phi_{(0)} + \rho^{m+n} \langle \mathcal{O}_\Phi \rangle. \tag{3.2.7}$$

This identification allows for a more precise statement of dynamical equivalence of the

[4] Note that non-BPS operators do not map to supergravity modes, and are instead believed to be dual to string modes.

[5] Note that, unlike in flat space, the squared masses m^2 of fields in AdS do not need to be positive to ensure stability. In fact, m^2 can become negative so as long as it safisfies the *Breitenlohner-Freedman (BF) bound* [41, 42],

$$m^2 L^2 \geq -d^2/4. \tag{3.2.5}$$

This will be relevant for us in Part II when discussing chiral symmetry breaking in the context of AdS/CFT.

two theories which comes from equating the generating functionals. In particular, one equates the bulk partition function (for bulk fields with boundary asymptotics $\phi_{(0)}$) to the QFT partition function in the presence of sources,

$$Z[\phi_{(0)}] \equiv \int_{\Phi\sim\phi_{(0)}} \mathcal{D}\Phi\, e^{-S[\Phi]} = \left\langle e^{-\int \phi_{(0)}\mathcal{O}_\Phi} \right\rangle_{QFT}, \tag{3.2.8}$$

where the expectation value on the right hand side is taken over the QFT path integral and $S[\Phi]$ is the string action. In the supergravity limit the left hand side simplifies upon taking the leading saddle-point approximation, and the path integral localises on the classical solution. The above relation then leads to

$$S_{\text{on-shell}}[\phi_{(0)}] = -W_{QFT}[\phi_{(0)}] \tag{3.2.9}$$

where now $S_{\text{on-shell}}[\phi_{(0)}]$ is the supergravity action evaluated *on-shell* (i.e. with the equations of motion and appropriate asymptotics satisfied) and $W_{QFT}[\phi_{(0)}]$ is the generating function of QFT connected graphs defined by $Z_{\text{QFT}}[J] = e^{W_{\text{QFT}}[J]}$. In the AdS_5/CFT_4 correspondence discussed in Section 3.1 for example, $S_{\text{on-shell}}[\phi_{(0)}]$ would be the KK reduction of the type IIB supergravity action on S^5, evaluated on a solution with boundary asymptotics $\phi_{(0)}$.

Connected correlation functions can now be readily computed in the usual way by functionally differentiating the generating functional with respect to the sources and then setting the sources to zero,

$$\langle \mathcal{O}_\Phi(x)\rangle = \left.\frac{\delta S_{\text{on-shell}}}{\delta\phi_{(0)}(x)}\right|_{\phi_{(0)}=0} \tag{3.2.10}$$

$$\langle \mathcal{O}_\Phi(x_1)\mathcal{O}_\Phi(x_2)\rangle = -\left.\frac{\delta^2 S_{\text{on-shell}}}{\delta\phi_{(0)}(x_1)\delta\phi_{(0)}(x_2)}\right|_{\phi_{(0)}=0} \tag{3.2.11}$$

$$\langle \mathcal{O}_\Phi(x_1)\cdots\mathcal{O}_\Phi(x_n)\rangle = (-1)^{n+1}\left.\frac{\delta^n S_{\text{on-shell}}}{\delta\phi_{(0)}(x_1)\cdots\delta\phi_{(0)}(x_n)}\right|_{\phi_{(0)}=0}. \tag{3.2.12}$$

3.2.3 Holographic Renormalization

An outstanding problem with the discussion in Section 3.2.2 is that the expressions on both sides of the relation (3.2.9) diverge, due to UV divergences in the QFT and IR divergences in AdS. In a QFT the usual procedure of renormalization deals with the UV divergences in a manner independent of the IR physics, and thus holographically one expects the divergences should be dealt with solely via a near-boundary analysis. This is the procedure of *holographic renormalization* [31, 43], a systematic method for renormalizing the bulk on-shell action via covariant counterterms. As a result, renormalized 1-point functions can be obtained (and higher-point functions given an exact solution).

The method proceeds as follows:

1. One solves the field equations with prescribed boundary conditions iteratively in a near-boundary expansion to obtain a solution of the form (3.2.6) - the two independent solutions correspond to the ρ^m and ρ^{m+n} terms.[6] This procedure determines all terms in the expansion (3.2.6) in terms of the source $\phi_{(0)}$, except for $\phi_{(2n)}$ which is left undetermined.

2. The asymptotic solution is then substituted into the action, which is regularized by restricting the radial coordinate to $\rho \geq \epsilon$ for $\epsilon \ll 1$. The action reduces to a contribution on the $\rho = \epsilon$ slice and the finite number of divergent terms can be isolated, which depend only on the source $\phi_{(0)}$,

$$S_{\text{reg}}[\phi_{(0)};\epsilon] = \int_{\rho=\epsilon} d^4x\sqrt{g_{(0)}}\left[\epsilon^{-\nu}a_{(0)} + \epsilon^{-\nu+1}a_{(2)} + \ldots - \log\epsilon\, a_{(2\nu)} + \mathcal{O}(\epsilon^0)\right], \tag{3.2.13}$$

   with $g_{(0)}$ the boundary metric, and $\nu > 0$.

3. A covariant counterterm action $S_{\text{ct}}[\Phi(x;\epsilon);\epsilon]$ can then be constructed by rewriting the divergent terms in (3.2.13) in terms of the bulk field $\Phi(x,\epsilon)$ on the cutoff surface, by inverting the series (3.2.6) order by order.

4. The combination

$$S_{\text{sub}}[\Phi(x;\epsilon);\epsilon] = S_{\text{reg}}[\phi_{(0)};\epsilon] + S_{\text{ct}}[\Phi(x;\epsilon);\epsilon] \tag{3.2.14}$$

   is then finite by construction in the limit $\epsilon \to 0$. This quantity is required in taking the variations to obtain correlation functions. The renormalized on-shell action as a function of the sources can then be obtained as

$$S_{\text{ren}}[\phi_{(0)}] = \lim_{\epsilon\to 0} S_{\text{sub}}[\Phi(x;\epsilon);\epsilon]. \tag{3.2.15}$$

5. One can then obtain the renormalized 1-point function of the operator $\mathcal{O}_\Phi$ dual to Φ as

$$\langle\mathcal{O}_\Phi\rangle_s \equiv \frac{1}{g_{(0)}}\frac{\delta S_{\text{ren}}}{\delta\phi_{(0)}} = \lim_{\epsilon\to 0}\left(\frac{1}{\epsilon^{d/2-m}}\frac{1}{\sqrt{\gamma}}\frac{\delta S_{\text{sub}}}{\delta F(x,\epsilon)}\right) \tag{3.2.16}$$

   where $\gamma_{\mu\nu}$ is the induced metric on the cutoff surface, and the subscript s denotes that this is the 1-point function in the presence of sources. Evaluating this explicitly and setting the sources to zero one finds

$$\langle\mathcal{O}_\Phi\rangle \sim \phi_{(2n)} \tag{3.2.17}$$

[6] In early treatments these were referred to as the *non-normalizable* and *normalizable* modes respectively.

and thus the VEV of the operator $\mathcal{O}_\Phi$ is proportional to the term $\phi_{(2n)}$ not determined by the near-boundary analysis, as claimed beneath equation (3.2.6).

Note that to obtain higher-point correlation functions, one needs an exact solution to the field equations to determine the term $\phi_{(2n)}$ - the n-point functions can then be calculated from (3.2.10).

3.3 Holographic RG Flows

Note that for a massive scalar in AAdS dual to an operator of dimension Δ, the procedure of Section 3.2.3 leads to an asymptotic expansion of the form [31]

$$\Phi = \rho^{(d-\Delta)/2}\phi_{(0)} + \cdots + \rho^{\Delta/2}\phi_{(2\Delta-d)} + \dots \tag{3.3.1}$$

with $\phi_{(0)}$ the source and $\phi_{(2\Delta-d)}$ proportional to the 1-point function. Recall that the isometries of AdS_{d+1} correspond to the conformal goup in d-dimensions - asymptotically AdS spaces more generally are conjectured to be dual to field theories with a UV fixed point i.e. they are conformal in the UV. Note that the situation in (3.3.1), with a non-trivial scalar field in AAdS space, therefore corresponds to a *deformation* of the dual boundary CFT, either via an operator deformation or a VEV deformation (where the conformal symmetry is spontaneously broken) for the boundary asymptotics $\rho^{(d-\Delta)/2}\varphi$ and $\rho^{\Delta/2}\varphi$ respectively.

More generally, a crucial step towards studying realistic strongly-coupled field theories is to construct *holographic RG flows* - supergravity backgrounds conjectured to be dual to a standard QFT renormalisation group flow. A simple example of the latter is $\mathcal{N} = 4$ SYM in the UV with the addition of marginal or relevant operators that generate the flow, such as that considered in [44] and its gravity dual constructed in [45]. This is an example of an interpolating *domain wall* flow, which are Einstein-scalar systems that interpolate between a CFT in the UV and IR - the metric accordingly asymptotes to AdS in both limits, with different radii that are determined by the value of the scalar field (which is constant in both the UV and IR). Such flows can be used, for example, to provide holographic proofs of the C-theorem [46].

Note that holographic RG flows are not limited to the 5-dimensional picture, and indeed there exist many examples within the framework of 10-dimensional supergravity e.g. [47–51]. We will see in Chapter 8 for example that probe branes in AdS/CFT can often be treated as deformations of the underlying CFT. In particular, there also exist examples within both frameworks that exhibit the property of confinement, which will be a central concept in Part II.

3.A Scalar Mass-Dimension Relation

Consider a massive scalar in AdS_{d+1} with action

$$S \sim \int dz d^d x \sqrt{-g} \left(g^{mn} \partial_m \Phi \partial_n \Phi + m^2 \Phi^2 \right). \tag{3.A.1}$$

Using the coordinates of (3.2.2) the Klein-Gordon equation is

$$\left(\Box_g - m^2 \right) \Phi = \left(\frac{1}{L^2} \left(z^2 \partial_z^2 - (d-1) z \partial_z + z^2 \eta_{\mu\nu} \partial^\mu \partial^\nu \right) - m^2 \right) \Phi = 0. \tag{3.A.2}$$

Let us assume in particular that the solution is asymptotically an eigenstate of dilatations in the z-direction i.e. it takes the form $\Phi \sim z^k$ for some k. The wave equation becomes

$$z^2 k(k-1) z^{k-2} - (d-1) z k z^{d-1} - m^2 L^2 z^k = 0 \tag{3.A.3}$$

which implies the quadratic equation

$$k^2 - dk - m^2 L^2 = 0 \tag{3.A.4}$$

with two independent solutions

$$k = \frac{d}{2} \pm \sqrt{\frac{d^2}{4} + m^2 L^2}. \tag{3.A.5}$$

A general solution to the wave equation thus goes asymptotically as

$$\Phi(x, z) \sim \phi_{(0)}(x) z^{d-k} + \langle \mathcal{O}_\Phi \rangle (x) z^k + \dots \tag{3.A.6}$$

where k satisfies $m^2 L^2 = k(k-d)$. By dimensional analysis $\phi_{(0)}$ and $\langle \mathcal{O}_\Phi \rangle$ can be associated with the source and VEV respectively of a boundary operator of conformal dimension k. Thus, identifying k with the conformal dimension Δ of the field theory operator $\mathcal{O}_\Phi$ dual to Φ, we obtain the mass-dimension relation (3.2.4).

Part II

Flavour and QCD

CHAPTER 4

Probe Branes and Low-Energy QCD

An important generalisation of the AdS/CFT correspondence for many purposes is the incorporation of *flavour* degrees of freedom in the QFT i.e. degrees of freedom that transform under the *fundamental* representation of the gauge group. $\mathcal{N} = 4$ SYM, being a supersymmetric pure gauge theory, necessarily only contains fields that transform under the *adjoint* representation since supersymmetry and gauge symmetry commute. To attempt a holographic description of QCD or many strongly-coupled condensed matter systems for example, it is necessary to include matter degrees of freedom resembling quarks or electrons. Flavour degrees of freedom can be added to AdS/CFT by considering additional branes in the supergravity construction known as *probe branes* which will be relevant throughout the remainder of this thesis - we thus introduce them in detail in this chapter, mostly following the treatment in the review [52].

We also introduce some central concepts of low-energy QCD that will be relevant numerous times throughout the rest of Part II - namely, *confinement* and *chiral symmetry breaking*. These are responsible for many phenomenological aspects of QCD, and much progress has been made in realising them within the context of gauge/gravity duality, from both top-down models and a bottom-up approach known as *AdS/QCD*. We introduce both in the present chapter, again largely following [52], leaving a more detailed discussion of AdS/QCD to Chapter 6. As briefly mentioned in Section 3.3, such systems necessarily break conformality; supersymmetry is also necessarily broken upon chiral symmetry breaking. Such features thus move us away from the ideal and highly symmetric $\mathcal{N} = 4$ SYM theory towards more realistic physical systems. We will discuss many of these same features again in Chapter 5 within a slightly different context when we study holographic graphene.

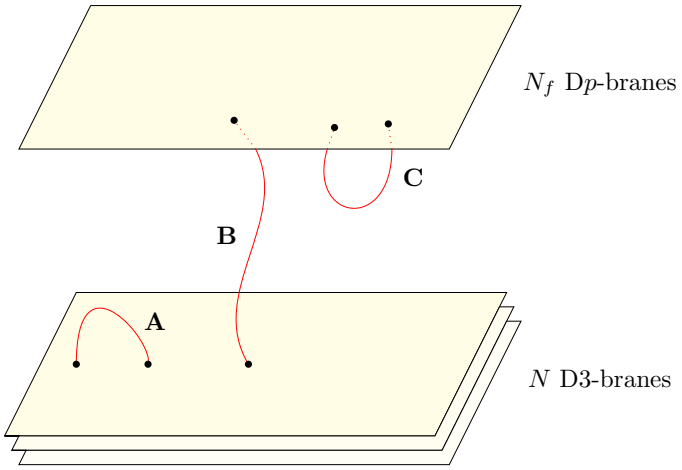

Figure 4.1.1: Schematic illustration of the flavour brane construction: strings **A** correspond to adjoint DoF (gauge bosons), strings **B** correspond to fundamental DoF ("quarks"), and strings **C** correspond to quark/anti-quark bilinears ("mesons"). When the Dp-branes are separated from the D3-branes, the flavour DoF corresponding to strings **B** become massive.

4.1 Adding Flavour to AdS/CFT

To introduce flavour degrees of freedom into AdS/CFT one follows a similar line of reasoning to that used in Section 2.1.3 where the worldvolume theory on a stack of D3-branes was discussed. The basic idea, beginning in [53], consists in including a stack of N_f Dp-branes ("flavour" branes) in addition to the original stack of N D3-branes ("colour" branes) - see Figure 4.1.1. The $3-p$ and $p-3$ strings generate excitations that transform under the (anti-)fundamental representation of the $SU(N)$ colour gauge group since they have only one endpoint on the D3-branes.[1] The $3-3$ strings will generate the gauge theory $\mathcal{N}=4$ SYM as before, and one builds the construction such that the $p-p$ strings dynamically decouple, leaving simply $\mathcal{N}=4$ SYM plus additional flavour degrees of freedom. The latter property arises by virtue of the expression for the gauge coupling in equation (2.1.12) - the ratio of the 't Hooft couplings for the theories on the D3-branes and Dp-branes thus goes as

$$\frac{\lambda_p}{\lambda_3} = \frac{N_f}{N}\,(2\pi)^{p-3}\,\alpha'^{\frac{p-3}{2}} \tag{4.1.1}$$

which vanishes in the Maldacena limit $\alpha' \to 0$ for the cases of $p=5,7$ which we will be mainly interested in throughout the following.[2] The $p-p$ strings thus decouple from the other strings, and the $SU(N_f)$ that they generate plays the role of a *global* flavour symmetry group from the perspective of the D3-branes worldvolume.

[1] Note that they also transform under the (anti-)fundamental of the flavour group $SU(N_f)$ since they have one endpoint on the Dp-branes, as is the case for quarks in QCD.

[2] D(-1)-branes do not contribute flavour degrees of freedom, D1-branes do not decouple, and D9-branes cannot be separated from the stack of D3-branes, which is required if one wants to consider massive flavour. Flavour D3-branes are also permitted but we will not consider them in the following

The $p-p$ strings are in the adjoint of the $SU(N_f)$ flavour group, and it is thus natural to associate them with *mesons* i.e. gauge-invariant bilinear operators formed from a quark and anti-quark. Since these strings can be considered small perturbations of the Dp-branes, one conjectures that mesons in the gauge theory are dual to fluctuations of the flavour branes in the background geometry - the precise mapping between fluctuations and operators for particular intersections can be given [54, 55], as for the mapping between supergravity modes and $\mathcal{N}=4$ SYM operators discussed in Section 3.2.2. Furthermore, this new conjecture provides a very useful method for computing meson spectra from gauge/gravity duality, by solving for the eigenmodes of linearized fluctuations of the branes about their vacuum embedding. We will consider examples of this at length in Chapter 6, though from a less string-theoretic perspective.

In general, the addition of flavour branes will create source terms in the type IIB supergravity equations that result from (2.1.1), and the $AdS_5\times S^5$ background will no longer be a solution to the full system that results. A large simplification occurs however when one takes the *probe limit* $N_f/N\to 0$.[3] The flavour branes can then be treated as probes, so-called *probe branes* [56], since their backreaction on the near-horizon geometry generated by the stack of D3-branes can be neglected. On the field theory side this corresponds to dropping quark loops from the gauge background, and is known as the *quenched approximation* which is commonly used in lattice QCD computations [57,58]. We will work in the probe limit numerous times throughout the following.

4.1.1 D3/D7 System

The D3/D7 system [53] provides the only example of a supersymmetric D3/Dp-brane intersection that allows flavour degrees of freedom to be introduced in the full 3+1-dimensions of the gauge theory. D3/D5 systems for example, which we will consider in Chapter 5, lead to a *defect field theory* with the flavour restricted to a submanifold. We will use the D3/D7 system at length in Chapter 8, and it is also the motivation behind the Dynamic AdS/QCD model used in Chapter 6.

The brane embedding can be represented diagrammatically as

	0	1	2	3	4	5	6	7	8	9
D3	-	-	-	-	•	•	•	•	•	•
D7	-	-	-	-	-	-	-	-	•	•

where - denotes a direction the brane extends in, and • denotes a transverse direction. This embedding has a manifest $SO(4)\times SO(2)$ isometry - the $SO(2)$ can be broken however by separating the D7-branes from the D3-branes in the 89-directions.[4] This

[3] Since we work in the 't Hooft limit where $N\to\infty$, the probe limit is satisfied so as long as N_f is kept finite.

[4] We will later relate this to a holographic model of chiral symmetry breaking - see Section 4.2.1.

corresponds to giving a mass to the flavour degrees of freedom,

$$m = \frac{l}{2\pi\alpha'}, \tag{4.1.2}$$

where l is the separation, since the 3-7 and 7-3 strings will have a minimum length l and consequently a minimum energy given by (4.1.2).

The dual field theory to the D3/D7 system can be constructed explicitly and is given by $\mathcal{N} = 4$ SYM coupled to $\mathcal{N} = 2$ hypermultiplets. The matter introduced thus really consists of fermions together with scalar superpartners - the latter become massive in the presence of any further supersymmetry breaking. The symmetries can easily be matched between the two sides of the correspondence - for example, the $SO(4) \times SO(2) \subset SO(6)$ isometry of the D7-brane embedding corresponds to the preserved subgroup of the $\mathcal{N} = 4$ SYM R-symmetry group[5], with the $SO(2) \cong U(1)$ factor being broken explicitly by the presence of a mass term in the field theory, as in the corresponding brane picture.

In the probe limit, the D3/D7 system can instead be viewed as a small number of D7 probes in an $AdS_5 \times S^5$ background. The new degrees of freedom can then be described by studying the D7-brane actions from Section 2.1.2 in this background, which recall also includes a profile for the form C_4 and a constant dilaton (see (2.1.15)). The bosonic actions (2.1.10) and (2.1.11) in this case thus reduce to

$$S_7 = -T_7 \int d^8\xi e^{-\Phi} \sqrt{-\det\left(G_{\alpha\beta} + 2\pi\alpha' F_{\alpha\beta}\right)} + \frac{(2\pi\alpha')^2}{2} \mu_7 \int P[C_4] \wedge F \wedge F \tag{4.1.3}$$

where the appropriate 8-form term in the Chern-Simons action has been extracted. For now let us set $F_2 = 0$, which can be done consistently - later, in Chapters 5 and 8, we will also consider non-zero F_2. The action thus reduces to (2.1.8),

$$S_7 \sim \int d^8\xi \sqrt{-\det G_{\alpha\beta}}, \tag{4.1.4}$$

as just the worldvolume of the brane.

For many purposes when embedding probe branes, it is convenient to write the $AdS_5 \times S^5$ metric in a form that illuminates the directions that the probe extends in and their symmetry, by splitting the space transverse to the D3-branes in a particular way. For the case of a D7 probe considered here one writes[6]

$$ds^2 = \frac{r^2}{L^2}\eta_{\mu\nu}dx^\mu dx^\nu + \frac{L^2}{r^2}\left(d\rho^2 + \rho^2 d\Omega_3^2 + dw^2 + w^2 d\phi^2\right) \tag{4.1.5}$$

[5] Technically, the $SO(4)$ decomposes to $SU(2)_R \times SU(2)_\Phi$ with $SU(2)_R$ the aforementioned R-symmetry factor, and $SU(2)_\Phi$ rotating the scalars in the adjoint hypermultiplet.

[6] Note that the ρ used here is a different coordinate to that of the same letter in Section 3.2.

with $r^2 = \rho^2 + w^2$ the radius in the transverse space (i.e. the AdS radius) as before.[7] One then embeds the probe such that it extends in the directions (x^μ, ρ, Ω_3), with (w, ϕ) the transverse coordinates - the coordinate ρ then effectively plays the role of the holographic RG scale r, though the distinction is of physical importance as we will see. We may consistently set $\phi =$ constant due to the symmetry in the directions transverse to the D7 probe. The induced metric on the D7 probe is then easily calculated as

$$ds^2_{D7} = \frac{\rho^2 + w^2}{L^2}\eta_{\mu\nu}dx^\mu dx^\nu + \frac{L^2}{\rho^2 + w^2}d\rho^2 + \frac{L^2\rho^2}{\rho^2 + w^2}d\Omega_3^2 \tag{4.1.6}$$

which asymptotically ($\rho \to \infty$) is $AdS_5 \times S^3$.

To find the exact ground state embedding, we work in static gauge (see Section 2.1.2) and search for a solution $w(\rho)$ of the equation of motion that results from the action (4.1.4) on the background (4.1.5), where this is a function of ρ only due to the $SO(4)$ symmetry of the S^3 and in order to preserve Poincaré invariance. The action then becomes

$$S_7 \sim \int d\rho\rho^3\sqrt{1 + (\partial_\rho w)^2} \tag{4.1.7}$$

with corresponding equation of motion

$$\frac{d}{d\rho}\left(\rho^3\frac{\partial_\rho w}{\sqrt{1 + (\partial_\rho w)^2}}\right) = 0. \tag{4.1.8}$$

This has a supersymmetric flat embedding solution $w(\rho) = l$ i.e. the D7 is separated from the D3 stack by a distance l. Physically, $w(\rho)$ can be interpreted as the running of the flavour mass under RG flow, and thus for these solutions the mass is non-renormalised, as expected for a supersymmetric gauge theory. For $l = 0$ conformal invariance is preserved, but otherwise it is broken by the scale l. Note that for non-zero l, the radius of the S^3 in (4.1.6) vanishes at $\rho = 0$ - this corresponds to the radial coordinate value $r = \sqrt{\rho^2 + w^2} = l$ and the brane embedding thus caps off smoothly in the space here. Physically, this corresponds to the intuition that the flavour degrees of freedom only exist at RG scales above their mass. In particular, in top-down models like this the meson spectra, which can be calculated by considering linear fluctuations about the vacuum embedding found above, is blind to scales below the constituent quark mass l. We will discuss this issue further in Chapter 6 in the context of Dynamic AdS/QCD.

It remains to discuss this additional duality a little more precisely, in light of the holographic dictionary discussed in Section 3.2. Asymptotically, the equation of motion

[7] Note also that for other purposes, such as holographic renormalisation and Kaluza-Klein holography, it is better to use a coordinate system that does not mix the AdS radial and S^5 coordinates in this way - in Chapter 8 we will thus use a different set of coordinates.

(4.1.8) has the leading contribution

$$\frac{d}{d\rho}\left(\rho^3\partial_\rho w\right) = 0 \tag{4.1.9}$$

with general solution

$$w = l + \frac{c}{\rho^2} + \dots \tag{4.1.10}$$

We wish to use the dictionary to identify the dimension of the dual operator, but a problem arises in that the kinetic term in the scalar action (4.1.7) is not canonically normalised. Making the field redefinition $w(\rho) = \rho\Phi(\rho)$ the asymptotic form of the action becomes, after an integration by parts,

$$S_7 \sim \int d\rho\rho^3 \left(\partial_\rho w\right)^2 \sim \int d\rho\rho^3 \left(\rho^2 \left(\partial_\rho \Phi\right)^2 - 3\Phi^2\right), \tag{4.1.11}$$

which is easily identified as the action for a free massive scalar in AdS_5, with mass $m^2 = -3$.[8] The corresponding asymptotic expansion of the field Φ is thus

$$\Phi = \frac{l}{\rho} + \frac{c}{\rho^3} + \dots \tag{4.1.12}$$

and since this scalar is canonically normalised, the result in equation (3.3.1) may be used (making the transformation $\rho \to 1/\rho^2$ to account for the different definition of the holographic radial coordinate used). One thus finds that Φ and consequently w describe a dimension-1 source (i.e. mass) and a dimension-3 operator, consistent with the mass-dimension relation (3.2.4) for a bulk scalar of mass $m^2 = -3$.

The dimension-3 operator in question is a supersymmetric generalisation of the usual fermion mass term $\mathcal{L}_m = m\bar{\psi}\psi$, and consequently its VEV is a generalisation of the *chiral condensate* $\langle\bar{\psi}\psi\rangle$ which we will discuss in the next section. This VEV must vanish if supersymmetry is present, and in the supersymmetric flat embedding $w_6 = l$ found previously, there is no subleading term and so the VEV indeed is zero. Some confusion arises however from the fact that in other coordinate systems the subleading terms may be zero. For example, in the coordinate system in which holographic renormalisation is most readily carried out, and which we use in Chapter 8, the subleading term is non-zero. Holographic renormalization provides the solution here however, as finite counterterms can be fixed by supersymmetry to ensure that the on-shell action is zero, and consequently one finds that the VEV automatically vanishes in this case [59]. For the remainder of Part II we will continue to work in coordinates analogous to those used here.

[8] Indeed, in [59] it was shown that asymptotically the general action (4.1.4) for a D7 probe is the same as that of a massive free scalar in AdS_5, which allowed the holographic renormalisation to be performed by simply borrowing the corresponding counterterms.

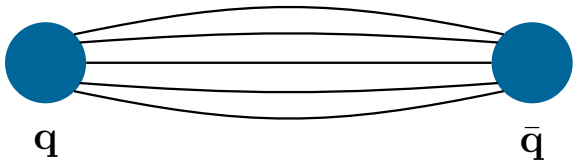

Figure 4.2.1: Mesons viewed as a quark and anti-quark joined via a string-like gluon flux tube: the tube causes a linear potential between the quarks that grows as their separatoin, $V(r) \propto r$, leading to the phenomenon of confinement.

4.2 QCD - Confinement and Chiral Symmetry Breaking

Quantum Chromodynamics (QCD), the theory of the strong interaction, describes the dynamics and interactions of quarks and gluons, and mathematically is given by a non-abelian gauge theory with gauge group $SU(3)$ coupled to N_f Dirac fermions,

$$\mathcal{L}_{\text{QCD}} = -\frac{1}{4}F^a_{\mu\nu}F^{\mu\nu}_a + \bar{\psi}_j\left(i\gamma^\mu D_\mu \delta^{jk} - M^{jk}\right)\psi_k. \tag{4.2.1}$$

If one assumes that all the quark masses are equal then there is a $U(N_f)$ global flavour symmetry, and the beta function of the theory (for the case of general colour N) can be calculated as [60]

$$\beta(g) \equiv \frac{dg}{d\ln\mu} = -\frac{g^3}{48\pi^2}\left(11N - 2N_f\right) \tag{4.2.2}$$

where μ is the RG scale. This is manifestly negative for $11N > 2N_f$, which is satisfied for the observed case of $N = 3, N_f = 6$. The coupling thus vanishes in the UV ($\mu \to \infty$), a property known as *asymptotic freedom* [61, 62], whereas the IR ($\mu \to 0$) is strongly coupled - in fact, the coupling diverges at a finite value of $\mu = \Lambda_{\text{QCD}}$ known as the *Landau pole* (though of course the perturbative analysis must be treated with suspicion in this regime).

The strongly-coupled nature of the IR in QCD leads to a number of important phenomenological implications (see e.g. [63]) that are observed experimentally, though currently without analytic proof since the large coupling defies analysis via traditional perturbative methods. Perhaps the most crucial of these is *confinement*, which is the property that no colour-charged particles can be isolated, but must instead exist in colour-singlet bound states. For example, quarks are observed to form *hadron* bound states either as *mesons* ($\bar{q}q$) or *baryons* (qqq), and gluons similarly are believed to form *glueballs* (see e.g. [64, 65]). Important signatures of confinement in a theory are the existence of a discrete spectrum of bound states, together with a *mass gap* i.e. strictly positive value for the lowest mass in the theory - in QCD for example, although the gluons are massless, glueballs must have a lower mass bound.[9]

Confinement can be understood by thinking of quarks in bound states as being held

[9] An analytic proof of confinement is still missing even in pure Yang-Mills theory, but it can be demonstrated in lattice QCD [66].

together by gluon flux tubes or 'strings' - see Figure 4.2.1. The energy between quarks grows as one tries to separate them, with a linear potential $V(r) \propto r$ for separation r.[10] Such a feature is known to lead to an 'area law' for the expectation value of the Wilson loop $\langle W_{\mathcal{C}} \rangle$, which can then be taken as an indication of confinement in a theory (confinement can then be tested for in a given theory holographically, since $\langle W_{\mathcal{C}} \rangle$ has a simple dual description [67]). Furthermore, the linear potential implies the *Regge trajectory* between mass and spin $M^2 \propto J$ - this was in fact the original motivation for string theory as a theory of the strong interaction in the 1960s, since it correctly described the patterns of hadrons being observed in particle accelerators. We will discuss Regge trajectories further in Chapter 6 in the context of AdS/QCD.

Another key aspect of low-energy QCD dynamics is *chiral symmetry breaking* [68]. Due to a large separation of scales in the quark masses, at low energies only the three lightest quarks need be considered i.e. the up, down and strange quarks. As mentioned previously, for equal mass quarks the QCD Lagrangian has a $U(N_f)$ flavour symmetry - taking the three lightest quarks to be approximately equal mass, there is thus a $U(3)$ flavour symmetry. In the limit that these masses are approximately zero, the so-called *chiral limit*, this symmetry is in fact enhanced to $SU(3)_L \times SU(3)_R$ which rotates the left and right-handed chiral projections of the Dirac fermions independently. In other words, the massless QCD Lagrangian

$$\mathcal{L}_{\text{QCD}|_{m=0}} = -\frac{1}{4} F^a_{\mu\nu} F_a^{\mu\nu} + i\bar{\psi}_L \gamma^\mu D_\mu \psi_L + i\bar{\psi}_R \gamma^\mu D_\mu \psi_R \tag{4.2.3}$$

is invariant under

$$\psi_L \to e^{-i\theta_L \cdot \lambda} \psi_L \qquad \psi_R \to e^{-i\theta_R \cdot \lambda} \psi_R \tag{4.2.4}$$

where λ^a are the $SU(3)$ Gell-Mann matrices. These transformations can equivalently be written as vector and axial-vector transformations of the full Dirac fermion

$$\psi \to e^{-i\theta_V \cdot \lambda} \psi \qquad \psi \to e^{-i\theta_A \cdot \lambda \gamma_5} \psi \tag{4.2.5}$$

with symmetry $SU(3)_V \times SU(3)_A$.[11]

Of course real QCD is not chiral, and indeed chiral symmetry is explicitly broken by mass terms for the fermions

$$\mathcal{L}_m = -m\bar{\psi}\psi = -m\bar{\psi}_L \psi_R - m\bar{\psi}_R \psi_L \tag{4.2.6}$$

which are not invariant under (4.2.4), but only the subgroup $SU(3)_V$. However, the situation is slightly more complicated since there is evidence that the chiral symmetry in

[10] Note that separating the quarks far enough can cause the string or flux tube to break, with the resulting fragments then independently forming new bound states.

[11] Of the remaining $U(1)_V \times U(1)_A$ that one would expect to be present, $U(1)_A$ is anomalous [69, 70] (except at large N) whereas $U(1)_V$ corresponds to baryon number conservation and is indeed preserved in the full quantum theory.

QCD is in fact *spontaneously broken*. Spontaneous symmetry breaking can occur if, although there are no mass terms for quarks, the dynamics generates a vacuum expectation value for the mass operator i.e.

$$\langle\bar{\psi}\psi\rangle = \langle\bar{\psi_L}\psi_R\rangle + \langle\bar{\psi_R}\psi_L\rangle \neq 0 \tag{4.2.7}$$

This is known as the *chiral condensate* as mentioned in Section 4.1.1, and is manifestly not invariant under chiral symmetry transformations (4.2.4).[12] Following Goldstone's theorem [71, 72], one would expect 8 massless bosons present in the spectrum when breaking $SU(3)_L \times SU(3)_R \to SU(3)_V$. In reality these will be pseudo-Goldstone bosons with non-zero mass due to the only approximate chiral symmetry present in nature. In QCD, these pseudo-Goldstone bosons are the pions, kaons, and eta mesons, and their light masses compared to the rest of the spectrum (which cannot be explained via small explicit mass terms for the light quarks - see [73]) can be understood to be generated via this chiral symmetry breaking mechanism.[13]

4.2.1 Top-Down Holographic Models

Although a full gravity dual of QCD is not within reach at present, considerable work has been done in trying to realise these features of low-energy QCD within the gauge/gravity framework. For example, confinement can be realised by considering supergravity backgrounds that have a divergence in the interior of the bulk at a finite value $r = r_0$ of the holographic radial coordinate. This obstruction or "wall" in the IR leads to a linear relationship between separation and energy for a string that dips deep into the AdS space and thus can be viewed as leading to confinement following [67]. Examples of such constructions exist within both the bottom-up and top-down pictures, such as the 5-dimensional *GPPZ* flow [74, 75] or the 10-dimensional *Constable-Myers* flow [76] - the latter is generated by a running of the dilaton and is a completely non-supersymmetric background.

For the following we are mostly interested in top-down models of chiral symmetry breaking from probe branes. We will study a new example of this in Chapter 5, and Chapter 6 is largely concerned with similar issues within the Dynamic AdS/QCD framework which, although a bottom-up construction, is directly inspired by top-down probe brane models of chiral symmetry breaking.

The simplest example of realising chiral symmetry breaking within gauge/gravity duality is to consider D7 probe branes within a confining, non-supersymmetric background

[12] Note that, as mentioned in Section 4.1.1, chiral condensates can only exist in the absence of supersymmetry.

[13] Another heuristic argument for spontaneous chiral symmetry breaking can be given on the basis that QCD is confining. Since the energy between quarks grows as one tries to separate them, it might be energetically favourable for the ground state to contain many quark and anti-quark pairs bound together. By Poincaré invariance the only possibility is a condensate of the form (4.2.7) [60].

such as the Constable-Myers flow (chiral symmetry breaking can also be triggered via a background magnetic field [77], as we discuss more in Chapter 5). The symmetry in question that is broken is the $U(1)$ of the 89-directions transverse to the D7 probe, which corresponds to part of the R-symmetry in the field theory as discussed in Section 4.1.1. This symmetry is broken by a non-trivial brane embedding, and in the field theory is correspondingly broken by either an explicit mass term or a condensate $\langle\bar{\psi}\psi\rangle$. The case of spontaneous symmetry breaking is given by solutions of the brane embedding of the form (4.1.12) with $l = 0, m \neq 0$ i.e. zero mass but non-zero condensate. Note that the anomalous $U(1)_A$ symmetry of QCD becomes restored at large N (with finite N_f) as discussed in Section 4.2, and is similarly broken by the formation of a condensate - we thus take the spontaneous breaking of the $U(1)$ symmetry in the D7 system as a model for the breaking of this $U(1)_A$ in QCD at large N.

It is also possible to construct holographic models of chiral symmetry breaking for non-abelian symmetries, which more faithfully represent the full pattern of symmetry breaking present in QCD. For example, the *Sakai-Sugimoto* model [78, 79] is a D4-D8 system within the framework of type IIA string theory, and breaks the full $SU(N_f) \times SU(N_f)$ of QCD. In Chapter 5 we will see an example of D5 probe branes breaking an $SO(3)$ symmetry.

4.2.2 AdS/QCD

A complementary approach to studying QCD within gauge/gravity duality (though one that does not strictly use the holographic dictionary) is to use bottom-up models that have come to be known collectively as *AdS/QCD* [80,81]. These are simple 5-dimensional gravity models that are not derived from any top-down string theory model, and consequently the details of the dual field theory are not known. By choosing the ingredients of the 5-dimensional theory carefully however, it can be conjectured to be dual to a confining gauge theory similar to QCD, and useful calculations about the latter can be performed with relative ease.

A full gravity dual of QCD should of course contain an infinite number of bulk fields dual to the infinite number of operators in QCD, in accordance with the field-operator map discussed in Section 3.2.2. However, if one is interested in studying the dynamics of chiral symmetry breaking then only a small number of operators contribute - the chiral order paramater, and the left and right symmetry currents $\bar{\psi}_L\gamma^\mu\psi_L$ and $\bar{\psi}_R\gamma^\mu\psi_R$ associated with the $SU(N_f) \times SU(N_f)$ chiral symmetry.

Within this approach for example, there exist models that can be viewed as the gravitational counterpart to *chiral perturbation theory* [68] - this is a low-energy effective field theory of QCD that dispenses with notions of quarks and gluons and instead takes as its degrees of freedom the light mesons that are the pseudo-Goldstone modes of chiral symmetry breaking, as discussed in Section 4.2. One collects these modes π^a into a

single field

$$U = e^{i\pi^a(x)T_a/f_\pi} \tag{4.2.8}$$

with f_π the pion decay constant and T_a the $SU(3)$ generators, and then constructs a phenomenological Lagrangian as a derivative expansion. Correspondingly, one can consider a bulk scalar field of the form

$$X(z,x) = X_0(z)e^{2i\pi^a(x)T_a} \tag{4.2.9}$$

where π^a encodes the light mesons and $X_0(z)$ encodes the quark mass and condensate via its asymptotics

$$X_0(z) \sim \frac{1}{2}Mz + \frac{1}{2}\Sigma z^3 \tag{4.2.10}$$

with M and Σ the mass and condensate matrices respectively - the asymptotics are appropriate to describe a scalar operator of dimension 3. Here z is the radial coordinate in a simple 5-dimensional AdS space, but with a cutoff or *hard wall* at $z = z_0$. This breaks conformal symmetry, and the scale z_0 introduces a mass gap and ensures confinement. Similarly the model contains two gauge fields that are dual to the left and right symmetry currents. Altogether one has the action

$$S = -\int_0^{z_0} d^5x\sqrt{-g}\ \mathrm{Tr}\left[|DX|^2 + 3|X|^2 + \frac{1}{4g_5^2}(F_L^2 + F_R^2)\right] \tag{4.2.11}$$

with g_5 the gauge coupling, and the scalar mass $m^2 = -3$ chosen to describe a dimension 3 operator in the field theory according to (3.2.4) - the gauge fields dual to the symmetry currents are massless according to the relation $m^2 = (\Delta - 1)(\Delta - 3)$, which is the analogue of (3.2.4) for vector fields in $d = 4$.

Given this model, one can then compute meson spectra and decay constants by considering fluctuations about the ground state solution - the method gives results that are within 10% agreement with experimental measurements [80]. One problem with the hard wall feature present in this model is that it leads to a scaling behaviour $M^2 \sim n^2, s^2$ for the meson masses with excitation number and spin, whereas QCD is known to follow Regge behaviour $M^2 \sim n, s$ as dicussed in Section 4.2. For this reason one often considers *soft wall* models within AdS/QCD that circumvent this difficulty, though at the expense of potentially creating new problems. This issue forms the subject matter of Chapter 6.

An extension of this simple model, known as *Dynamic AdS/QCD* [82, 83], makes some improvements, and is inspired by the D3/probe D7 model discussed in Section 4.1.1. In particular, the generation of the quark condensate and soft wall in the IR occur dynamically, rather than needing to be put in by hand, though one does put in the gauge theory dynamics as input through the running of the anomalous dimension of the quark/antiquark bilinear. A useful application of this model is to study the N_f-dependence of the

gauge theory, since one can simply vary the form of the anomalous dimension that is used as input - such an approach has been used to study a variety of physical problems, such as the conformal window [84] and walking gauge theories [83, 85]. We discuss the Dynamic AdS/QCD model in detail in Chapter 6.

CHAPTER 5

Holographic Graphene in a Cavity

The material in the present chapter is based largely on [1].

5.1 Introduction

The low-energy description of graphene [86] is given by a theory of 2+1-dimensional massless fermions interacting through classically conformal 3+1-dimensional electromagnetism. Holographic descriptions of $\mathcal{N} = 4$ super Yang-Mills theory with defect D5-probe branes [87–91] (and other related systems [92–97]) provide a calculable system with similar overall properties - fermions living on the defect interacting via higher-dimension conformal gauge fields. The holographic description is of course only valid in a regime where the gauge fields are strongly coupled (formally, the large N limit). It has been argued however that the graphene system may be close to strong coupling since the effective speed of light of the fermionic theory is much less than the vacuum value [98]. Nevertheless, graphene may be in a different universality class from the holographic systems, lying closer to perturbative expectations. One way to drive graphene's interactions to stronger coupling is to place the theory in a cavity, by placing a sheet between two mirrors for example. The separation of the mirrors Δz enters the effective 2+1-dimensional electromagnetic coupling as $g_2^2 \sim g_3^2/\Delta z$ (see also discussion of the Purcell effect in the condensed matter literature [99]) and can be used to control the coupling strength. It is therefore possible that graphene could be forced into the strongly coupled regime experimentally. Holographic models may then provide useful guidance as to the expected phenomena in real world systems (although the holographic theories typically contain remnants of super-partners of the fields involved, and so no predictions are likely to be quantitatively correct).

Motivated by this idea, in this chapter we study the holographic D3/D5 system in a compact space and in a cavity. The simplest example is to study the $\mathcal{N} = 4$ theory in a space with one compact dimension, introducing a scale Δz - the gravity dual is given by the AdS-soliton configuration [100] (the circumference of the space is computed in Appendix 5.A). In Section 5.2.1 we place a single D5-probe in the geometry and show that a mass gap is generated by the probe brane bending in the holographic description (the system is a simple lower-dimensional extrapolation of the well explored D4/D6 system [101]). This is a clean example of dynamical mass gap generation using AdS/CFT, similar to the mass gap generated by an external magnetic field [102]. Previously, a mass gap has also been shown to develop in a system of two D5-probes in $AdS_5 \times S^5$ representing spatially separated defects [59, 97, 103, 104] - here the condensation occurs due to the D5 and anti-D5-branes joining in the interior of AdS and represents "exciton" condensation between the fermions on one defect with those on the other. In [105] the phase transition between that phase and the phase in a magnetic field, where condensation occurs on each brane alone, was investigated. In the present case, the conformal symmetry breaking of the IR length scale is not sufficient to generate a transition, but a similar transition does occur again when a magnetic field of sufficient strength is applied as discussed in Section 5.2.3.

Using the $\mathcal{N} = 4$ system to model electromagnetic interactions between mirrors is more difficult since it is unclear whether any true model would include such a configuration that describes both the $\mathcal{N} = 4$ vacuum and the mirrors. The AdS-soliton configuration again appears to be the appropriate way to initially introduce the IR length scale. In [106] a proposal was made for AdS-duals for $\mathcal{N} = 4$ SYM with boundaries. Amongst these proposals is one for a strip of the gauge theory between two boundaries of constant tension. The dual geometry is the AdS-soliton but with a cut-off in the AdS space corresponding to the position of the boundaries (the tension of the boundary is matched to that of the plasma within). We study probe D5-branes in this system but fail to find a regular description of a single defect since the D5-brane solutions hit the interior cut-off. Most likely this shows that the system with a tensionful wall at the edges of the strip is not a physical system that could be generated in a complete theory. However, the discussion shows that the behaviour of the gauge fields in a cavity would likely be very similar to that in the space with a compact dimension. We therefore use the AdS-soliton to describe the vacuum state of the gauge fields and simply place probe D5-branes and their mirror image partners into the space by hand. A new phase is identified in which the probe has a mass gap as a result of exciton condensation with its mirror image if the sheet comes within a quarter of the separation of the mirrors to either mirror. The complicated phase diagram for bilayer configurations is also computed in this case in Section 5.3.2.

5.2 $\mathcal{N} = 4$ Super Yang-Mills on a Compact Space

Motivated by the previous discussion, we will here loosely represent QED interactions by the large N dynamics of $\mathcal{N} = 4$ super Yang-Mills theory on the surface of a stack of D3-branes. The theory in flat 3+1-dimensional space is described at zero temperature by $AdS_5 \times S^5$,

$$ds^2 = \frac{(\rho^2 + L^2)}{R^2}(dx_{2+1}^2 + dz^2) + \frac{R^2}{(\rho^2 + L^2)}(d\rho^2 + \rho^2 d\Omega_2^2 + dL^2 + L^2 d\tilde{\Omega}_2^2)\,, \tag{5.2.1}$$

where we have written the geometry to display the directions the D3-branes lie in (x_{2+1}, z). A 2+1-dimensional defect with an $\mathcal{N} = 2$ chiral multiplet on its surface can be introduced by embedding a probe D5-brane on $(x_{2+1}, \rho, \Omega_2)$ with the transverse directions $(L, \tilde{\Omega}_2, z)$ where z is the spatial 3-direction. Here we denote the AdS radius as R.

$\mathcal{N} = 4$ SYM on a space that is compact in the z-direction is instead described holographically by the AdS-soliton [100]

$$ds^2 = \frac{R^2}{r^2}h^{-1}(r)dr^2 + \frac{r^2}{R^2}\left(dx_{2+1}^2 + h(r)dz^2\right) + R^2 d\Omega_5^2 \tag{5.2.2}$$

with

$$h(r) = 1 - \left(\frac{r_0}{r}\right)^4. \tag{5.2.3}$$

The circumference of the space can be found by looking in the $r - z$ plane near the horizon at r_0 and demanding regularity after coordinate transformations, in a similar fashion to how one determines the temperature of a black hole. One finds (see Appendix 5.A) that the circumference of the z-direction is $R^2\pi/r_0$.

To embed a probe D5-brane into the space it's convenient to make a change of coordinates such that the 6-plane transverse to the D3-branes can be split as in Section 4.1.1. We thus require that

$$\frac{h^{-1}}{r^2}dr^2 = \frac{d\omega^2}{\omega^2} \tag{5.2.4}$$

which is satisfied by

$$\omega = \left(r^2 + \sqrt{r^4 - r_0^4}\right)^{1/2}. \tag{5.2.5}$$

It is simple to check that the required inverse is

$$r^2 = \frac{\omega^4 + r_0^4}{2\omega^2} \tag{5.2.6}$$

and the metric thus becomes

$$ds^2 = \frac{w^2}{R^2}\left(g_x dx_{2+1}^2 + g_z dz^2\right) + \frac{R^2}{w^2}(dw^2 + w^2 d\Omega_5^2) \tag{5.2.7}$$

where

$$g_x = \left(\frac{w^4 + r_0^4}{2w^4}\right) \tag{5.2.8}$$

$$g_z = \frac{(w^4 - r_0^4)^2}{2w^4(w^4 + r_0^4)}. \tag{5.2.9}$$

We can now split the transverse 6-plane as before,

$$ds^2 = \frac{(\rho^2 + L^2)}{R^2}(g_x dx_{2+1}^2 + g_z dz^2) + \frac{R^2}{(\rho^2 + L^2)}(d\rho^2 + \rho^2 d\Omega_2^2 + dL^2 + L^2 d\tilde{\Omega}_2^2)\,. \tag{5.2.10}$$

5.2.1 A Single Graphene Sheet

We now introduce quenched matter via a probe D5-brane - the analysis proceeds similarly to that of the D3/D7 system in Section 4.1.1. The matter content is a single Dirac fermion and scalar superpartners (that will become massive in the presence of any supersymmetry breaking) restricted to the x_{2+1} directions. The underlying brane configuration is as follows:

	0	1	2	3	4	5	6	7	8	9
D3	-	-	-	‖	•	•	•	•	•	•
D5	-	-	-	•	-	-	-	•	•	•

where ‖ corresponds to the compact direction. Note that there is an $SO(3)$ symmetry associated with the directions $(L, \tilde{\Omega}_2)$ transverse to the D5-brane. We expect the vacuum configuration for a single D5-probe to be described by a profile $L(\rho)$ at fixed z. We work at zero temperature and density (with all other fields switched off) and the action for the D5-probe is thus just its world volume,

$$\begin{aligned} S &\sim -\int d^6\xi e^{\Phi}\sqrt{-\det[G]} \\ &\sim -\int d\rho\, \left(1 + \frac{1}{(\rho^2 + L^2)^2}\right)^{3/2} \rho^2 \sqrt{1 + L'^2}\,, \end{aligned} \tag{5.2.11}$$

where Φ is the dilaton (which is constant here as in pure AdS) and we have dropped angular factors on the 2-sphere which are a constant multiplicative factor for all the solutions we compute. We have also rescaled each of L and ρ by a factor of r_0.

One can solve for the numerical embedding $L(\rho)$ by shooting from $\rho = 0$ subject to the boundary condition $L'(0) = 0$ for regularity. The asymptotic solutions fall off as $L(\rho) = m + c/\rho + ...$ where m is proportional to the quark mass and c to the quark condensate[1] (strictly it is only the quark condensate in the massless limit [92]). To find the massless embedding one shoots to find the solution with $L(\infty) = 0$. The minimum

[1]Note that the dimensions are consistent here, since the fermions are confined to live on a 2+1-dimensional defect i.e. the fermion mass term is now $\int d^3x m\bar{\Psi}\Psi$, which means that $\bar{\Psi}\Psi$ and thus c is of dimension 2.

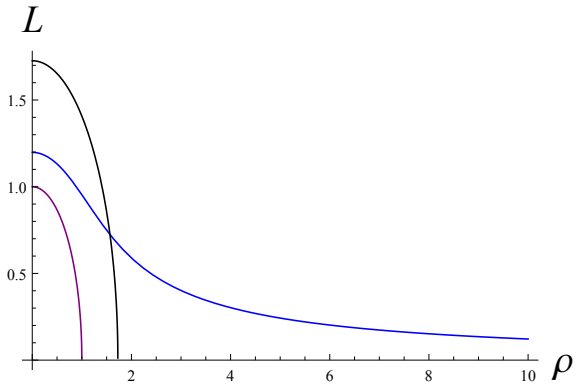

Figure 5.2.1: The embedding of a single D5 brane for a massless quark in the AdS-soliton background is shown for $r_0 = 1$. The dual of the compact space therefore closes off on the smaller circle shown - note the D5 brane embedding is regular avoiding this line. We also show the solution of (5.3.3) with the tension chosen so that the interval between the walls has radius $R^2\pi/r_0$ - the D5 embedding hits this cut off on the space.

energy solution is shown in Figure 5.2.1 (the position in the $\rho - L$ plane of the singularity at $\omega = 1$ is also shown, so one sees that the embedding never enters the singular region). Numerical computation of $-S$ evaluated on a solution gives the vacuum energy since the configuration is static. This energy suffers from an IR divergence which goes as Λ^3 for large cutoff Λ, as can be seen from equation (5.2.11) since $L'(\rho) \to 0$ as $\rho \to \infty$ on our solution. Of course this is expected within holography, and can be dealt with via the usual procedure of holographic renormalisation [59]. Here it is sufficient to include a counterterm of the form $L_1 = -\frac{1}{3}\sqrt{\gamma}$ to cancel the single divergence above, where γ is in the induced metric on the cutoff slice $\rho = \Lambda$.[2]

The curved solution in Figure 5.2.1 is already an interesting result. It breaks the $SO(3)$ symmetry of the $L = 0$ (supersymmetric massless) embedding to $SO(2)$ and the non-zero value of $L(0)$ can be interpreted as a dynamically generated IR quark mass. This response is familiar from other cases in the literature describing the dynamical generation of a mass gap [101, 102, 107]. This graphene-like configuration on a compact space thus provides an example of a completely controlled AdS/CFT computation of a dynamically generated mass gap (the case with a magnetic field [90, 91] is the only other known case for a single probe D5-brane).

5.2.2 Bilayer Configurations

Another example of a holographically computable dynamical mass gap is provided by a bilayer configuration of probe D5-branes in AdS. A joined D5/anti-D5-brane U-shaped configuration, analogous to the Wilson loop configuration of an interacting quark and anti-quark [67], describes "exciton" condensation between the fermions on the two defects. The separation of the defects provides the conformal symmetry breaking scale. It

[2] Note that no finite counterterms are possible for D5-branes.

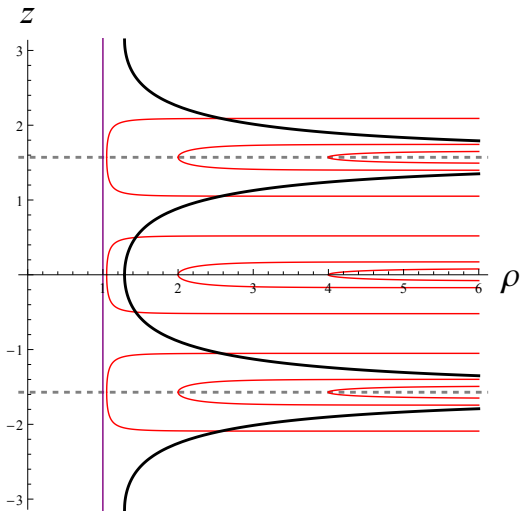

Figure 5.2.2: U-shaped bilayer configurations in the AdS-soliton background. The space has circumference π in the z-direction - we repeat the space to show configurations wrapping both ways around the circle. Note that configurations which reach down to $r_0 = 1$ describe defects separated by $\pi/2$ in z. We also plot the solution of (5.3.3) with the tension chosen so that the interval between the walls has radius $R^2\pi/r_0$ - the probe configurations hit this boundary. If the figure is viewed as that for an interval between two mirrors then configurations corresponding to exciton condensation with the mirror partner exist if the probe lies within $\pi/4$ of the mirror.

is therefore interesting to also explore this configuration in the compact space.

We will allow for an embedding of the probe D5-brane in the z-direction. Allowing z to depend on ρ only, the action for the case $L = 0$ now becomes

$$S \sim -\int d\rho \left(1+\frac{1}{\rho^4}\right)^{3/2} \rho^2 \sqrt{1+\frac{(\rho^4-1)^2}{2(\rho^4+1)} z'^2}\,. \tag{5.2.12}$$

We have again scaled ρ by r_0, and now also scaled z by a factor of $R^2 r_0$ (the circumference of the compact z-direction is now π in these coordinates). In general there may be solutions with non-zero z and L simultaneously but we shall not consider such configurations - they were explored in [105] for the B-field case but shown to only represent local maxima of the effective potential. The action for the brane configurations here is very similar to that in [105] with an IR wall introduced by an effective dilaton factor - the main difference is just the power in the dilatonic factor and so we expect the vacuum structure to be similar.

Since the action is independent of z, there is a constant of motion Π_z given by

$$\Pi_z = \frac{z'\sqrt{1+1/\rho^4}(\rho^4-1)^2}{\rho^2\sqrt{2+z'^2(\rho^4+4/(1+\rho^4)-3)}}. \tag{5.2.13}$$

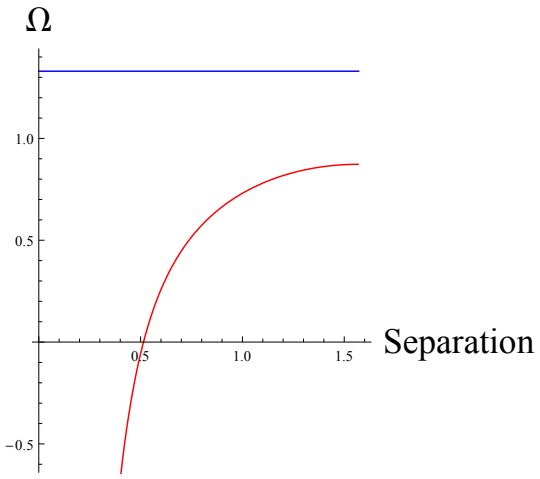

Figure 5.2.3: The regularized energy of two D5s in the configuration of Fig 5.2.1 (which is independent of separation) and that of the U-shaped joined embedding against separation in z (which cannot exceed $\pi/2$). The U-shaped configurations are always preferred.

As mentioned, these solutions represent two branes joining, and extend a finite distance into the bulk of the space at which point they turn around. There thus exists some ρ_0 at which $z' \to \infty$. From equation (5.2.13) one then finds that

$$\Pi_z = \frac{\sqrt{1+1/\rho_0^4}(\rho_0^4-1)^2}{\rho_0^2\sqrt{\rho_0^4+4/(1+\rho_0^4)-3}}. \tag{5.2.14}$$

From equation (5.2.13) one also finds

$$z' = \pm\frac{\sqrt{2}\Pi_z\rho^2}{\sqrt{(1+1/\rho^4)(\rho^4-1)^4-\Pi_z^2\rho^4(\rho^4+4/(1+\rho^4)-3)}} \tag{5.2.15}$$

giving a first order ODE for $z(\rho)$ which one can directly integrate up numerically. One can also find the separation Δz of the branes in a given solution by integrating equation (5.2.15) over $\rho \in [\rho_0, \infty]$. The solutions for various values of ρ_0 are shown in Figure 5.2.2.

An interesting feature is that there are no linked configurations with separation greater than $\pi/2$ (half the circumference of the compact direction). The maximum $\pi/2$ separation is realized precisely when the linked configurations fall into the scale r_0. For a compact space the dual has thus provided us with precisely the minimum number of configurations to describe all possible D5-probe separations - two D5-probes cannot be separated by more than half the circumference of the z-direction. The solutions do not however provide us with configurations that wind further around the compact direction.

For the purposes of computing the energies of these solutions, the expression given in equation (5.2.15) can be substituted directly into the action in (5.2.12). The asymptotic behaviour can then easily be read off and again reveals a single divergence which goes

as Λ^3, and can be cancelled by the same counterterm $L_1 = -\frac{1}{3}\sqrt{\gamma}$. The results for the two embeddings are given in Fig 5.2.3. The linked embedding always has lower energy than the separated embeddings - exciton condensation between the sheets is preferred over separated sheets with condensation on the single sheets at all separations on the z circle.

5.2.3 Applying a Magnetic Field

For the compact space, U-shaped probe configurations were always energetically preferred over the configuration in Figure 5.2.1 for bilayers. It is known however that the configuration of Figure 5.2.1 is heavily preferred when a large background constant magnetic field is applied [90–92]. Here we do not mean a component of the $\mathcal{N} = 4$ SYM fields, but instead a B-field associated with the $U(1)$ baryon number symmetry which has a dual description in terms of a gauge field in the DBI action of the brane. The DBI action with the worldvolume gauge field is now given by

$$S \sim -\int d^6\xi e^{\Phi}\sqrt{-\det[G + 2\pi\alpha' F]}. \tag{5.2.16}$$

For the 2+1-dimensional defect field theory in question, the only possibility for introducing an external magnetic field is via $F_{yx} = -F_{xy} = B_z \equiv B$. Following through the analysis as before, one finds that the actions retain the forms (5.2.11) and (5.2.12) but with an additional factor that can be identified as an effective dilaton profile,

$$e^{\Phi} = \sqrt{1 + \frac{(2\pi\alpha')^2 B^2}{g_x^2(\rho^2 + L^2)^2}}. \tag{5.2.17}$$

Equations (5.2.14) and (5.2.15) for the bilayer configurations now become

$$\Pi_z = \frac{\sqrt{1 + 1/\rho_0^4}(\rho_0^4 - 1)^2\sqrt{1 + 4B^2\rho_0^4/(1+\rho_0^4)^2}}{\rho_0^2\sqrt{\rho_0^4 + 4/(1+\rho_0^4) - 3}} \tag{5.2.18}$$

and

$$z' = \frac{\sqrt{2}\Pi_z\rho^2}{\sqrt{\mathcal{A} - \mathcal{B}}} \tag{5.2.19}$$

$$\begin{aligned} \mathcal{A} &= (1 + 1/\rho^4)(\rho^4 - 1)^4\left(1 + \tfrac{4B^2\rho^4}{(1+\rho^4)^2}\right) \\ \mathcal{B} &= \Pi_z^2\rho^4(\rho^4 + 4/(1+\rho^4) - 3) \end{aligned} \tag{5.2.20}$$

where we are writing B in units of $1/2\pi\alpha'$. One finds that for any value of B, the maximum possible separation of the branes (corresponding to $\rho_0 = 1$) is again given by $\Delta z = \pi/2$. Of course, the equation of motion for L also changes accordingly, and for a given value of B one again shoots numerically to find the solution with $L(\infty) = 0$, corresponding to the massless embedding.

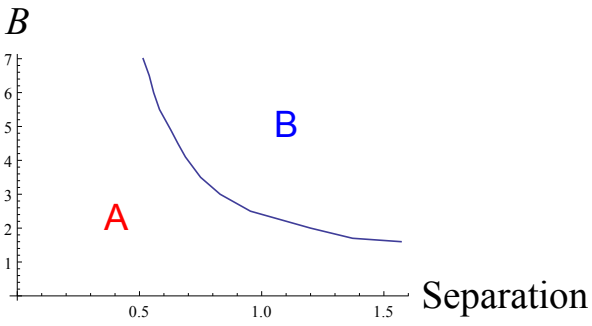

Figure 5.2.4: Phase diagram of bilayer D5-probes in AdS with one compact direction and an applied B field. Phase A is U-shaped configurations. In phase B the probes separate and take up configurations similar to Figure 5.2.1.

For both types of embedding the same regularisation as before holds, as the new factor introduces no new divergences. The energies of the solutions are increased as one increases the strength of the magnetic field but this does not happen at the same rate, and so a phase transition exists above a certain value of B. The phase diagram of the theory is shown in Figure 5.2.4 - at low B the U-shaped configurations are preferred (phase A in the figure) whilst at large B the separated brane configurations have lowest energy (phase B in the figure). The closer the probe branes, the larger the B-field needed to trigger the transition.

5.3 $\mathcal{N} = 4$ Super Yang-Mills in a Cavity

We would now like to describe the background $\mathcal{N} = 4$ SYM fields enclosed in a cavity, for example between two mirrors placed Δz apart. If the vacuum of the theory is locally determined then one would expect the description of the vacuum state to match that of the theory on a compact space since one can consider the space to simply repeat every Δz period - the soliton geometry of (5.2.2) thus seems the good candidate. Whether this is true or not depends on the boundary, where there can potentially be boundary terms associated with the "mirror".

5.3.1 AdS/BCFT

In [106] a proposal was given for constructing the holographic duals of boundary conformal field theories - the so-called *AdS/BCFT* duality. The idea is to extend the CFT d-dimensional boundary manifold M (itself with d-1-dimensional boundary ∂M) to a d+1-dimensional AAdS space N such that $\partial N = M \cup Q$, where Q is a d-dimensional submanifold of N such that $\partial Q = \partial M$ i.e. Q forms a new boundary in the interior of the bulk space[3]. One can add matter degrees of freedom localised to this boundary - the

[3]Note that Neumann boundary conditions (rather than Dirichlet) are imposed at the new boundary Q, since it should be dynamical from the holographic viewpoint and not fixed by CFT data.

simple case of a constant matter Lagrangian can be interpreted as a surface of constant tension $\mathcal{T}$, and the bulk plus boundary action becomes

$$\begin{aligned} I &= \frac{1}{16\pi G_N}\int_{\text{bulk}}\sqrt{-g}(R-2\Lambda) \\ &\quad +\frac{1}{8\pi G_N}\int_{\text{bound}}\sqrt{-h}(K-\mathcal{T}) \end{aligned} \tag{5.3.1}$$

where K_{ab} is the extrinsic curvature. The boundary condition

$$K_{ab} = (K-\mathcal{T})h_{ab} \tag{5.3.2}$$

results.

For the case of a strip of $\mathcal{N}=4$ SYM between two such boundaries, one starts with the AdS-soliton geometry, and the above boundary condition then gives the differential equation

$$z'(r) = \pm\frac{R\mathcal{T}}{r^2 h(r)\sqrt{4h(r)-R^2\mathcal{T}^2}} \tag{5.3.3}$$

where the sign depends on which side of the strip the boundary sits. The solutions of this equation represent the radial evolution of the position where the tension of the boundary matches the pressure of the interior gauge fields. The solutions are U-shaped dipping down to a distance r_* in the bulk - at the mid-point $4h(r_*) = R^2\mathcal{T}^2$. One can then integrate (5.3.3) from $r = r_*$ to ∞ and require that Δz matches that from the regularity condition of the geometry (5.2.2) found previously - this fixes the tension $\mathcal{T}$. We plot the solutions of (5.3.3) in Figure 5.2.1 and Figure 5.2.2 previously. They represent a cut-off on the space in this construction.

5.3.2 Adding Probe Branes and Mirror Images

We are now interested in including probe D5-branes in the space. The Euler-Lagrange equations describing the embeddings in the new space are identical to those in the compact space and we would hope the probes close off before hitting the new boundaries - in Figure 5.2.1 and Figure 5.2.2 we see that this is not the case however. It is possible that one needs to invoke new boundary conditions when the probes meet the cut-off to reflect the physics of the interaction between the fields on the probes and the barrier physics. Equally likely though is that the construction does not make complete sense - one is attempting to construct a theory with mirrors and a region of space with the vacuum of $\mathcal{N}=4$ SYM, but such a theory may well not exist because the matter needed to construct the mirror would need to be part of the vacuum in the strip.

We do not resolve these complex issues here - instead we will take the most naive prescription of simply using the soliton geometry as our description of the vacuum of the theory between two mirrors and place probe branes with their mirror images in that space, à la the method of images. The embedding solutions are then simply those we

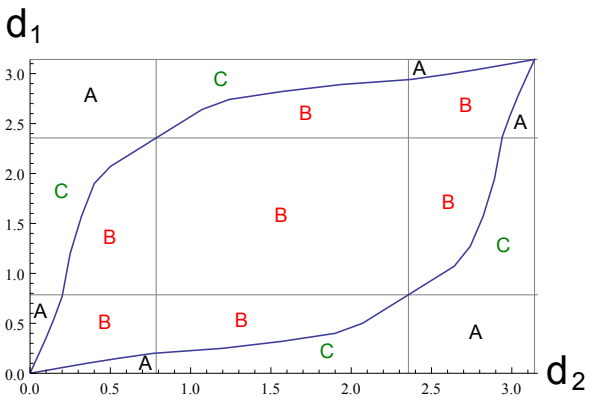

Figure 5.3.1: The phase diagram of the bilayer theory in an interval between two mirrors of separation π. d_1 and d_2 measure the distance from one mirror to the first and second defect respectively. We have marked the lines $d_{1/2} = \pi/4, 3\pi/4$ because these are the separations within which condensation with the mirror image are possible. In phase A both D5-branes are well separated and condense with their mirror images. In phase B the two D5-branes form a U-shaped configuration. In phase C the probe nearest the mirror displays exciton condensation with its mirror partner whilst the other probe takes up the lone configuration of Figure 5.2.1.

have already displayed for the compact space. We hope that this will reveal the qualitative new physics correctly.

Let us first take this approach for a single probe D5-brane between the mirrors. The immediate assumption is that the configuration is that shown in Figure 5.2.1 - there will be condensation of the fermions on the brane triggered by the conformal symmetry breaking scale Δz. However, there is an additional interesting possibility which is that there can be exciton style condensation with the mirror images of the probe. When the probe is at the mid-point between the mirrors it is a distance Δz from its reflections. There are no U-shaped configurations for probes separated by more than $\Delta z/2$ and so the single configuration of Figure 5.2.1 is correct. If the probe is moved within $\Delta z/4$ of the mirror however, then joined configurations exist with lower energy than the single configuration and exciton condensation with the mirror image will occur. In a sense this is a new form of mass gap formation for this system.

For two probe branes several configurations are possible depending on the separation of the branes from each other and from their mirror partners. Both branes can condense with their mirrors, one can condense with the mirror and one have condensation of only its own fields, or the two branes can display exciton condensation with each other. One works through all possibilities and computes the energetically preferred configuration - the phase diagram is shown in Figure 5.3.1.

5.4 Conclusions

In this chapter we have studied D5-probe embeddings in an AdS-soliton configuration. The geometry is dual to $\mathcal{N} = 4$ SYM with one spatial direction of the 3+1-dimensional space compact. We have also argued that it is dual to the vacuum of the theory of $\mathcal{N} = 4$ SYM confined to a compact region between two mirrors (although as we discussed this is ambiguous and essentially assumes the mirrors do not contribute to the form of the vacuum configuration of the $\mathcal{N} = 4$ fields except through the introduction of a length scale). The conformal symmetry breaking scale introduced through the finite distance in z in both cases generates fermion condensation and mass gap formation. For a compact space a single defect exhibits a fermion condensate on its surface. For a bilayer configuration the energetically preferred condensation is exciton condensation between the fermions on the two sheets. If one includes mirror images of the probes in the case of the interval then an extra phase appears in which a single fermion, when close enough to the mirror, displays exciton condensation with its mirror image. The bilayer phase structure, displayed in Figure 5.3.1, is then considerably complicated.

The hope is that graphene sheets could be engineered into a strongly-coupled phase by placing them in a cavity. The qualitative expectations from our results are that a mass gap will form in this regime. Further predictions would then be that there would be a first order phase transition to condensation with the mirror partner if the single sheet were brought close to the mirror. For bilayer configurations we also showed that an applied magnetic field can cause a first order transition from an exciton condensation phase to a phase with separate condensation on each sheet. Potentially these sorts of features could be looked for experimentally.

5.A Circumference of AdS-Soliton

We review here how the circumference of the AdS-soliton is determined for any number of spatial dimensions d. The metric is given by

$$ds^2 = \frac{R^2}{r^2}\left(1-\left(\frac{r_0}{r}\right)^d\right)^{-1}dr^2 + \frac{r^2}{R^2}\left(1-\left(\frac{r_0}{r}\right)^d\right)dz^2 + r^2 dx^2_{0..d-2}. \tag{5.A.1}$$

We will from now on exclude the part of the metric corresponding to the $x_{0..d-2}$ coordinates. We have

$$ds^2_{r-z} = \frac{1}{r^2}\left[\left(1-\left(\frac{r_0}{r}\right)^d\right)^{-1}dr^2 + r^4\left(1-\left(\frac{r_0}{r}\right)^d\right)dz^2\right]. \tag{5.A.2}$$

We look at the metric near the horizon by writing $r = r_0 + \bar{r}$ for small $\bar{r}$. The horizon factor $h(r)$ can then be written

$$1 - \left(\frac{r_0}{r}\right)^d = \frac{(r_0+\bar{r})^d - r_0^d}{(r_0+\bar{r})^d} = \frac{\bar{r}d}{r_0} + \mathcal{O}(\bar{r}^2). \tag{5.A.3}$$

The trick involves performing a coordinate transformation that brings the $r - z$ metric into the canonical form for a two-plane i.e we would like to identify the metric in the form $(d\sigma^2 + \sigma^2 d\alpha^2)/r^2$ where $r = r(\sigma)$ is some function of σ which will not affect regularity and so is not important in the following. We write

$$\left(1 - \left(\frac{r_0}{r}\right)^d\right)^{-1} dr^2 = \frac{r_0}{\bar{r}d} dr^2 \equiv \sigma^2 \tag{5.A.4}$$

and noting trivially that $dr = d\bar{r}$ (since $r = r_0 + \bar{r}$) we thus have

$$\frac{d\sigma}{dr} = \frac{d\sigma}{d\bar{r}} = \left(\frac{r_0}{d}\right)^{1/2} \frac{1}{\bar{r}^{1/2}} \quad \rightarrow \quad \sigma = \left(\frac{r_0}{d}\right)^{1/2} 2\bar{r}^{1/2}. \tag{5.A.5}$$

The desired coordinate transformation is then

$$\bar{r} = \frac{\sigma^2 d}{4r_0}. \tag{5.A.6}$$

The near-horizon metric becomes (where we are now ignoring the overall factor of $1/r(\sigma)^2$)

$$ds^2 = d\sigma^2 + (r_0+\bar{r})^4 \frac{\bar{r}d}{r_0} dz^2 \simeq d\sigma^2 + r_0^4 \frac{\bar{r}d}{r_0} dz^2 \tag{5.A.7}$$

and using the coordinate transformation we thus find

$$ds^2 = d\sigma^2 + \sigma^2 \frac{d^2 r_0^2}{4} dz^2. \tag{5.A.8}$$

This indeed takes the form $d\sigma^2 + \sigma^2 d\alpha^2$ where $\alpha \equiv z r_0 d/2$. By regularity α must have period 2π and thus z must have period $4\pi/r_0 d$.

CHAPTER 6

Soft Walls in Dynamic AdS/QCD and the Techni-Dilaton

The material in the present chapter is based largely on [3].

6.1 Introduction

The AdS/CFT correspondence combined with the introduction of flavour branes provides a quantitative method for computation of the physics of quarks in (at least some) strongly-coupled gauge theories, as introduced in Chapter 4. For example, the light meson spectrum of the $\mathcal{N} = 2$ theory with a small number of quark multiplets in the background of $\mathcal{N} = 4$ super Yang-Mills is known [54]. It has been natural to attempt to move these techniques towards more QCD-like theories, but a more phenomenological bottom-up methodology has been the only way to directly proceed to QCD thus far. AdS/QCD (see Section 4.2.2) is the broadest brush-stroke example, being the maximally simplified model in the spirit of a D7-probe action embedded in $AdS_5 \times S^5$. It was recognised early on however that the model suffers from radially excited states whose masses grow as n (the excitation number) [108,109] and, if minimally extended to include higher spin states, masses that grow as s (the spin). In QCD, meson Regge trajectories typically show $\sqrt{n}$ and $\sqrt{s}$ behaviour and indeed this was the original motivation for string theory in the 1960s. In AdS/CFT the strong coupling limit leaves a classical supergravity theory for the lightest states without strings in the AdS space, to match the expectation that quarks are joined by extended gluonic flux tubes in QCD.

In [110] it was pointed out that modifications of the IR AdS geometry or the IR behaviour of the dilaton in AdS could be used to achieve the expected Regge form for the masses. This clever trick undoes the argument that a gravity dual cannot describe this aspect of

the QCD spectrum. However, the trick is not completely convincing since the mesonic spectrum is determined by modifications of the theory in the deep IR well below the constituent quark mass and confinement scale, which appears to be a peculiar violation of decoupling. Nevertheless, such IR modifications have been incorporated into models such as [111–116] that provide a remarkably good description of QCD (see also for example the recent work [117]).

In this chapter we will present an analysis in which we introduce soft-wall behaviour in the Dynamic AdS/QCD model [82–85]. The model is a slightly more sophisticated version of AdS/QCD, retaining a few more features of probe brane embeddings in rigorous string theory settings. In particular, it allows one to smoothly move (in a phenomenological rather than a rigorous manner) from the $\mathcal{N} = 2$ theory to more QCD-like behaviour. It also provides an interpretation of the chiral symmetry breaking condensation as the dynamical generation of a IR quark mass. We will see in Section 6.3 that to introduce a soft wall and obtain a Regge meson spectrum requires a rather peculiar profile for the dynamical mass (one certainly not seen in top-down models) in order to allow physics in the deep IR to enter the meson physics - in particular, the dynamical quark mass must vanish in the deep IR. This analysis provides some support for those who claim that there is an inherent tension in the use of non-stringy descriptions of QCD states.

Recent work [82–85, 113–116, 118] has considered extending AdS/QCD models beyond just QCD to theories with arbitrary N_f and N_c, including theories speculated to run to IR fixed points and to behave as walking theories [119]. These models hopefully provide guidance to lattice practitioners who are attempting to simulate such theories [120–130] and one hopes that broad trends in the behaviours of meson masses as one enters this regime will be correctly displayed. The key extra ingredient beyond the simplest AdS/QCD models is to allow the mass squared of the scalar which describes the quark condensate (and encodes its dimension via $M^2 = \Delta(\Delta - 4)$) to run with RG scale. Chiral symmetry breaking occurs at the scale where the BF bound (c.f. (3.2.5)) is violated - $M^2 = -4$ in AdS_5 corresponding to $\Delta = 2$, or an anomalous dimension for $\bar{q}q$ of $\gamma = 1$.

An interesting debate about walking theories is whether the pseudo-conformal regime generates a bound state in the spectrum that is anomalously light since it is a Goldstone mode for conformal symmetry breaking. Interestingly, in Dynamic AdS/QCD the spin zero σ or f_0 meson was observed to become light [82–85] (the models of [131, 132] also describe a light dilaton holographically). On the other hand, in the model of [113–116] its mass did not fall relative to other states in this regime. Here we wish to suggest that the key difference between these models is that the latter incorporates a soft wall IR (the IR behaviour of their tachyon field is also crucial to this dynamics) whilst the former do not. To test this we show in Section 6.4 that if soft wall behaviour is introduced into the Dynamic AdS/QCD model (however artificially) then the shift to the IR behaviour of the quark mass introduces rather strong conformal symmetry breaking and the resulting σ

becomes heavy. This at least makes it clear that the behaviour of this state is sensitive to how the mesonic physics decouples at strong coupling at scales beneath the scale of the dynamically generated quark mass.

6.2 Hard & Soft Wall AdS/QCD

We begin by reviewing briefly the hard [80, 81] and soft wall [110] AdS/QCD models as the construction within Dynamic AdS/QCD later will be analogous. We assume the $s = 1$ rho meson is created by the operator $\bar{q}\gamma^{\mu}q$. Higher Regge states of greater spin are associated with operators containing terms like $\bar{q}\gamma^{\{\mu}\partial^{\nu}\dots\partial^{\lambda\}}q$ with $s-1$ derivatives inserted - these operators have dimension $2+s$. Holographically each of these operators will be associated with a symmetric s-index field $A^{\mu\cdots}$ in the dual geometry.

6.2.1 Hard Wall

In the hard wall model the dilaton Φ is a constant and one uses the AdS_5 metric

$$ds^2 = r^2 dx_4^2 + \frac{1}{r^2}dr^2. \tag{6.2.1}$$

r has the usual interpretation as an energy scale and is subject to a sharp cut-off at some r_0. The quadratic action is then schematically

$$S \sim \int d^4x dr \ \sqrt{-g}e^{-\Phi}r^{(4s-4)}(\partial^{\mu}A^{\nu\lambda\cdots})^2. \tag{6.2.2}$$

Note that, as discussed in [110], it can be argued that no further terms (such as those one would expect from covariant derivatives) contribute to the action due to the residual gauge freedom that remains in axial gauge, $A_{r\cdots} = 0$, for the case of higher spins in AdS[1]. The factors of r present are for the same reason, and as a result the fields $A^{\mu\cdots}$ have dimension $2-s$.

To find the bound state masses we consider linearized solutions of the form $V(r)\epsilon^{\mu\cdots}e^{-ik.x}$, with the polarisation tensor taking indices in the QFT directions only, and arrive at the equation of motion

$$\partial_r\left[r^{1+2s}\partial_r V\right] + r^{2s-3}M_n^2 V = 0 \tag{6.2.3}$$

where $k^2 = -M_n^2$. The large r solutions take the form

$$V = c + \frac{c'}{r^{2s}}. \tag{6.2.4}$$

Since V has dimension $2-s$, the constant c' has dimension $2+s$ which is appropriate to describe the operators under discussion, and c has dimension $2-s$ as is appropriate

[1]It should be noted that writing down an action for higher spin fields is inherently very complicated and runs into many issues, such as the need for auxiliary fields - here we have simply written the most naive possibility.

for the source.

To provide intuition into the solutions we wish to remove the first derivative terms and move to a Schrödinger equation form by setting $z = 1/r$ and $V = z^{s-1/2}\psi$ giving

$$-\psi'' + U(z)\psi = M_n^2\psi, \qquad U(z) = \frac{(s^2 - 1/4)}{z^2}. \tag{6.2.5}$$

At small $z \to 0$ (i.e. the UV) the potential grows rapidly, and in the IR the hard wall presents another barrier - this is thus asymptotically a square well and the eigenstates behaviour is known, $M_n^2 \sim n^2$. Furthermore, since the well is proportional in magnitude to s^2, it also follows that $M_s^2 \sim s^2$. Hard wall AdS/QCD is thus at odds with expectations from QCD and experiment.

6.2.2 Soft Wall

In soft wall models the IR metric and/or dilaton are allowed to take different forms to replace the hard wall cut-off. If we consider an IR metric

$$ds^2 = e^{2A(z)}(dx_4^2 + dz^2) \tag{6.2.6}$$

then e^A now carries energy dimension (as the coordinate r did before) and the actions for our fields are

$$S \sim \int d^4x dr \ \sqrt{-g} e^{-\Phi} e^{(4s-4)A} (\partial^\mu A^{\nu\lambda\ldots})^2 \tag{6.2.7}$$

analogously to before. The equation of motion becomes

$$\partial_z \left[e^{(2s-1)A-\Phi} \partial_z V \right] + e^{(2s-1)A-\Phi} M_n^2 V = 0. \tag{6.2.8}$$

The choices $\Phi =$ constant, $A = -z^2$ and the redefinition of fields $V = e^{(s-1/2)z^2}\psi$ gives the Schrödinger form

$$-\psi'' + U(z)\psi = M_n^2\psi, \qquad U(z) = (4s^2 + 1)z^2 \tag{6.2.9}$$

Here the potential is that of a simple harmonic oscillator and the solutions are known to scale as $M_n^2 \sim n$, as required for Regge behaviour. However, the s dependence in the potential means that the behaviour with s is not the desired $M_s^2 \sim s$.

Alternatively, one can return to (6.2.7) leaving the metric untouched and generate the soft wall through a dilaton profile $\Phi \sim 1/r^2 \sim z^2$. The equation of motion is then that in (6.2.8) with $A = -\log z$ i.e. the metric is just AdS. On setting $V = e^{(\Phi-(2s-1)A)/2}\psi$ we find

$$-\psi'' + U(z)\psi = M_n^2\psi, \quad U(z) = z^2 + 2(s-1) + \frac{s^2 - 1/4}{z^2} \tag{6.2.10}$$

which has eigenvalues

$$M_{n,s}^2 = 4(n+s). \tag{6.2.11}$$

This is the preferred scenario in [110].

Our initial goal is to realize these soft wall scenarios in the Dynamic AdS/QCD model.

6.3 Dynamic AdS/QCD

Dynamic AdS/QCD was introduced in detail in [82, 83] and is a variant of AdS/QCD (c.f. Section 4.2.2) with some additional features taken from top-down D7-probe models (c.f. Section 4.1.1). In particular, the soft wall in the model is dynamically determined and corresponds to the presence of a quark condensate.

The five dimensional action of our effective holographic theory is

$$S = \int d^4x\, d\rho\, e^{-\Phi} \mathrm{Tr}\, \rho^3 \left[\frac{1}{\rho^2 + |X|^2} |DX|^2 + \frac{\Delta m^2}{\rho^2} |X|^2 + \frac{1}{2} F_V^2 \right]. \tag{6.3.1}$$

The field X describes the quark condensate degree of freedom, with fluctuations in $|X|$ around its vacuum configuration describing the scalar meson. The π fields are the phase of X,

$$X = L(\rho)\, e^{2i\pi^a T^a}. \tag{6.3.2}$$

F_V are vector fields that will describe the vector mesons.

We work with the five dimensional metric

$$ds^2 = \frac{d\rho^2}{(\rho^2 + |X|^2)} + (\rho^2 + |X|^2) dx^2, \tag{6.3.3}$$

which will be used for contractions of the space-time indices. ρ is the holographic coordinate (with $\rho = 0$ the IR, and $\rho \to \infty$ the UV) and $|X| = L$ enters into the effective radial coordinate in the space, i.e. there is an effective $r^2 = \rho^2 + |X|^2$. This is how the quark condensate generates a soft IR wall for the linearized fluctuations that describe the mesonic states - when $|X|$ is nonzero the theory will exclude the deep IR at $r = 0$.

The vacuum structure of the theory can be determined by setting all fields except $|X| = L$ to zero. We assume that L will have no dependence on the x coordinates. The action for L is then given by

$$S = \int d^4x\, d\rho\, \rho^3 \left[(\partial_\rho L)^2 + \Delta m^2 \frac{L^2}{\rho^2} \right]. \tag{6.3.4}$$

If $\Delta m^2 = 0$ then the scalar L describes a dimension 3 operator and dimension 1 source as is required for it to represent $\bar{q}q$ and the quark mass m - that is, in the UV the solution for the L equation of motion is $L = m + \bar{q}q/\rho^2$. This case is in fact the $\mathcal{N} = 2$ SYM theory

of [54] and Dynamic AdS/QCD generates the known spectrum for the rho meson. A non-zero Δm^2 allows us to introduce an anomalous dimension for the quark bilinear operator. If the mass squared of the scalar violates the BF bound of $M^2 = -4$ ($\Delta m^2 = -1$, $\gamma = 1$) then the scalar field L becomes unstable and the theory enters a chiral symmetry breaking phase. A controlled example is that of introducing a magnetic field into the $\mathcal{N} = 2$ SYM theory [102] by an effective dilaton factor,

$$e^{-\Phi} = \sqrt{1 + \frac{B^2}{(\rho^2 + L^2)^2}}. \tag{6.3.5}$$

One could alternatively expand this to quadratic order in L and treat the quadratic term as a ρ-dependent Δm^2 term. The induced $L(\rho)$ function is schematically of the form $L \sim 1/(1 + \rho^2)$ for $B \sim 1$. This function can be thought of as the RG flow of the quark mass from a current quark mass of zero in the UV to a non-zero constituent quark IR value.

Our immediate goal here is not to fix Δm^2 and derive $L(\rho)$, but instead to investigate the form of $L(\rho)$ and $\Phi(\rho)$ which will give soft wall behaviour for the rho meson and its Regge tower of bound states.

6.3.1 The ρ Regge Trajectory

We again assume that the $s = 1$ rho meson is created by the operator $\bar{q}\gamma^\mu q$, with the higher Regge states of greater spin associated with operators which contain terms like $\bar{q}\gamma^{\{\mu}\partial^\nu \dots \partial^{\lambda\}}q$ with $s - 1$ derivatives inserted.

Holographically each of these operators will be associated with a symmetric s-index field in the geometry with quadratic action

$$S \sim \int d^4x\, d\rho\ \frac{\rho^{1+2s} e^{-\Phi}}{(\rho^2 + L^2)^{1-s}} (\partial^\mu A^{\nu\lambda\dots})^2 \tag{6.3.6}$$

in analogy to before. Note that there is some ambiguity here about what factors of ρ or factors of $\sqrt{\rho^2 + L^2}$ occur (they are fixed by top-down models [54] only for the rho meson) but for the generic conclusions we reach below this will not be important. Here they can be understood as being determined by requiring the corresponding operators to have the appropriate dimensions.

We seek linearized solutions of the form $V(r)\epsilon^{\nu\lambda\dots}e^{-ik.x}$ with $k^2 = -M_n^2$ and arrive at the equation of motion

$$\partial_\rho \left[\rho^{1+2s} e^{-\Phi} \partial_\rho V\right] + \frac{\rho^{1+2s} e^{-\Phi}}{(\rho^2 + L^2)^2} M_n^2 V = 0. \tag{6.3.7}$$

The large ρ solutions (assuming $e^{-\Phi}$ becomes constant) again take the form $V = c + c'/\rho^{2s}$.

We now seek to place the equation into Schrödinger form so that we can easily understand the potential that generates the masses of the tower of radially excited states. We first change coordinates so the $\partial^2 V$ term and the $M_n^2 V$ terms have the same coefficient,

$$\partial_\rho = \frac{1}{\rho^2 + L^2}\partial_z, \tag{6.3.8}$$

giving

$$\frac{\rho^{1+2s}}{(\rho^2+L^2)^2}\partial_z^2 V + \left(\partial_\rho\left[\frac{\rho^{1+2s}}{\rho^2+L^2}\right] - \frac{\rho^{1+2s}}{\rho^2+L^2}\partial_\rho\Phi\right)\partial_z V + \frac{\rho^{1+2s}}{(\rho^2+L^2)^2}M_n^2 V = 0 \tag{6.3.9}$$

where $\rho = \rho(z)$ is implicit. To remove the first derivative terms in (6.3.9), we rescale $\psi = aV$. The coefficient of the ψ' term (where $'$ denotes ∂_z) is

$$\frac{\rho^{1+2s}}{(\rho^2+L^2)^2}2a' + \left(\partial_\rho\left[\frac{\rho^{1+2s}}{\rho^2+L^2}\right] - \frac{\rho^{1+2s}}{\rho^2+L^2}\partial_\rho\Phi\right)a. \tag{6.3.10}$$

Setting this to zero we thus require

$$\frac{1}{a}\partial_\rho a = -\frac{1+2s}{2\rho} + \frac{1}{2}\partial_\rho\Phi + \frac{\rho}{\rho^2+L^2} + \frac{\partial_\rho L^2}{2(\rho^2+L^2)} \tag{6.3.11}$$

where recall that $a' = (\rho^2+L^2)\partial_\rho a$. From this one easily derives

$$\begin{aligned}\tfrac{1}{a}\partial_\rho^2 a &= \tfrac{1+2s}{2\rho^2} + \tfrac{1}{2}\partial_\rho^2\Phi + \tfrac{1}{\rho^2+L^2} + \tfrac{\partial_\rho^2 L^2}{2(\rho^2+L^2)} \\ &\quad - \tfrac{(\partial_\rho L^2)(2\rho+\partial_\rho L^2)}{2(\rho^2+L^2)^2} - \tfrac{\rho(2\rho+\partial_\rho L^2)}{(\rho^2+L^2)^2} + \left(\tfrac{1}{a}\partial_\rho a\right)^2\end{aligned} \tag{6.3.12}$$

which is needed in the potential below.

The equation of motion is now of Schrödinger form,

$$-\psi'' + U\psi = M_n^2\psi, \tag{6.3.13}$$

with the potential

$$\begin{aligned}U &= -\tfrac{(\rho^2+L^2)^2}{a\rho^{1+2s}e^{-\Phi}}\partial_\rho\left[\rho^{1+2s}e^{-\Phi}\partial_\rho a\right] \\ &= -(\rho^2+L^2)^2\left[\tfrac{(1+2s)}{\rho}\left(\tfrac{1}{a}\partial_\rho a\right) - \partial_\rho\Phi\left(\tfrac{1}{a}\partial_\rho a\right) + \tfrac{1}{a}\partial_\rho^2 a\right].\end{aligned} \tag{6.3.14}$$

This expression is still in the ρ coordinates, and needs to be rewritten in z using the result of the coordinate transformation in (6.3.8) for the given function $L(\rho)$ in each of the examples in the following.

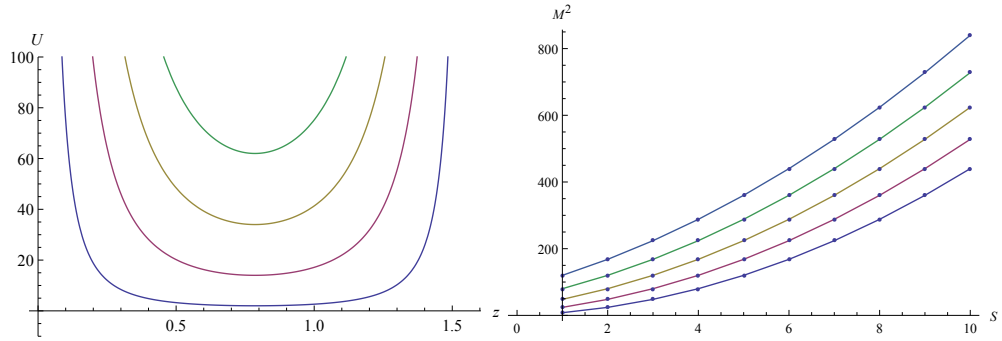

Figure 6.3.1: The Schrödinger wells for the $\mathcal{N}$=2 model for $s = 1, 2, 3, 4$ which give a spectrum $M^2 = 4(n+s)(n+s+1)$, and a plot of the mass trajectories vs spin, s, for the excitation numbers $n = 1, 2, 3, 4, 5$.

6.3.2 Examples

In this section we will look at the spectrum of the rho meson and its Regge partners which emerge from a variety of choices of the function $L(\rho)$ in Dynamic AdS/QCD. We begin with the controlled case of the $\mathcal{N} = 2$ SYM theory and move away phenomenologically towards more QCD-like spectra.

$\mathcal{N} = 2$ SQCD

The model includes the D3/probe D7 model which describes an $\mathcal{N} = 2$ gauge theory [54]. In this case L is a constant (which, up to a constant, is the quark mass and the only scale of the theory), and Φ is also constant. The change of variables in (6.3.8) gives for $m = 1$

$$\partial_\rho = \frac{1}{\rho^2+1}\partial_z, \qquad z = \arctan[\rho]. \tag{6.3.15}$$

The key point here is that $0 < \rho < \infty$ maps to $0 < z < \pi/2$. Since z is of restricted range, a square well-like potential asymptotically is unavoidable. This is directly related to the fact that in a D7-probe model the rho meson physics lives on the D7 world-volume and does not access scales below the quark mass (here $r < 1$). In the field theory the constituent quark mass provides a cut-off in RG scale and the meson masses are determined only in the theory above that cut-off.

In Figure 6.3.1 we show the Schrödinger wells generated for different s. The meson spectra in these potentials can be found from solving (6.3.13) - we shoot from $z = 0$ and require the field and its derivative to vanish at the endpoints of the well. The known analytic spectrum $M^2_{n,s} = 4(n+s)(n+s+1)$ results - some sample masses are also plotted in Figure 6.3.1 showing $M^2_{n,s}$ grows as $n^2,\ s^2$.

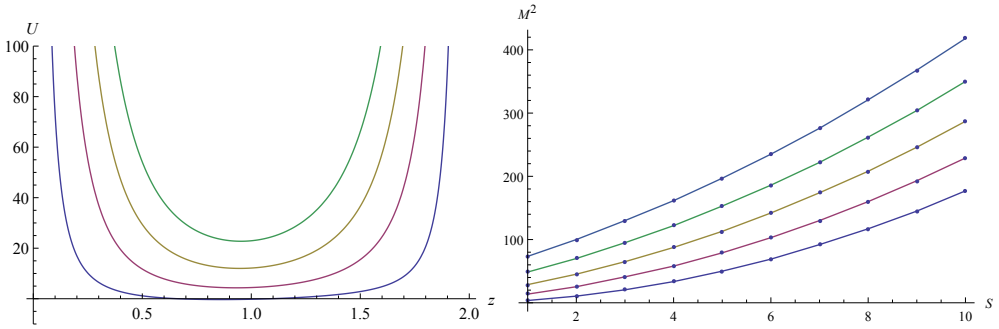

Figure 6.3.2: The Schrödinger wells for the Dynamically Generated Mass model for $s = 1, 2, 3, 4$ and a plot of the mass trajectories vs spin, s, for the excitation numbers $n = 1, 2, 3, 4, 5$.

A Model of a Dynamically Generated Mass

In models with a dynamically generated mass (e.g. [102, 107]) a typical profile for the embedding L is

$$L = \frac{1}{1+\rho^2} \tag{6.3.16}$$

which falls off as $1/\rho^2$ at large ρ but deviates from passing through $r^2 = \rho^2 + L^2 = 0$ yet has $\partial_\rho L(0) = 0$. Such models are very similar to the $\mathcal{N} = 2$ case though in that at large ρ the L dependence in (6.3.8) is negligible, whilst at small ρ we have $L \simeq$ constant. Again we take Φ to be a constant. Solving (6.3.8) numerically one again finds that the z coordinate is bounded in extent and the Schrödinger well must be square asymptotically. In Figure 6.3.2 we plot the Schrödinger well and masses for this case - $M^2_{n,s}$ again grows as n^2 and s^2.

Of course this is only a toy example since the running of dilaton-like factors that might induce this shape in L are not included. However, it is important to stress that the change of variables to z is independent of the dilaton - it is this change of variables that leads to a truncated range in z and hence a square well and n^2-like spectrum. No choice of dilaton in the bulk or on the brane could change that result.

Engineering with L

We can now try to engineer a behaviour for the meson masses that goes as $\sqrt{n}$ or $\sqrt{s}$. Let's first ask what choice of $L(\rho)$, which sets the form of the soft wall, would achieve this. We need in the IR ($\rho \to 0$) for L to dominate in the factor $(\rho^2 + L^2)$ in (6.3.8) - if $L \sim \rho^p$ then we need $0 < p < 1$. Note that in this case the IR corresponds to $z \to \infty$ (in the previous two cases it corresponded to $z \to 0$). For $p < 1/2$ the z coordinate resulting from (6.3.8) is bounded by a maximum value and the asymptotics must look like a square well. For $p > 1/2$ the IR potential well falls to zero and the spectrum is not discrete. More interesting behaviours can be found in the region fine tuned close to $p = 1/2$

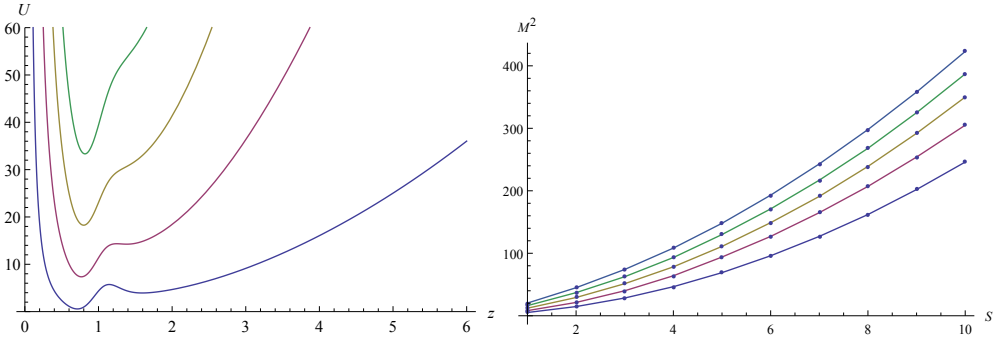

Figure 6.3.3: The Schrödinger wells for the soft wall model with L given by (6.3.22) for $s = 1, 2, 3, 4$ and a plot of the mass trajectories vs spin, s, for the excitation numbers $n = 1, 2, 3, 4, 5$.

We can, for example, engineer the soft wall potential of [110] for the rho mesons. We set Φ to a constant and look at $s = 1$. The equation of motion (6.3.7) becomes

$$\partial_\rho \left[\rho^3 \partial_\rho V\right] + \frac{\rho^3}{(\rho^2 + L^2)^2} M_n^2 V = 0. \tag{6.3.17}$$

We enforce the change of variables

$$e^{-z^2} \partial_z = -\rho^3 \partial_\rho \tag{6.3.18}$$

which in the IR (i.e. small ρ, large z) implies

$$\rho^2 = z e^{-z^2}. \tag{6.3.19}$$

In the IR limit (where L dominates in $\rho^2 + L^2$) the equation of motion (6.3.17) thus becomes

$$\partial_z (e^{-z^2} \partial_z V) + \frac{\rho^6 e^{z^2}}{L^4} M_n^2 V = 0. \tag{6.3.20}$$

Thus if we pick

$$\frac{\rho^6 e^{z^2}}{L^4} = e^{-z^2}, \qquad i.e. \quad L^2 = z\rho \tag{6.3.21}$$

in the IR, we achieve the soft wall model of (6.2.8) at $s = 1$. Note that, up to a log factor, we indeed sit on the $p = 1/2$ boundary.

As an example complete model of this type we can choose

$$L = \frac{z^{1/2} \rho^{1/2}}{\sqrt{1 + z\rho^5}}. \tag{6.3.22}$$

This falls off asymptotically in the UV as $1/\rho^2$ but matches the IR behaviour needed. We display the Schrödinger well and Regge trajectories in Figure 6.3.3. The potential has

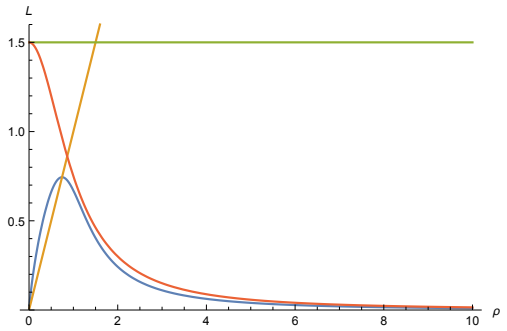

Figure 6.3.4: The function $L(\rho)$ which reproduces the soft wall behaviour of [110] with a constant dilaton. Also shown are examples of the profiles for the $\mathcal{N} = 2$ theory ($L =$ constant) and for the dynamically generated mass example ($L = 1/(1+\rho^2)$). The line $L = \rho$ is also plotted to show where the on mass-shell condition is satisfied.

a harmonic oscillator form at large z which leads to the linear Regge behaviour in n. However, it is not yet clear that this is a success. To investigate, we first plot the function $L(\rho)$ - see Figure 6.3.4. Physically, $L(\rho)$ in the top-down models is a plot of the quark mass against RG scale. Here this function is very peculiar, at least in the context of top-down models - the quark mass grows until the on mass-shell scale but then below that scale falls to zero in the deep IR. In particular, in this construct the rho meson physics is determined by radial distances (RG scales) all the way down to zero. This is in sharp contrast to top-down models where the rho physics is immune to scales below the IR quark mass. The construct of a soft wall thus requires non-decoupling of quarks in the IR of a strongly coupled gauge theory - of course this generic point is true in any soft wall model. Many authors have expressed the view that soft walls are not the way to produce linear Regge behaviour (and that one should instead use true stringy behaviour), and the interpretation in Dynamical AdS/QCD most likely supports this view.

Functionally there is a second problem with this model. By manipulating L we have effectively realized linear trajectories in an equivalent way to the use of "e^A" in [110]. As there, the trajectories for higher s states do not have the same slope as $s = 1$ - see Figure 6.3.4. In the next example we will provide a model that mixes a dilaton flow and L profile, and achieves the best case of [110].

Engineered Dilaton and L

As we saw in the second example above, one cannot use a bulk dilaton to engineer an IR soft wall model with any finite value for $L(0)$, because the quark physics will not see the deep IR behaviour of that dilaton. An example solution to this problem is to take $L \sim \rho$ in the IR, so that the induced metric on the embedding is just AdS, and take a dilaton $\Phi = z^2$. We set as an example

$$L = \frac{\rho}{1+\rho^3}, \qquad \Phi = z^2. \tag{6.3.23}$$

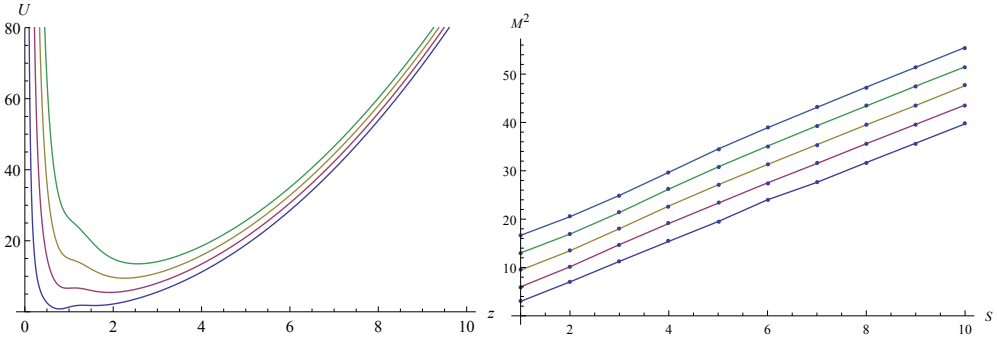

Figure 6.3.5: The Schrödinger wells for the soft wall model with L given by (6.3.23) for $s = 1, 2, 3, 4$ and a plot of the mass trajectories vs spin, s, for the excitation numbers $n = 1, 2, 3, 4, 5$.

We plot the Schrödinger wells and mass trajectories in Figure 6.3.5 where the linearity in n and s is clear.

The complaint that the rho physics is determined by RG scales below the IR quark mass still remains in this model however. Note that we have not attempted to find profiles for Δm^2 which would dynamically generate these profiles for L - they would clearly need to be quite peculiar relative to the standard expectation from the perturbation theory running.

6.4 Techni-Dilaton

In this final section we turn our attention to the impact of soft wall dynamics on the so called techni-dilaton state in walking gauge theories. There is considerable interest in the behaviour of QCD-like $SU(N_c)$ gauge theories with varying number of flavours N_f [133–144]. For $N_f < 11N_c/2$ the theories become asymptotically free. There is believed to be a region of N_f below this value where the theory runs to an IR fixed point at which the coupling grows in strength as N_f decreases. At some critical value, roughly estimated as $N_f \simeq 4N_c$, the coupling at the fixed point becomes strong enough to trigger chiral symmetry breaking, and IR conformality is lost. The transition is triggered when the anomalous dimension of $\bar{q}q$ becomes $\gamma \simeq 1$ [113, 118, 145] and is of a BKT or Miransky scaling type [146, 147]. Just below the critical value of N_f for chiral symmetry breaking, the theories are supposed to display walking behaviour. The coupling runs to an IR theory with $\gamma \simeq 1$ from below. For theories close to the critical coupling the running in the IR theory is very slow and the scale where chiral symmetry breaking occurs is in a theory that is very close to conformal [119]. A number of authors have predicted that a light dilaton-like state (relative to the rest of the spectrum) will emerge in these theories [148–153].

Several groups have recently developed holographic models of walking theories and the conformal window [82–85, 113–116, 118]. These theories do not predict the dynam-

ics of the running of the couplings or anomalous dimensions but include them either directly or through chosen potentials for supergravity fields. They do however predict the meson spectrum as a function of N_f and N_c after those assumptions have been included. Interestingly, Dynamic AdS/QCD was used to show the presence of a light $\bar{q}q$ scalar state [83], but the model of [113] does not see such a state. Here we wish to argue that it is the incorporation of soft wall dynamics in [113] that explains this difference. In particular, as we have seen in the sections above, to achieve $M_n^2 \sim n$ Regge trajectories in AdS/QCD models it is necessary to allow the meson physics to be determined by the deep IR regime below the chiral symmetry breaking scale. In [113] this is achieved by the tachyon field that describes the $\bar{q}q$ condensate diverging in the IR only at the scale $r = 0$. In Dynamic AdS/QCD the probe-brane-like action terminates at the on mass-shell condition for the quarks. The running in the gauge theory is near conformal down to that on mass-shell condition scale, but below where the quarks decouple from the running of the gauge coupling the Yang-Mills like running of the glue theory is very non-conformal. We believe that whether a light mesonic state is seen or not depends on whether its dynamics is sensitive to the conformal symmetry breaking deep IR or not. To demonstrate this logic we simply study the mass of the scalar $\bar{q}q$ state in Dynamic AdS/QCD with and without soft wall behaviour. When we decouple the mesonic action at the quark mass scale the state is light, but if we allow it to see the non-conformal IR running then the state becomes heavy with mass of order the chiral symmetry breaking scale. This at least highlights the role of quark decoupling in these holographic descriptions. Top-down probe brane models appear to us to support the idea that mesonic physics should be blind to the deep IR below the quark mass, but this would invalidate the soft wall mechanism.

6.4.1 Walking Dynamics in Dynamic AdS/QCD

The gauge dynamics is input into Dynamic AdS/QCD through the running of γ, the anomalous dimension of $\bar{q}q$. In the holographic description γ enters through the term Δm^2 in (6.3.1).

We will fix the form of Δm^2 using the two loop running of the gauge coupling in QCD with N_f flavours transforming under a representation R. This of course is a naive extrapolation of perturbative results beyond their regime of validity, but is widely used to motivate the presence of a conformal window and walking. The running takes the form

$$\mu \frac{d\alpha}{d\mu} = -b_0 \alpha^2 - b_1 \alpha^3, \tag{6.4.1}$$

where

$$b_0 = \frac{1}{6\pi}(11 N_c - 2 N_f), \tag{6.4.2}$$

and

$$b_1 = \frac{1}{24\pi^2}\left(34N_c^2 - 10N_cN_f - 3\frac{N_c^2-1}{N_c}N_f\right). \tag{6.4.3}$$

Asymptotic freedom is present provided $N_f < 11N_c/2$. There is an IR fixed point with value

$$\alpha_* = -b_0/b_1\,, \tag{6.4.4}$$

which rises to infinity at $N_f \sim 2.6N_c$.

The one loop result for the anomalous dimension of the quark mass is

$$\gamma_1 = \frac{3C_2}{2\pi}\alpha, \qquad C_2 = \frac{(N_c^2-1)}{2N_c}\,. \tag{6.4.5}$$

Thus, using the fixed point value α_*, the condition $\gamma = 1$ occurs at $N_f^c \sim 4N_c$ (precisely $N_f^c = N_c(100N_c^2 - 66)/(25N_c^2 - 15)$).

We will identify the RG scale μ with the AdS radial parameter $r = \sqrt{\rho^2 + L^2}$ in our model. Note it is important that L enters here - if it did not (and the scalar mass was only a function of ρ) then, were the mass to violate the BF bound at some ρ, it would leave the theory unstable no matter how large L grew. Including L means that the creation of a non-zero but finite L can remove the BF bound violation, leading to a stable solution.

Working perturbatively from the AdS result $m^2 = \Delta(\Delta - 4)$ we have

$$\Delta m^2 = -2\gamma_1 = -\frac{3(N_c^2-1)}{2N_c\pi}\alpha\,. \tag{6.4.6}$$

This will then fix the r dependence of the scalar mass through Δm^2 as a function of N_c and N_f.

The vacuum structure for a given choice of representation, N_f and N_c, must be identified first. The Euler-Lagrange equation for the vacuum embedding L_v is given at fixed Δm^2 by the solution of

$$\frac{\partial}{\partial\rho}\left(\rho^3\partial_\rho L_v\right) - \rho\Delta m^2 L_v = 0. \tag{6.4.7}$$

Note that if Δm^2 depends on L_v at the level of the Lagrangian then there would be an additional term $-\rho L^2\partial\Delta m^2/\partial L_v$. We neglect this term and instead impose the running of Δm^2 at the level of the equation of motion. The reason is that the extra term introduces an effective contribution to the running of γ that depends on the gradient of the running coupling. Such a term is not present in perturbation theory in our QCD-like theories - we wish to keep the running of γ in the holographic theory as close to the perturbative guidance from the gauge theory as possible.

In order to find $L_v(\rho)$ we solve the equation of motion numerically with shooting techniques with an input IR initial condition. A sensible first guess for the IR boundary con-

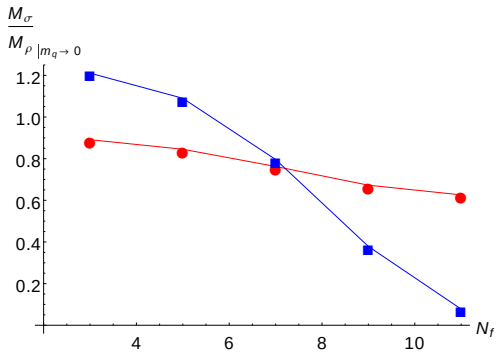

Figure 6.4.1: A plot of the σ meson mass in units of the ρ meson mass against N_f in Dynamic AdS/QCD. The points that fall to zero at the chiral transition at $N_f = 12$ are those computed where the action is cut-off at the on-shell mass of the quark so the theory is blind to the deep IR conformal symmetry breaking, whilst the points that asymptote to a non-zero value at $N_f = 12$ are for the soft wall variant.

dition is

$$L_v(\rho = L_0) = L_0, \qquad L_v'(\rho = L_0) = 0. \tag{6.4.8}$$

This IR condition is similar to that from top-down models [78,101,102,107] but imposed at the RG scale where the flow becomes "on mass-shell". Here we are treating $L(\rho)$ as a constituent quark mass at each scale ρ. To continue the flow below this quark mass scale we would need to address the issue of the decoupling of the quarks from the running function γ - previously we have not addressed this challenge but we will show some of the subtly below when we include a soft wall.

The isoscalar $\bar{q}q$ (σ) mesons are described by linearized fluctuations of L about its vacuum configuration, L_v. We look for space-time dependent excitations, i.e. $|X| = L_v + \delta(\rho)e^{iq.x}$ with $q^2 = -M_\sigma^2$. The linearized equation of motion for δ is

$$\begin{aligned}\partial_\rho(\rho^3\delta') - \Delta m^2\rho\delta - \rho L_v\delta \left.\frac{\partial\Delta m^2}{\partial L}\right|_{L_V} \\ + M_\sigma^2 R^4 \frac{\rho^3}{(L_v^2+\rho^2)^2}\delta = 0.\end{aligned} \tag{6.4.9}$$

We seek solutions with asymptotics of $\delta = 1/\rho^2$ in the UV and with $\partial_\rho\delta|_{L_0} = 0$ in the IR, giving a discrete meson spectrum. This calculation has already been presented in [82–85] and the σ meson mass, in units of the rho meson mass, falls to zero as $N_f \to 4N_c$ where the Miransky phase transition occurs. We summarize this result for the $N_c = 3$ theory in Figure 6.4.1.

We will now include an IR soft wall behaviour into the model in the spirit of the fourth example given in Section 6.3.2, with an IR profile for $L(\rho)$ and the dilaton . To demonstrate this idea, rather than cooking Δm^2 below the quark on mass-shell scale, we will include the soft wall by hand in the L_v profile and just compute the bound state masses.

We take for the IR wall

$$L(\rho) = L_0 \sin(\pi\rho/2L_0), \quad \rho < L_0 \tag{6.4.10}$$

which is linear at small ρ and matches to the solutions already found above $\rho = L_0$. We then include a dilaton of the form

$$\Phi(\rho) = 1 + e^{-1/\rho^2} - e^{-1/L_0^2} \tag{6.4.11}$$

which grows from unity at the matching scale to take the form $\exp(-z^2)$ in the IR. We again compute the rho and σ spectrum as a function of N_f for the $N_c = 3$ theory, except now imposing the boundary conditions $V'(0) = 0$ and $\delta'(0) = 0$. We display the results in Figure 6.4.1 as well - the σ meson now does not become light because it is sensitive to the IR conformal symmetry breaking that picks out the scale L_0.

6.5 Conclusions

Dynamic AdS/QCD is an AdS/QCD model derived from the quadratically expanded D3/probe D7 system, with the running of the anomalous dimension of $\bar{q}q$ replaced by hand to match a particular theory. The field $|X| = L$ holographically dual to the quark bilinear can be thought of as the running quark mass, and generates a soft wall in the action for the mesonic fluctuations. In this chapter we have studied manipulating L to mimic a soft wall model in the spirit of [110]. The idea is to use the deep IR behaviour of the metric or the dilaton to transform the mesonic spectra from that associated with a square well potential ($M_n \sim n$) to that associated with a simple harmonic oscillator ($M_n \sim \sqrt{n}$). Although this can be done, it requires $L \to 0$ in the IR which is not the behaviour seen in top-down models, nor what would be naively expected for the IR behaviour of the quark mass - the mesonic physics becomes determined by RG scales well below the on-shell quark mass. Nevertheless, we have shown examples of this behaviour in the model.

We have also highlighted the consequences of soft wall dynamics in models of the light σ meson that emerges in walking theories near the chiral transition from the conformal window. If the mesonic physics is determined by scales above the on-shell mass of the quark then the near-conformal dynamics of these theories can lead to a light σ meson relative to the rest of the spectrum. However, if soft wall dynamics is included then the meson physics is determined at scales both above and below the on-shell mass. Since here the mass function falls to zero in the IR, the dynamics is very non-conformal and the σ meson mass is determined by the on-shell mass scale. This highlights the cause of the difference in spectrum between the results in [113–116] and [145]. Of course, in the holographic models the decoupling behaviour of the quarks or mesonic physics is input by hand, so one must decide which scheme is most plausible.

Our intuition has been led by top-down models such as the D3/probe D7 system with

a magnetic field [102], where the mesonic physics lives on the probe and does not see the geometry below the IR mass scale. Another example is given by the Sakai Sugimoto model [78] in which, firstly, meson physics is restricted to the probe brane energy scales which are sharply cut off at the IR mass, and, secondly, the deep IR of the background geometry is capped off by confinement. We feel that the decoupling in [145] is more realistic, though one might expect some interaction with scales just below the quark mass that may tend to raise the techni-dilaton mass. It seems likely that the lattice will be the only way to find a definitive conclusion on the issue.

Part III

Entanglement for Flavour and Top-Down Models

CHAPTER 7

Holographic Entanglement Entropy

Of the many diverse areas of application that gauge/gravity duality has been utilised for over the past two decades, the subject of quantum *entanglement* is one that has received particular attention. Entanglement has been a contentious philosophical topic since the Einstein-Podolsky-Roson (EPR) [154] gedankenexperiments of the 1930s, which seemed to wreak havoc on accepted notions of locality central to our basic understanding of physics. The phenomenon was partially enlightened by the work of Bell [155, 156] on quantum correlations in the 1960s, and entanglement came to be understood as a central aspect of quantum physics, crucially distinguishing it from its classical counterpart. It has since been exploited in numerous ingenious ways in the field of quantum information, which is both deepening our understanding of the foundations of quantum mechanics and leading to exciting new technologies that might revolutionarize many aspects of modern life.

Another area where discussions of entanglement have borne fruit is the field of condensed matter theory, where the entanglement structure of many-body system wavefunctions encodes important information about the underlying quantum state. For example, certain measures of entanglement can be used as order paramaters for phase transitions in topological systems (see e.g. [157, 158]), in situations where no local quantity signifies any transition. One such quantity, which we shall be primarily interested in, is the *entanglement entropy* - as its name suggests it is formally defined in a similar manner to the usual quantum thermodynamic entropy, but can be actually viewed as encoding information about the entanglement between subsystems. Much interest into entanglement entropy has been generated due to the fact that, whilst being laborious to compute in a general quantum field theory, it admits a simple geometrical description

in those that have holographic duals. We will define both the field theory and holographic quantities in the present chapter, and much of Part III will consist in computing this quantity in gravity duals.

Another significant impact that holography has had on discussions of entanglement entropy, and one potentially even more important, is the birth of deep connections between quantum entanglement and gravity. As we will discuss in the following, the holographic prescription for calculating entanglement entropy relates a simple geometrical quantity in the bulk to entanglement, an intrinsically quantum phenomenon, in the boundary QFT. That such a relation should exist is surprising, and has motivated many authors to investigate the emergence of spacetime geometry in holography out of QFT entanglement data [159–161]. The protypical example of this is the thermofield double state [162], where one observes that macroscopic entanglement in the QFT leads to spacial connectivity in the holographic dual - such studies have led to the summarising slogan "ER=EPR" [163], with 'ER' here referring to *Einstein-Rosen bridges* or wormholes, directly highlighting the connection between a geometric notion and quantum entanglement. We will touch upon such issues again in Chapter 8 when we discuss a quantity known as the *differential entropy*, which was motivated from related considerations.

7.1 Definition of Entanglement Entropy

Consider a generic quantum system in a state with density matrix ρ, which we take to be in a pure state so that $\rho = |\Psi\rangle\langle\Psi|$ for some state vector $|\Psi\rangle$. One considers the situation where the Hilbert space of the system $\mathcal{H}$ can be partitioned into two factors, $\mathcal{H} = \mathcal{H}_A \otimes \mathcal{H}_{A^c}$. For example, one could consider a simple system of two qubits where the partitioning is manifest. In general, one can define the *reduced density matrix* for subsystem A by tracing over the degrees of freedom in $\mathcal{H}_{A^c}$,

$$\rho_A \equiv \mathrm{Tr}_{A^c}[\rho]. \tag{7.1.1}$$

For an observer making measurements in system A with no knowledge of A^c, this is the effective density matrix required to compute expectation values i.e. $\langle \mathcal{O}_A \rangle = \mathrm{Tr}[\rho_A \mathcal{O}_A]$. The *entanglement entropy (EE)* (see e.g. [164]) is then the usual von Neumann entropy of this reduced density matrix,

$$S_A \equiv -\mathrm{Tr}_A[\rho_A \log \rho_A]. \tag{7.1.2}$$

The intuition here is that, in taking the trace in (7.1.1), subsystem A has complete ignorance about the state of A^c. If the original state vector $|\Psi\rangle$ was separable (i.e. factorises into a state for A and a state for A^c), then one will end up with a pure state in $\mathcal{H}_A$ and consequently the entanglement entropy (7.1.2) will be zero. If the the original state is entangled however, then one will end up with a mixed state in $\mathcal{H}_A$ and consequently there will be non-zero entropy (7.1.2) that can be taken as a measure of this entangle-

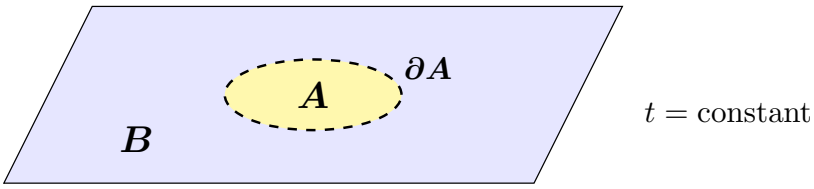

Figure 7.1.1: The entanglement entropy for a QFT is defined by partitioning the Hilbert space geometrically for a spatial (constant time) slice.

ment. Heuristically, the entanglement entropy can be viewed as counting the number of EPR pairs between the two systems.

This discussion applies for any quantum system with such a partitioning of the Hilbert space. In particular, one may take a discrete lattice with degrees of freedom confined to the lattice sites, and imagine a spatial partitioning of the system to give the corresponding partitioning of the Hilbert space. Taking the limit where the lattice spacing goes to zero, one can then extend this discussion to quantum field theories. We assume the QFT spacetime is globally hyperbolic and thus can consider a spatial (Cauchy) slice[1], and partition the Hilbert space by geometrically partitioning this slice - see Figure 7.1.1. An outstanding issue exists for gauge theories however, in that no decomposition of the Hilbert space can be done in a gauge-invariant manner - the gauge-invariant operators are link variables between sites, not at the sites themselves. Many authors [165–169] have proposed prescriptions in which a choice is made about which region, A or A^c, the variables belong to when cutting through the links with an entangling surface.

There are in addition computational difficulties with extending the discussion to quantum field theories, since taking the logarithm of a continuum operator as in (7.1.2) is not without technical problems. The standard approach is to use the *replica trick* [170] whereby one computes the *Renyi entropies* [171]

$$S_A^{(n)} \equiv \frac{1}{1-n}\log \mathrm{Tr}_A(\rho_A^n) \tag{7.1.3}$$

using the path integral formalism, and then extracts the EE from the limit

$$S_A = \lim_{n\to 1} S_A^{(n)}. \tag{7.1.4}$$

In particular, one can write this as

$$S_A = -\frac{\partial}{\partial n}\mathrm{tr}_A \rho_A^n|_{n=1} \tag{7.1.5}$$

[1]We will assume the state is time-independent throughout this thesis.

and the task then becomes to compute $\mathrm{tr}_A \rho_A^n$, which can be written as

$$\mathrm{tr}_A \rho_A^n = \frac{Z_n}{(Z_1)^n}. \tag{7.1.6}$$

Here, Z_1 is the usual partition function, and Z_n is the partition function on an n-sheeted Riemann surface formed by gluing together n copies of the original spacetime along ∂A. The argument of [172] for the holographic entanglement entropy proposal essentially makes use of a gravitational counterpart to this replica trick.[2] Although one in principle has the above prescription for calculating the EE in any QFT, there are nevertheless very few such analytical calculations in interacting theories and in spacetime dimensions greater than two, due to the technical complexity of the procedure. As we will see in Section 7.2, holography provides a considerably simpler method for computing the EE in field theories that admit a gravity dual.

7.1.1 Properties

An important property of the entanglement entropy is that it is divergent, which follows from the usual UV short-range correlations in a local QFT. Intuitively, one can understand the divergence as arising from short-range correlations between EPR pairs across the entangling surface, and consequently the leading divergence (in the ground state) is proportional to the area of this surface [173, 174],

$$S_A = \gamma \frac{\mathrm{Area}(\partial A)}{\epsilon^{d-2}} + \ldots, \tag{7.1.7}$$

where ϵ is a UV regulator, and γ is a theory-dependent coefficient that scales with the number of degrees of freedom.[3] Of the subleading divergences, although most are scheme-dependent, there is a *universal* term which (for even d) goes as

$$S_A = \cdots + (-1)^{\frac{d-2}{2}} s_A \log\left(\frac{L}{\epsilon}\right) + \mathcal{O}(\epsilon^0) \tag{7.1.8}$$

where L is a measure of the size of region A. We shall discuss this universal term more in Section 8.6.

Note that for a pure quantum state (as in the zero temperature case) one finds that (see e.g. [164])

$$S_A = S_{A^c} \tag{7.1.9}$$

which explicitly shows that the EE, unlike the thermal entropy, is not an extensive quantity. This identity no longer holds at finite temperature however, since the entanglement entropy then contains thermal contributions.

The EE also satisfies a number of inequalities [175–177] that follow from its definition

[2] We discuss this argument further in Section 9.7.

[3] The area law would not be expected to hold in a non-local theory however.

(7.1.2) - one of particular importance, and which is used in motivations of the differential entropy discussed in Section 8.7, is the property of *strong subbadditivity*, which for a tripartite system $\mathcal{H} = \mathcal{H}_A \otimes \mathcal{H}_B \otimes \mathcal{H}_C$ can be stated as

$$S_{A\cup B} + S_{B\cup C} \geq S_{A\cup B\cup C} + S_B, \tag{7.1.10}$$

$$S_{A\cup B} + S_{B\cup C} \geq S_A + S_C. \tag{7.1.11}$$

This property can in turn be derived from the monotonicity of the *relative entropy* [178]

$$S(\rho||\sigma) = \text{Tr}[\rho\log\rho] - \text{Tr}[\rho\log\sigma] \tag{7.1.12}$$

which is a measure of distinguishability between two quantum states. For small changes of the state, the monotocity of the relative entropy can be written in a form suggestive of thermodynamics, and leads to an equality known as the *first law of entanglement* [179]. This identity has gained interest within holography since it has been argued to be equivalent to the linearized gravitational equations in the bulk [180, 181], again alluding to the strong connection between boundary entanglement and bulk gravity.[4]

All of these properties can be readily observed in the holographic description, which we introduce in the following section.

7.2 Holographic Entanglement Entropy

We now state the holographic prescription for computing the EE in a QFT. We focus on the time-independent case as this is our main interest throughout the rest of this thesis. The *Ryu-Takayangi (RT)* [183] proposal for computing the EE for a region A states that one should form the codimension two bulk surface Σ with boundary $\partial\Sigma = \partial A$ that is homologous to A and has *minimal area*. The EE is then given by the familiar Bekenstein-Hawking expression

$$S_A = \min_{\partial\Sigma=\partial A} \frac{\text{Area}(\Sigma)}{4G_N}. \tag{7.2.1}$$

Computationally one minimises the area functional

$$S_A = \frac{1}{4G_N}\int_\Sigma d^{d-1}\sigma\sqrt{\gamma} \tag{7.2.2}$$

where γ is the induced metric on Σ - we compute many such examples throughout Chapters 8 and 9. The setup is illustrated in Figure 7.2.1. Intuitively one may motivate this by viewing the surface Σ as the bulk counterpart of smearing out region B by hiding a corresponding part of the bulk spacetime from A, with the minimal area condition coming from the entropy bound [184, 185].

[4] It has also been argued [182] that the full non-linear gravitational equations should follow from the first law of entanglement.

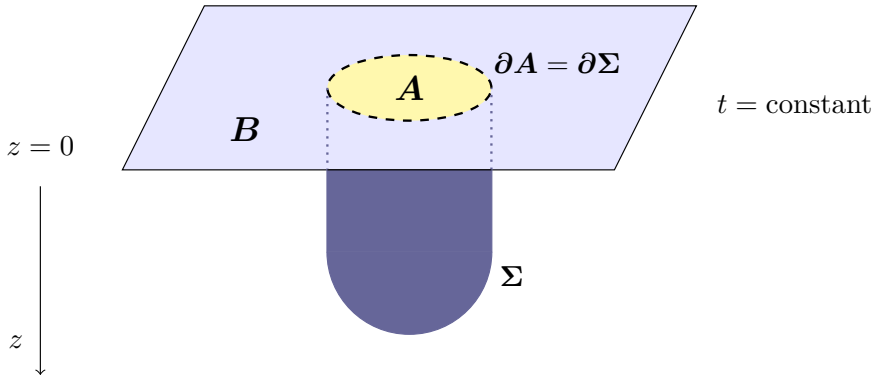

Figure 7.2.1: Ryu-Takayanagi prescription for holographic entanglement entropy: one constructs the codimension two minimal bulk surface homologous to the boundary entangling region.

Note that Σ is a surface in a spatial slice of the bulk AdS space, in the same way that the entangling surface in the QFT is defined on a spatial slice of the boundary. If there are multiple solutions causing the area functional to vanish, then one picks the solution with minimum area.[5] This prescription can be extended to general time-dependent situations using the covariant holographic EE proposal of [186], which proposes an extremal surface prescription similar in structure to (7.2.1).

There have been numerous checks of equation (7.2.1), which was proven for spherical entangling regions in CFTs in [187] by conformally mapping the EE to the thermal entropy of a black hole. In the last few years a general argument [172] for its validity has been given based on generalised gravitational entropy and the replica trick, as we discuss in Section 9.7. It is simple to demonstrate that this holographic quantity satisfies the properties discussed in Section 7.1.1: the property of complementarity in equation (7.1.9) is manifest by definition; the leading divergence in (7.1.7) is readily observed from expected volume divergences of submanifolds in AdS [188–191], with the power of ϵ following from the form of the metric and the area law property simply following from the fact that $\partial\Sigma = \partial A$; the property of strong subadditivity in (7.1.10)-(7.1.11) is also easily demonstrated using simple geometrical arguments [192].

Note that this construction implicitly works within the lower-dimensional gravity picture i.e. in AAdS without the compact space present. The question of how to compute the EE holographically in a top-down setting is the subject matter of Chapter 9. It was originally proposed that one could just directly extend (7.2.1) by taking a codimension two surface in the full higher-dimensional spacetime and similarly minimising the area functional - many studies followed this prescription for computing the EE in top-down settings (see e.g. [183, 193–206]). As we will see, there is strong evidence that this is indeed the case, but the identification with the quantity that one gets from computation

[5] That any non-trivial minimal surfaces exist is due to the fact that the setup is in AAdS space rather than flat space.

in the lower-dimensional picture is very non-trivial.

Considering entanglement in a top-down setting also leads naturally to discussions of *generalised entanglement entropy* as studied in [207, 208]. A distinct field theory quantity, known as the *global symmetry entanglement entropy*, can be considered holographically by taking a codimension two bulk minimal surface that asymptotically fills the spatial background but partitions the compact space. Further quantities still in the field theory, so-called *field-space entanglement*, can also be considered by partitioning the Hilbert space in field-space rather than geometrically - the latter is more difficult to realise holographically, but can be done in certain cases when the bulk spacetime has decoupled inner throat regions as discussed in [208]. An important property about these alternative measures of entanglement is that their leading terms scale with volume rather than area, since when one integrates out degrees of freedom, the entanglement between these and those remaining occurs everywhere in the space.

One final issue concerns the UV divergences of the entanglement entropy. We discuss these further for example in Section 8.6 in relation to the universal terms in the flavour contribution to the EE. For many purposes however one is often interested in the finite terms - these can be used as order parameters for phase transitions (see e.g. [194, 209], but also Section 8.3.4), and are also relevant in studies of the F-theorem [210]. A common approach to extracting the finite terms involves differentiating the EE with respect to geometric parameters that characterise the entangling region, or with respect to the mass. This is a simple procedure both in the field theory and holographically and will be the approach we use in Chapter 8, but there are certain problems with such methods since they only hold for specific entangling geometries, and it is difficult to relate them to usual procedures of renormalisation for other quantities in the QFT. Holographically these divergences arise from near-boundary behaviour, and one would expect that they can be dealt with systematically using the holographic renormalisation procedure of Section 3.2.3. This is indeed the case, as was recently carried out in [211] - one finds that (7.2.2) needs to be supplemented with a counterterm action to obtain the renormalised functional

$$S_{\text{ren}} = \frac{1}{4G_N}\int_{\Sigma} d^{d-1}\sigma\sqrt{\gamma} - \frac{1}{4G_N}\int_{\partial\Sigma} d^{d-2}x\sqrt{\tilde{\gamma}}\left(\frac{1}{d-2}+\dots\right) \tag{7.2.3}$$

where $\tilde{\gamma}$ is the induced metric on $\partial\Sigma$. As mentioned however, we shall not need to make use of this formalism in the following - in Chapter 8 we use renormalisation by differentiation where required since we study only particular entangling geometries, and in Chapter 9 we mostly work at the level of the bare entanglement area functional.

CHAPTER 8

Entanglement Entropy and Differential Entropy for Massive Flavours

The material in the present chapter is based largely on [2].

8.1 Introduction

The focus of this chapter is on the computation of holographic entanglement entropy in top-down brane probe systems, which are widely used in phenomenological applications of holography as discussed in Part II. Entanglement entropy is a new computable for such systems and, following the pioneering works of [194, 209], can act as an order parameter for confinement and other phase transitions.

A top-down brane probe system is expressed in terms of a ten-dimensional supergravity background and a brane embedding into this background. The Ryu-Takayanagi prescription is however based on extremal surfaces in the reduced Einstein $(d+1)$-dimensional metric, where d is the dimension of the dual field theory. One of the main results of this chapter is a systematic method to compute the holographic entanglement entropy for any top-down brane probe system, using the method of Kaluza-Klein holography [24] to extract the lower-dimensional Einstein metric. This method reproduces earlier results of [212–215] but allows entanglement entropy to be computed for any brane system with arbitrary worldvolume fluxes (earlier results for massless flavours at finite density can be found in [216]). We illustrate our methodology using the example of the D3/D7 system at finite mass and density. We compute the holographic entanglement entropy for massive flavours, with arbitrary mass and various entangling region geometries, and use our new methodology to address the case of finite density.

Brane systems provide a new testing ground for the dependence of entanglement en-

tropy on the field theory and on the shape of entangling region, topics of considerable current interest, see for example [217–222]. In particular, one can explore the structure of universal logarithmic terms; these are well-understood for conformal field theories (see e.g. [223, 224]) and recent papers have explored the behaviour of entanglement entropy under relevant perturbations using conformal perturbation theory [225–230]. It was shown in [227] that for a CFT deformed by a relevant operator

$$I \to I + \lambda \int d^d x \mathcal{O} \tag{8.1.1}$$

there is a new logarithmic divergence in the entanglement entropy of the half space

$$\delta S = \mathcal{N}\lambda^2 \frac{(d-2)}{4(d-1)} \frac{\pi^{\frac{d+2}{2}}}{\Gamma(\frac{d+2}{2})} \mathcal{A} \log\left(\frac{\epsilon_{UV}}{\epsilon_{IR}}\right) \tag{8.1.2}$$

when $\Delta = (d+2)/2$ with $\mathcal{A}$ the area of the dividing surface and $\mathcal{N}$ the normalisation of the two point function of the operator $\mathcal{O}$. Here ϵ_{UV} and ϵ_{IR} correspond to UV and IR cutoffs respectively.

In Section 8.6 we prove (8.1.2) by analysing the volume divergences of the holographic entanglement entropy and show that (as postulated in [227]) such a divergence occurs for an entangling surface with arbitrary geometry. We also show explicitly that (8.1.2) agrees with the logarithmic terms in the entanglement entropy for the D3/D7 system at finite mass, using the probe brane holographic renormalisation results of [59] to determine the holographic two point function normalisation. As well as matching the universal terms in the entanglement entropy, we explain the origin of finite terms in the entanglement entropy for massive flavour systems, in terms of the effective IR description of the system in terms of a CFT deformed by irrelevant operators.

As discussed in Chapter 7, there is a growing literature connecting quantum entanglement with the global structure of the bulk spacetime, see in particular [163, 182]. In [231] a relation between the area of generic (non-minimal) surfaces and entanglement was proposed and this idea was sharpened with the introduction of differential entropy [232–237]. We verify that the differential entropy in the D3/D7 system indeed computes the area of a hole in the reduced Einstein metric; the agreement is somewhat subtle since the depth of the hole is itself corrected by the presence of the probe branes.

In Section 8.8 we discuss the implications of the fact that the entanglement and differential entropy are related to the reduced Einstein metric, rather than the ten-dimensional metric: even if entanglement allows us to reconstruct the reduced Einstein metric completely, this information does not suffice to reconstruct the ten-dimensional geometry. Moreover, the causal structure in ten dimensions only agrees with that of the reduced Einstein metric in special cases (e.g. product metrics); the global structure is qualitatively different between five and ten dimensions even for well-understood examples

such as the Coulomb branch of $\mathcal{N}=4$ SYM. Reconstruction of the full ten-dimensional geometry would therefore seem to require a generalized notion of entanglement in the dual field theory, such as those discussed in Chapter 7.

The plan of this chapter is as follows. In Section 8.2 we briefly review the features of the D3/D7 system relevant to the present discussion. In Sections 8.3 and 8.4 we compute the entanglement entropy for slab, half space and spherical entangling regions for the massive D3/D7 system. In Section 8.5 we present a general method to compute the entanglement entropy in any brane probe system using Kaluza-Klein holography and illustrate our method with the D3/D7 system at finite mass and density. We discuss the field theory interpretation of our results in Section 8.6 and give a holographic proof of (8.1.2) for generic entangling regions. In Section 8.7 we show that the differential entropy computes the area of a hole in the Einstein metric and we discuss the meaning of entanglement and differential entropy for top-down solutions in Section 8.8, illustrating our discussions with Coulomb branch geometries.

8.2 Massive Flavours

In this chapter we will explore entanglement entropy for massive brane systems, focussing for the most part on the specific example of the D3/D7 brane system discussed in Chapter 4 - we briefly review the results here in a form appropriate to the present work. Consider N_c D3-branes and $N_f \ll N_c$ parallel coincident D7-branes. As discussed previously the decoupling limit gives rise to $\mathcal{N}=4$ SYM coupled to N_f massless flavours; the resulting field theory is an $\mathcal{N}=2$ SCFT. Taking the background $AdS_5 \times S^5$ metric to be of unit radius

$$ds^2 = \frac{1}{z^2}\left(dz^2 + dx^\mu dx^\mu\right) + d\theta^2 + \sin^2\theta d\Omega_3^2 + \cos^2\theta d\phi^2, \tag{8.2.1}$$

the flat embedding solution of a probe D7-brane corresponding to a massless flavour is described in these coordinates by ϕ constant and $\theta = \pi/2$, i.e. the probe D7-brane wraps $AdS_5 \times S^3$.

Suppose one separates the D7-branes from the stack of D3-branes; the resulting open strings are massive and the field theory in the decoupling limit corresponds to $\mathcal{N}=4$ SYM coupled to N_f massive flavours [53] (we discuss the massive deformation of the $\mathcal{N}=2$ SCFT further in Section 8.6). The corresponding D7-brane embedding in $AdS_5 \times S^5$ is described by ϕ being constant and the angle θ depending on the radial coordinate z as

$$\sin^2\theta = (1 - m^2 z^2), \tag{8.2.2}$$

where m corresponds to the flavour mass, or equivalently the separation of the D7 and D3 branes. Note that the probe brane wraps the equator of the S^5 as $z \to 0$ and smoothly caps off at a finite value of $z = 1/m$, controlled by the flavour mass.

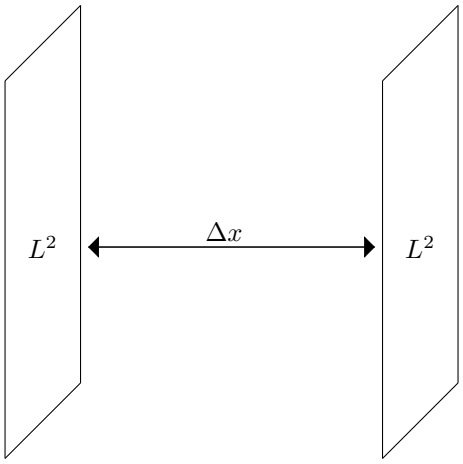

Figure 8.3.1: Illustration of a slab boundary region: $\Delta x = l$ is the width of the region, and L^2 is the regularized area of its boundary faces.

The D3/D7 brane system can be used to model mesons holographically. Considerable work has been done on generalizations of the probe brane embeddings to finite temperature and finite density, see the review [52], and on the backreaction of the flavour branes onto the geometry [238–240]. In particular, note that interesting meson melting phase transitions are observed at finite temperature and density, see for example [241, 242]. Backreacting massive flavours is non-trivial even at zero temperature and density, since the flavours break the global symmetry to $SO(4)$ and the resulting ten-dimensional metric is therefore of cohomogeneity three. Smearing the branes over the compact space reduces the cohomogeneity of the metric but this is obscure from the field theory perspective as it corresponds to an averaging over different field theories.

In this chapter we will calculate the entanglement entropy and the differential entropy for the massive flavour system at zero temperature and zero density, and match our results with field theory results based on conformal perturbation theory. We will also present a method to compute the entanglement entropy for any probe brane system (with or without worldvolume gauge fields) and illustrate this method with the case of massive flavours at finite density. The method is equally applicable at finite temperature, although at finite temperature the entanglement entropy will include both thermal and quantum contributions; matching with field theory results is considerably harder as few results for finite temperature exist. It would however be interesting to explore the finite temperature results in the context of melting phase transitions.

8.3 Entanglement Entropy for Slabs

In this section we compute the entanglement entropy for a slab on the boundary (see Figure 8.3.1), working to leading order in the ratio of the number of flavours to colors, N_f/N_c.

Let us begin by reviewing the computation of entanglement entropy for a slab in AdS_5. We define a slab region on the boundary of width $\Delta x = l$ by $x \in [0, l]$, and take as an embedding ansatz $z = z(x)$ on a $t = 0$ hypersurface. Defining the regularised lengths of the other spatial directions as L, it is then easy to show that the Ryu-Takayanagi entanglement entropy functional [183] for the embedding surface is

$$S = \frac{L^2}{4G_N}\int_0^l dx \frac{\sqrt{1+z'^2}}{z^3}, \tag{8.3.1}$$

where G_N is the Newton constant. Since we chose the AdS_5 to have unit radius, the Newton constant is dimensionless and can be related to the number of colors N_c as

$$\frac{1}{8\pi G_N} = \frac{N_c^2}{4\pi^2}. \tag{8.3.2}$$

The Lagrangian is independent of x explicitly and hence the associated Hamiltonian is a constant of motion. Rearranging the expression for this constant of motion one easily finds

$$z' = \frac{\sqrt{\tilde{z}^6 - z^6}}{z^3} \tag{8.3.3}$$

where $\tilde{z}$ is clearly the turning point of the solution since $z'(\tilde{z}) = 0$. The entanglement entropy is then obtained by substituting this solution into the entropy functional, resulting in

$$S = \frac{L^2\tilde{z}^3}{2G_N}\int_\epsilon^{\tilde{z}} \frac{dz}{z^3\sqrt{\tilde{z}^6 - z^6}}. \tag{8.3.4}$$

Here we have included a factor of two, from the two halves of the entangling surface, i.e. $0 < x < l/2$ and $l/2 < x < l$. It is useful to define the dimensionless parameter $s \equiv z/\tilde{z}$ so that $z \in [\epsilon, \tilde{z}] \to s \in [a, 1]$ where $a \equiv \epsilon/\tilde{z}$ is also dimensionless. We obtain, for example

$$\frac{dx}{dz} = \frac{s^3}{\sqrt{1-s^6}}. \tag{8.3.5}$$

Note that the entanglement entropy is thereby manifestly dimensionless

$$\begin{aligned} S &= \frac{L^2}{2\tilde{z}^2 G_N}\int_a^1 \frac{ds}{s^3\sqrt{1-s^6}} \\ &= \frac{L^2}{2\tilde{z}^2 G_N}\left(\frac{\sqrt{\pi}\Gamma(-\frac{1}{3})}{6\Gamma(\frac{1}{6})} + \frac{1}{2a^2}{}_2F_1\left(-1/3, 1/2, 2/3, a^6\right)\right); \\ &= \frac{L^2}{2G_N}\left(\frac{1}{2\epsilon^2} + \frac{\sqrt{\pi}\Gamma(-\frac{1}{3})}{6\Gamma(\frac{1}{6})\tilde{z}^2}\right), \end{aligned} \tag{8.3.6}$$

where in the latter equation we retain only terms which are finite or divergent as the cutoff $\epsilon \to 0$.

It is simple to find the induced metric of the entangling surface and its associated stress

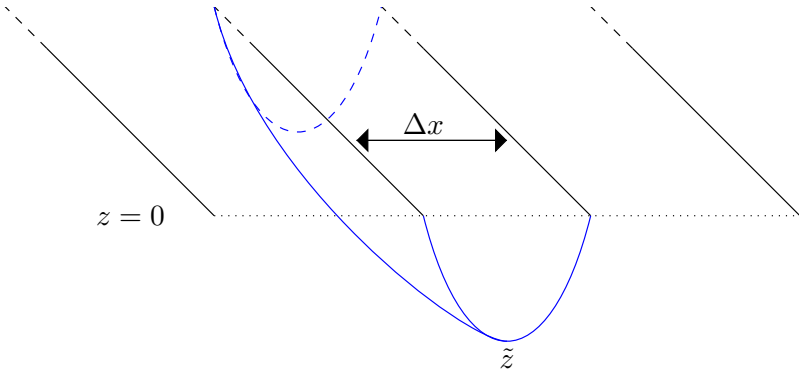

Figure 8.3.2: The minimal surface for a slab boundary region - the boundary is at $z = 0$ and $z = \tilde{z}$ is the turning point of the surface.

tensor. The induced metric is given by $\gamma_{ab}^{\min} = \partial_a X^\mu \partial_b X^\nu g_{\mu\nu}$ where $a, b = (s, y, w)$ run over the surface indices and μ, ν run over all AdS_5 indices. The induced metric is therefore

$$\gamma_{ab}^{\min} = \left(\frac{1}{s^2(1-s^6)}, \frac{1}{s^2\tilde{z}^2}, \frac{1}{s^2\tilde{z}^2} \right). \tag{8.3.7}$$

We note for further use that

$$\sqrt{\gamma^{\min}} = \frac{1}{\tilde{z}^2 s^3 \sqrt{1-s^6}}. \tag{8.3.8}$$

Differentiating the action functional, the stress tensor for the surface is given by

$$T_{min}^{\mu\nu} \equiv \frac{2}{\sqrt{\gamma^{\min}}} \frac{\delta \sqrt{\gamma^{\min}}}{\delta g_{\mu\nu}} \tag{8.3.9}$$

which evaluates to:

$$T_{min}^{\mu\nu} = \gamma^{\min\, ab} \partial_a X^\mu \partial_b X^\nu \tag{8.3.10}$$

after using the chain rule. It is then a simple matter to calculate these components, resulting in

$$T_{min}^{\mu\nu} = \left(s^2(1-s^6)\tilde{z}^2, 0, s^8\tilde{z}^2, s^2\tilde{z}^2, s^2\tilde{z}^2 \right) \tag{8.3.11}$$

which we will make use of below. Note also that the relation between the width of the slab, l, and the turning point of the minimal surface is

$$l = 2\int_0^{\tilde{z}} \frac{z^3 dz}{(\tilde{z}^6 - z^6)^{\frac{1}{2}}} = 2\tilde{z}\int_0^1 \frac{s^3 ds}{(1-s^6)^{\frac{1}{2}}} = \frac{2\sqrt{\pi}\Gamma(\frac{2}{3})}{\Gamma(\frac{1}{6})}\tilde{z}. \tag{8.3.12}$$

8.3.1 Flavour Contribution

Now let us compute the change in the entanglement entropy caused by the presence of N_f flavour branes, with $N_f \ll N_c$. A priori, to compute this change one would expect

that one needs to compute the backreaction of the branes to linear order in N_f/N_c and then extract from the backreacted geometry the change in the five-dimensional Einstein metric and hence the change in the area of the minimal surface. As mentioned earlier, it is hard to compute the backreacted ten-dimensional geometry because of the high cohomogeneity of the problem; smeared solutions are known and entanglement entropy was computed for these smeared solutions in [201].

It is important to note however that entanglement entropy is defined in terms of the five-dimensional Einstein metric, not the ten-dimensional (Einstein-frame) metric. One would not in general expect to obtain the correct answer for the entanglement entropy by computing the area of a minimal surface in the ten-dimensional metric, see Section 8.5. Note that [201] used the ten-dimensional metric rather than the five-dimensional Einstein metric.

Computing the full ten-dimensional backreaction without smearing and extracting the effective five-dimensional Einstein metric is intractable for general probe brane systems. Several methods have therefore been developed to extract the entanglement entropy from the probe brane embedding, see [212–215]. The methods of [212, 214, 215] are particularly applicable to spherical entangling regions, for which the CHM map [187] may be exploited. In this section our discussion will follow that of [213], which is applicable to all entangling region geometries.

On general grounds the change in the entanglement entropy for any perturbation in the five-dimensional Einstein metric is

$$\delta S = \frac{1}{4G_N}\int d^3x\sqrt{\gamma^{\min}}\frac{1}{2}T^{\mu\nu}_{\min}h^E_{\mu\nu} \tag{8.3.13}$$

where $h^E_{\mu\nu}$ is the perturbation in the five-dimensional Einstein metric, $T^{\mu\nu}_{\min}$ is the energy momentum tensor of the minimal (entangling) surface in the background and the integral is over the original entangling surface. Therefore one can compute the entanglement entropy provided one can extract the change in the five-dimensional Einstein metric. For general brane embeddings the computation of the perturbation in the five-dimensional Einstein metric is subtle; in Section 8.5 we present a method to compute the Einstein metric for all types of brane embeddings.

It was observed in [213] that the perturbation in the five-dimensional Einstein metric is straightforward to compute whenever the brane embedding has an induced world-volume metric which is diagonal (a product of a non-compact part and a compact part which is embedded in the sphere part of the background geometry) and furthermore the non-compact part of the metric has no dependence on the sphere coordinates. In such a case the linearised backreaction on the metric for probe branes can be computed [214] as

$$h^E_{\mu\nu} = \frac{1}{z^2}\mathrm{diag}\left(f(z), -h(z), h(z), h(z), h(z)\right) \tag{8.3.14}$$

where the metric perturbation is sourced by the effective brane energy momentum tensor $T^{\text{eff}}_{\mu\nu}$ i.e.

$$G_{\mu\nu}(h^E) = 8\pi G_N T^{\text{eff}}_{\mu\nu}. \tag{8.3.15}$$

This effective stress energy tensor is obtained by reducing the brane action over the three-sphere

$$I = -T_7 \int_{AdS_5} d^5\sigma \int_{S^3} d^3\sigma \sqrt{-\gamma} = -T_7 \int_{AdS_5} d^5\sigma (2\pi^2)(1-m^2z^2)^{\frac{3}{2}} \sqrt{-\gamma_{(s)}}, \tag{8.3.16}$$

where $\gamma_{\alpha\beta}$ is the worldvolume metric for the brane.[1] The worldvolume metric is diagonal for the given embedding and therefore the determinant factorises, allowing the integral over the three-sphere to be evaluated. The resulting effective action then depends only on the non-compact part of the worldvolume metric, $\gamma_{(s)\mu\nu}$, but note that the effective tension of this brane is z-dependent. Varying this effective action with respect to the non-compact part of the background metric results in the effective energy momentum tensor

$$(T^{\text{eff}})^{\mu\nu} = 2\pi^2 T_7 (1-m^2z^2)\gamma_s^{\mu\nu}. \tag{8.3.17}$$

Note that this method for computing the effective source term for the five-dimensional Einstein metric relies on the fact that the worldvolume brane metric is a direct product of non-compact and compact parts. The method is also not applicable for brane embeddings in which worldvolume gauge fields are non-zero or worldvolume fields source other supergravity fields as well as the metric. In Section 8.5 we will discuss a more generally applicable method for computing the entanglement entropy contributions from probe branes which does not rely on a diagonal worldvolume metric.

Substituting (8.3.17) into (8.3.15) gives the following equation

$$f(z) + zh'(z) \equiv \tilde{f}(z) = \frac{t_0}{12}(1-m^2z^2)^2. \tag{8.3.18}$$

Here t_0 is the backreaction parameter, proportional to the number of flavours $\mathcal{N}_f$

$$t_0 = 16\pi G_N T_o; \qquad T_o = 2\pi^2 T_7 \tag{8.3.19}$$

where T_7 is the tension of a D7-brane. Only the gauge invariant combination $\tilde{f}(z)$ is determined by the Einstein equations. However, continuity of the metric and of the extrinsic curvature at $z = 1/m$ requires that $h(z)$ satisfies $h(1/m) = h'(1/m) = 0$.

Substituting the metric perturbation and the minimal surface stress energy tensor into

[1] Note that we denote the worldvolume metric for the brane as γ and the induced metric on the entangling surface as $\gamma^{\min}$.

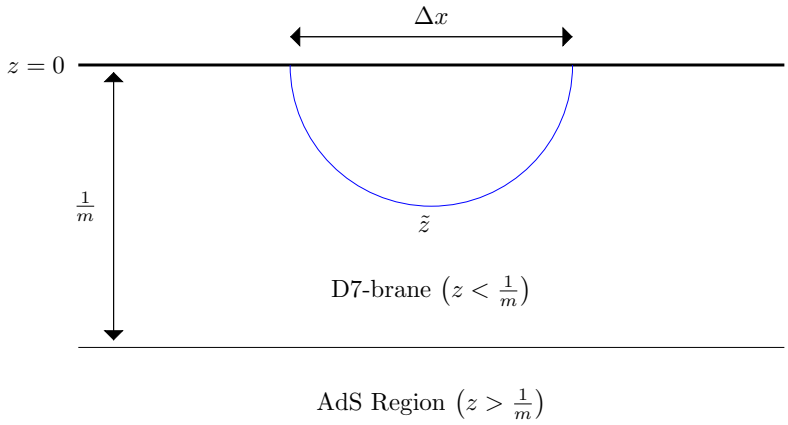

Figure 8.3.3: The relationship between the original minimal surface and the D7-probe embedding - when $\tilde{z} < 1/m$ the entire minimal surface lies within the probe brane embedding.

(8.3.13) thus gives

$$\delta S = \frac{1}{4G_N}\int dsdwdy \frac{1}{2\tilde{z}^2 s^3\sqrt{1-s^6}}\left(f(\tilde{z}s)(1-s^6)+h(\tilde{z}s)(s^6+2)\right) \tag{8.3.20}$$

where this integral is over the original entangling surface with coordinates (s, w, y). Defining $\alpha \equiv L^2/(4G_N\tilde{z}^2)$ for convenience (where we have computed the trivial y, w-integrals to give the factor L^2 and taken into account the factor of two arising from the two halves of the entangling surface), and unpacking $f(\tilde{z}s)$ we find

$$\delta S = \alpha\int ds\left(\frac{\sqrt{1-s^6}}{s^3}\tilde{f}(\tilde{z}s) - \frac{\sqrt{1-s^6}}{s^2}\tilde{z}h'(\tilde{z}s) + \frac{(s^6+2)}{s^3\sqrt{1-s^6}}h(\tilde{z}s)\right). \tag{8.3.21}$$

Integrating the second term by parts, the bulk contribution cancels the third term and one is left with a boundary contribution

$$\delta S = \alpha\left(\int_a^b ds\frac{\sqrt{1-s^6}}{s^3}\tilde{f}(\tilde{z}s) - \left[h(\tilde{z}s)\frac{\sqrt{1-s^6}}{s^2}\right]_{s=a}^{s=b}\right) \tag{8.3.22}$$

where $a = \epsilon/\tilde{z}$ and $b = 1, 1/\mu$ for $\mu < 1, \mu > 1$ respectively. Here $\mu \equiv m\tilde{z}$ is the dimensionless mass parameter. This latter distinction occurs because, although the integral runs over the original entangling surface which has $z \in [\epsilon, \tilde{z}]$, the integral in fact only receives a non-zero contribution when $h^E_{\mu\nu} \neq 0$, i.e. for $z < 1/m$. When $\tilde{z} < 1/m$ (i.e. $\mu < 1$), the entire entangling surface lies within the brane embedding, and the upper limit is thus $z = \tilde{z}$ or $s = 1$. When $\tilde{z} > 1/m$ (i.e. $\mu > 1$) however, the upper limit will depend on the mass and be given by $z = 1/m$ i.e. $s = 1/\mu$ (see Figure 8.3.3).

For both cases, the boundary term at $s = b$ actually vanishes. The expression within square brackets trivially vanishes at $s = 1$ for the case $\mu < 1$, and it vanishes for $\mu \geq 1$

using the continuity condition $h(1/m) = 0$. The expression for both cases is thus given by

$$\delta S = \alpha \left(\int_a^b ds \frac{\sqrt{1-s^6}}{s^3} \tilde{f}(\tilde{z}s) + h(\epsilon) \frac{\sqrt{1-a^6}}{a^2} \right) \tag{8.3.23}$$

with b depending on the case as mentioned above. Expanding for $\tilde{f}$ this becomes

$$\delta S = \frac{t_0 \alpha}{12} \left(\int_a^b ds \frac{\sqrt{1-s^6}}{s^3} (1-\mu^2 s^2)^2 + h(\epsilon) \frac{\sqrt{1-a^6}}{a^2} \right) \tag{8.3.24}$$

Note that the entanglement entropy depends explicitly on the gauge fixing for the metric perturbation. One choice of scheme would be to set $f(z) = 0$, corresponding to Fefferman-Graham coordinates while a second natural choice of scheme is to fix $h(z)$ such that the cutoff is unchanged to linear order and one then obtains the relation

$$h(\epsilon) = \frac{t_0}{12} \left(1 - \frac{2}{3} m^2 \epsilon^2 + \frac{1}{5} m^4 \epsilon^4 \right) + \mathcal{O}(t_0^2). \tag{8.3.25}$$

For this gauge choice one obtains

$$\begin{aligned} \delta S &= \frac{t_0 L^2}{48 G_N} \left(\frac{1}{\tilde{z}^2} \int_a^b ds \frac{\sqrt{1-s^6}}{s^3} (1-\mu^2 s^2)^2 + \left(\frac{1}{\epsilon^2} - \frac{2m^2}{3} + \mathcal{O}(\epsilon^2) \right) \right) \\ &= \frac{t_0 L^2}{48 G_N} \left(\frac{1}{\tilde{z}^2} \int_a^b ds \frac{\sqrt{1-s^6}}{s^3} (1-\mu^2 s^2)^2 \right) + \delta S_{\text{gauge}}(m, \epsilon), \end{aligned} \tag{8.3.26}$$

where we note that the gauge dependent contribution δS_{gauge} is independent of the turning point $\tilde{z}$, since $h(0)$ is finite. We will discuss this point further below. In what follows we will retain the gauge dependence explicitly, rather than fixing a gauge, and show that this gauge dependence drops out of universal terms.

In computing the integral we first specialise to the case of small mass so $b = 1$. Performing the integral directly over the range $s \in [a, 1]$ and expanding the answer in a gives the following up to $\mathcal{O}(a)$

$$\begin{aligned} \int_a^1 ds \frac{\sqrt{1-s^6}}{s^3} (1-\mu^2 s^2)^2 &= \frac{1}{2a^2} + \frac{2}{3}\mu^2 + \frac{\sqrt{\pi}}{12} \frac{\Gamma(-1/3)}{\Gamma(7/6)} \\ &+ \mu^4 \frac{\sqrt{\pi}}{12} \frac{\Gamma(1/3)}{\Gamma(11/6)} - \frac{2}{3}\mu^2 \log 2 + 2\mu^2 \log a. \end{aligned} \tag{8.3.27}$$

The result thus becomes

$$\begin{aligned} \delta S &= \frac{t_0 L^2}{48 G_N} \left(\frac{1}{2\epsilon^2} + \frac{2}{3} m^2 + \frac{\sqrt{\pi}}{12 \tilde{z}^2} \frac{\Gamma(-1/3)}{\Gamma(7/6)} + m^4 \tilde{z}^2 \frac{\sqrt{\pi}}{12} \frac{\Gamma(1/3)}{\Gamma(11/6)} \right. \\ &+ \left. \frac{2}{3} m^2 \log(\epsilon^3 / 2\tilde{z}^3) \right) + \delta S_{\text{gauge}}(m, \epsilon). \end{aligned} \tag{8.3.28}$$

We next consider the case of large mass so $b = 1/\mu$. The result is given in terms of generalised hypergeometric functions

$$\begin{aligned}\int_a^{1/\mu} ds \frac{\sqrt{1-s^6}}{s^3}(1-\mu^2 s^2)^2 &= \frac{1}{2a^2} + \frac{1}{6\mu^4}{}_3F_2\left(\{1/2,1,1\},\{2,2\},1/\mu^6\right) \\ &\quad -\frac{\mu^2}{2}{}_2F_1\left(-1/2,-1/3,2/3,1/\mu^6\right) \\ &\quad +\frac{\mu^2}{2}{}_2F_1\left(-1/2,1/3,4/3,1/\mu^6\right) + 2\mu^2\log(\mu a) + \mathcal{O}(a^2).\end{aligned} \tag{8.3.29}$$

Expanding for large mass one then obtains

$$\begin{aligned}\delta S &= \frac{t_0 L^2}{48 G_N}\left(\frac{1}{2\epsilon^2} + 2m^2\log(m\epsilon) - \frac{1}{48 m^4 \tilde{z}^6}\mathcal{O}\left(\frac{\epsilon^2}{\tilde{z}^2}\right)\right. \\ &\quad \left. + \mathcal{O}\left(\frac{1}{m^{10}\tilde{z}^{12}}\right)\right) + \delta S_{\text{gauge}}(m,\epsilon).\end{aligned} \tag{8.3.30}$$

Note that the power and log-divergent terms agree for $\mu \leq 1$ and $\mu \geq 1$.

We can immediately obtain the change in the entanglement entropy for the half space from the $\tilde{z} \to \infty$ limit of the above expression. In this case the entangling surface extends throughout the bulk and has no turning point. The contribution to the entanglement entropy from the brane is then

$$\delta S = \frac{t_0 L^2}{48 G_N}\left(\frac{1}{4\epsilon^2} + m^2\log(m\epsilon)\right). \tag{8.3.31}$$

Note that the divergent terms differ from (8.3.30) by an overall factor of two, since the entangling surface in the field theory no longer has two disconnected parts. We will discuss the field theory computation of (8.3.31) in Section 8.6.

8.3.2 Changes in Turning Point and Entanglement Surface

The perturbed entangling surface has a turning point for which the relation between the turning point and the width of the slab $\Delta x = l$ is changed relative to (8.3.12). The equation for the perturbed entangling surface is obtained analogously to (8.3.3) and given by

$$(z')^2 = \left(\frac{\tilde{z}^6}{z^6} - 1\right) + h(z)\left(\frac{4\tilde{z}^6}{z^6} - 1\right) - f(z)\left(\frac{\tilde{z}^6}{z^6} - 1\right). \tag{8.3.32}$$

for some constant $\tilde{z}$, and where $f(z)$ and $h(z)$ are the metric perturbations discussed previously. The width of the slab is then given by

$$\frac{l}{2} = \int_0^{\tilde{z}} \frac{z^3 dz}{(\tilde{z}^6 - z^6)^{\frac{1}{2}}} + \frac{1}{2}\int_0^{\frac{1}{m}} z^3 dz \frac{(f + zh')}{(\tilde{z}^6 - z^6)^{\frac{1}{2}}} - \frac{1}{2}\left[\frac{z^4 h}{(\tilde{z}^6 - z^6)^{\frac{1}{2}}}\right]_0^{\frac{1}{m}}, \tag{8.3.33}$$

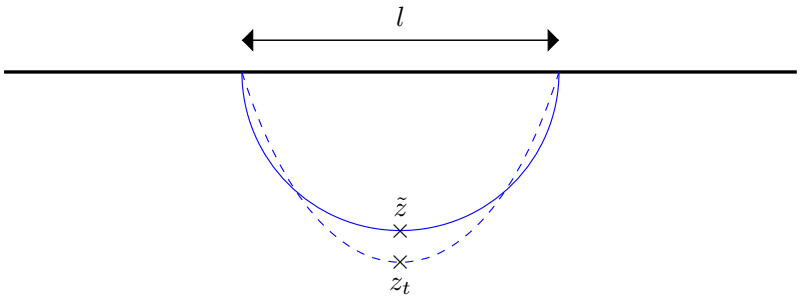

Figure 8.3.4: Illustration of the change in the turning point of the minimal surface - $\tilde{z}$ is the turning point of the original minimal surface (i.e. the one that is actually used to compute the flavour contribution to the entanglement entropy (8.3.13)), whereas z_t is the turning point of the minimal surface in the backreacted geometry.

where the upper limits of integration are explained as follows: for $\mu \geq 1$, the surface ends in the region in which the perturbations $f(z)$ and $h(z)$ vanish; from (8.3.32) the turning point therefore remains at $z = \tilde{z}$, and we continue to use the definition $\mu \equiv m\tilde{z}$.

The boundary term in (8.3.33) vanishes since $h(1/m) = 0$ and $h(0)$ is finite and therefore the relation between the turning point and the slab width depends only on the gauge invariant combination of metric perturbations. Substituting this combination using (8.3.18) one hence obtains

$$\frac{l}{2} = \tilde{z}\left(\frac{\sqrt{\pi}\Gamma(\frac{2}{3})}{\Gamma(\frac{1}{6})} + \frac{t_0}{24}\int_0^{\mu^{-1}} ds s^3 \frac{(1-\mu^2 s^2)^2}{(1-s^6)^{\frac{1}{2}}}\right), \tag{8.3.34}$$

where note that $\mu = m\tilde{z}$ depends on $\tilde{z}$ implicitly. The integral can be computed resulting in

$$\begin{aligned}\int_0^{\mu^{-1}} ds s^3 \frac{(1-\mu^2 s^2)^2}{(1-s^6)^{\frac{1}{2}}} &= \frac{1}{24\mu^4}\left(16\mu^3(-\mu^3+\sqrt{\mu^6-1})\right. \\ &\left. + 6\,{}_2F_1\left(\frac{1}{2},\frac{2}{3},\frac{5}{3},\frac{1}{\mu^6}\right) + 3\,{}_2F_1\left(\frac{1}{2},\frac{4}{3},\frac{7}{3},\frac{1}{\mu^6}\right)\right)\end{aligned} \tag{8.3.35}$$

and expanding for $\mu \gg 1$ one finds

$$\frac{l}{2} = \tilde{z}\left(\frac{\sqrt{\pi}\Gamma(\frac{2}{3})}{\Gamma(\frac{1}{6})} + \frac{t_0}{576 m^4 \tilde{z}^4}\right). \tag{8.3.36}$$

For the small mass case the situation is more complicated, since from equation (8.3.32) we find that the turning point of the surface is itself changed (see Figure 8.3.4). Let the perturbed turning point be

$$z_t = \tilde{z} + t_0 \delta\tilde{z}. \tag{8.3.37}$$

The latter is computed by setting $z' = 0$ in (8.3.32), resulting in

$$t_0 \delta\tilde{z} = \frac{1}{2}\tilde{z}h(\tilde{z}). \tag{8.3.38}$$

Note that the shift in the turning point depends on the metric perturbation $h(z)$ explicitly, rather than the gauge independent combination.

The relation between l and z_t is now calculated using the relation (8.3.32) which can be rewritten as

$$z^3 z' = \left((1+h(\tilde{z}))(z_t^6 - z^6) - f(z)(z_t^6 - z^6) + H(z)(4\tilde{z}^6 - z^6)\right)^{\frac{1}{2}}, \tag{8.3.39}$$

where we define

$$h(z) = H(z) + h(\tilde{z}), \tag{8.3.40}$$

with $H(\tilde{z})$ by construction being zero. In relation (8.3.39) we implicitly work to first order in t_0, which in particular implies that $\tilde{z}$ can be replaced by z_t in terms multiplying $f(z)$ and $H(z)$, which are already of order t_0. Therefore

$$\frac{l}{2} = \frac{1}{(1+h(\tilde{z}))^{\frac{1}{2}}}\int_0^{z_t}\frac{z^3 dz}{(z_t^6 - z^6)^{\frac{1}{2}}} + \frac{1}{2}\int_0^{z_t} z^3 dz \frac{(f + zH')}{(z_t^6 - z^6)^{\frac{1}{2}}} - \frac{1}{2}\left[\frac{z^4 H}{(\tilde{z}^6 - z^6)^{\frac{1}{2}}}\right]_0^{z_t}. \tag{8.3.41}$$

The boundary term vanishes at $z = 0$ and the contribution at $z = z_t$ is zero since $H(z_t) = 0$ to order t_0. Since $h'(z) = H'(z)$ the combination appearing in the second integral is the gauge invariant combination as before and therefore

$$\frac{l}{2} = z_t(1 - \frac{1}{2}h(\tilde{z}))\int_0^1 \frac{s^3 ds}{(1-s^6)^{\frac{1}{2}}} + \frac{z_t}{24}t_0\int_0^1 ds \frac{s^3(1-\mu^2 s^2)^2}{(1-s^6)^{\frac{1}{2}}}. \tag{8.3.42}$$

where now $\mu \equiv m z_t$. Computing the integrals we obtain

$$\begin{aligned} l &= z_t(1 - \frac{1}{2}h(\tilde{z}))\frac{2\sqrt{\pi}\Gamma(\frac{2}{3})}{\Gamma(\frac{1}{6})} \\ &\quad + \frac{t_0 z_t}{12}\left(\frac{\sqrt{\pi}\Gamma(\frac{2}{3})}{\Gamma(\frac{1}{6})} - \frac{2\mu^2}{3} + \frac{\mu^4\sqrt{\pi}\Gamma(\frac{4}{3})}{6\Gamma(\frac{11}{6})}\right). \end{aligned} \tag{8.3.43}$$

Note that $h(\tilde{z}) = h(z_t)$ at this order.

Even though we only needed the original entangling surface to compute the entanglement entropy above, these changes to the turning point are important to keep track of when comparing the differential entropy to the gravitational entropy of the corresponding hole in the bulk, as we will discuss in Section 8.7.

8.3.3 Finite Contributions

To understand the infra-red behaviour of the entanglement entropy it is often useful to isolate the finite contributions.

A dimensionless, cut-off independent quantity was defined in [243, 244] by differentiating with respect to the mass as

$$S_m = m^4 \frac{\partial^2 S}{\partial (m^2)^2}. \tag{8.3.44}$$

Note that this expression is valid for four-dimensional quantum field theories, with different expressions being proposed in lower dimensions. Implicitly, ϵ and $\tilde{z}$ (or equivalently l) are held fixed. A priori, since the gauge dependent terms depend on the mass it is not obvious that this quantity will be independent of the gauge. However, on general grounds the gauge dependent terms must make the form

$$\delta S_{\text{gauge}} = a_{-2} \frac{L^2}{\epsilon^2} + a_0 m^2 L^2 + \mathcal{O}(\epsilon^2) \tag{8.3.45}$$

with a_{-2} and a_0 dimensionless coefficients. This form follows from the fact that the entanglement entropy is extensive, i.e. it is proportional to the area of each slab L^2, and the underlying theory is conformal. This implies that the only finite terms in the scheme dependent part of the entanglement entropy must be proportional to $m^2 L^2$, since m is the only other cutoff independent scale in the problem. Since neither a_{-2} nor a_0 contribute to (8.3.44), the quantity computed by (8.3.44) is indeed independent of the gauge.

Computing this quantity one finds that for $\mu \leq 1$

$$\delta S_m = \frac{t_0 L^2}{48 G_N} \left(\frac{\sqrt{\pi}\Gamma(\frac{1}{3})}{6\Gamma(\frac{11}{6})} m^4 \tilde{z}^2 \right) \tag{8.3.46}$$

while for $\mu \geq 1$

$$\delta S_m = \frac{t_0 L^2}{32 G_N} \frac{\mu^2}{3\tilde{z}^2} {}_2F_1[-1/2, 1/3, 4/3, 1/\mu^6] \tag{8.3.47}$$

which can be expanded for $\mu \gg 1$

$$\delta S_m = \frac{t_0 L^2}{48 G_N} \left(m^2 - \frac{1}{8 m^4 \tilde{z}^6} + \mathcal{O}\left(\frac{1}{m^{10} \tilde{z}^{12}} \right) \right) \tag{8.3.48}$$

For slab geometries an alternative method of defining a cut-off independent quantity is (see for example [245–248][2])

$$S_l = l \frac{\partial S}{\partial l}. \tag{8.3.49}$$

[2] S_l is always positive and decreasing in two dimensions and plays the role of a c-function.

This quantity is manifestly independent of the coordinate choice $h(z)$, since δS_{gauge} is a local quantity, which is hence independent of the (non-local) slab width l, as we saw explicitly below (8.3.26). For $\mu \leq 1$ this quantity evaluates to

$$\delta S_l = \frac{t_0 L^2}{48 G_N}\left(-\frac{\sqrt{\pi}}{6\tilde{z}^2}\frac{\Gamma(-\frac{1}{3})}{\Gamma(\frac{7}{6})} + \frac{\sqrt{\pi}\Gamma(\frac{1}{3})}{6\Gamma(\frac{11}{6})} m^4 \tilde{z}^2 \right) \tag{8.3.50}$$

while for $\mu \gg 1$ one obtains

$$\delta S_l = \frac{t_0 L^2}{48 G_N}\left(\frac{1}{8 m^4 \tilde{z}^6} + \mathcal{O}\left(\frac{1}{m^{10}\tilde{z}^{12}} \right) \right). \tag{8.3.51}$$

The limit $\mu \gg 1$ probes the IR of the theory: for fixed m this corresponds to taking an entangling surface which extends deep into the bulk. Therefore a finite quantity should in this limit decouple from UV physics. Comparing (8.3.48) and (8.3.51), the first quantity does not fulfil this criterion (as the term of order m^2 derives from the logarithmic divergence) whereas the latter quantity does. We will hence use (8.3.51) in Section 8.6 when discussing the IR physics.

8.3.4 Phase Transitions

The flavour contributions to the entanglement entropy (8.3.28) and (8.3.29) match at $m\tilde{z} = 1$, i.e. when the turning point of the entangling surface is at the location where the metric perturbation vanishes. This matching was guaranteed by the continuity of the metric perturbation and its derivative at $z = 1/m$. There are however discontinuities in the derivatives of the flavour contribution at $m\tilde{z} = 1$, induced by the discontinuities of higher derivatives of the metric perturbation at $z = 1/m$. In particular, there is a discontinuity in the fourth derivative of the entanglement entropy with respect to the slab width (at fixed mass)

$$\left(\frac{\partial^4 S}{\partial l^4}\right)_{m\tilde{z}=1} \tag{8.3.52}$$

From the field theory perspective it is more natural to fix the mass (i.e. the theory) and vary the slab width (i.e. the entangling region). However, if one instead looks at the variation of the entanglement entropy with respect to the mass at fixed slab width, the fourth derivative is also discontinuous

$$\left(\frac{\partial^4 S}{\partial m^4}\right)_{m\tilde{z}=1} \tag{8.3.53}$$

Correspondingly the finite quantities δS_m and δS_l have discontinuities in their second and third derivatives, respectively.

The discontinuity arises from the discontinuity in second derivatives of the metric at

$z = 1/m$. The fourth derivative of the entanglement entropy contains the terms

$$\left(\frac{\partial^4 S}{\partial l^4}\right)_{\tilde{z}=1/m} \sim \frac{1}{8G_N}\left(\frac{\partial \tilde{z}}{\partial l}\right)^4_{\tilde{z}=1/m} \frac{\partial^3}{\partial \tilde{z}^3}\left(\sqrt{\gamma}T^{\mu\nu}_{\min}h^E_{\mu\nu}(\tilde{z})\right)_{\tilde{z}=1/m} \tag{8.3.54}$$

Note that the discontinuity does not arise at lower order in derivatives since the volume element of the entangling surface vanishes at the turning point.

At first sight one might try to assign a physical interpretation to the discontinuity of the entanglement entropy, i.e. a phase transition. However, the discontinuity is inherited from the discontinuity in the metric derivatives and correspondingly in the curvature. This discontinuity is likely to be an artefact of the probe approximation: in a fully back-reacted solution for the D3 and D7 branes there should be no source terms in the energy momentum tensor and hence no discontinuities in the curvature of the metric. In other words, one would expect from gauge/gravity duality that the backreacted solution should solve the type IIB equations with no sources. The metric and curvature should hence be continuous and the metric for the back-reacted solution should be smoothened around $z = 1/m$, over a radial coordinate range $\Delta z \ll 1/m$.

It is interesting to note that at any finite density the brane probe extends throughout the bulk and therefore there is no longer any discontinuity at finite z: as we show in Section 8.5 the backreacted solution is indeed smoothened around $z = 1/m$, over a small but finite radial coordinate range.

8.4 Entanglement Entropy for Spherical Regions

In this section we compute the entanglement entropy for the case of a spherical entangling surface, extending the small mass results of [214] to generic mass. The methods of [212, 214, 215] are in principle applicable to spherical entangling regions but in practice the CHM map [187] becomes intractable for finite mass, as the probe brane embedding in the hyperbolic black hole is extremely complicated. Therefore again our discussion will follow closely the method of [213].

Writing the boundary metric in spherical coordinates we have

$$ds^2 = \frac{1}{z^2}(-dt^2 + dr^2 + r^2 d\Omega_2^2 + dz^2) \tag{8.4.1}$$

for the AdS_5 metric. We define a ball on the boundary by $r \leq R$ and take as an embedding ansatz $z = z(r)$ at $t = 0$. The functional for the entangling surface is then

$$S = \frac{\pi}{G_N}\int_0^R dr \frac{\sqrt{1 + z'^2}}{z^3} r^2, \tag{8.4.2}$$

where we have done the trivial integral over the two-sphere. It is easy to show that

the resulting equations of motion are solved by the hemisphere $r^2 + z^2 = R^2$, and the desired extremal surface is thus a hemisphere in r and z of radius R that wraps the 2-sphere S^2 - this surface will be parametrised by $\{s, \Omega_2\}$ where s is defined by $z = Rs$ and $r = R\sqrt{1-s^2}$ and $\Omega_2 = (\theta, \phi)$.

We can now compute the induced metric on this extremal surface using the expression $\gamma_{ab}^{min} = \partial_a X^\mu \partial_b X^\nu g_{\mu\nu}$ where now $a, b = (s, \theta, \phi)$. One finds

$$\gamma_{ab}^{min} = \left(\frac{1}{s^2(1-s^2)}, \frac{(1-s^2)}{s^2} g_{S^2} \right) \tag{8.4.3}$$

where we note for further use that

$$\sqrt{\gamma^{min}} = \frac{\sqrt{1-s^2}}{s^3} \sqrt{g_{S^2}}. \tag{8.4.4}$$

We can then compute the stress tensor of the surface and one finds (computing only the diagonal components since this quantity will be contracted with $h_{\mu\nu}^E$ which is diagonal)

$$T_{min}^{\mu\nu} = \left(s^2 R^2 (1-s^2), 0, R^2 s^4, \frac{s^2}{1-s^2}, \frac{s^2}{1-s^2} \text{cosec}^2(\theta) \right). \tag{8.4.5}$$

We are now in a position to compute the entanglement entropy, but we must first write the metric backreaction in the coordinate system (z, t, r, θ, ϕ)

$$h_{\mu\nu}^E = \frac{1}{z^2} \text{diag}\left(f(z), h(z), h(z), h(z) g_{S^2} \right). \tag{8.4.6}$$

The resulting entanglement entropy becomes

$$\delta S = \frac{\pi}{2G_N} \int_a^b ds \frac{\sqrt{1-s^2}}{s^3} \left((s^2+2) h(Rs) - (s^2-1) f(Rs) \right) \tag{8.4.7}$$

where $a \equiv \epsilon/R$ and $b = 1, 1/\mu$ for $\mu < 1, \mu > 1$ respectively as for the slab, where now $\mu \equiv mR$. Expanding out $f(Rs)$ and again using partial integration on the $h'(Rs)$ term as in the slab case one obtains

$$\delta S = \frac{\pi}{2G_N} \int_a^b ds \frac{(1-s^2)^{3/2}}{s^3} \tilde{f}(Rs) - \frac{\pi}{2G_N} \left[h(Rs) \frac{(1-s^2)^{3/2}}{s^2} \right]_a^b \tag{8.4.8}$$

again reducing the contribution of $h(z)$ to a boundary term. The term at $s = b$ vanishes for both possible values of b for the same reasons as before, leading to

$$\delta S = \frac{t_0 \pi}{24 G_N} \int_a^b ds \frac{(1-s^2)^{3/2}}{s^3} \left(1 - (\mu s)^2 \right)^2 + \frac{\pi}{2G_N} h(\epsilon) \frac{1}{a^2} \left(1 - a^2 \right)^{3/2}. \tag{8.4.9}$$

Since $h(\epsilon)$ depends upon the gauge choice, we can rewrite this expression as in the pre-

vious section as

$$\delta S = \frac{t_0\pi}{24G_N}\int_a^b ds\frac{(1-s^2)^{3/2}}{s^3}\left(1-(\mu s)^2\right)^2 + \delta S_{\rm gauge}(\epsilon,R,m). \tag{8.4.10}$$

The gauge dependent contribution depends in this case on all three parameters: the cutoff ϵ, the mass m and the radius of the spherical region R (note that in the previous expression the mass dependence is contained implicitly in the metric function $h(z)$). Note the difference relative to the case of the slab: since the dual theory is local, the gauge dependent terms for the slab cannot depend on the slab width. The radius of the sphere however relates to the intrinsic curvature of the entangling region, which is a local quantity and therefore can appear in the gauge dependent terms. In particular, since $h(0)$ is finite, the non-vanishing terms in $\delta S_{\rm gauge}$ will be either quadratic in R or independent of R in any scheme.

Let us now consider the small and large mass cases separately. For $\mu \leq 1$ the contribution from the $s=b$ limit to the integral vanishes where $b=1$. One therefore obtains

$$\delta S = \frac{t_0\pi}{8G_N}\left(\frac{R^2}{6\epsilon^2}+\frac{4\mu^2+3}{6}\log\frac{\epsilon}{2R}+\frac{1}{4}+\frac{8\mu^2}{9}+\frac{\mu^4}{15}\right)+\delta S_{\rm gauge}(\epsilon,R,m). \tag{8.4.11}$$

Using the same regularisation scheme as before to fix $h(\epsilon)$ one obtains as in [214]

$$\delta S = \frac{t_0\pi}{8G_N}\left(\frac{R^2}{2\epsilon^2}+\frac{4\mu^2+3}{6}\log\frac{\epsilon}{2R}-\frac{1}{4}+\frac{2\mu^2}{3}+\frac{\mu^4}{15}\right), \tag{8.4.12}$$

where

$$\delta S_{\rm gauge}(\epsilon,R,m) = \frac{\pi t_0}{24G_N}\left(\frac{R^2}{\epsilon^2}-\frac{2}{3}\mu^2-\frac{3}{2}+\cdots\right). \tag{8.4.13}$$

For $\mu \geq 1$ the extra contribution from the $s=b$ limit of integration is given by

$$\frac{t_0\pi}{24G_N}\left(-\sqrt{1-\frac{1}{\mu^2}}\left(\frac{8}{15}+\frac{83\mu^2}{30}+\frac{\mu^4}{5}\right)+\frac{1}{2}(3+4\mu^2)\log\left(\mu+\mu\sqrt{1-\frac{1}{\mu^2}}\right)\right). \tag{8.4.14}$$

This vanishes at $\mu=1$ as we would expect by continuity. Thus the total contribution to the entanglement entropy for $\mu \geq 1$ is given by

$$\begin{aligned}\delta S \;=\; & \frac{t_0\pi}{8G_N}\left(\frac{R^2}{6\epsilon^2}+\frac{4\mu^2+3}{6}\log\frac{\epsilon}{2R}+\frac{1}{4}+\frac{8\mu^2}{9}+\frac{\mu^4}{15}\right. \\ & -\frac{1}{3}\sqrt{1-\frac{1}{\mu^2}}\left(\frac{8}{15}+\frac{83\mu^2}{30}+\frac{\mu^4}{5}\right)+\frac{1}{6}(3+4\mu^2)\log\left(\mu+\mu\sqrt{1-\frac{1}{\mu^2}}\right)\Bigg) \\ & +\delta S_{\rm gauge}(\epsilon,R,m).\end{aligned} \tag{8.4.15}$$

For $\mu \gg 1$ this expression asymptotes to

$$\delta S = \frac{t_0 \pi}{8 G_N}\left(\frac{R^2}{6\epsilon^2}+\left(\frac{2\mu^2}{3}+\frac{1}{2}\right)\log(m\epsilon)+\frac{3}{8}-\frac{1}{48\mu^2}+\mathcal{O}\left(\frac{1}{\mu^4}\right)\right) + \delta S_{\text{gauge}}(\epsilon, R, m). \tag{8.4.16}$$

As for the slab, the expressions for the entanglement entropy match at $\mu = 1$, i.e. when the turning point of the entangling surface reaches $z = 1/m$. Derivatives of the entanglement entropy with respect to R at fixed m or with respect to m at fixed R become discontinuous at $\mu = 1$ because of the metric discontinuity. For spherical entangling surfaces the discontinuity arises at fifth order i.e.

$$\left(\frac{\partial^5 S}{\partial R^5}\right)_{m=1/R} \tag{8.4.17}$$

is discontinuous. The discontinuity again arises from the discontinuity in second derivatives of the metric at $z = 1/m$, and is hence expected to be absent in a fully back-reacted solution without sources. The fifth derivative of the entanglement entropy contains the terms

$$\left(\frac{\partial^4 S}{\partial l^4}\right)_{\tilde{z}=1/m} \sim \frac{1}{8G_N}\frac{\partial^4}{\partial \tilde{z}^4}\left(\sqrt{\gamma} T^{\mu\nu}_{\min} h^E_{\mu\nu}(\tilde{z})\right)_{\tilde{z}=1/m}. \tag{8.4.18}$$

Note that the discontinuity does not arise at lower order in derivatives since the terms contracted with the metric perturbation are zero when the turning point lies at $\tilde{z} = 1/m$, and their first derivative is also zero; see the form of the integrand in (8.4.8).

8.4.1 Finite Contributions

For a spherical region one can define a finite quantity by differentiating with respect to the mass, (8.3.44). For $\mu \leq 1$ this gives

$$\delta S_m = \frac{\pi t_0}{60 G_N}\mu^4. \tag{8.4.19}$$

For $\mu \gg 1$ one obtains

$$\delta S_m = -\frac{\pi t_0}{8 G_N}\left(\frac{\mu^2}{3}-\frac{1}{4}-\frac{1}{24\mu^2}+\mathcal{O}\left(\frac{1}{\mu^4}\right)\right). \tag{8.4.20}$$

The quantity (8.3.49) is not finite for a spherical region and it is proposed to use instead [249, 250]

$$S_{LM} = R\frac{\partial}{\partial R}\left(R\frac{\partial}{\partial R}-2\right)S. \tag{8.4.21}$$

Note that this quantity vanishes for all terms which are independent of R or quadratic in R, which in particular guarantees that the gauge dependent terms drop out of S_{LM}.

For $\mu \leq 1$ one obtains

$$\delta S_{LM} = \frac{\pi t_0}{8G_N}\left(1 - \frac{4}{3}\mu^2 + \frac{8}{15}\mu^4\right). \tag{8.4.22}$$

For $\mu \gg 1$ one obtains

$$\delta S_{LM} = \frac{\pi t_0}{48G_N\mu^2} + \cdots, \tag{8.4.23}$$

with all terms with higher order powers in μ cancelling.

As for the slab the limit $\mu \gg 1$ probes the IR of the theory: for fixed m this corresponds to taking an entangling surface which extends deep into the bulk. Therefore a finite quantity should in this limit decouple from UV physics. Comparing (8.4.20) and (8.4.23), the first quantity again does not fulfil this criterion (as the term of order m^2 derives from the logarithmic divergence) whereas the latter quantity does. We will hence use (8.4.23) in Section 8.6 when discussing the IR physics.

8.5 Entanglement Entropy from Kaluza-Klein Holography

In this section we describe a new method for computing the entanglement entropy of probe brane systems using Kaluza-Klein holography [24]. This method is applicable to any probe brane system, i.e. for any shape entangling region with any worldvolume gauge fields, and can also be used for other systems such as Coulomb branch geometries.

The holographic entanglement entropy for any static asymptotically anti-de Sitter geometry is given by the Ryu-Takayanagi functional in terms of the area of a minimal surface in the Einstein frame metric. Probe brane systems are however described by top-down constructions. In other words, we first specify a ten-dimensional supergravity solution for which a holographic interpretation is known, the usual examples being geometries which are asymptotic to the products of anti-de Sitter and Sasaki-Einstein manifolds. The probe system is then specified by the brane embedding into the ten-dimensional background and the worldvolume fields on the brane. The backreaction onto the ten-dimensional supergravity solution is computed by viewing the D-brane action as sourcing the supergravity fields, with the sources being localised on the brane embedding. Computation of the backreaction therefore involves solving all of the ten-dimensional supergravity equations.

Even after computing the backreacted ten-dimensional supergravity solution, one cannot immediately compute the entanglement entropy, because the latter requires the five-dimensional Einstein metric. For any supergravity solution which can be viewed as a perturbation of anti-de Sitter cross a Sasaki-Einstein manifold the method of Kaluza-Klein holography can however be used to extract the five-dimensional Einstein metric [24]. This method implies that, if one only wishes to compute the entanglement entropy, it is not actually necessary to compute all of the backreaction of the brane onto

the ten-dimersional supergravity fields: one only needs to know the backreaction for those field components which contribute to the five-dimensional Einstein metric.

In the rest of the section we will describe the computation of the entanglement entropy using the Kaluza-Klein holography approach for massive D7-branes in an $AdS_5 \times S^5$ background. At the end of the section we will discuss further applications and generalisations of this method.

8.5.1 Kaluza-Klein Holography

The backreaction of the D7-branes onto $AdS_5 \times S^5$ results in a supergravity background which can be expressed as a perturbation of $AdS_5 \times S^5$. Thus the metric can be expressed as

$$\begin{aligned} ds^2 &= (g^o_{MN} + h_{MN}) dx^M dx^N; \\ &= \frac{1}{z^2}(dz^2 + dx^\mu dx_\mu) + (d\theta^2 + \sin^2\theta d\Omega_3^2 + \cos^2\theta d\phi^2) + h_{MN}(x^m, \theta_a) dx^M dx^N, \end{aligned} \tag{8.5.1}$$

where we denote ten-dimensional indices as x^M; θ^a collectively denote the five sphere coordinates and x^m denote the five-dimensional coordinates, i.e. (z, x^μ). Thus g^o_{MN} is the background $AdS_5 \times S^5$ metric and h_{MN} is the metric perturbation. The other type IIB supergravity fields are the dilaton ϕ, the NS-NS three form field strength H_{MNP} and the RR field strengths F_M, F_{MNP} and F_{MNPQR}. Only the self-dual five-form field strength has a background profile

$$\begin{aligned} F_{MNPQR} &= F^o_{MNPQR} + f_{MNPQR}; \\ F^o &= \frac{1}{z^5} dz \wedge dt \wedge dw \wedge dx \wedge dy + \sin^3\theta \cos\theta d\theta \wedge d\Omega_3 \wedge d\phi, \end{aligned} \tag{8.5.2}$$

with f_{MNPQR} being the perturbation of the five form field strength. Our normalisation conventions are that the Einstein equations for type IIB supergravity are given by

$$R_{MN} = \frac{1}{6} F_{MPQRS} F_N^{\ PQRS} + \cdots \tag{8.5.3}$$

The Einstein equations are quadratic in the dilaton gradients and form field strengths. Therefore, working to linearized order in the perturbations, the Einstein equation decouples from the perturbations of ϕ, H_{MNP}, F_M and F_{MNP} since the latter do not have profiles in the $AdS_5 \times S^5$ background. Similarly the only contributions to the five-form equation of motion at linearised order are from the metric perturbations and the five-form field strength perturbations.

The fluctuations can be expanded in S^5 harmonics [36]

$$\begin{aligned} h_{mn}(x,y) &= \sum h^{I_1}_{mn}(x)Y^{I_1}(y) \\ h_{ma}(x,y) &= \sum (B^{I_5}_{(v)m}(x)Y^{I_5}_a(y) + B^{I_1}_{(s)m}(x)D_aY^{I_1}(y)) \\ h_{(ab)}(x,y) &= \sum (\phi^{I_{14}}_{(t)}(x)Y^{I_{14}}_{(ab)}(y) + \phi^{I_5}_{(v)}(x)D_{(a}Y^{I_5}_{b)}(y) + \phi^{I_1}_{(s)}(x)D_{(a}D_{b)}Y^{I_1}(y)) \\ h^a_a(x,y) &= \sum \pi^{I_1}(x)Y^{I_1}(y) \end{aligned} \tag{8.5.4}$$

and

$$\begin{aligned} f_{mnrst}(x,y) &= \sum 5D_{[m}b^{I_1}_{nrst]}(x)Y^{I_1}(y) \\ f_{amnrs}(x,y) &= \sum (b^{I_1}_{mnrs}(x)D_aY^{I_1}(y) + 4D_{[m}b^{I_5}_{nrs]}(x)Y^{I_5}_a(y)) \\ f_{abmnr}(x,y) &= \sum (3D_{[m}b^{I_{10}}_{nr]}(x)Y^{I_{10}}_{[ab]}(y) - 2b^{I_5}_{mnr}(x)D_{[a}Y^{I_5}_{b]}(y)) \\ f_{abcmn}(x,y) &= \sum (2D_{[m}b^{I_5}_{n]}(x)\epsilon_{abc}{}^{de}D_dY^{I_5}_e(y) + 3b^{I_{10}}_{mn}(x)D_{[a}Y^{I_{10}}_{bc]}(y)) \\ f_{abcdm}(x,y) &= \sum (D_mb^{I_1}_{(s)}(x)\epsilon_{abcd}{}^eD_eY^{I_1}(y) + (\Lambda^{I_5}-4)b^{I_5}_m(x)\epsilon_{abcd}{}^eY^{I_5}_e(y)) \\ f_{abcde}(x,y) &= \sum b^{I_1}_{(s)}(x)\Lambda^{I_1}\epsilon_{abcde}Y^{I_1}(y) \end{aligned} \tag{8.5.5}$$

Numerical constants in these expressions are inserted so as to match with the conventions of [36]. Parentheses denote a symmetric traceless combination (i.e. $A_{(ab)} = 1/2(A_{ab}+A_{ba}) - 1/5 g_{ab}A^a_a$). $Y^{I_1}, Y^{I_5}_a, Y^{I_{14}}_{(ab)}$ and $Y^{I_{10}}_{[ab]}$ denote scalar, vector and tensor harmonics whilst Λ^{I_1} and Λ^{I_5} are the eigenvalues of the scalar and vector harmonics under (minus) the d'Alembertian. The subscripts t, v and s denote whether the field is associated with tensor, vector or scalar harmonics respectively, whilst the superscript of the harmonic label I_n derives from the number of components n of the harmonic.

Not all fluctuations are independent - some are diffeomorphic to each other or to the background. This issue can be dealt with by imposing a gauge; for example, the de Donder-Lorentz gauge fixing condition is

$$D^a h_{(ab)} = D^a h_{am} = 0 \tag{8.5.6}$$

which sets to zero the coefficients $B^{I_1}_{(s)m}, \phi^{I_5}_{(v)}, \phi^{I_1}_{(s)}$. A more elegant way of dealing with this issue is to construct gauge invariant combinations of the fluctuations. Such gauge invariant combinations of the fluctuations were constructed in [24], with the combinations reducing to the de Donder-Lorentz gauge fluctuations on imposing this gauge.

In [24] the equations of motion satisfied by the fluctuations were constructed to quadratic order in the fluctuations, and the relation between five-dimensional fields and ten-dimensional fields was also constructed up to quadratic order in the fluctuations. In the current context we are only interested in the five-dimensional Einstein metric and we work only to linear order in the fluctuations. We can therefore read off from [24, 36]

the relationship between the five-dimensional Einstein metric perturbation h^E_{mn} and the ten-dimensional fields as

$$h^E_{mn} = h^0_{mn} + \frac{1}{3}\pi^0 g^o_{mn}, \tag{8.5.7}$$

where the superscripts indicate that these are zero modes, i.e. associated with the trivial constant scalar harmonic.

The type IIB supergravity equations lead to the linearized equation for the Einstein metric

$$(\mathcal{L}_E + 4)h^E_{mn} = 0, \tag{8.5.8}$$

where $\mathcal{L}_E$ is the Einstein operator, defined as usual by

$$\mathcal{L}_E h^E_{mn} = \frac{1}{2}\left(-\Box h^E_{mn} + D_p D_m h^{Ep}_n + D_p D_n h^{Ep}_m - D_m D_n h^{Ep}_p\right). \tag{8.5.9}$$

The five-dimensional equation of motion in turn can be seen to follow from reducing the ten-dimensional action

$$I_{IIB} = \frac{1}{2\kappa^2_{10}}\int d^{10}x\sqrt{-\det(g_{MN})}\left(R(g_{MN}) - \frac{4}{5!}F_{MNPQR}F^{MNQR} + \cdots\right) \tag{8.5.10}$$

over the five-sphere[3]. This results in

$$I = \frac{N_c^2}{2\pi^2}\int d^5x\sqrt{-\det(g_{mn})}\left(\frac{1}{4}R(g_{mn}) + \cdots\right), \tag{8.5.11}$$

where we use the relation

$$\frac{1}{2\kappa^2_{10}}V_{S^5} = \frac{\pi^3}{2\kappa^2_{10}} = \frac{1}{2\kappa^2_5} = \frac{N_c^2}{8\pi^2}, \tag{8.5.12}$$

which is applicable when the AdS radius L is set to one. Thus the effective Newton constant is given by

$$\frac{1}{16\pi G_N} = \frac{N_c^2}{8\pi^2}. \tag{8.5.13}$$

For the probe brane system, the type IIB supergravity equations are solved with source terms, from the D-brane action, which in turn implies that the linearized Einstein equations in five dimensions are sourced. The complete ten-dimensional action is

$$I = I_{IIB} + I_{D7} \tag{8.5.14}$$

where

$$I_{D7} = -T_7\int d^{10}x\int d^8\sigma\delta(x^M - X^M(\sigma^\alpha))e^{-\phi}\sqrt{-\det(g_{MN}\partial_\alpha X^M\partial_\beta X^N) + \cdots}. \tag{8.5.15}$$

[3]Note that the 10d action must be supplemented with a self-duality constraint for the five form field strength.

Here σ^α denote the world-volume coordinates and the ellipses denote terms involving the world-volume gauge fields and Wess-Zumino couplings. The latter do not contribute in the case of the D7-brane embeddings under consideration here.

The source term results in a stress energy tensor [251]

$$T^{MN} = -T_7 \int d^8\sigma \sqrt{-\gamma} e^{-\phi} (\gamma^{\alpha\beta} \partial_\alpha X^M \partial_\beta X^N) \frac{\delta(x^M - X^M(\sigma^\alpha))}{\sqrt{-\det(g_{MN})}}, \tag{8.5.16}$$

where we denote the worldvolume induced metric as $\gamma_{\alpha\beta} = g_{MN}\partial_\alpha X^M \partial_\beta X^N$. The sourced IIB equation is thus

$$(R_{MN} - \frac{1}{6} F_{MPQRS} F_N^{\ PQRS} + \cdots) = \kappa_{10}^2 (T_{MN} - \frac{1}{8} T g_{MN}) \equiv \kappa_{10}^2 \bar{T}_{MN}, \tag{8.5.17}$$

with $T = g^{MN} T_{MN}$. The trace adjusted stress energy tensor can be expanded in S^5 harmonics, using the same harmonic basis as for the metric:

$$\begin{aligned}
\bar{T}_{mn}(x,y) &= \sum \bar{T}^{I_1}_{mn}(x) Y^{I_1}(y) \\
\bar{T}_{ma}(x,y) &= \sum (\tilde{T}^{I_5}_{(v)m}(x) Y^{I_5}_a(y) + \tilde{T}^{I_1}_{(s)m}(x) D_a Y^{I_1}(y)) \\
\bar{T}_{(ab)}(x,y) &= \sum \bar{T}^{I_{14}}_{(t)}(x) Y^{I_{14}}_{(ab)}(y) + \bar{T}^{I_5}_{(v)}(x) D_{(a} Y^{I_5}_{b)}(y) + \bar{T}^{I_1}_{(s)}(x) D_{(a} D_{b)} Y^{I_1}(y)) \\
\bar{T}^a_a(x,y) &= \sum \tilde{T}^{I_1}(x) Y^{I_1}(y)
\end{aligned} \tag{8.5.18}$$

The correction to the five-dimensional Einstein equation only depends on the following zero modes (see Appendix 8.A):

$$(\mathcal{L}_E + 4) h^E_{mn} = \kappa_{10}^2 (\bar{T}^0_{mn} + \frac{1}{3} \tilde{T}^0 g^o_{mn}) \equiv \bar{t}_{mn}, \tag{8.5.19}$$

where we have used the fact that the D7-brane embedding of interest does not source the RR five-form field strength.

Given the D7-brane embedding, i.e. $\theta(z) = \cos^{-1}(mz)$, the ten-dimensional energy momentum tensor source can be computed as

$$T_{MN} = -T_7 \mathcal{T}_{MN} \delta(\theta - \theta(z)) \delta(\phi), \tag{8.5.20}$$

with

$$\begin{aligned}
\mathcal{T}_{zz} &= \frac{1}{z^2}(1 - m^2 z^2)^2; \qquad \mathcal{T}_{\mu\nu} = \frac{1}{z^2}(1 - m^2 z^2)\eta_{\mu\nu}; \\
\mathcal{T}_{\Omega_3} &= (1 - m^2 z^2)^2 g_{\Omega_3}; \qquad \mathcal{T}_{\phi\phi} = 0; \\
\mathcal{T}_{\theta\theta} &= m^2 z^2 (1 - m^2 z^2).
\end{aligned} \tag{8.5.21}$$

where note that $\mathcal{T} \equiv g^{MN}\mathcal{T}_{MN} = 8(1 - m^2 z^2)$. Here we denote the metric on the unit three-sphere by g_{Ω_3}. The energy momentum tensor source can be projected onto

spherical harmonics using Fourier decompositions of the delta functions:

$$\begin{aligned}\delta(\theta-\theta(z)) &= \frac{2}{\pi}+\sum_{m=1}^{\infty}\frac{4}{\pi}\cos(m\theta(z))\cos(m\theta);\\ \delta(\phi) &= \frac{1}{2\pi}+\sum_{m=1}^{\infty}\frac{1}{\pi}\cos(m\phi).\end{aligned} \tag{8.5.22}$$

By projecting onto the zero mode, one then immediately shows that the ten-dimensional energy momentum tensor source is such that

$$\bar{T}^0_{zz}=-T_7\frac{m^2}{\pi^2}(1-m^2z^2);\qquad \bar{T}^0_{\mu\nu}=0, \tag{8.5.23}$$

with

$$\bar{T}^0=\frac{T_7}{\pi^2}(1-m^2z^2)(m^2z^2-2), \tag{8.5.24}$$

and hence using (8.5.19) we find that

$$\bar{t}_{zz}=-\frac{t_0}{3z^2}(1-m^4z^4);\qquad \bar{t}_{\mu\nu}=\frac{t_0}{6z^2}(1-m^2z^2)(m^2z^2-2)\eta_{\mu\nu}, \tag{8.5.25}$$

where as before

$$t_0=16\pi G_N(2\pi^2T_7). \tag{8.5.26}$$

Given the five-dimensional stress tensor $t_{mn}=\bar{t}_{mn}-\frac{1}{2}\bar{t}g^o_{mn}$, it is straightforward to see that the perturbation of the Einstein metric induced by this source is in agreement with that given in (8.3.14) and (8.3.18).

8.5.2 Generalizations to Other Probe Brane Systems

For a general probe brane system, the complete ten-dimensional action is

$$I=I_{IIB}+I_{Dp} \tag{8.5.27}$$

where

$$\begin{aligned}I_{Dp} &= -T_p\int d^{10}x\int d^{p+1}\sigma\delta(x^M-X^M(\sigma^\alpha))e^{-\phi}\sqrt{-\det(\gamma_{\alpha\beta}+\mathcal{F}_{\alpha\beta})}\\ &\quad +T_p\int d^{10}x\int\delta(x^M-X^M(\sigma^\alpha))\left[e^{\mathcal{F}}\wedge\sum_q C_q\right],\end{aligned} \tag{8.5.28}$$

with

$$\begin{aligned}\gamma_{\alpha\beta} &= g_{MN}\partial_\alpha X^M\partial_\beta X^N;\\ \mathcal{F}_{\alpha\beta} &= B_{MN}\partial_\alpha X^M\partial_\beta X^N+F_{\alpha\beta};\\ C_{\alpha_1\cdots\alpha_q} &= C_{M_1\cdots M_1}\partial_{\alpha_1}X^{M_1}\cdots\partial_{\alpha_q}X^{M_q}.\end{aligned} \tag{8.5.29}$$

We consider embedding a brane into a type IIB background which is either $AdS_5 \times S^5$ or AdS_5 Schwarzschild $\times S^5$, so that the only background field profiles are for the metric and the five-form. Following the arguments in the previous section, we therefore only need to consider the equations for the metric and five-form perturbations, as the other perturbation equations decouple.

The energy momentum tensor source is [92, 251]

$$T^{MN} = -T_p \int d^{p+1}\sigma \sqrt{-M} e^{-\phi} (M^{\alpha\beta} \partial_\alpha X^M \partial_\beta X^N) \frac{\delta(x^M - X^M(\sigma^\alpha))}{\sqrt{-\det(g_{MN})}}, \tag{8.5.30}$$

where we define $M_{\alpha\beta} = \gamma_{\alpha\beta} + \mathcal{F}_{\alpha\beta}$ with $M^{\alpha\beta}$ being its inverse. The source in the five form equation of motion is

$$\begin{aligned} \partial_M \left(\sqrt{-g} F^{MNPQR}\right) &= 2\kappa_{10}^2 T_p \int d^{p+1}\sigma \delta(x^M - X^M(\sigma^\alpha)) \epsilon^{\alpha_1 \cdots \alpha_{p+1}} \mathcal{F}_{\alpha_1\alpha_2} \\ &\quad \cdots \partial_{\alpha_{p-2}} X^N \partial_{\alpha_{p-1}} X^P \partial_{\alpha_p} X^Q \partial_{\alpha_{p+1}} X^R \end{aligned} \tag{8.5.31}$$

Note that for a D7-brane this term only contributes if $\mathcal{F} \wedge \mathcal{F} \neq 0$. Therefore, provided that $\mathcal{F} \wedge \mathcal{F} = 0$, the correction to the five-dimensional Einstein equation due to source D7-branes still depends only on the stress energy tensor zero modes,

$$(\mathcal{L}_E + 4) h^E_{mn} = \kappa_{10}^2 (\bar{T}^0_{mn} + \frac{1}{3} \bar{T}^0 g^o_{mn}) \equiv \bar{t}_{mn}. \tag{8.5.32}$$

One can thus compute the perturbation to the five-dimensional Einstein metric by projecting the brane energy momentum source onto the appropriate combination of (spherical) zero modes. It would be straightforward to relax the condition $\mathcal{F} \wedge \mathcal{F} = 0$ and obtain the correction to the five-dimensional Einstein equation, taking into account the sources in the RR field equations, but we will not analyse this case in detail here.

The analysis above immediately allows us to treat D7-branes at finite mass, density (and temperature). The finite temperature background can be written as

$$\begin{aligned} ds^2 &= \rho^2 \left[-\frac{f^2}{\tilde{f}} dt^2 + \tilde{f} dx^2 \right] + \frac{d\rho^2}{\rho^2} + d\Omega_5^2; \\ f(\rho) &= 1 - \frac{u_0^4}{\rho^4}; \qquad \tilde{f}(\rho) = 1 + \frac{u_0^4}{\rho^4}. \end{aligned} \tag{8.5.33}$$

with the temperature being $T = \sqrt{2} u_0 / \pi$. The D7-brane embeddings can be expressed in terms of two scalar functions $\chi(\rho)$ and $a(\rho)$:

$$\theta(\rho) = \cos^{-1}(\chi(\rho)); \qquad F_{\rho t} = \partial_\rho a(\rho) \equiv E(\rho), \tag{8.5.34}$$

where the potential is $A_t = a(\rho)$. These embeddings can be found numerically, see

[241, 242]. The main feature is that at any finite density, i.e. whenever the asymptotic form of the potential is

$$A_t = \mu - \frac{\tilde{d}}{\rho^2} + \cdots \tag{8.5.35}$$

with non-zero charge density $\tilde{d}$, the embeddings do not close off at finite radius. At finite temperature the embeddings have a spike which extends into the horizon, while at zero temperature this spike passes through the Poincaré horizon. In other words, asymptotically as $\rho \to \infty$, the brane wraps the equator $\theta = \pi/2$ of the five sphere but there is a spike, $\theta \to 0$ as $\rho \to u_0$. In the zero temperature limit, the spike solution becomes analytic for $\rho \to 0$,

$$E(\rho) \approx \mathcal{E}; \qquad \theta(\rho) \approx \theta_1 \rho, \tag{8.5.36}$$

with $\mathcal{E}$ and θ_1 constant.

Focussing on the zero temperature limit for simplicity, the effective source stress energy tensor of (8.5.32) is given in terms of $\theta(\rho)$ and $E(\rho)$ by

$$\begin{aligned}
\bar{t}_{\rho\rho} &= -t_0 \frac{\sin^3\theta}{2\rho^2(1+\rho^2\dot{\theta}^2 - E^2)^{\frac{1}{2}}}\left(-\frac{2}{3} - \frac{4\rho^2\dot{\theta}^2}{3} + E^2\right); \\
\bar{t}_{tt} &= t_0 \frac{\rho^2\sin^3\theta}{2(1+\rho^2\dot{\theta}^2 - E^2)^{\frac{1}{2}}}\left(-\frac{2}{3} - \frac{\rho^2\dot{\theta}^2}{3} + E^2\right); \\
\bar{t}_{ij} &= -t_0 \frac{\rho^2\sin^3\theta}{2(1+\rho^2\dot{\theta}^2 - E^2)^{\frac{1}{2}}}\left(-\frac{2}{3} - \frac{\rho^2\dot{\theta}^2}{3}\right)\delta_{ij}.
\end{aligned} \tag{8.5.37}$$

Here $\dot{\theta}$ denotes $\partial_\rho\theta(\rho)$. To compare with the previous sections we change coordinates to $z = 1/\rho$, and use the five-dimensional stress tensor $t_{mn} = \bar{t}_{mn} - \frac{1}{2}\bar{t}g^o_{mn}$,

$$\begin{aligned}
t_{zz} &= -t_0 \frac{\sin^3\theta}{2z^2(1+z^2\theta_z^2 - E^2)^{\frac{1}{2}}}; \\
t_{tt} &= t_0 \frac{z^2\sin^3\theta}{2(1+z^2\theta_z^2 - E^2)^{\frac{1}{2}}}\left(1+z^2\theta_z^2\right); \\
t_{ij} &= -t_0 \frac{z^2\sin^3\theta}{2(1+z^2\theta_z^2 - E^2)^{\frac{1}{2}}}\left(1+z^2\theta_z^2 - E^2\right)\delta_{ij},
\end{aligned} \tag{8.5.38}$$

where $\theta_z = \partial_z\theta$.

The metric perturbation induced by such sources can then be expressed as

$$\delta(ds^2) = \frac{f(z)}{z^2}dz^2 - \frac{g(z)}{z^2}dt^2 + \frac{h(z)}{z^2}dx^i dx_i. \tag{8.5.39}$$

As previously the gauge invariant combination is

$$\tilde{f}(z) = f(z) + zh'(z) \tag{8.5.40}$$

and there are now two independent Einstein equations:

$$\begin{aligned} -\tilde{f} - \frac{1}{4}z(g' - h') &= \frac{1}{6}z^2 t_{zz}; \\ \frac{3}{2}z(h' - g') + \frac{1}{2}z^2(g'' - h'') &= z^2(t_{tt} + t_i), \end{aligned} \tag{8.5.41}$$

where we define $t_{ij} = t_i \delta_{ij}$. These equations can be integrated to give

$$\begin{aligned} \tilde{f}(z) &= -\frac{1}{6}z^2 t_{zz} - \frac{1}{2}z^4 \int \frac{dz}{z^3}\left(t_{tt} + t_i\right); \\ (g(z) - h(z)) &= 2\int^z d\tilde{z}\tilde{z}^3 \int^{\tilde{z}} \frac{dw}{w^3}\left(t_{tt}(w) + t_i(w)\right). \end{aligned} \tag{8.5.42}$$

These equations can be solved analytically as $z \to 0$ and $z \to \infty$. The near boundary expansions of the fields χ and E are

$$\begin{aligned} \chi &= mz + cz^3 + \cdots \\ E &= 2\tilde{d}z^3 + \cdots, \end{aligned} \tag{8.5.43}$$

where m is the quark mass, c determines the quark condensate and $\tilde{d}$ is the density. The corresponding asymptotic expansions of the gauge invariant metric perturbations are

$$\begin{aligned} \tilde{f}(z) &= \frac{t_0}{12}\left(1 - 2m^2 z^2 + \mathcal{O}\left(m^4 z^4, mcz^4\right) + \cdots\right); \\ (g(z) - h(z)) &= \frac{t_0}{3}\tilde{d}z^6 + \cdots \end{aligned} \tag{8.5.44}$$

Note that in fixing a Fefferman-Graham gauge as $z \to 0$ one needs to take into account the shift in the AdS radius. The Fefferman-Graham gauge is obtained by choosing

$$f(z) = \frac{t_0}{12}, \tag{8.5.45}$$

which then implies that

$$zh'(z) = \frac{t_0}{6}\left(-m^2 z^2 + \mathcal{O}\left(m^4 z^4, mcz^4\right) + \cdots\right), \tag{8.5.46}$$

and hence

$$h(z) = \frac{t_0}{12}\left(1 - m^2 z^2 + \mathcal{O}\left(m^4 z^4, mcz^4\right) + \cdots\right), \tag{8.5.47}$$

where the integration constant is fixed by the AdS radius.

In the opposite limit of $z \to \infty$ we can use the spike solution (8.5.36) to show that

$$\begin{aligned} \tilde{f}(z) &= \frac{t_0\theta_1^3}{4z^3(1-\mathcal{E}^2)^{\frac{1}{2}}}\left(\frac{1}{3}+\frac{\mathcal{E}^2}{7}\right); \\ (g(z)-h(z)) &= -\frac{t_0\theta_1^3\mathcal{E}^2}{42z^3(1-\mathcal{E}^2)^{\frac{1}{2}}}, \end{aligned} \tag{8.5.48}$$

and hence the metric perturbations are bounded in the deep interior.

The effect of the metric perturbation (8.5.39) on the entanglement entropy is expressed in exactly the same way as in previous sections, since $g(z)$ does not enter the entanglement entropy. Thus for a slab, following (8.3.22), the brane contribution to the entanglement entropy is

$$\delta S = \frac{L^2}{4G_N\tilde{z}^2}\left(\int_a^b ds\frac{\sqrt{1-s^6}}{s^3}\tilde{f}(\tilde{z}s) - \left[h(\tilde{z}s)\frac{\sqrt{1-s^6}}{s^2}\right]_{s=a}^{s=b}\right) \tag{8.5.49}$$

where $\tilde{z}$ is the turning point of the original minimal surface and $a = \epsilon/\tilde{z}$. At zero density $\tilde{f}(z)$ is zero for $z \geq 1/m$ and continuity of the metric and its derivatives requires $h(1/m) = h'(1/m) = 0$. At any finite density $\tilde{f}(z)$ is non-zero at finite z and there is no need to impose that the function $h(z)$ vanishes at a finite value of z. In the finite density case the integration is therefore over the entire entangling surface, i.e. the upper limit $b = 1$ and

$$\delta S = \frac{L^2}{4G_N\tilde{z}^2}\left(\int_a^1 ds\frac{\sqrt{1-s^6}}{s^3}\tilde{f}(\tilde{z}s) + \left[h(\epsilon)\frac{\sqrt{1-a^6}}{a^2}\right]\right), \tag{8.5.50}$$

since the other boundary term vanishes at $s = 1$.

Note that δS has no discontinuities in its derivatives with respect to mass or to the width of the slab at finite density since $\tilde{f}(z)$ has no discontinuities in its derivatives at finite density. This provides another reason for viewing as unphysical the discontinuities discussed earlier.

It is useful to define the difference between the entanglement entropy at finite density and that at zero density, for the same mass,

$$\delta S - \delta S_{\tilde{d}=0} = \frac{L^2}{4G_N\tilde{z}^2}\left(\int_a^1 ds\frac{\sqrt{1-s^6}}{s^3}\delta\tilde{f}(\tilde{z}s) + \left[\delta h(\epsilon)\frac{\sqrt{1-a^6}}{a^2}\right]\right), \tag{8.5.51}$$

where

$$\begin{aligned} \delta\tilde{f}(z) &= \tilde{f}(z) - \frac{t_0}{12}(1-m^2z^2)^2; \\ \delta h(z) &= h(z) - h(z)_{\tilde{d}=0}, \end{aligned} \tag{8.5.52}$$

where we have used the analytic expression for $\tilde{f}(z)$ at zero density. From the asymp-

totic expansions (8.5.44), we can infer that the asymptotic expansion of $\delta\tilde{f}$ is

$$\delta\tilde{f}(z) = t_0\mathcal{O}(mcz^4) + \cdots \tag{8.5.53}$$

We can also always choose a gauge such that

$$\delta h(z) = t_0\mathcal{O}(z^4) + \cdots ; \tag{8.5.54}$$

this simply corresponds to matching the gauge asymptotically at zero and finite density. Substituting into (8.5.51) the difference between the entanglement entropy at finite density and that at zero density is UV finite[4] and only the integrated term contributes,

$$\delta S - \delta S_{\tilde{d}=0} = \frac{L^2}{4G_N\tilde{z}^2}\int_a^1 ds\frac{\sqrt{1-s^6}}{s^3}\delta\tilde{f}(\tilde{z}s). \tag{8.5.55}$$

Note however that this quantity does have discontinuities in its derivatives at $\tilde{z} = 1/m$, since the zero density quantity has such discontinuities.

8.5.3 Numerical Calculation of the Entanglement Entropy at Finite Density

We now consider in detail the embeddings in (8.5.34) with the aim to explicitily carry out the computation of the flavour entanglement entropy in the case of finite density. We follow the analysis in [241,242], though unlike the latter we focus on the zero temperature case. The background, instead of (8.5.33), is therefore $AdS_5 \times S^5$

$$ds^2 = \rho^2[-dt^2 + dx_3^2] + \frac{d\rho^2}{\rho^2} + d\theta^2 + \sin^2\theta d\Omega_3^2 + \cos^2\theta d\phi^2 \tag{8.5.56}$$

and the probe D7-brane extends in $\{t, x_3, \rho, \Omega_3\}$. We consider an embedding $\theta(\rho)$, and in addition we introduce a $U(1)$ gauge field $A_t(\rho)$ on the worldvolume of the D7-brane in order to study the gauge theory at finite density and chemical potential. The DBI action for this probe brane then evaluates to

$$I_{D7} = -T_7\int d^8\sigma\frac{\rho^3}{4}(1-\chi^2)\sqrt{1-\chi^2+\rho^2(\partial_\rho\chi)^2 - 2(1-\chi^2)F_{\rho t}^2} \tag{8.5.57}$$

where $\chi(\rho) \equiv \cos[\theta(\rho)]$ and $F_{\rho t}(\rho) = \partial_\rho A_t(\rho)$ is the electric field. The equation of motion for the gauge field has solutions with asymptotics given by (8.5.35), and since I_{D7} does not depend explicitly on A_t, there is a constant of motion $d \equiv \delta I_{D7}/\delta F_{\rho t}$.

For solving the resulting equations of motion it is useful to eliminate the gauge field A_t from the action by performing a Legendre transform with respect to d. The equation of

[4] Earlier discussions of the UV finiteness of terms in the entanglement entropy induced by a chemical potential may be found in [252–254].

motion for χ can then be obtained from the Legendre transformed action $\tilde{I}_{D7}$ as

$$\partial_\rho \left[\frac{\rho^5(1-\chi^2)\dot{\chi}}{\sqrt{1-\chi^2+\rho^2\dot{\chi}^2}} \sqrt{1+\frac{8\tilde{d}^2}{\rho^6(1-\chi^2)^3}} \right] = \tag{8.5.58}$$
$$-\frac{\rho^3\chi}{\sqrt{1-\chi^2+\rho^2\dot{\chi}^2}} \sqrt{1+\frac{8\tilde{d}^2}{\rho^6(1-\chi^2)^3}} \left[3(1-\chi^2)+2\rho^2\dot{\chi}^2 - 24\tilde{d}^2 \frac{1-\chi^2+\rho^2\dot{\chi}^2}{\rho^6(1-\chi^2)^3+8\tilde{d}^2} \right]$$

where $\dot{\chi} \equiv \partial_\rho \chi$ and $\tilde{d} \equiv d/T_{D7}$. It is straightforward to show that asymptotically solutions to this equation take the form given in (8.5.43).

We solve (8.5.58) numerically for a given $\tilde{d}$ with regular boundary conditions imposed in the deep interior. Recalling that $\chi = \cos\theta$ the spike solution is such that $\chi(0) \to 1$. However, since $\dot{\chi}(\rho) = -\sin\theta\dot{\theta}$, $\dot{\chi}(0) = 0$ and is independent of the value of $\dot{\theta}(0)$. Therefore we instead set boundary conditions at $\rho = \rho_0 \ll 1$,

$$\chi(\rho_0) = 1 - \frac{1}{2}\delta^2; \qquad \dot{\chi}(\rho_0) = -\alpha, \tag{8.5.59}$$

with $\alpha > 0$ and $\delta^2 \ll 1$. These boundary conditions correspond to

$$\theta(\rho_0) = \delta; \qquad \dot{\theta}(\rho_0) = \frac{\alpha}{\delta}. \tag{8.5.60}$$

Such conditions are consistent with the spike solution $\theta = \theta_1\rho + \cdots$ in (8.5.36) provided that $\alpha \sim \delta^2/\rho_0$; if the latter condition is satisfied the solutions can be smoothly continued to $\rho = 0$. These boundary conditions differ from those used in [241, 242] due to the fact that we work at zero temperature. Note that the quark mass can be extracted from the embedding using $\lim_{\rho\to\infty}(\rho\chi)$ due to (8.5.43).

The equations of motion for the gauge field are then given by Hamilton's equations with $\tilde{I}_{D7}$ as Hamiltonian, which reproduce the fact that $\tilde{d}$ is a constant, together with the equation

$$\partial_\rho A_t = 2\tilde{d} \frac{\sqrt{1-\chi^2+\rho^2\dot{\chi}^2}}{\sqrt{(1-\chi^2)[\rho^6(1-\chi^2)^3+8\tilde{d}^2]}}. \tag{8.5.61}$$

This equation can be integrated to give

$$A_t(\rho) = 2\tilde{d}\int_0^\rho d\rho' \frac{\sqrt{1-\chi^2+\rho'^2\dot{\chi}^2}}{\sqrt{(1-\chi^2)[\rho'^6(1-\chi^2)^3+8\tilde{d}^2]}} \tag{8.5.62}$$

where we have set $A_t(\rho) \to 0$ as $\rho \to 0$. The chemical potential μ is then given by $A_t(\infty)$ in the previous expression. Once the embedding $\chi(\rho)$ has been found above, one can compute $F_{\rho t} \equiv \partial_\rho A_t$ and μ from (8.5.61) and (8.5.62) respectively. Note that the parameter

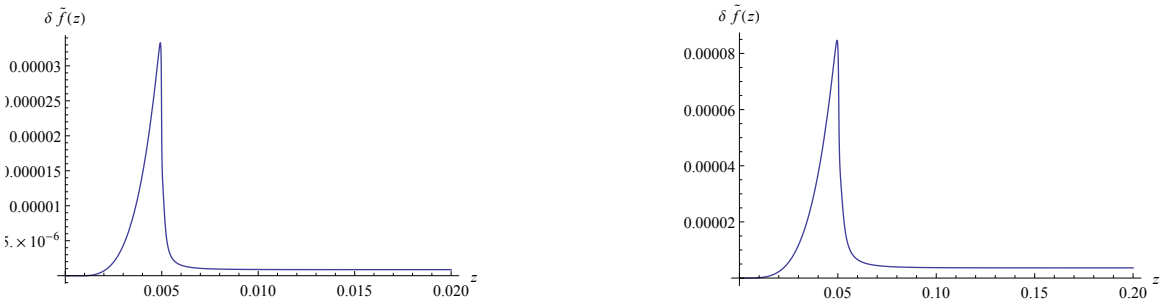

(a) $\tilde{d} = 200,\ m = 200$ (b) $\tilde{d} = 0.5,\ m = 20$

Figure 8.5.1: Plots of $\delta\tilde{f}(z)$ for various values of $\tilde{d}$ and m. In all cases $\delta\tilde{f}(z)$ asymptotes to zero as $z \to \infty$.

$\tilde{d}$ indeed characterises the density since

$$\lim_{\rho\to\infty}(\rho^3\partial_\rho A_t) = 2\tilde{d}, \tag{8.5.63}$$

in agreement with (8.5.35).

To compute the entanglement entropy one must change coordinates as in the previous section. At zero temperature the coordinate transformation is trivial and simply amounts to setting $z = 1/\rho$ whilst leaving the other coordinates unchanged. One can then compute the five-dimensional stress tensor components in (8.5.38), and thus the gauge-invariant metric perturbation $\tilde{f}(z)$ as defined by (8.5.42). We plot $\delta\tilde{f}(z)$, as defined in (8.5.52), in Figure 8.5.1 for various values of $\tilde{d}$ and m, the latter being fixed by the choice of both $\tilde{d}$ and $\chi'(0)$. The same general features are observed for all values of the parameters; $\delta\tilde{f}(z)$ peaks around $z = 1/m$ and has a long spike slowly asymptoting to zero as $z \to \infty$. Although one might expect intuitively that the thickness of this spike is determined by the ratio $\tilde{d}/m$ (with a larger ratio leading to a thicker spike), the results indicate that it is in fact the magnitude of $\chi'(0)$ that determine this thickness, with a larger value of $\chi'(0)$ corresponding to a thicker spike (and a larger magnitude of $\delta\tilde{f}(z)$ overall).

It is a simple matter to compute the background subtracted entanglement entropy using (8.5.55): the result for $\tilde{d} = 200$, $m = 200$ is shown in Figure 8.5.2. The graph shows the entanglement entropy as a function of the depth of the entangling surface $\tilde{z}$, which is proportional to the slab width l. It follows from (8.5.53) that the subtracted entanglement entropy increases quadratically with $\tilde{z}$ for $\tilde{z} \ll 1$; if $\delta f = \lambda z^4$ then

$$\delta S - \delta S_{\tilde{d}=0} = \frac{L^2\lambda}{48G_N}\frac{\sqrt{\pi}\Gamma(1/3)}{\Gamma(11/6)}\tilde{z}^2. \tag{8.5.64}$$

The metric perturbation δf reaches a maximum around $z \sim 1/m$ and is very small for

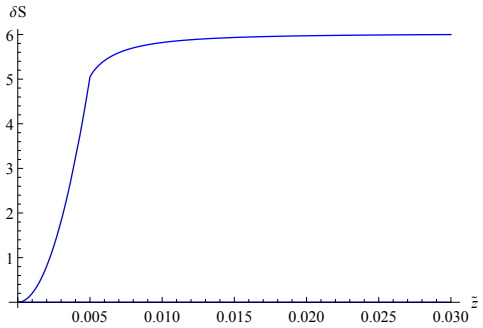

Figure 8.5.2: Plot of the background subtracted entanglement entropy for $\tilde{d} = 200$, $m = 200$ as the width of the slab is increased. The entanglement entropy increases quadratically until the depth of the entangling surface is $1/m$ and then slowly saturates to a constant value as the width of the slab is increased further.

$z > 1/m$, and therefore the entanglement entropy of surfaces which extend to turning points $\tilde{z} \gg 1/m$ saturates.

The D3/D7 system has a rich structure of phase transitions as the chemical potential, temperature and magnetic field are varied, see [255, 256]. It would be interesting to use entanglement entropy to explore these phase transitions, extending the above results. Note that the entanglement entropy for massless flavours at finite density was discussed in [216]; our method would give the same results for massless flavours, and it would be interesting to explore how the entanglement entropy changes as one increases the ratio of density to mass.

8.6 Field Theory Interpretation

The D3/D7 system is dual to $\mathcal{N} = 4$ SYM coupled to $\mathcal{N} = 2$ massive hypermultiplets. The key features of this field theory are as follows. The field content of $\mathcal{N} = 4$ consists of the gauge fields A_μ, scalars X^A transforming in the fundamental of the R symmetry group $SO(6)$ and spinors λ^i transforming in the spinor representation of $SO(6)$. The hypermultiplets consist of scalars χ and fermions η transforming in the bifundamental of the $SU(N_c)$ and $SU(N_f)$ gauge groups. In the massless case the addition of these hypermultiplets preserves an $SO(4) \times SO(2)$ subgroup of the R symmetry group of $\mathcal{N} = 4$ SYM. The hypermultiplets are coupled to the $\mathcal{N} = 4$ SYM fields by potential terms of the form

$$I = \int d^4x \mathrm{Tr}_{SU(N_c)} \mathrm{Tr}_{SU(N_f)} \left(X^A \chi^\dagger \chi X^A \right). \tag{8.6.1}$$

Separating the branes by a distance m (in string units) corresponds to introducing a mass term m for the hypermultiplets, which breaks the conformal invariance and breaks the R symmetry group further to $SO(4)$.

There are two distinct regimes of interest: the mass parameter m being small relative to energy scales of interest, and the mass parameter being large compared to scales of

interest. In the former case the theory is clearly described in terms of a small mass perturbation of a conformal field theory, and we can use the underlying conformal invariance to understand the entanglement entropy. Entanglement entropy for relevant perturbations has been studied recently [227] and we will discuss the relation to our results below.

In the opposite regime, of high mass, at energy scales much lower than m we can integrate out the hypermultiplets, effectively setting $\chi \sim \frac{1}{m}$. The potential term above controls the leading deformation to the $\mathcal{N} = 4$ SYM theory: at low energies the effective description must be

$$I = I_{SYM} + \frac{1}{m^2} \int d^4x \mathcal{O}_6, \tag{8.6.2}$$

where $\mathcal{O}_6$ is an operator of dimension six in the $\mathcal{N} = 4$ SYM theory, i.e. it is an irrelevant deformation of the SYM conformal field theory. The dimension six operator explicitly breaks the R symmetry from $SO(6)$ to $SO(4)$ and is therefore charged with respect to the $SO(6)$ R symmetry of $\mathcal{N} = 4$ SYM. The backreaction of this deformation on the stress energy tensor, which is an R symmetry singlet, is necessarily quadratic in this deformation, i.e. the stress energy tensor is only affected at order $1/m^4$. The behaviour of entanglement entropy under irrelevant deformations has been less studied and we will explore this case in more detail below.

8.6.1 Zero Mass: Marginal Deformation of CFT

In the limit of zero mass, the brane contribution to the entanglement entropy of the slab is

$$\delta S = \frac{t_0 L^2}{48 G_N} \left(\frac{3}{2\epsilon^2} + \frac{\sqrt{\pi}}{2\tilde{z}^2} \frac{\Gamma(-1/3)}{\Gamma(1/6)} \right), \tag{8.6.3}$$

where implicitly we have fixed a gauge choice such that

$$h(z) = \frac{t_0}{12}. \tag{8.6.4}$$

Note that this expression is proportional to the entanglement entropy of a slab in AdS_5

$$S = \frac{L^2}{2G_N} \left(\frac{1}{2\epsilon^2} + \frac{\sqrt{\pi}}{6\tilde{z}^2} \frac{\Gamma(-1/3)}{\Gamma(1/6)} \right). \tag{8.6.5}$$

The entanglement entropy of a spherical surface in AdS_5 is

$$S = \frac{\pi}{G_N} \left(\frac{R^2}{2\epsilon^2} + \frac{1}{2} \log(\epsilon/\epsilon_{IR}) - \frac{1}{4} \right). \tag{8.6.6}$$

The brane contribution to the entanglement entropy for a spherical surface at zero mass is

$$\delta S = \frac{t_0 \pi}{8 G_N} \left(\frac{R^2}{2\epsilon^2} + \frac{1}{2} \log(\epsilon/\epsilon_{IR}) - \frac{1}{4} \right), \tag{8.6.7}$$

which is again proportional to the AdS result.

This is to be expected, see also [213, 215]: suppose that the AdS radius is scaled as

$$L_{AdS} \to L_{AdS}\,(1+\delta_{AdS}) \tag{8.6.8}$$

with $\delta_{AdS} \ll 1$. Since the bulk entangling surface is of dimension three, this implies that

$$S \to S\,(1+\delta_{AdS})^{\frac{3}{2}} \approx S\left(1+\frac{3}{2}\delta_{AdS}\right). \tag{8.6.9}$$

In the case at hand, the effect of the brane is to shift the AdS radius as

$$\delta_{AdS} = \frac{t_0}{12} \tag{8.6.10}$$

The brane contribution to the entanglement entropy at zero mass is therefore precisely

$$\delta S = \frac{3}{2}\delta_{AdS} S, \tag{8.6.11}$$

explaining the results above.

8.6.2 Small Mass: Relevant Deformation of CFT

In the small mass regime, the mass m is smaller than the energy scales of interest, so the system can be viewed as a mass perturbation of an underlying CFT.

Half space: Let us consider first the case in which the size of the slab $l \to \infty$, i.e. the space is divided into two regions by a plane; the brane contribution to the entanglement entropy is given in (8.3.31). In particular the logarithmic divergence is

$$\delta S = \frac{t_0 L^2}{48 G_N} m^2 \log(m\epsilon) = \frac{\pi}{3} T_0 (m^2 L^2) \log(m\epsilon), \tag{8.6.12}$$

where in the latter expression we use (8.3.19) i.e. T_0 is the effective tension of the D7-brane, reduced over the three sphere.

The mass deformation in the field theory is associated with the following slipping mode of the D7-brane on the three sphere: letting the five sphere metric be

$$d\Omega_5^2 = d\theta^2 + \sin^2\theta\, d\Omega_3^2 + \cos^2\theta\, d\phi^2 \tag{8.6.13}$$

then the slipping mode is associated with the angle θ, i.e. we retain only the following terms in the D7-brane action

$$I = T_0 \int d^5x \sqrt{g}\sin^3\theta \sqrt{1+g^{\mu\nu}\partial_\mu\theta\partial_\nu\theta}, \tag{8.6.14}$$

where we have integrated over the three-sphere, because the mode of interest is an

$SO(4)$ singlet and hence there is no dependence on the three sphere coordinates. The metric $g_{\mu\nu}$ denotes the AdS_5 metric and we work here in Euclidean signature as we need to compute correlation functions. The resulting equation of motion for θ is

$$0 = \Box\theta - 3\cot\theta - \frac{1}{2}\frac{g^{\mu\nu}\partial_\mu\theta(g^{\rho\sigma}\partial_\rho\theta\partial_\sigma\theta)}{1+g^{\mu\nu}\partial_\mu\theta\partial_\nu\theta} \tag{8.6.15}$$

where $\Box$ is the Laplacian in the Euclidean AdS_5 metric. Linearising this equation around $\theta = \pi/2$ gives

$$0 = \Box\theta + 3\theta, \tag{8.6.16}$$

i.e. the scalar is dual to an operator of dimension three.

As we will discuss shortly, we are interested in computing the normalization of the two point function of this operator, and it thus suffices to consider the solution to the linearized equation of motion (8.6.16). From [59], we can read off the operator one point function in terms of the asymptotic expansion of the scalar field

$$\langle\mathcal{O}_3\rangle = T_0\left(-2\theta_{(2)} + \frac{1}{3}\theta_{(0)}^3 + \frac{R_0}{12}\theta_{(0)} + \Box_{(0)}\theta_{(0)}\right) \tag{8.6.17}$$

where

$$\theta = z(\theta_{(0)} + \theta_{(1)}z + \theta_{(2)}z^2 + \tilde{\theta}_{(2)}z^2\log(z) + \cdots) \tag{8.6.18}$$

Here $\Box_{(0)}$ refers to the Laplacian in the boundary metric $g_{(0)}$ and $R_{(0)}$ is the scalar curvature of this metric, which is zero in our case. Working in momentum space, the regular solution to the linearized field equation (8.6.16) is

$$\theta = \theta_{(0)}(k)(z^2K_1(kz)), \tag{8.6.19}$$

with k the momentum and $\theta_{(0)}(k)$ corresponding to the Fourier transform of the source. One then expands (8.6.19) about $z = 0$ to identify the various terms in (8.6.18), for example

$$\theta_{(2)}(k) = \theta_{(0)}(k)\left(\frac{1}{4}(-1+2\gamma)k^2 + \frac{1}{2}k^2\log\left(\frac{k}{2}\right)\right) \tag{8.6.20}$$

where γ is the Euler constant. Functionally differentiating the one point function (8.6.17) with respect to the source $\theta_{(0)}$, and setting the source to zero, therefore gives

$$\langle\mathcal{O}_3(k)\mathcal{O}_3(-k)\rangle = T_0k^2\log\left(\frac{k}{2}\right) + \cdots, \tag{8.6.21}$$

where contact terms have been dropped. Fourier transforming back to position space gives

$$\langle\mathcal{O}_3(x)\mathcal{O}_3(0)\rangle = \frac{4T_0}{\pi^2}\mathcal{R}\left(\frac{1}{x^6}\right), \tag{8.6.22}$$

where $\mathcal{R}$ denotes differential renormalization, see [31].

In [227] it was shown that for a CFT deformed by a relevant operator

$$I \to I + \lambda \int d^d x \mathcal{O}, \tag{8.6.23}$$

the change in the entanglement entropy of the half space is

$$\delta S = \mathcal{N}\lambda^2 \frac{(d-2)}{4(d-1)} \frac{\pi^{\frac{d+2}{2}}}{\Gamma(\frac{d+2}{2})} \mathcal{A} \log\left(\frac{\epsilon_{UV}}{\epsilon_{IR}}\right), \tag{8.6.24}$$

where ϵ_{UV} and ϵ_{IR} correspond to UV and IR cutoffs, respectively, $\mathcal{A}$ is the area of the dividing surface while $\mathcal{N}$ is the normalisation of the two point function of $\mathcal{O}$, i.e. at separated points

$$\langle \mathcal{O}(x)\mathcal{O}(0)\rangle = \frac{\mathcal{N}}{x^{2\Delta}}, \tag{8.6.25}$$

with $\Delta = (d+2)/2$ the (relevant) operator dimension. Note that the entanglement entropy is unchanged to first order in the perturbation λ.

In our case the normalisation is given in (8.6.22), $\lambda = m$ and $\mathcal{A} = L^2$. Hence

$$\delta S = \frac{\pi T_0}{3} m^2 L^2 \log\left(\frac{\epsilon_{UV}}{\epsilon_{IR}}\right). \tag{8.6.26}$$

which exactly agrees with (8.6.12), taking the IR cutoff to be $\epsilon_{IR} = 1/m$.

Sphere: For the spherical entangling region the logarithmically divergent terms are

$$\delta S = \frac{t_0 \pi}{8 G_N}\left(\frac{2\mu^2}{3} + \frac{1}{2}\right)\log(m\epsilon) = T_0\left(\frac{4}{3}(\pi m R)^2 + \pi^2\right)\log(m\epsilon). \tag{8.6.27}$$

The second of these terms was explained above. The first is proportional to the mass deformation and can be expressed in the same form as (8.6.24), with

$$\mathcal{A} = 4\pi R^2; \qquad \mathcal{N} = \frac{4T_0}{\pi^2}, \tag{8.6.28}$$

setting the IR cutoff to be $\epsilon_{IR} = 1/m$.

Slab: For a slab of finite width, the logarithmically divergent terms are precisely twice those for the half space,

$$\delta S = \frac{2\pi T_0}{3} m^2 L^2 \log\left(\frac{\epsilon_{UV}}{\epsilon_{IR}}\right). \tag{8.6.29}$$

Taking into account that the area of the entangling surface is in this case $2L^2$, we again find exact agreement with (8.6.24).

At first sight it may seem surprising that the expression (8.6.24), which was derived for the half space using the known modular Hamiltonian, is applicable to other entangling geometries, with the entangling area replaced by the appropriate value. However, from

the field theory perspective, one could derive the result for the spherical region by conformal transformations (the modular Hamiltonian is also known) and the divergent contributions for a slab, being local, must necessarily give exactly twice the result for an infinite slab. It was argued in [227] that the result should hold for any geometry, since any entangling surface is locally flat; of course for a curved surface there are additional contributions to the entanglement entropy beyond this universal contribution. The dilaton effective action approach was also used in [257, 258] to derive the logarithmic divergences for any shape entangling region, up to a universal coefficient computable from the dilaton effective action.

There is also a very simple holographic way to understand why the formula (8.6.24) is applicable to the logarithmic divergences of any shape entangling surface, generalising the work of [230, 259]. Deforming the conformal field theory by an relevant scalar operator corresponds in the bulk to coupling gravity to a massive scalar Φ i.e. we consider

$$I = \frac{1}{16\pi G_N}\int d^{d+1}x\left(R + d(d+1) - \frac{1}{2}(\partial\Phi)^2 - \frac{1}{2}M^2\Phi^2 + \cdots\right), \tag{8.6.30}$$

where $M^2 = \Delta(\Delta - d)$, with $\Delta < d$ the dimension of the dual operator. Here implicitly we are working perturbatively in the scalar field so we include only quadratic terms in Φ with the ellipses denoting higher order terms. The normalisation of the operator two point function is [31, 260]

$$\langle\mathcal{O}(x)\mathcal{O}(0)\rangle = \frac{(2\Delta - d)\Gamma(\Delta)}{16\pi G_N \pi^{\frac{d}{2}}\Gamma(d - \frac{\Delta}{2})}\frac{1}{x^{2\Delta}}, \tag{8.6.31}$$

for $\Delta = d/2 + k$ with k an integer. In particular we can write

$$\mathcal{N} = \frac{\Gamma(d/2+1)}{8\pi^{d/2+1}G_N} \tag{8.6.32}$$

for $\Delta = d/2 + 1$.

Working perturbatively around an AdS_{d+1} background, a scalar field profile

$$\Phi = \lambda z^{d-\Delta} \tag{8.6.33}$$

corresponds to deforming the field theory by the dimension Δ operator, with λ characterising the deformation. At quadratic order in the source there is a backreaction on the metric. Letting the metric perturbation be as before

$$\delta(ds^2) = \frac{1}{z^2}\left(f(z)dz^2 + h(z)dx^\mu dx_\mu\right) \tag{8.6.34}$$

then the Einstein equation implies that the gauge invariant combination of these per-

turbations is given by

$$f(z) + zh'(z) = \frac{(\Delta - d)}{2(d-1)}\lambda^2 z^{2(4-\Delta)}. \tag{8.6.35}$$

Working in Fefferman-Graham gauge we may set $f(z) = 0$ in which case

$$h(z) = -\frac{1}{4(d-1)}\lambda^2 z^{2(d-\Delta)} = -h_0\lambda^2 z^{2(d-\Delta)}. \tag{8.6.36}$$

Now consider an entangling surface in the deformed metric. Let the induced metric for the minimal surface be $\gamma_{ab} = \partial^a X^\mu \partial^b X^\mu g_{\mu\nu}$ and fix a static gauge such that

$$Z = z; \qquad X^a = \sigma^a; \qquad X^i = X^i(z, \sigma^a) \tag{8.6.37}$$

where asymptotically as $z \to 0$

$$X^i(z, \sigma^a) = X^i(\sigma^a) + \cdots \tag{8.6.38}$$

The entanglement entropy contains divergent terms from

$$S = \frac{1}{4G_N}\int d^{d-1}x\sqrt{\gamma} \approx \frac{1}{4G_N}\int dz d\sigma^a \sqrt{\gamma^o}\frac{1}{z^{d-1}}(1 + \cdots + \frac{(d-2)}{2}h(z) + \cdots) \tag{8.6.39}$$

where

$$\gamma^o_{ab} = \partial_a X^i(\sigma^c)\partial_b X^j(\sigma^c)\delta_{ij} \tag{8.6.40}$$

is the induced metric for the entangling surface on the boundary. Integrating over the radial coordinate one finds the usual power law volume divergence

$$\frac{1}{4G_N(d-2)\epsilon^{d-2}}\int d\sigma^a\sqrt{\gamma^0} = \frac{\mathcal{A}}{4G_N(d-2)\epsilon^{d-2}}, \tag{8.6.41}$$

with $z = \epsilon$ being the UV cutoff and $\mathcal{A}$ being the volume of the entangling surface in the boundary. From the relevant perturbation one obtains a logarithmic divergence whenever

$$\Delta = \frac{1}{2}(d+2) \tag{8.6.42}$$

where

$$\delta S = \frac{\mathcal{A}}{8G_N}(d-2)\lambda^2 h_0 \log(\epsilon/\epsilon_{IR}). \tag{8.6.43}$$

Using the identity (8.6.32) we thence obtain

$$\delta S = \mathcal{N}\mathcal{A}\lambda^2 \frac{(d-2)\pi^{d/2+1}}{4(d-1)\Gamma(d/2+1)}\log(\epsilon/\epsilon_{IR}), \tag{8.6.44}$$

which is exactly (8.6.24) but does not assume any geometry for the entangling surface. It would be interesting to prove this result from the field theory; the modular Hamiltonian for generic entangling surfaces is not known but the holographic result suggests that one

should be able to compute the logarithmic divergences without complete knowledge of the modular Hamiltonian.

Note that this result has a straightforward generalisation to irrelevant deformations. Deforming the conformal field theory by an irrelevant scalar operator corresponds in the bulk to coupling gravity to a massive scalar Φ with $M^2 = \Delta(\Delta - d)$, with $\Delta > d$ the dimension of the dual operator. Following the same steps we see that the entanglement entropy contains divergent terms from

$$S = \frac{1}{4G_N}\int d^{d-1}x\sqrt{\gamma} \approx \frac{1}{4G_N}\int dz d\sigma^a \sqrt{\gamma^o}\frac{1}{z^{d-1}}(1 + \frac{(d-2)}{2}h(z) + \cdots) \tag{8.6.45}$$

but since $\Delta > d$ the metric perturbation $h(z)$ always gives rise to additional UV divergences:

$$\delta S = -\frac{\lambda^2(d-2)}{32G_N(d-1)(2\Delta - d - 2)}\frac{\mathcal{A}}{\epsilon^{2\Delta-d-2}}. \tag{8.6.46}$$

Using the identity (8.6.32) we thence obtain

$$\delta S = -\mathcal{N}\lambda^2\frac{(d-2)\pi^{d/2+1}}{4(d-1)(2\Delta - d - 2)\Gamma(d/2+1)}\frac{\mathcal{A}}{\epsilon^{2\Delta-d-2}}, \tag{8.6.47}$$

where $\mathcal{N}$ is the operator normalisation. As for the usual power law divergences, such terms are not universal but nonetheless will be given an interpretation in the following section.

8.6.3 Large Mass: Irrelevant Deformation of CFT

By large mass, we mean that the mass scale m is higher than the energy scales of interest. This implies in particular that $m \gg 1/l$, where l characterises the size of the entangling region, i.e. the width of the slab or the radius of the sphere. Thus we are always working in the regime $\mu \gg 1$. The UV divergent contributions to the entanglement entropy have already been explained above and here we are interested in explaining the leading finite contributions for $\mu \gg 1$. To decouple such contributions from the divergent terms, it is useful to look at the differentiated quantities (8.3.51) and (8.4.23) (which we argued previously do not receive contributions from UV divergent terms).

As stated above, for large mass, the effective IR description is in terms of an irrelevant deformation of SYM. It is easy to understand the effects of such a deformation on the entanglement entropy from the dual perspective. For a deformation by an operator of dimension six with $\lambda \sim 1/m^2$ the change in the metric behaves as $1/(mz)^4$. The metric perturbation can only be viewed as small relative to the background AdS_5 metric when $(mz)^4 \gg 1$.

Slab: Now it is straightforward to infer the effect of the irrelevant deformation on the entanglement entropy of a slab. Since the latter scales extensively with the volume of

the slab, L^2, and the metric is corrected at order $1/m^4$, the change in the entanglement entropy goes as L^2/m^4. The underlying theory is conformal so the only scale in the problem is the width of the slab l. Since the entanglement entropy is dimensionless the effect of the massive modes is to change the entanglement entropy as

$$\delta S \sim \frac{L^2}{m^4 l^6}, \tag{8.6.48}$$

which indeed agrees with the term found in (8.3.51).

We can infer this answer using (8.6.47), which in the case of $\Delta = 6$ and $d = 4$ gives

$$\delta S \sim \lambda^2 \frac{\mathcal{A}}{\epsilon^6}. \tag{8.6.49}$$

In the case at hand $\lambda \sim 1/m^2$. The description in terms of an irrelevant deformation of SYM is only valid provided that we consider entangling surfaces for which $l \gg 1/m$. The effective cutoff should therefore be $\epsilon \sim l \gg 1/m$ and hence we reproduce the formula above.

Sphere: For a spherical entangling surface the leading contribution to the differentiated entanglement entropy at large μ behaves as (8.4.23)

$$\delta S \sim \frac{1}{m^2 R^2} + \mathcal{O}\left(\frac{1}{m^4 R^4}\right). \tag{8.6.50}$$

Thus although there is a $1/m^4$ term (as above) this is not the leading contribution. A simple way to understand the origin of this term is by exploiting the CHM map [187]. The entanglement entropy for the spherical region is then computed by computing the entropy in the mass deformed theory on a hyperbolic space. Since the fields are conformally coupled the action contains the terms

$$I = \frac{1}{2}\int d^4x\sqrt{-g}\left((\partial\chi)^2 + m^2\chi^2 + \frac{1}{6}\mathcal{R}\chi^2\right), \tag{8.6.51}$$

where χ is a hypermultiplet scalar and $\mathcal{R} \sim 1/R^2$ is the Ricci scalar. Now when we integrate out the hypermultiplets we obtain additional terms in (8.6.2): setting $\chi \sim 1/m$ we obtain a contribution from the curvature coupling of order $1/(m^2R^2)$, which is in agreement with the expression above.

8.6.4 Conformal Perturbation Theory at Higher Orders

The brane contributions to the entanglement entropy for the half space (8.3.31) consist of only the divergent term arising from the shift in the AdS radius and the logarithmic divergence discussed above. Since the logarithmic divergence is expressed entirely in terms of the coefficient of the two point function for the dimension three (fermion mass) operator, this contribution to the entanglement entropy is trivially not renormalized rel-

ative to the weak coupling result: since the operator dimension is protected, there is such a contribution regardless of the coupling. The result (8.3.31) only includes powers of m up to m^2, which follows on dimensional grounds: the dimensionless entanglement entropy scales extensively with the slab area L^2 and therefore the only way that contributions at order m^3 or higher could arise in the entanglement entropy would be if the latter was IR divergent, i.e. the contributions would have to scale as

$$\delta S \sim L^2 m^k \Lambda_{IR}^{k-2} \tag{8.6.52}$$

where the IR cutoff $\Lambda_{IR} \gg 1$ (relevant perturbations cannot introduce UV power law divergences so an IR cutoff is the only possibility). However, the entanglement entropy is an IR safe quantity and therefore no such dependence on an IR cutoff should arise.

From the perspective of conformal perturbation theory, it is not obvious that there are not contributions to the entanglement entropy from higher order terms, i.e. terms of order m^3 or higher. The change in the entanglement entropy is in general expressed as [225–227]

$$\delta S = -m\langle \mathcal{O}K\rangle + \frac{1}{2}m^2\left(\langle \mathcal{O}KK\rangle - \langle \mathcal{O}\mathcal{O}\rangle\right) + \mathcal{O}(m^3) \tag{8.6.53}$$

where $\mathcal{O}$ is the deforming operator and K is the modular Hamiltonian. The first term vanishes by conformal invariance and the second term gives the logarithmic divergence. By the argument above, higher order terms (dependent on higher order correlation functions) must vanish and it would be interesting to show this explicitly.

8.7 Differential Entropy

Given the expression for the entanglement entropy of a slab, we now proceed to compute the differential entropy. Following [232–237], the differential entropy should correspond to the area of a surface in the backreacted geometry - see Figure 8.7.1.

The differential entropy is defined as

$$E = \sum_{k=1}^{\infty}[S(I_k) - S(I_k \cap I_{k+1})] \tag{8.7.1}$$

where $\{I_k\}$ is a set of intervals that partitions the boundary. We will cover the boundary with n intersecting slabs - we take I_k to be a slab of width Δx, and the intersection $I_k \cap I_{k+1}$ is thus a strip of width $\Delta x - L_x/n$ where L_x is the regularised length of the x-direction. At the end we will take the limit $n \to \infty$.

For a slab in AdS_5 there is a relation between the strip width Δx, and the maximum bulk depth of the associated extremal surface $\tilde{z}$, see (8.3.12). When the slab lies in the perturbed geometry this relation is modified (see for example (8.3.36)), and therefore it

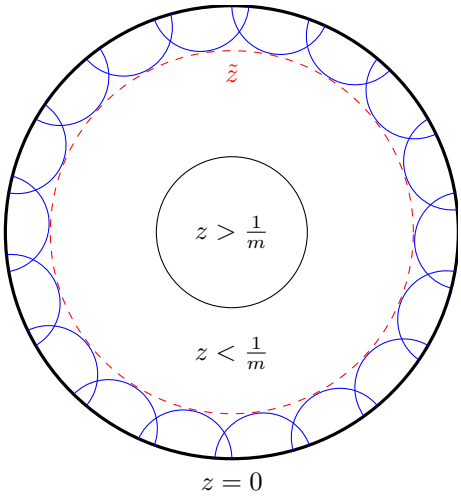

Figure 8.7.1: An illustration of the equivalence between the differential entropy of a boundary partition and the area of a corresponding hole in the bulk. As the number of strips partitioning the boundary tends to infinity, the turning points of the associated minimal surfaces (blue) form a smooth hole in the bulk (red) whose area equals the differential entropy.

is useful to leave the relation implicit as

$$\Delta x = c\tilde{z} = (c_0 + c_1 t_0 + \mathcal{O}(t_0^2))\tilde{z}. \tag{8.7.2}$$

with

$$c_0 = \frac{2\sqrt{\pi}\Gamma(\frac{2}{3})}{\Gamma(\frac{1}{6})}; \tag{8.7.3}$$

and c_1 depends on whether μ is greater than or less than one. The differential entropy takes the following form

$$E = \lim_{n\to\infty} n[S(\Delta x) - S(\Delta x - L_x/n)] \tag{8.7.4}$$

where the overall factor of n arises from the fact that all slabs are of equal width. For AdS_5 this gives

$$E = \frac{L^2\sqrt{\pi}\Gamma(-\frac{1}{3})}{12\Gamma(\frac{1}{6})G_N} \lim_{n\to\infty} n\left[\frac{c^2}{(\Delta x)^2} - \frac{c^2}{(\Delta x - L_x/n)^2}\right] \tag{8.7.5}$$

and hence

$$E = -\frac{V\sqrt{\pi}\Gamma(-\frac{1}{3})}{6\Gamma(\frac{1}{6})G_N}\frac{c^2}{(\Delta x)^3}, \tag{8.7.6}$$

where $V = L^2 L_x$ is the regularised three-volume. Using (8.7.3) this expression can be rewritten as

$$E = \frac{V}{4G_N}\frac{c_0^3}{(\Delta x)^3}, \tag{8.7.7}$$

and the latter is manifestly equal to the volume of the turning point surface (i.e. the hole) divided by $4G_N$.

8.7.1 Large Mass $\mu \gg 1$

Proceeding to calculate the flavour contributions, we begin with the very large mass case. The relevant expression for the entanglement entropy is (8.3.30). The two leading terms are manifestly independent of $\tilde{z}$ and thus of Δx which implies that the differential entropy vanishes in this limit,

$$\delta E = \lim_{n\to\infty} n[\delta S(\Delta x) - \delta S(\Delta x - L_x/n)] \to 0. \tag{8.7.8}$$

The limit $\mu \gg 1$ means $\tilde{z} \gg 1/m$ and thus the hole formed in the bulk is far away from the probe brane (which ends at $z = 1/m$). In the large μ limit the leading contribution to the differential entropy arises from the third term in (8.3.30) and hence

$$\begin{aligned} \delta E &= -\frac{t_0 L^2}{2304 m^4 G_N} \lim_{n\to\infty} n \left[\frac{c^6}{\Delta x^6} - \frac{c^6}{(\Delta x - L_x/n)^6}\right] \\ &= \frac{t_0 V c_0^6}{384 m^4 (\Delta x)^7 G_N}, \end{aligned} \tag{8.7.9}$$

where c_0 is defined by (8.7.3). Note that since the gauge dependent terms are independent of Δx they also automatically cancel in the differential entropy.

Now let us compare the differential entropy with the volume of a hole of radius $\tilde{z}$. Since the backreaction on the AdS_5 metric in this region is zero one might naively expect that the change in the differential entropy is zero. However, this does not take into account the fact that the relation between the turning point radius $\tilde{z}$ and the width of the boundary slabs Δx is modified (8.3.36). In other words, the gravitational entropy of the hole remains

$$E_{grav} = \frac{V}{4G_N}\frac{1}{\tilde{z}^3}, \tag{8.7.10}$$

since the metric is AdS_5, but to express this quantity in terms of Δx we need to use the relation in (8.7.2) to first order in the perturbation, resulting in

$$E_{grav} = \frac{V}{4G_N}\left(\frac{c_0^3}{(\Delta x)^3} + \frac{3c_0^2 c_1 t_0}{(\Delta x)^3}\right) = \frac{V c_0^3}{4G_N(\Delta x)^3} + \frac{t_0 V c_0^6}{384 m^4 (\Delta x)^7 G_N}, \tag{8.7.11}$$

where we use

$$c_1 = \frac{1}{288 m^4 \tilde{z}^4} = \frac{c_0^4}{288 m^4 (\Delta x)^4}. \tag{8.7.12}$$

where the latter equality is to order t_0. The second term in (8.7.11) is in exact agreement with the calculation of the perturbation in the differential entropy (8.7.9); we will see in Section 8.7.3 that this agreement holds for all $\mu > 1$.

8.7.2 Small Mass $\mu < 1$

We proceed with the small mass case. Extracting from (8.3.28) the terms which depend on $\tilde{z}$ one obtains

$$\delta S = \frac{t_0 L^2}{48 G_N}\left(\frac{\sqrt{\pi}}{12}\frac{\Gamma(-1/3)}{\Gamma(7/6)}\frac{1}{\tilde{z}^2} + \frac{\sqrt{\pi}}{12}\frac{\Gamma(1/3)}{\Gamma(11/6)} m^4 \tilde{z}^2 - 2m^2 \log\tilde{z} + \cdots\right) \tag{8.7.13}$$

From these terms in the entanglement entropy we can now proceed to compute the differential entropy using (8.7.4). Again it is clear that all divergent and gauge dependent terms cancel from the differential entropy, since they are independent of Δx. Noting that

$$(\Delta x)^2 - (\Delta x - L_x/n)^2 = 2\Delta x \frac{L_x}{n} + \mathcal{O}(1/n^2) \tag{8.7.14}$$

$$\frac{1}{(\Delta x)^2} - \frac{1}{(\Delta x - L_x/n)^2} = -\frac{2}{\Delta x^3}\frac{L_x}{n} + \mathcal{O}(1/n^2) \tag{8.7.15}$$

$$\log\frac{\Delta x - L_x/n}{\Delta x} = -\frac{1}{\Delta x}\frac{L_x}{n} + \mathcal{O}(1/n^2) \tag{8.7.16}$$

we obtain the perturbation in the differential entropy

$$\delta E = -\frac{t_0 V}{48 G_N}\left(-\frac{3c_0^3}{2\Delta x^3} - m^4\frac{\sqrt{\pi}}{6}\frac{\Gamma(1/3)}{\Gamma(11/6)}\frac{\Delta x}{c_0^2} + \frac{2m^2}{\Delta x}\right), \tag{8.7.17}$$

where c_0 is as given in (8.7.3).

Now let us compare this expression with the gravitational entropy of a hole of radius z_t,

$$E_{grav} = \frac{V}{4G_N}\frac{1}{z_t^3}\left(1 + \frac{3}{2}h(z_t)\right), \tag{8.7.18}$$

where we take into account the metric perturbation relative to AdS_5. In this case the relation between z_t and Δ is given by

$$\Delta x = c_0 z_t(1 - \frac{1}{2}h(z_t)) + c_1' t_0 z_t, \tag{8.7.19}$$

where c_0 is defined in (8.7.3) and

$$c_1' = -\frac{1}{24}\left(-c_0 + \frac{4\mu^2}{3} - \frac{\mu^4\sqrt{\pi}\Gamma(\frac{1}{3})}{9\Gamma(\frac{11}{6})}\right) \tag{8.7.20}$$

Thus we note that the gauge dependent quantity $h(z_t)$ cancels from the entropy of the hole, with

$$E_{grav} = \frac{V}{4G_N}\frac{1}{(\Delta x)^3}\left(c_0^3 + 3c_0^2 c_1' t_0\right), \tag{8.7.21}$$

and moreover the change in gravitational entropy of the hole agrees exactly with the change in the differential entropy (8.7.17).

8.7.3 $\mu > 1$

We now proceed with the case $\mu > 1$, without requiring $\mu \gg 1$. The entanglement entropy for $\mu > 1$ is given by equations (8.3.29) and (8.3.30)

$$\begin{aligned}\delta S &= \frac{t_0 L^2}{48G\tilde{z}^2}\left(\frac{1}{2a^2}+\frac{1}{6\mu^4}{}_3F_2\left(\{1/2,1,1\},\{2,2\},1/\mu^6\right)\right. \\ &\quad -\frac{\mu^2}{2}{}_2F_1\left(-1/2,-1/3,2/3,1/\mu^6\right)+\frac{\mu^2}{2}{}_2F_1\left(-1/2,1/3,4/3,1/\mu^6\right) \\ &\quad \left.+2\mu^2\log(\mu a)\right)+\delta S_{\text{scheme}}(m,\epsilon)\end{aligned} \tag{8.7.22}$$

Recalling that $\mu = m\tilde{z}$ and $a = \epsilon/\tilde{z}$, the divergent and log parts are independent of $\tilde{z}$ (and thus Δx) and so do not contribute to the differential entropy, nor do the gauge dependent terms. Also recall that $\tilde{z} = \Delta x/c$, where throughout the following we can replace $c \to c_0$ to order t_0 since δS already contains an overall factor of t_0. We thus have

$$\begin{aligned}\delta S &= \frac{t_0 L^2}{48G}\left(\frac{c^6}{6m^4\Delta x^6}{}_3F_2\left(\{1/2,1,1\},\{2,2\},\frac{c^6}{m^6\Delta x^6}\right)\right. \\ &\quad \left.-\frac{m^2}{2}{}_2F_1\left(-1/2,-1/3,2/3,\frac{c^6}{m^6\Delta x^6}\right)+\frac{m^2}{2}{}_2F_1\left(-1/2,1/3,4/3,\frac{c^6}{m^6\Delta x^6}\right)\right)+\ldots\end{aligned} \tag{8.7.23}$$

where the ellipses denote $\tilde{z}$-independent terms. We want to compute the differential entropy

$$\delta E = \lim_{n\to\infty} n[\delta S(\Delta x) - \delta S(\Delta x - L_x/n)] \tag{8.7.24}$$

which requires the relations

$$\begin{aligned}&{}_2F_1\left(-1/2,1/3,4/3,\frac{a}{x^6}\right)-{}_2F_1\left(-1/2,1/3,4/3,\frac{a}{(x-L_x/n)^6}\right)= \\ &\qquad \frac{3aL_x}{4x^7}{}_2F_1\left(1/2,4/3,7/3,\frac{a}{x^6}\right)\frac{1}{n}+\mathcal{O}(1/n^2)\end{aligned} \tag{8.7.25}$$

$$\begin{aligned}&{}_2F_1\left(-1/2,-1/3,2/3,\frac{a}{x^6}\right)-{}_2F_1\left(-1/2,-1/3,2/3,\frac{a}{(x-L_x/n)^6}\right)= \\ &\qquad -\frac{3aL_x}{2x^7}{}_2F_1\left(1/2,2/3,5/3,\frac{a}{x^6}\right)\frac{1}{n}+\mathcal{O}(1/n^2)\end{aligned} \tag{8.7.26}$$

$$\begin{aligned}&\frac{1}{x^6}{}_3F_2\left(\{1/2,1,1\},\{2,2\},\frac{a}{x^6}\right)- \\ &\quad \frac{1}{(x-L_x/n)^6}{}_3F_2\left(\{1/2,1,1\},\{2,2\},\frac{a}{(x-L_x/n)^6}\right)= \\ &\qquad \frac{12L_x}{ax}\left(-1+\sqrt{1-\frac{a}{x^6}}\right)\frac{1}{n}+\mathcal{O}(1/n^2)\end{aligned} \tag{8.7.27}$$

where here $a/x^6 < 1$ since we are considering $\mu > 1$. For the former two results we have used the standard identity

$$\frac{d}{dz}{}_2F_1(a,b,c,x) = \frac{ab}{c}{}_2F_1(a+1,b+1,c+1,x) \tag{8.7.28}$$

and for the latter result we have used the following relation,

$${}_3F_2\left(\{1/2,1,1\},\{2,2\},x\right) = \frac{4}{x}\left(\log\left(\frac{1+\sqrt{1-x}}{2}\right) - \sqrt{1-x}+1\right) \tag{8.7.29}$$

where, again, here $x < 1$ since we are considering $\mu > 1$. The differential entropy is then calculated to be

$$\begin{aligned}\delta E &= \frac{t_0 V}{384G}\frac{c_0^2}{(\Delta x)^3\mu^4}\left(16\mu^6\left(-1+\sqrt{1-\frac{1}{\mu^6}}\right)\right. \\ &\quad \left. +6{}_2F_1\left(\frac{1}{2},\frac{2}{3},\frac{5}{3},\frac{1}{\mu^6}\right)+3{}_2F_1\left(\frac{1}{2},\frac{4}{3},\frac{7}{3},\frac{1}{\mu^6}\right)\right)\end{aligned} \tag{8.7.30}$$

where recall $V \equiv L^2 L_x$, and we leave some Δx-dependence implicit in μ for notational clarity.

We now want to compute the corresponding change in the gravitational entropy of the hole. As shown in Section 8.7.1, the change in gravitational entropy of the hole is given by

$$\delta E_{\text{grav}} = \frac{V}{4G_N}\frac{3c_0^2 c_1 t_0}{\Delta x^3} \tag{8.7.31}$$

where c_1 is defined by equation (8.7.2) and is given by equations (8.3.34)-(8.3.35)

$$\begin{aligned}c_1 &= \frac{1}{288\mu^4}\left(16\mu^6\left(-1+\sqrt{1-\frac{1}{\mu^6}}\right)\right. \\ &\quad \left. +6{}_2F_1\left(\frac{1}{2},\frac{2}{3},\frac{5}{3},\frac{1}{\mu^6}\right)+3{}_2F_1\left(\frac{1}{2},\frac{4}{3},\frac{7}{3},\frac{1}{\mu^6}\right)\right).\end{aligned} \tag{8.7.32}$$

The equality of the differential entropy and the gravitational entropy of the hole is then manifest.

8.8 Entanglement and Differential Entropy for Top-Down Solutions

The main focus of this chapter has been to develop a systematic method for computing the entanglement entropy for top-down brane probe systems. Our method however immediately generalises to any top-down solution which can be viewed as a perturbation of $AdS_5 \times S^5$ (or indeed a perturbation of the finite temperature AdS_5 Schwarzschild $\times\, S^5$): using the Kaluza-Klein holography dictionary we can extract the effective five-dimensional Einstein metric and thence compute the entanglement entropy.

It is worth noting that given a general asymptotically $AdS_5 \times S^5$ supergravity solution one cannot extract the five-dimensional Einstein metric, except asymptotically around the conformal boundary. Brane probe systems in which the perturbations relative to $AdS_5 \times S^5$ are small everywhere, and thus the Kaluza-Klein dictionary can be used to compute the five-dimensional Einstein metric at all scales, are special cases. In general the Kaluza-Klein dictionary becomes intractable when the metric perturbations relative to the $AdS_5 \times S^5$ background are of order one, i.e. at some finite distance from the conformal boundary.

Another subset of ten-dimensional supergravity solutions can be expressed in terms of the uplifts of five-dimensional gauged supergravity solutions, for which the Einstein metric is known from the lower-dimensional theory. For example, specific cases of Coulomb branch solutions are realised as solutions of $\mathcal{N} = 8$ gauged supergravity in five dimensions; generic Coulomb branch solutions are however not realised as lower-dimensional solutions. The Coulomb branch examples also illustrate the fact that the causal structure of the five-dimensional Einstein metric is generically not the same as that of the uplifted ten-dimensional metric: the former can have naked timelike singularities which correspond to harmless null horizons in the uplifted solutions. One could thus envisage a scenario where the lower-dimensional metric had no entanglement shadows of the type discussed in [235] but the uplifted solution had shadow regions which could not be probed by five-dimensional fields at all.

The entanglement entropy is computed from the five-dimensional Einstein metric and the differential entropy (built from entanglement entropy) therefore reconstructs areas of holes in the five-dimensional Einstein metric. The ten-dimensional metric cannot be reconstructed just from the five-dimensional Einstein metric: the uplift map requires all the matter fields in the lower-dimensional theory. Therefore the standard entanglement entropy and differential entropy cannot in principle reconstruct the ten-dimensional geometry without additional information.

8.8.1 Coulomb Branch Examples

To illustrate the above discussions we consider a particular Coulomb branch solution discussed in [45, 261]. The Coulomb branch of $\mathcal{N} = 4$ SYM corresponds to the spontaneous breaking of the gauge symmetry by giving VEVs to the scalars - on the gravity side, these solutions are represented by multi-centre D3-brane solutions. These flows break superconformal invariance but preserve sixteen supercharges.

[261] studies particular Coulomb branch solutions which admit consistent truncations. These flows are described in five-dimensional gauged supergravity by a single scalar field $\chi(r)$ where r is a radial coordinate for the 5-dimensional metric

$$ds^2 = e^{2A(r)} dx_\nu dx^\nu + dr^2 \tag{8.8.1}$$

where $r \to \infty$ corresponds to the conformal boundary. The BPS conditions can be written as

$$\frac{d\chi}{dr} = \frac{g}{2}\frac{\partial W}{\partial \chi} \qquad \frac{dA}{dr} = -\frac{g}{3}W \tag{8.8.2}$$

where $W(\chi)$ is the superpotential and g is the gauged supergravity coupling constant. In particular, we will be interested in the solution which, from the ten-dimensional point of view, corresponds to the D3-branes being uniformly distributed on a disc of radius σ in the transverse space, preserving $SO(4) \times SO(2)$ of the $SO(6)$ symmetry in the conformal $AdS_5 \times S^5$ solution. In this case one has

$$W(\chi) = -e^{\frac{2}{\sqrt{6}}\chi} - \frac{1}{2}e^{-\frac{4}{\sqrt{6}}\chi} \tag{8.8.3}$$

$$A(\chi) = \frac{1}{2}\log\left|\frac{e^{\frac{2}{\sqrt{6}}\chi}}{1-e^{\sqrt{6}\chi}}\right| + \log(\sigma) \tag{8.8.4}$$

where we have as usual set the radius of curvature of AdS_5 to be one.

Redefining the radial coordinate one can write the metric as

$$ds^2 = \lambda^2\rho^2\left(dx_\nu dx^\nu + \frac{d\rho^2}{\rho^4\lambda^6}\right) \qquad \lambda^6 = \left(1+\frac{\sigma^2}{\rho^2}\right), \tag{8.8.5}$$

where $\rho \to \infty$ at the conformal boundary and the metric is AdS_5 for $\sigma = 0$. The uplifted ten-dimensional metric is then expressed as

$$ds_{10}^2 = \Delta^{-2/3}ds^2 + ds_K^2, \tag{8.8.6}$$

where the warp factor Δ depends on the sphere coordinates and ds_K^2 is a metric on a warped sphere. Explicitly

$$\begin{aligned} \Delta^{-2/3} &= \frac{\zeta}{\lambda^2} \qquad \zeta = (1+\frac{\sigma^2}{\rho^2}\cos^2\theta); \\ ds_K^2 &= \frac{1}{\zeta}\left(\zeta^2 d\theta^2 + \cos^2\theta d\Omega_3^2 + \lambda^6\sin^2\theta d\phi^2\right). \end{aligned} \tag{8.8.7}$$

The five-dimensional metric has a naked timelike singularity at $\rho = 0$ but the uplifted geometry has a null horizon at $\rho = 0$.

The five-dimensional metric satisfies an a-theorem: the warp factor $A(r)$ in (8.8.1) decreases monotonically as r decreases. Correspondingly the entanglement entropy and the differential entropy monotonically decrease as the scale of the entangling region is increased. Working for convenience in the coordinate system (8.8.5) the entanglement entropy of a slab is

$$S = \frac{L^2}{4G_N}\int_{\rho_0}^{\Lambda} d\rho \frac{\rho^3(\rho^2+\sigma^2)^{1/2}}{\sqrt{\rho^4(\rho^2+\sigma^2)-\rho_0^4(\rho_0^2+\sigma^2)}}, \tag{8.8.8}$$

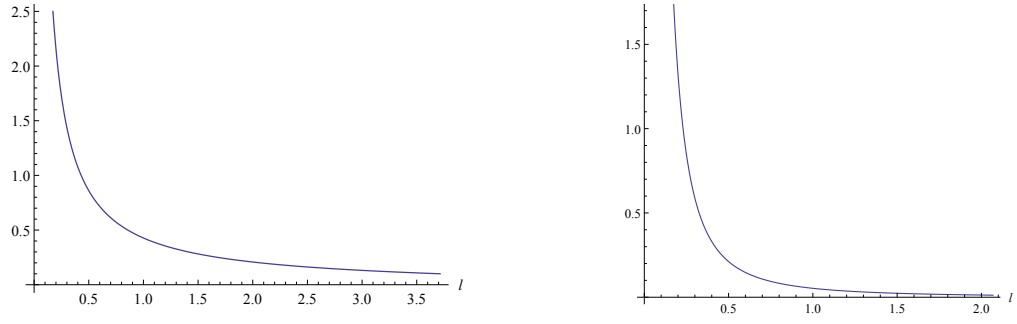

Figure 8.8.1: Plots of ρ_0 and ΔS as functions of l for $\sigma = 0.1$. Both functions asymptote to zero as $l \to \infty$.

where Λ is the UV cutoff and ρ_0 is the turning point. The quantity

$$\Delta S = S - \frac{\Lambda^2 L^2}{2G_N} \tag{8.8.9}$$

is UV finite by construction. The relation between the width of the slab l and the turning point is

$$l = 2\rho_0^2(\rho_0^2+\sigma)^{1/2}\int_{\rho_0}^{\infty}\frac{d\rho}{\sqrt{\rho^2(\rho^2+\sigma^2)(\rho^4(\rho^2+\sigma^2)-\rho_0^4(\rho_0^2+\sigma^2))}}. \tag{8.8.10}$$

The quantity $\Delta S(l)$ monotonically decreases as l is increased. We can express the differential entropy associated with strips of width l as

$$E(l) = L_x\frac{\partial(\Delta S)}{\partial l}, \tag{8.8.11}$$

and this quantity also decreases monotonically with l. This had to be true since (by construction) $E(l)$ can be expressed in terms of the warp factor in (8.8.1), which is known to satisfy the a-theorem, see [45]. It is interesting to note that the differential entropy is proportional to the finite entropy (8.3.49), which in turn is known to play the role of a c-function in two spacetime dimensions. In any holographic background dual to a RG flow, the differential entropy is by construction expressed in terms of the warp factor in (8.8.1), which satisfies the a-theorem provided that appropriate energy conditions are imposed on the bulk stress energy tensor [45], and therefore the differential entropy has the correct property to correspond to an a-function (in any dimension).

Entanglement for Coulomb branch geometries has been discussed in earlier papers [203, 207] from a ten-dimensional perspective, i.e. minimal surfaces in the ten dimensional geometry were explored. As emphasised throughout this chapter, the standard entanglement entropy should be computed from the five-dimensional Einstein metric, which can only be extracted near the boundary in the case of separated brane stacks

discussed in [203, 207], since no consistent truncation to five-dimensional supergravity exists (Kaluza-Klein holography allows us to extract the Einstein metric near the conformal boundary, where the metric is close to AdS_5 but deep in the interior the metric is not close to AdS_5 and therefore the method cannot be used there, see [24, 25]). It is however an interesting and non-trivial question whether the entanglement entropy can equally well be computed via codimension two minimal surfaces in the uplifted geometry. One must refine the boundary conditions in this case to distinguish whether one is computing the usual entanglement entropy or the generalised entanglement entropy discussed in Section 7.2. We return to this issue, as well as the discussion of entanglement entropy for Coulomb branch solutions, in Chapter 9.

8.9 Conclusions

One of the main results of this chapter is a systematic method to compute the effective lower-dimensional Einstein metric for top-down brane probe systems, using which one can extract the entanglement entropy. We have illustrated this method with the case of quarks at finite mass and density, at zero temperature. It would be interesting to explore the finite temperature behaviour of the entanglement entropy and how it captures the phase transitions found in [241, 242]. Our method is applicable to any brane probe system and could for example be used to evaluate the entanglement entropy in models of quantum Hall physics [262, 263] and in top-down models of the Kondo effect [264]. One could also explore entanglement entropy in the presence of flavours for ABJM theory, see earlier results in [202, 204].

We were able to match the structure of all terms in the entanglement entropy for finite mass quarks at zero density with field theory expectations, and the logarithmic divergences were matched exactly. Few field theory results exist for entanglement entropy at finite temperature and density; see the recent papers [265, 266] for discussions of specific universal thermal corrections in conformal field theories. It would be interesting to explore whether conformal perturbation techniques analogous to those of [227] can be used to extract universal terms at finite mass and density; just like the mass, the chemical potential breaks conformal invariance even at zero temperature but can be treated in conformal perturbation theory. Results on entanglement entropy using conformal perturbation theory in the context of higher spin theory can be found in [267–269].

The entanglement entropy calculated using the ten-dimensional metric is in general expected to be qualitatively different to that computed using the lower-dimensional Einstein metric[5]. It is interesting to note however that the entanglement entropy computed using the top-down metric for smeared solutions such as [202] seems to give answers

[5] As demonstrated in [24] and subsequent works on Kaluza-Klein holography, quantities computed using the upstairs ten-dimensional metric qualitatively differ from those computing using the systematic Kaluza-Klein holography approach of extracting the lower-dimensional Einstein metric, and other lower-dimensional fields, directly dual to field theory operators.

which agree with F-theorem expectations. In such examples the ten-dimensional metric has a very special form, in which all warp factors depend only on the radial coordinate, and thus the lower-dimensional Einstein metric is simply related to the top-down metric. It would be interesting to understand the relationship between the metrics in more detail, and to compare the entanglement entropy computed in [202] with what is obtained using the method developed here. This general issue forms the subject matter of Chapter 9.

Note that the entanglement entropy is not the only interesting quantity which is computable from the effective lower-dimensional Einstein metric: correlation functions involving only the transverse traceless components of the field theory stress energy tensor can also be computed from perturbations of the Einstein metric. Kaluza-Klein holography allows such energy momentum tensor correlation functions to be accessed without computing the entire backreaction in ten dimensions.

8.A Source Terms in Linear Equations

In this appendix we discuss the derivation of (8.5.19) from (8.5.17) using the results for the linearised field equations around an $AdS_5 \times S^5$ background given in [36]. The components of the Einstein equations in the non-compact directions are

$$\begin{aligned}&\frac{1}{2}(\Box_x+\Box_y+2)H_{mn}+3g^o_{mn}H^p_p-\frac{1}{2}\nabla_m\nabla^p H_{np}-\frac{1}{2}\nabla_n\nabla^p H_{mp} \\ &\quad+\frac{1}{2}\nabla_m\nabla_n H^p_p-\frac{1}{2}\nabla_m\nabla^a h_{na}-\frac{1}{2}\nabla_n\nabla^a h_{ma}-\frac{1}{6}g^o_{mn}(\Box_x+\Box_y)h^a_a \\ &\quad-\frac{16}{3}g^o_{mn}h^a_a+\frac{1}{3}g^o_{mn}\epsilon^{pqrst}f_{pqrst}=\kappa_{10}^2\bar{T}_{mn}.\end{aligned} \tag{8.A.1}$$

Here ∇_m and ∇_a denote covariant derivatives while $\Box_x$ and $\Box_y$ denote the d'Alambertians; $H_{np}=h_{np}+\frac{1}{3}h^a_a g^o_{mn}$.

Projecting this equation onto the zeroth spherical harmonic results in

$$\begin{aligned}&\frac{1}{2}(\Box_x+2)h^E_{mn}+3g^o_{mn}(h^E)^p_p-\frac{1}{2}\nabla_m\nabla^p h^E_{np}-\frac{1}{2}\nabla_n\nabla^p h^E_{mp} \\ &\quad+\frac{1}{2}\nabla_m\nabla_n(h^E)^p_p-\frac{1}{6}g^o_{mn}\Box_x\pi^0-\frac{16}{3}g^o_{mn}\pi^0+\frac{1}{3}g^o_{mn}\epsilon^{pqrst}\partial_p b^0_{pqrst}=\kappa_{10}^2\bar{T}^0_{mn},\end{aligned} \tag{8.A.2}$$

where h^E_{mn} was defined in (8.5.7).

To obtain an equation for the Einstein metric perturbation h^E_{mn} we need to eliminate π^0 and b^0_{pqrs}. The trace of the Einstein equation over the five sphere gives

$$\begin{aligned}&\frac{1}{2}(\Box_x-\frac{1}{15}\Box_y-32)h^a_a+\frac{1}{2}\Box_y H^p_p-\frac{1}{2}\nabla^a\nabla^p h_{ap} \\ &\quad-\nabla^a\nabla^b h_{(ab)}+\frac{5}{3}\epsilon^{abcde}f_{abcde}=\kappa_{10}^2\bar{T}^a_a.\end{aligned} \tag{8.A.3}$$

Projecting this equation onto the zeroth spherical harmonic results in

$$\frac{1}{2}(\Box_x - 32)\pi^0 = \kappa_{10}^2 \tilde{T}^0. \tag{8.A.4}$$

The five-form self duality equation along the non-compact directions gives

$$5\partial_{[m}c_{npqr]} = \frac{1}{4!}\epsilon_{mnpqr}^{\quad abcde}\partial_a c_{bcde} + \frac{1}{2}(H_p^p - \frac{8}{3}h_a^a)\epsilon_{mnpqr} \tag{8.A.5}$$

which projected onto the zeroth spherical harmonics gives

$$5\partial_{[m}b^0_{npqr]} = \frac{1}{2}((h^E)_p^p - \frac{8}{3}\pi^0)\epsilon_{mnpqr}. \tag{8.A.6}$$

Inserting (8.A.4) and (8.A.6) into (8.A.2) then gives

$$(\mathcal{L}_E + 4)h^E_{mn} = \kappa_{10}^2(\bar{T}^0_{mn} + \frac{1}{3}\tilde{T}^0 g^o_{mn}). \tag{8.A.7}$$

CHAPTER 9

Entanglement Entropy in Top-Down Models

The material in the present chapter is based largely on [4].

9.1 Introduction

The focus of this chapter is on the computation of holographic entanglement entropy in top-down systems. By "top-down" we mean solutions of ten and eleven dimensional supergravity which are asymptotic to AdS cross a compact space. In the context of phenomenological applications of holography, it is considered important to use top-down models wherever possible, to ensure that the quantities calculated are consistent. Entanglement entropy is a novel computable for top-down models and, following the pioneering works of [194, 209], it can be used as an order parameter to characterise confinement and other phase transitions.

The original Ryu-Takayanagi proposal [183] is applicable to (asymptotically locally) anti-de Sitter spacetimes which are static. Given an entangling region on a spatial hypersurface of constant time in the boundary field theory, the entanglement entropy is computed holographically from the area A of a bulk minimal surface of codimension two which is homologous to the boundary entangling region,

$$S_{\rm RT} = \frac{A}{4G_N} \tag{9.1.1}$$

where G_N is the Newton constant. Note that the area of the minimal surface is computed in the Einstein frame metric.

In this chapter we will focus on entanglement entropy in top-down models, assuming

that the solutions are globally static (the latter is a reasonable assumption in many phenomenological models, in which holographic duals of Poincaré invariant field theories are being constructed, but the static assumption does exclude finite temperature and density models).

Consider a bulk solution which is asymptotic to $AdS_{d+1} \times X$ where X is a compact space. Given an entangling region on a spatial hypersurface of the non-compact part of the boundary, then it has been suggested by [183, 193] that the holographic entanglement entropy can be computed from the area of a codimension two minimal surface which asymptotically wraps the compact space X and is homologous to the entangling region. Hence

$$S_{\text{top}-\text{down}} = \frac{\mathcal{A}}{4\mathcal{G}_N} \tag{9.1.2}$$

where $\mathcal{A}$ is the area of the minimal surface (in the Einstein frame metric) and $\mathcal{G}_N$ is the higher dimensional Newton constant. This prescription for the top-down entanglement entropy was used in [194] to explore phase transitions in top-down models. Other applications of the top-down prescription can be found in [195–206].

The purpose of this chapter is to explore the relationship between (9.1.1) and (9.1.2). In particular, we will give strong evidence that the two formulae agree whenever we can uplift an asymptotically anti-de Sitter spacetime to a top-down solution. We will also give a proof that (9.1.2) indeed correctly calculates the holographic entanglement entropy in situations where consistent truncations of the top-down model do not exist, i.e. one does not know how to calculate the lower-dimensional Einstein metric. Our explicit examples focus primarily on asymptotically $AdS_5 \times S^5$ geometries, although the arguments and methodology could be straightforwardly generalized to other holographic dualities.

As we review in Section 9.2, the agreement between (9.1.1) and (9.1.2) is manifest for top-down solutions which are globally direct products between an asymptotically locally AdS geometry and a compact space X. The agreement between (9.1.1) and (9.1.2) is far less obvious even in the context of consistent truncations of top-down models to gauged supergravity. The map between the top-down Einstein metric and the lower-dimensional Einstein metric is quite complicated for consistent truncations, with warp factors depending non-trivially on both the lower-dimensional coordinates and on the position in the compact space, see for example (9.3.6).

In Sections 9.3 and 9.4 we show that the top-down entanglement entropy computed via (9.1.2) indeed agrees with that computed using (9.1.1) in consistent truncations to gauged supergravities and in consistent truncations involving massive vectors. The agreement involves non-trivial cancellations of warp factors depending on compact space coordinates.

A generic asymptotically $AdS_5 \times S^5$ solution of ten-dimensional supergravity cannot be

expressed as a solution of a five-dimensional theory which is a consistent truncation. For example, only special Coulomb branch solutions can be reduced to give gauged supergravity solutions (see examples in [45,261]) and only a subgroup of LLM solutions [270] can be reduced to gauged supergravity solutions. However, in a finite region near the conformal boundary, one can always systematically reduce the ten-dimensional solutions over the sphere to obtain the five-dimensional Einstein metric as a Fefferman-Graham expansion; the reduction uses the methods of Kaluza-Klein holography developed in [24, 25].

In Section 9.5 we use Kaluza-Klein holography to compare the top-down entanglement entropy (9.1.2) with that obtained from the five-dimensional Einstein metric using (9.1.1), working up to quadratic order in the near boundary expansion. Even though the relationship between the five-dimensional and ten-dimensional Einstein metrics is extremely complicated (involving derivative field redefinitions), the expressions (9.1.1) and (9.1.2) indeed agree.

Entanglement entropy has also been computed for flavour brane solutions (used to describe flavours in the dual field theory), using both probe branes and backreacted (smeared) solutions. For probe branes, one can calculate the backreaction of the probe branes onto the lower-dimensional Einstein metric using Kaluza-Klein holography, as in Chapter 8, and show that this gives an equivalent answer to that obtained using (9.1.2). Entanglement entropy for backreacted smeared solutions has previously been computed using (9.1.2). In Section 9.6 we show that the same answer is obtained by extracting the lower-dimensional Einstein metric using Kaluza-Klein holography and applying (9.1.1), again confirming the matching between (9.1.1) and (9.1.2).

Having established the agreement between (9.1.1) and (9.1.2) in a number of examples, we give general arguments for why the formulae agree in Section 9.7, building on the approach of [172]. In particular, assuming that the replica trick may be used, we can express entanglement in terms of partition functions for replica spaces. The latter can be computed holographically to leading order using the onshell action and therefore the equality of (9.1.1) and (9.1.2) is essentially inherited from the equality of ten-dimensional and five-dimensional onshell actions.

In Section 9.7 we also give an alternative argument for the origin of (9.1.1) and (9.1.2), using the replica trick approach of [172] in combination with old results of Gibbons and Hawking on gravitational instanton symmetries [271]. The latter suggests that for generic entangling regions there may be additional contributions to the holographic entanglement entropy (even at leading order) if the circle direction used in the replica trick is non-trivially fibered over the boundary of the entangling region. In practice one does not usually consider entangling regions such that the circle direction is non-trivially fibered but it would nonetheless be interesting to explore this situation further.

We conclude in Section 9.8 by discussing the implications of our results for top-down

holography and spacetime reconstruction. Extracting field theory data from a top-down solution is in general very subtle and computationally involved: one has to expand the ten-dimensional equations of motion perturbatively, and then use non-linear field redefinitions to obtain the effective five-dimensional equations of motion. Given the effective five-dimensional equations of motion and the asymptotic expansions of the five-dimensional fields, one can then read off field theory data using holographic renormalization [24, 25]. We should note that these steps are required even when one calculates quantities in the conformal vacuum: indeed, non-linear field redefinitions between ten-dimensional and five-dimensional fields were first introduced in [37] for the computation of three point functions in $\mathcal{N} = 4$ SYM.

The lower-dimensional metric is a particularly important quantity for holography, as it relates to the dual energy momentum tensor. One must identify the lower-dimensional metric to compute one point functions and higher correlation functions of the stress energy tensor in the dual theory. The latter are in turn used in many contexts, including discussions of a theorems and also of energy correlations, following [272]. Yet, as we review in Section 9.5, the relation between the lower-dimensional metric and the ten-dimensional metric is very complicated. The matching of (9.1.1) and (9.1.2) implies simple constraints relating the two metrics which can be used to check Kaluza-Klein holography calculations and perhaps even to deduce the lower-dimensional metric (see Section 9.6 for an example).

There has been a great deal of interest in relating entanglement to the reconstruction of the holographic spacetime. Since (9.1.2) relates the entanglement entropy to minimal surfaces in the top-down geometry, entanglement implicitly knows about the compact part of the geometry. It would be interesting to explore further how entanglement can be used to understand the global structure of the ten-dimensional geometry.

9.2 Entanglement Entropy for $AdS_5 \times S^5$

We begin by reviewing the computation of entanglement entropy for a strip on the boundary of $AdS_5 \times S^5$ from both ten-dimensional and five-dimensional perspectives.

Consider a strip A defined by $x \in [0, l]$ on the boundary of AdS_5,

$$ds_5^2 = \frac{1}{\rho^2}\left(dx_\mu dx^\mu + d\rho^2\right) \tag{9.2.1}$$

where $x^\mu = (t, x, y, z)$, the conformal boundary is at $\rho \to 0$, and we set the AdS radius to one throughout for convenience.

To compute the entanglement entropy one calculates the area of a bulk codimension

two minimal surface Σ with boundary $\partial\Sigma = \partial A$,

$$S_5 = \frac{1}{4G_5}\int_{\{\Sigma|\partial\Sigma=\partial A\}} d^3\xi\sqrt{\det\gamma_3} \tag{9.2.2}$$

where γ_3 is the induced metric on the minimal surface and ξ_i $(i = 1, 2, 3)$ are the world-volume coordinates. Since the metric is static we work on a fixed-time slice $t = t_0$, and the surface is thus given by $\Sigma = (t_0, x(\xi_i), y(\xi_i), z(\xi_i), \rho(\xi_i))$. By symmetry of the metric and boundary conditions it is clear that the surface cannot have non-trivial dependence on the y, z-directions, and (choosing static gauge to identify the ξ_i with a subset of the spacetime coordinates) we can thus describe the minimal surface by an embedding of the form $x = x(\rho)$ or $\rho = \rho(x)$, where it is implicit that the surface extends in the y, z-directions. Taking $x = x(\rho)$ for concreteness the induced metric on Σ is

$$ds^2_{ind} = \frac{1}{\rho^2}\left[dy^2 + dz^2 + \left(x'^2 + 1\right)d\rho^2\right] \tag{9.2.3}$$

and one can thus easily compute the entanglement entropy as

$$S_5 = \frac{V_2}{2G_5}\int_\delta^{\rho_0}\frac{d\rho}{\rho^3}\sqrt{x'^2+1} \tag{9.2.4}$$

where V_2 is the regularised area of ∂A, ρ_0 is the turning point of the surface, and δ is the UV cutoff.

Now consider the calculation of the entanglement entropy from the ten-dimensional perspective, using the ten-dimensional (Einstein) metric for $AdS_5 \times S^5$,

$$ds^2_{10} = \frac{1}{\rho^2}\left(dx_\nu dx^\nu + d\rho^2\right) + d\theta^2 + \cos^2\theta d\Omega_3^2 + \sin^2\theta d\phi^2 \tag{9.2.5}$$

The proposed generalisation of the Ryu-Takayanagi prescription in this case is to calculate the area of a codimension two minimal surface Σ, now in the full ten-dimensional spacetime,

$$S_{10} = \frac{1}{4G_{10}}\int_{\{\Sigma|\partial\Sigma=\partial A\}} d^8\xi\sqrt{\det\gamma_8} \tag{9.2.6}$$

where γ_8 is the induced metric on the minimal surface and ξ_i $(i = 1, ..., 8)$ are the world-volume coordinates.

Consider again the case of a strip on the boundary of the AdS_5 factor. In a similar fashion to before we can describe the corresponding minimal surface by an embedding of the form $x = x(\rho, \theta, \Omega_3, \phi)$, or $\rho = \rho(x, \theta, \Omega_3, \phi)$, or $\theta = \theta(x, \rho, \Omega_3, \phi)$ etc., where we again have chosen static gauge, have assumed no dependence on the y, z-directions, and are working on a fixed-time slice $t = t_0$. However, due to the S^5 factor one must refine the boundary conditions to include the internal space. As before we take the boundary condition that the surface Σ is anchored on ∂A, and consider further the condition that Σ

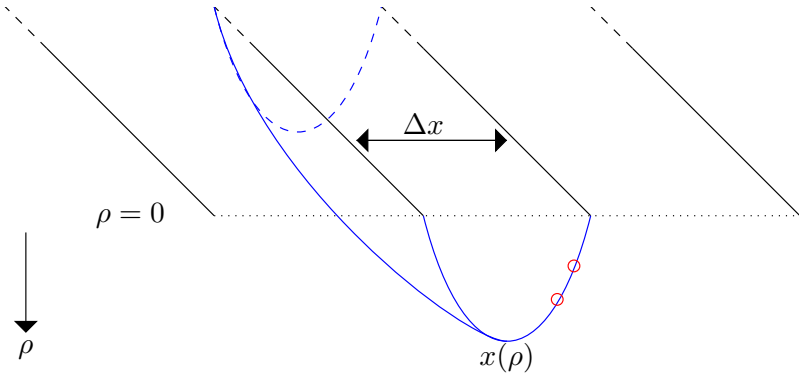

Figure 9.2.1: The entangling surface for a slab boundary region - the conformal boundary is at $\rho \to 0$ and the minimal surface is described by $x(\rho)$. The minimal surface is a direct product of a codimension two surface in anti-de Sitter with the five sphere (the latter being indicated in red).

wraps the S^5 asymptotically. Alternative boundary conditions would describe different quantities in the dual field theory - see discussions on generalised entanglement entropy [207, 208].

The boundary conditions respect the symmetries of the S^5, and together with the fact that $AdS_5 \times S^5$ is a product space it is clear by symmetry as before that the minimal surface cannot depend non-trivially on the S^5 coordinates. Thus the embedding is of the form $x = x(\rho)$ or $\rho = \rho(x)$ as in the five-dimensional case, where it is now implicit that it both extends in the y, z-directions and wraps the S^5, see Figure 9.2.1. Taking $x = x(\rho)$ for concreteness as before the induced metric on Σ is just:

$$ds^2_{ind} = \frac{1}{\rho^2}\left[dy^2 + dz^2 + \left(x'^2 + 1\right) d\rho^2\right] + d\theta^2 + \cos^2\theta d\Omega_3^2 + \sin^2\theta d\phi^2 \tag{9.2.7}$$

The entanglement entropy is thus easily calculated to be

$$S_{10} = \frac{V_2 V_{S^5}}{2G_{10}} \int_\delta^{\rho_0} \frac{d\rho}{\rho^3}\sqrt{x'^2 + 1} \tag{9.2.8}$$

which is identical to the 5-dimensional result since the Newton constants are related as $G_5 = G_{10}/V_{S^5}$.

In the above example one hence obtains the same result for the entanglement entropy when computed from both the ten and five dimensional perspectives. This example had a particularly high level of symmetry, however, and it is not clear that the above equivalence should carry over to less trivial cases.

The general problem one would like to study is the relationship between the entanglement entropy as calculated in a given downstairs metric and the entanglement entropy calculated in the uplifted solution, in cases where this uplift map is known or can be computed. Certain Coulomb branch geometries, which we study first in the following

section, provide a good example of such a scenario, admitting a known ten-dimensional uplift which is not a simple product space, instead containing warp factors that depend on both the holographic radial coordinate and a sphere coordinate.

9.3 Consistent Truncations of the Coulomb Branch

In this section we continue the discussion of Section 8.8.1 and study particular Coulomb Branch solutions discussed in [45, 261] that admit consistent truncations to solutions of five-dimensional gauged supergravity, comparing the entanglement entropy computed from five and ten dimensions.

9.3.1 Solutions with $SO(4) \times SO(2)$ Symmetry

Let us discuss first Coulomb branch solutions which, from the ten-dimensional point of view, correspond to D3-branes being uniformly distributed on a disc of radius σ in the transverse space. These supergravity solutions hence preserve $SO(4) \times SO(2)$ of the $SO(6)$ symmetry in the $AdS_5 \times S^5$ solution. These Coulomb branch geometries admit consistent truncations to (a particular sector of) 5-dimensional gauged supergravity, with action given by

$$I = \frac{1}{16\pi G_5}\int d^5x \left(-\frac{1}{4}R + \frac{1}{2}(\partial\alpha)^2 - \left(\frac{g^2}{8}\left(\frac{\partial W}{\partial \alpha}\right)^2 - \frac{g^2}{3}W^2\right)\right) \tag{9.3.1}$$

where α is a scalar field, W is the superpotential and g is the coupling constant. The five-dimensional Einstein frame metric for the solutions was considered in Section 8.8.1 and can be written as

$$ds^2 = \lambda^2 w^2 \left(dx_\nu dx^\nu + \frac{dw^2}{w^4\lambda^6}\right) \qquad \lambda^6 = \left(1 + \frac{\sigma^2}{w^2}\right), \tag{9.3.2}$$

which clearly reduces to an AdS_5 metric for $\sigma = 0$. (In the latter case the conformal boundary is at $w \to \infty$.)

Consider again a strip on the boundary defined by $x \in [0, l]$. As above we can describe the minimal surface by an embedding of the form $x = x(w)$ or $w = w(x)$. Taking $x = x(w)$ the induced metric on the surface is easily calculated to be

$$ds^2_{ind} = \lambda^2 w^2 \left[dy^2 + dz^2 + \left(x'^2 + \frac{1}{w^4\lambda^6}\right)dw^2\right] \tag{9.3.3}$$

where $x' \equiv dx/dw$, and thus one finds

$$\sqrt{\det\gamma} = \lambda^3\rho^3\sqrt{x'^2 + \frac{1}{w^4\lambda^6}} \tag{9.3.4}$$

The entanglement entropy for the slab is thus

$$S = \frac{V_2}{2G_5}\int_{w_0}^{\Lambda} dw\lambda^3 w^3\sqrt{x'^2+\frac{1}{w^4\lambda^6}} \tag{9.3.5}$$

where w_0 is the turning point of the minimal surface and Λ is the UV cutoff.

The five-dimensional metric in (9.3.2) can be uplifted to the following ten-dimensional Einstein frame metric [45, 261],

$$ds_{10}^2 = \Delta^{-2/3}ds^2 + ds_K^2, \tag{9.3.6}$$

where the warp factor Δ depends both on the holographic radial coordinate and on one of the sphere coordinates, while ds_K^2 is a metric on a warped sphere. Explicit expressions for these quantities are

$$\Delta^{-2/3} = \frac{\zeta}{\lambda^2} \qquad\qquad \zeta = (1+\frac{\sigma^2}{w^2}\cos^2\theta) \tag{9.3.7}$$

$$ds_K^2 = \frac{1}{\zeta}\left(\zeta^2 d\theta^2 + \cos^2\theta d\Omega_3^2 + \lambda^6\sin^2\theta d\phi^2\right). \tag{9.3.8}$$

Note that $\zeta, \lambda \to 1$ as $w \to \infty$ and thus the solution is indeed asymptotically $AdS_5 \times S^5$. To compute the entanglement entropy for the strip we now proceed as before, with the additional boundary condition that the minimal surface wraps the S^5 asymptotically.

However, in the present case there are non-trivial warp factors that mix the holographic radial coordinate w and the sphere coordinate θ. Thus, although we can continue to assume the minimal surface has trivial dependence on Ω_3 and ϕ, we can no longer a priori assume that the minimal surface has trivial dependence on θ. We thus may assume an embedding of the form $x = x(w,\theta)$, or $w = w(x,\theta)$ or $\theta = \theta(x,w)$. Choosing $x = x(w,\theta)$ (as the boundary conditions will be clearest in this choice) one calculates the induced metric to be

$$\begin{aligned} ds_{ind}^2 &= \zeta w^2\left[dy^2+dz^2+\left(x'^2+\frac{1}{w^4\lambda^6}\right)d\rho^2\right] + 2\zeta w^2 x'\dot{x}d\rho d\theta \\ &\quad +\zeta(1+\dot{x}^2w^2)d\theta^2 + \frac{\cos^2\theta}{\zeta}d\Omega_3 + \frac{\lambda^6}{\zeta}\sin^6\theta d\phi \end{aligned} \tag{9.3.9}$$

where $\dot{x} \equiv dx/d\theta$. One thus finds that the ten-dimensional entanglement functional is

$$S = \frac{1}{4G_{10}}\int d^8x\sqrt{\det\gamma} \tag{9.3.10}$$

where

$$\sqrt{\det\gamma} = \sqrt{\det g_{\Omega_3}}\cos^3\theta\sin\theta\lambda^3w^2\left[\left(\rho^2x'^2+\frac{1}{w^2\lambda^6}\right)(1+\dot{x}^2w^2) - \dot{x}^2x'^2w^4\right]^{1/2} \tag{9.3.11}$$

Notice that all factors of ζ, which depend on the sphere coordinate θ, cancel out and the spherical prefactors combine to become $\sqrt{\det g_{\Omega_5}}$. The only additional dependence on the spherical coordinates thus comes through the fact that $x(w,\theta)$ depends on θ

$$\sqrt{\det\gamma} = \sqrt{\det g_{\Omega_3}}\cos^3\theta\sin\theta\lambda^3 w^2\sqrt{w^2x'^2 + \frac{\dot{x}^2}{\lambda^6} + \frac{1}{w^2\lambda^6}} \tag{9.3.12}$$

One can immediately make an interesting observation. The equations of motion admit the solution $\dot{x}=0$, since the action is quadratic in $\dot{x}$ and θ does not appear explicitly in the non-trivial square root part of the action functional. For solutions in which $\dot{x}=0$, the entanglement entropy is thus

$$S = \frac{V_2 V_{S^5}}{4G_{10}}\int_{w_0}^{\Lambda} dw\lambda^3 w^3\sqrt{x'^2 + \frac{1}{w^4\lambda^6}} \tag{9.3.13}$$

i.e. identical to (9.3.5) since $G_5 = G_{10}/V_{S^5}$.

Although one can thus consistently set $\dot{x}=0$ to obtain a solution to the ten-dimensional equation of motion, it remains to show that this is indeed the minimal solution. This can be done using the radial Hamiltonian formalism as follows. One first assumes a given θ-independent solution of the equations of motion and then considers θ-dependent perturbations to this background. By computing the Hamiltonian one then shows that these perturbations lead to a larger Hamiltonian and thus the minimal solution (at least perturbatively) is indeed the one that is independent of θ. The independence of the minimal surface on the compact coordinates is a point we will return to in Section 9.5.2.

9.3.2 Other Coulomb Branch Solutions

Similar conclusions can be reached for other consistent truncations of Coulomb branch solutions with different symmetries. In [45,261] they also consider solutions with $SO(3)\times SO(3)$ and $SO(5)$ symmetry in addition to the $SO(4)\times SO(2)$ solution considered above, corresponding to various symmetric distributions of D3-branes. The $SO(3)\times SO(3)$ case has the following 10d metric

$$ds_{10}^2 = \zeta w^2\lambda\left(dx_\mu^2 + \frac{dw^2}{w^4\lambda^6}\right) + \frac{1}{\lambda\zeta}\left(\zeta^2 d\theta^2 + \cos^2\theta d\Omega_2^2 + \lambda^4\sin^2\theta d\tilde{\Omega}_2^2\right) \tag{9.3.14}$$

$$\Delta^{-2/3} = \frac{\zeta}{\lambda} \tag{9.3.15}$$

while the $SO(5)$ case has the following 10d metric

$$ds_{10}^2 = \frac{\zeta w^2}{\lambda^3}\left(dx_\mu^2 + \frac{dw^2}{w^4\lambda^6}\right) + \frac{\lambda^3}{\zeta}\left(\zeta^2 d\theta^2 + \cos^2\theta d\Omega_4^2\right) \tag{9.3.16}$$

$$\Delta^{-2/3} = \frac{\zeta}{\lambda} \tag{9.3.17}$$

In both cases the definitions of λ and ζ are as before, and the expression for Δ shows the relationship between the ten-dimensional and five-dimensional metrics c.f. (9.3.6). Given what has been deduced from the $SO(4) \times SO(2)$ case previously, it is immediate that the same equivalence will occur in these cases, since the factors of ζ cancel in the determinant and indeed one can explicitly check that the powers of λ come out the same in the two cases.

We will continue the discussion of entanglement entropy for more general Coulomb branch solutions in Section 9.5.

9.4 Consistent Truncations with Massive Vector Fields

In this section we consider the entanglement entropy for particular backgrounds which admit consistent truncations with massive vector fields, as discussed in [273]. Consider again type IIB supergravity but now with the metric, the dilaton Φ, the 5-form F_5, and the 3-form $H = \mathrm{d}B$ switched on. Our conventions for the action in Einstein frame are

$$I = \frac{1}{16\pi G_{10}} \int d^{10}x\sqrt{-g_{10}} \left[R - \frac{1}{2}\partial_A\Phi\partial^A\Phi - \frac{1}{2\cdot 3!}e^{-\Phi}H_{ABC}H^{ABC} - \frac{1}{2\cdot 5!}F^2_{(5)} \right] \tag{9.4.1}$$

where as usual we need to impose in addition the self-duality constraint on F_5.

Now consider the following ansatz for the ten-dimensional fields

$$ds^2_{10} = e^{-\frac{2}{3}(4U+V)}ds^2_M + e^{2U}ds^2_{B_{KE}} + e^{2V}\eta^2 \tag{9.4.2}$$

$$B = A \wedge \eta + \theta\omega \tag{9.4.3}$$

$$F_5 = 4e^{-4U-V}(1+\star)vol_M \tag{9.4.4}$$

where M is the 5-dimensional spacetime with metric ds^2_M and volume form vol_M. Furthermore, $ds^2_{B_{KE}} + \eta^2$ is a Sasaki-Einstein metric c.f. the representation of S^5 as a $U(1)$ fibration over $\mathbb{CP}^2$. The scalars U, V and Φ are taken to be functions on M, as is the one-form A. Expressions for the quantities θ and ω will not be important in what follows but may be found in [273].

Reducing the field equations over the internal space, one obtains equations of motion which may in turn be derived from the following 5-dimensional action for the fields (g_5, U, V, Φ, A)

$$\begin{aligned} I \;=\; & \frac{1}{16\pi G_5}\int d^5x\sqrt{-g_5}\Big[R + 24e^{-u-4v} - 4e^{-6u-4v} - 8e^{-10v} - 5(\partial u)^2 \\ & - \frac{15}{2}(\partial v)^2 - \frac{1}{2}(\partial\Phi)^2 - \frac{1}{4}e^{-\Phi+4u+v}F_{mn}F^{mn} - 4e^{-\Phi-2u-3v}A_mA^m\Big] \end{aligned} \tag{9.4.5}$$

where $F = dA$, $u = \frac{2}{5}(U-V)$ and $v = \frac{4}{15}(4U+V)$. It was shown in [273] that this reduction is consistent i.e. any solution of the resulting five-dimensional equations of

motion can be uplifted to a solution of type IIB supergravity using the map (9.4.2)-(9.4.4).

Note that from the reduced action (9.4.5) one finds that the mass of the vector field A around the AdS_5 background is $m^2 = 8$, showing these solutions are indeed associated with massive vector fields. As is clear from (9.4.2)-(9.4.3) however, this vector field does not appear in the ten-dimensional metric but instead appears in the ten-dimensional two-form field and thus it does not directly contribute to the ten-dimensional entanglement entropy.

We can immediately compute the ten-dimensional entanglement entropy, which as before is given by

$$S_{10} = \frac{1}{4G_{10}} \int_{\{\Sigma | \partial\Sigma = \partial A\}} d^8\xi \sqrt{\det \gamma_8} \tag{9.4.6}$$

where implicitly we work with the metric in Einstein frame. One can now immediately obtain the ten-dimensional entanglement entropy for an arbitrary entangling region, only assuming that we again work on a fixed time slice and that the entangling surface wraps the internal space asymptotically. Since the warp factors in the metric do not depend at all on the internal directions the entangling surface will therefore also wrap the internal space deep in the bulk. Since the entangling surface is consequently codimension two with respect to the five-dimensional spacetime M one trivially obtains

$$\sqrt{\gamma_8} = (e^{-\frac{2}{3}(4U+V)})^{\frac{3}{2}} (e^{2U})^{\frac{4}{2}} (e^{2V})^{\frac{1}{2}} \sqrt{\gamma_5}\, vol_{SE} = \sqrt{\gamma_5}\, vol_{SE} \tag{9.4.7}$$

where vol_{SE} is the volume form on the internal space, and thus it is immediate that the entanglement entropy as computed from ten dimensions will be equivalent to the five-dimensional entanglement entropy.

A particular example of interest in this solution class is given by backgrounds with non-relativistic scaling symmetries, in particular the Schrödinger backgrounds discussed in [273]. These are deformations of AdS that have a metric that can be written in the following form

$$ds^2_{M_z} = -b^2 r^{2z} (dx^+)^2 + \frac{dr^2}{r^2} + r^2 \left(-dx^- dx^+ + dx^2 + dy^2\right) \tag{9.4.8}$$

where $x^\pm$ are lightcone coordinates, z is the dynamical exponent and b is a parameter that characterizes the deformation from AdS_5. This metric is a solution to the equations of motion one obtains from the following action

$$S = \frac{1}{16\pi G_{D+3}} \int d^{D+2}x dr \sqrt{-g} \left(R - 2\Lambda - \frac{1}{4} F_{mn} F^{mn} - \frac{m^2}{2} A_m A^m \right) \tag{9.4.9}$$

where the vector field solution is $A_+ \propto r^z$, provided that $\Lambda = -(D+1)(D+2)/2$ and $m^2 = z(z+D)$.

One can check that the metric (9.4.8) for $z = 2$ (and $D = 2$) together with $U = V =$

$\Phi = 0$ and $A_+ = br^2$ is a solution to the equations of motion one derives from (9.4.5) - indeed, (9.4.5) reduces to (9.4.9) under these conditions, where in the present case $m^2 = 8$ as expected. Checking explicitly the equivalence of the ten-dimensional and five-dimensional entanglement entropies is trivial in this case since all the warp factors in (9.4.2) evaluate to one and thus the metric is a simple product space. Note that an identical analysis can be performed for consistent truncations that have vector fields with mass $m^2 = 24$ found in [273], and the equivalence between the ten-dimensional and five-dimensional entanglement entropy carries over in the same way in such cases.

9.5 Kaluza-Klein Holography

A generic ten dimensional supergravity solution which is asymptotic to $AdS_5 \times S^5$ cannot be expressed as the uplift of a five dimensional supergravity solution. However, in the vicinity of the conformal boundary the ten-dimensional solution can always be expressed as a perturbation of $AdS_5 \times S^5$. Dual field theory data can be expressed in terms of these perturbations using the method of Kaluza-Klein holography [24,25] as discussed in Section 8.5.1. We briefly review here the main features relevant to the present work.

Let us express the $AdS_5 \times S^5$ metric as

$$ds^2 = g^o_{AB} dx^A dx^B \equiv \frac{1}{\rho^2}\left(d\rho^2 + dx^\mu dx_\mu\right) + d\Omega_5^2 \tag{9.5.1}$$

with the five form flux being

$$F = F^o \equiv \eta_{AdS_5} + \eta_{S^5} \tag{9.5.2}$$

where η denotes the volume form. The Einstein metric of a solution of the type IIB equations which is a deformation of $AdS_5 \times S^5$ can therefore be expressed as

$$g_{AB} = g^o_{AB} + h_{AB}. \tag{9.5.3}$$

The metric fluctuation can always be decomposed in terms of spherical harmonics on the sphere. The metric fluctuations are decomposed as

$$\begin{aligned} h_{mn} &= \sum h^I_{mn} Y^I; \\ h_{ma} &= \sum \left(B^{I_v}_m Y^{I_v}_a + b^I_m D_a Y^I\right); \\ h_{(ab)} &= \sum \left(\phi^{I_t} Y^{I_t}_{(ab)} + \psi^{I_v} D_{(a} Y^{I_v}_{b)} + \chi^I D_{(a} D_{b)} Y^I\right); \\ h^a_a &= \sum \pi^I Y^I \end{aligned} \tag{9.5.4}$$

where Y^I are scalar harmonics, $Y^{I_v}_a$ are vector harmonics and $Y^{I_t}_{(ab)}$ are symmetric traceless tensor harmonics; D_a denotes the covariant derivative. We will not need explicit forms for the spherical harmonics in what follows but note that the defining equations

are

$$\begin{aligned} \Box Y^I &= \Lambda^I Y^I \qquad \Lambda^I = -k(k+4) \qquad k = 0, 1, 2, \cdots \\ \Box Y_a^{I_v} &= \Lambda^{I_5} Y_a^{I_v} \qquad \Lambda^{I_v} = -(k^2+4k-1) \qquad k = 1, 2, \cdots \\ \Box Y_{(ab)}^{I_t} &= \Lambda^{I_t} Y_{(ab)}^{I_t} \qquad \Lambda^{I_t} = -(k^2+4k-2) \qquad k = 2, 3, \cdots \end{aligned} \tag{9.5.5}$$

where $\Box$ is the D'Alambertian and $D^a Y_a^{I_v} = D^a Y_{(ab)}^{I_t} = 0$. The spherical harmonic labels denote both the degree of the harmonic and additional quantum numbers, i.e. charges under the Cartan of $SO(6)$.

The fluctuations are not all independent, as some of the modes are diffeomorphic to each other or to the background. To derive the spectrum around AdS it is usual to impose a gauge fixing condition such as the de Donder-Lorentz gauge

$$D^a h_{(ab)} = D^a h_{am} = 0 \tag{9.5.6}$$

which sets to zero b_m^I, ψ^{I_v} and χ^I. The remaining modes h_{mn}^I, $B_m^{I_v}$, ϕ^{I_t} and π^I are then related to tensor, vector and scalar fields in five dimensions. Although this gauge choice is very convenient for deriving the spectrum, it can be less useful when analysing a generic solution, as typically such solutions will not naturally be expressed in this gauge. Instead of gauge fixing the symmetry, one can instead derive gauge invariant combinations of the fluctuations; the latter are the five-dimensional fields [24, 25].

Working to linear order in the perturbations the five-dimensional Einstein metric $g_{mn}^5 = g_{mn}^o + H_{mn}$ is related to the ten-dimensional metric perturbations given above as

$$H_{mn} = h_{mn}^0 + \frac{1}{3}\pi^0 g_{mn}^o, \tag{9.5.7}$$

i.e. it depends only on the zero mode of the tensor perturbation and the breathing mode on the sphere. The origin of the second term is the Weyl rescaling needed to bring the five dimensional metric into Einstein frame. This was the main Kaluza-Klein holography result used in Section 8.5 to calculate the entanglement entropy contribution of probe branes. In the present chapter we also wish to go to higher order however.

Working to quadratic order in the perturbations, the expression for the five-dimensional metric in terms of the ten-dimensional metric perturbations is considerably more complicated and indeed it has not been worked out in generality. At quadratic order the schematic form of the appropriately gauge-invariant metric perturbation is

$$h_{mn} = h_{mn}^0 + \frac{1}{3}\pi^0 g_{mn}^o + h_{(2)mn} \tag{9.5.8}$$

where $h_{(2)mn}$ is quadratic in perturbations.

For example, for modes associated with the scalar spherical harmonics the quadratic

contributions are [24]

$$\begin{aligned} h_{(2)mn} &= -\sum_I z(k)\left(\frac{1}{2}\Lambda^I(\chi^I\hat{h}^I_{mn}+\frac{1}{2}D_m\chi^I D_n\chi^I)\right. \\ &\left. + D_m\hat{b}^{pI}\hat{h}^I_{np}+D_n\hat{b}^{pI}\hat{h}^I_{mp}+\hat{b}^{pI}D_p\hat{h}^I_{mn}+D_m\hat{b}^{pI}D_n\hat{b}^I_p+\hat{b}^{pI}\hat{b}^I_p g^o_{mn}-\hat{b}^I_m\hat{b}^I_n\right) \end{aligned} \tag{9.5.9}$$

where

$$\begin{aligned} \hat{b}^I_m &= b^I_m-\frac{1}{2}D_m\chi^I \\ \hat{h}^I_{mn} &= h^I_{mn}-D_m b^I_n-D_n b^I_m \end{aligned} \tag{9.5.10}$$

are gauge invariant combinations at linear order in the fluctuations. Note that if we work in de Donder-Lorentz gauge $h_{(2)mn}=0$.

It is important however to note that h_{mn}, while appropriately gauge invariant with respect to the ten-dimensional symmetries and transforming as a five-dimensional metric, is still not the five-dimensional Einstein metric fluctuation. The combination h_{mn} satisfies an Einstein equation

$$(\mathcal{L}_E+4)h_{mn}=T_{(2)mn} \tag{9.5.11}$$

where $\mathcal{L}_E$ is the usual linearized Einstein operator and the effective stress energy tensor is $T_{(2)mn}$. This effective stress energy tensor is quadratic in the fluctuations but involves derivative interactions. For example, terms quadratic in the fields π^I have the general structure

$$T_{(2)mn}=\sum_I\left(a_I D_m D_p D_r\pi^I D_n D^p D^r\pi^I+b_I D_m D_p\pi^I D_n D^p\pi^I+\cdots\right) \tag{9.5.12}$$

with certain coefficients $(a_I,b_I,\cdots)$. The effective five-dimensional action does not contain derivative interactions, and therefore the five-dimensional fields must be related to ten-dimensional fields by non-linear field redefinitions, as first noted in [37]. In particular the five-dimensional Einstein metric perturbation H_{mn} is related to the metric fluctuation h_{mn} as

$$H_{mm}=h_{mn}+\sum_I\left(A_I D_m D_p\pi^I D_n D^p\pi^I+B_I D_m\pi^I D_n\pi^I+\cdots\right) \tag{9.5.13}$$

where again the coefficients $(A_I,B_I,\cdots)$ are computable. Thus the explicit form of the five-dimensional Einstein metric is extremely complicated at quadratic order since it involves infinite sums with coefficients $(A_I,B_I,\cdots)$ which are very arduous to compute; see [24] for explicit expressions.

9.5.1 General Coulomb Branch solutions

As an example of solutions which can be understood using Kaluza-Klein holography, we consider general Coulomb branch solutions i.e. solutions that do not necessarily admit a consistent truncation. The metric for such solutions takes the following form,

$$ds^2 = H(y)^{-1/2} dx_\mu dx^\mu + H(y)^{1/2} dy_i dy^i \tag{9.5.14}$$

where x_μ are the brane directions and y_i are transverse directions, and $H(y)$ is a harmonic function on R^6. Near the conformal boundary the harmonic function takes the form

$$H = \frac{L^4}{r^4}\left(1 + \sum_{k\geq 2} \frac{a_k^I Y_k^I}{r^k}\right) \tag{9.5.15}$$

where we have written

$$dy_i dy^i = dr^2 + r^2 d\Omega_5^2 \tag{9.5.16}$$

while Y_k^I are scalar harmonics of degree k on S^5 and a_k^I are coefficients defining the brane distribution. Implicitly we have taken the decoupling limit of the brane solution, i.e. dropped the constant term in the harmonic function.

We can now express the Coulomb branch metric asymptotically as a perturbation of $AdS_5 \times S^5$. The background asymptotes to

$$ds^2 = g^o_{AB} dx^A dx^B = \frac{r^2}{L^2} dx_\mu dx^\mu + \frac{L^2}{r^2} dr^2 + L^2 d\Omega_5^2 \tag{9.5.17}$$

To match with earlier conventions we set $L^2 = 1$ (the curvature radius can be reinstated in final formulae if required). Near the conformal boundary

$$g_{AB} = g^o_{AB} + h_{AB} \tag{9.5.18}$$

where working to linear order in the coefficients a_n^I we can read off

$$\begin{aligned} h_{\mu\nu} &= -\sum_{k\geq 2} \frac{a_k^I Y_k^I}{2r^{k-2}} \eta_{\mu\nu}; \\ h_{rr} &= \sum_{k\geq 2} \frac{a_k^I Y_k^I}{2r^{k+2}}; \\ h_{ab} &= \sum_{k\geq 2} \frac{a_k^I Y_k^I}{2r^k} g^o_{ab}. \end{aligned} \tag{9.5.19}$$

Hence the non-zero perturbations are

$$\pi^I = \frac{5a_k^I}{2r^k} \tag{9.5.20}$$

and

$$h^I_{\mu\nu} = -\frac{a^I_k}{2r^{k-2}} \qquad h^I_{rr} = \frac{a^I_k}{2r^{k+2}}, \tag{9.5.21}$$

for harmonics of degree $k \geq 2$.

These perturbations are consistent with the diagonalised equations of motion at linear order found in [36]. Let

$$\pi^I = 10k\epsilon s^I \tag{9.5.22}$$

where ϵ is a small parameter and k is the degree of the associated spherical harmonic with $k \geq 2$. The equation of motion for s^I is

$$\Box s^I = k(k-4)s^I \tag{9.5.23}$$

where $\Box$ is the d'Alambertian in AdS_5.

The supergravity field equations at linear order then imply that such perturbations are necessarily accompanied by

$$\begin{aligned} h^I_{mn} = \epsilon h^I_{(1)mn} &= \epsilon\left(\frac{4}{(k+1)}D_{(m}D_{n)}s^I - \frac{6k}{5}s^I g^o_{mn}\right) \\ &= \epsilon\left(\frac{4}{(k+1)}D_mD_ns^I - \frac{2k}{k+1}(k-1)s^I g^o_{mn}\right) \end{aligned} \tag{9.5.24}$$

If one switches on only these modes at linear order, as in the Coulomb branch solutions, other metric perturbations are induced at order ϵ^2 or higher. In other words, other ten-dimensional perturbations can be induced by expanding the field equations to quadratic order in ϵ but these perturbations are not present at linear order. Comparing with (9.5.20) we find that

$$\epsilon s^I = \frac{a^I_k}{4kr^k} \tag{9.5.25}$$

which indeed satisfies (9.5.23).

For later use, let us note that if s^I depends only on the radial coordinate, ρ, then

$$D_\rho D_\rho s^I = (\partial^2_\rho s^I + \frac{1}{\rho}\partial_\rho s^I) \qquad D_\mu D_\nu s^I = -\frac{1}{\rho}\eta_{\mu\nu}\partial_\rho s^I \tag{9.5.26}$$

are the only non-vanishing components of $D_mD_ns^I$. Moreover, one can show that

$$\rho^2(D_\rho D_\rho s^I + \eta^{\mu\nu}D_\mu D_\nu s^I) = \rho^2\partial^2_\rho s^I - 3\rho\partial_\rho s^I = k(k-4)s^I \tag{9.5.27}$$

for onshell s^I depending only on the radial coordinate.

The general map between five-dimensional fields (and equations of motion) and ten-dimensional fluctuations was worked out to quadratic order in ϵ in [24]. In particular, working in de Donder-Lorentz gauge, the map between the five-dimensional Einstein

metric perturbation H_{mn} and ten-dimensional fields to quadratic order is

$$H_{mn} = h^0_{mn} + \frac{1}{3}\pi^0 g^o_{mn} + \epsilon^2 \sigma_{(2)mn} \tag{9.5.28}$$

where h^0_{mn} is the ten-dimensional metric perturbation associated with the trivial harmonic (to order ϵ^2), π^0 is the trace of the metric perturbation on the S^5 associated with the trivial harmonic (to order ϵ^2)[1] and

$$\begin{aligned} \sigma_{(2)mn} &= \sum_I z(k) \big(A_I D_p D_m s^I D^p D_n s^I + B_I s^I D_m D_n s^I \\ &\qquad + D_I (D_p s^I)(D^p s^I) g^o_{mn} + E_I (s^I)^2 g^o_{mn} \big) \end{aligned} \tag{9.5.29}$$

where the coefficients (A_I, B_I, D_I, E_I) depend on the degree of the harmonic. Explicit values for the coefficients in the case of $k = 2$ were given in [24],

$$A_2 = -\frac{4}{9}; \qquad B_2 = \frac{20}{3}; \qquad D_2 = -\frac{20}{9}; \qquad E_2 = \frac{64}{9}. \tag{9.5.30}$$

Restricting to the fields depending only on the radial coordinate and working onshell we find that

$$\begin{aligned} \sigma_{(2)\rho\rho} &= \sum_I z(k) \Big[(16A_I + D_I)(\partial_\rho s^I)^2 + (8k(k-4)A_I + 4B_I)\frac{s^I}{\rho}\partial_\rho s^I \\ &\qquad + (E_I + k(k-4)(k(k-4)A_I + B_I))\frac{(s^I)^2}{\rho^2} \Big] \\ \sigma_{(2)\mu\nu} &= \delta_{\mu\nu} \sum_I z(k) \left[(A_I + D_I)(\partial_\rho s^I)^2 - B_I \frac{s^I}{\rho}\partial_\rho s^I + E_I \frac{(s^I)^2}{\rho^2} \right] \end{aligned} \tag{9.5.31}$$

We should note however that the field redefinition (9.5.29) gives the reduced metric in a specific gauge: we can always make a diffeomorphism ξ_n which is quadratic in s^I such that

$$\delta H_{mn} = D_m \xi_n + D_n \xi_m. \tag{9.5.32}$$

In the case of interest, such a diffeomorphism must respect the Poincaré invariance and hence

$$\xi_m = D_m \left(\sum_I z(k) F_I (s^I)^2 \right) \tag{9.5.33}$$

with F_I being arbitrary. The effect of such a diffeomorphism is to shift the coefficients arising in (9.5.31), but the form of the expression remains unchanged. (A natural way to fix the gauge would be to impose a Fefferman-Graham gauge on the resulting five-dimensional metric but this condition was not imposed in [24]).

We also know from [24] that we can express the terms to quadratic order in π^0, which

[1] Note that π^0 vanishes at linear order in the Coulomb branch solutions.

we denote as $\pi^0_{(2)}$ as

$$\pi^0_{(2)} = \epsilon^2 \sum_I z(k) \left(J_I (s^I)^2 + L_I (D_m s^I)(D^m s^I) \right) \tag{9.5.34}$$

where the coefficients (J_I, L_I) can be determined explicitly from the ten-dimensional field equations at quadratic order. For $k = 2$ these coefficients are

$$J_2 = -72 \qquad L_2 = 8. \tag{9.5.35}$$

Note that the coefficients $(A_I, B_I, D_I, E_I, J_I, L_I)$ were not calculated for general values of k in [24].

9.5.2 Entanglement Entropy

Consider a solution which can be expressed as a perturbation of $AdS_5 \times S^5$ and which preserves full Poincaré invariance of the dual field theory. Then the metric can be written as

$$ds^2 = (g^o_{mn} + h_{mn}) dx^m dx^m + (g^o_{ab} + h_{ab}) dy^a dy^b \tag{9.5.36}$$

where the metric perturbations depend only on the radial coordinate ρ and on the sphere coordinates y^a. Now consider the entanglement entropy for a slab region in the dual field theory, with the slab being defined as the region $-l < x < l$; the slab is assumed to be longitudinal to the the y and z directions.

We can compute the entanglement entropy from the ten-dimensional metric by finding an eight-dimensional minimal surface on a fixed time slice for which the boundary conditions are $x \to \pm l$ as $\rho \to 0$, with the surface wrapping the whole five sphere. From symmetry the minimal surface is specified by the function

$$x(\rho, y^a). \tag{9.5.37}$$

We can equivalently express the minimal surface as $\rho(x, y^a)$. Moreover, working with the leading order metric (which depends only on ρ) this function is clearly independent of the spherical coordinates. Thus the entangling surface in the perturbed background can be expressed as

$$x(\rho, y^a) = x_0(\rho) + x_1(\rho, y^a) + \cdots \tag{9.5.38}$$

where implicitly $x_1(\rho, y^a)$ is linear in the metric perturbations and the ellipses denote higher order corrections.

The induced metric on the entangling surface is

$$\gamma_{\alpha\beta} = g_{AB} \partial_\alpha x^A \partial_\beta x^B \tag{9.5.39}$$

With the static gauge fixing used above the induced metric is therefore

$$\begin{aligned} \gamma_{ij} &= g_{ij} + g_{xx}\partial_i x \partial_j x \\ \gamma_{ia} &= g_{xx}\partial_i x \partial_a x \\ \gamma_{ab} &= g_{ab} + \partial_a x \partial_b x \end{aligned} \tag{9.5.40}$$

where $x^i = (\rho, y, z)$ are the non-compact coordinates of the entangling surface. Imposing the further condition that x is independent of y and z we find that

$$\gamma_{yy} = g_{yy} \qquad \gamma_{xx} = g_{xx} \qquad \gamma_{\rho\rho} = g_{\rho\rho} + g_{xx}(\partial_\rho x)^2 \qquad \gamma_{\rho a} = g_{xx}\partial_\rho x \partial_a x \tag{9.5.41}$$

and therefore the determinant of the induced metric is given by

$$\sqrt{\gamma} = \sqrt{g_{yy}g_{zz}g_{\rho\rho}}\sqrt{\det\left(g_{ab}(1 + \frac{g_{xx}}{g_{\rho\rho}}(\partial_\rho x)^2) + g_{xx}\partial_a x \partial_b x\right)}. \tag{9.5.42}$$

The entanglement entropy functional is then

$$S = \frac{1}{4G_{10}}\int d^3x d^5y \sqrt{\gamma}. \tag{9.5.43}$$

9.5.2.1 Linear Order

For an entangling surface lying near the conformal boundary, so that the metric can be expressed as a perturbation of $AdS_5 \times S^5$, the leading contribution to the entanglement entropy is that of a surface in $AdS_5 \times S^5$. Now consider the contribution to the entanglement entropy to linear order in the metric perturbations. Since x is independent of the spherical coordinates y^a to leading order, the term $\partial_a x \partial_b x$ appearing in (9.5.42) is at least quadratic in the metric perturbation and can be neglected at this order, so the entanglement entropy is simply

$$S = \frac{1}{4G_{10}}\int d^3x d^5y \sqrt{g_{yy}g_{zz}(g_{\rho\rho} + g_{xx}(\partial_\rho x)^2)}\sqrt{\det(g_{ab})}, \tag{9.5.44}$$

where implicitly we work only to linear order in the metric perturbations. However, since we integrate over the five sphere only zero mode spherical harmonics can contribute at linear order and therefore we can substitute

$$g_{mn} = g^o_{mn} + h^0_{mn}; \qquad g_{ab} = g^o_{ab}(1 + \frac{1}{5}\pi^0). \tag{9.5.45}$$

Moreover, we can also express the embedding function in terms of scalar spherical harmonics

$$x(\rho, y^a) = x_0(\rho) + \sum_I x_1^I(\rho)Y^I(y^a) + \cdots \tag{9.5.46}$$

and again only the zero mode can contribute at this order. Let us denote

$$\bar{x}(\rho) = x_0(\rho) + x_1^0(\rho), \tag{9.5.47}$$

i.e. the embedding function is to this order only dependent on the radial coordinate ρ.

The entanglement entropy integral then factorises as

$$\begin{aligned} S &= \frac{1}{4G_{10}} \int d^5y \sqrt{\det g^o_{ab}} \int d^3x \sqrt{g_{yy} g_{zz} (g_{\rho\rho} + g_{xx} (\partial_\rho \bar{x})^2)} (1 + \frac{1}{2}\pi^0) \\ &= \frac{1}{4G_5} \int d^3x \sqrt{g_{yy} g_{zz} (g_{\rho\rho} + g_{xx} (\partial_\rho \bar{x})^2)} (1 + \frac{1}{2}\pi^0), \end{aligned} \tag{9.5.48}$$

where we use

$$\frac{1}{G_{10}} = \frac{V_{S^5}}{G_5} \tag{9.5.49}$$

and V_{S^5} is the volume of the five sphere.

Now let us compare to the entanglement entropy computed directly from the five-dimensional Einstein metric g^5_{mn}. This is very similar to the expression above:

$$S = \frac{1}{4G_5} \int d^3x \sqrt{g^5_{yy} g^5_{zz} (g^5_{\rho\rho} + g^5_{xx} (\partial_\rho \bar{x})^2)}. \tag{9.5.50}$$

If we now recall that (up to linear order)

$$g^5_{mn} = g^o_{mn} + h^0_{mn} + \frac{\pi^0}{3} g^o_{mn} \tag{9.5.51}$$

we find that the ten-dimensional and five-dimensional expressions precisely agree.

An alternative derivation of this result can be given using the fact that the change in the entanglement entropy is (c.f. Chapter 8)

$$\delta S = \frac{1}{8G_{10}} \int d^3x d^5y \sqrt{\gamma^o} T^{AB} h_{AB} \tag{9.5.52}$$

where T_{AB} is the energy momentum tensor of the original minimal surface (with induced metric γ^o) and h_{AB} is the change in the background metric. Using the explicit form of the energy momentum tensor we then find that

$$\begin{aligned} \delta S &= \frac{1}{8G_{10}} \int d^3x d^5y \sqrt{\gamma^o} \Big(g^{oab} h_{ab} + g^{oyy} h_{yy} + g^{ozz} h_{zz} \\ &\quad + \gamma^{o\rho\rho} (h_{\rho\rho} + h_{xx} (\partial_\rho \bar{x})^2) \Big). \end{aligned} \tag{9.5.53}$$

As above the integration over the five sphere picks out the zero modes in the harmonic

expansions of the metric perturbations, resulting in

$$\begin{aligned}\delta S &= \frac{1}{8G_5}\int d^3x\sqrt{\gamma^o}\left(\pi^0 + g^{oyy}h^0_{yy} + g^{ozz}h^0_{zz} + \gamma^{o\rho\rho}(h^0_{\rho\rho} + h^0_{xx}(\partial_\rho\bar{x})^2)\right) \quad (9.5.54)\\ &= \frac{1}{8G_5}\int d^3x\sqrt{\gamma^o}\left(g^{oyy}H_{yy} + g^{ozz}H_{zz} + \gamma^{o\rho\rho}(H_{\rho\rho} + H_{xx}(\partial_\rho\bar{x})^2)\right)\end{aligned}$$

where H_{mn} is the five-dimensional Einstein metric perturbation to linear order, see (9.5.7). The latter expression is exactly equivalent to

$$\delta S = \frac{1}{8G_5}\int d^3x\sqrt{\gamma^o}T^{mn}H_{mn} \quad (9.5.55)$$

where T^{mn} is the energy momentum tensor of the minimal surface in five-dimensional anti-de Sitter, thus demonstrating the equivalence between the five-dimensional and ten-dimensional computations.

9.5.2.2 Quadratic Order

Now let us consider the entanglement entropy to quadratic order in the metric perturbations. Since the embedding function is independent of the sphere coordinates to at least quadratic order (c.f. (9.5.47)), the expression (9.5.44) is still valid. Moreover, if we expand the embedding as

$$x(\rho, y^a) = x_0(\rho) + \epsilon x^0_1(\rho) + \epsilon^2\sum_I x^I_2(\rho)Y^I(y) + \cdots \quad (9.5.56)$$

we can see that again only the zero mode of the second order term can contribute after integration over the five sphere. Thus x is also independent of the sphere coordinates to this order, and using recursion we see that x depends only on the radial coordinates to *all* orders in the expansion.

Thus the entanglement entropy computed from ten dimensions is

$$\begin{aligned}S &= \frac{1}{4G_{10}}\int d^3x d^5y\sqrt{g_{yy}g_{zz}(g_{\rho\rho} + g_{xx}(\partial_\rho x)^2)}\sqrt{\det(g_{ab})}, \quad (9.5.57)\\ &\equiv \frac{1}{4G_{10}}\int d^3x d^5y\sqrt{\det\gamma_{ij}}\sqrt{\det(g_{ab})},\end{aligned}$$

where γ_{ij} is the non-compact part of the induced metric and implicitly x is now taken to depend only on ρ.

To show the equivalence between (9.5.57) and (9.5.50) we need to know the explicit map between the five-dimensional Einstein metric and the ten-dimensional metric fluctuations to quadratic order. Since this map is not known in full generality, we will focus on the case of general Coulomb branch solutions, using the expressions for perturbations given in Section 9.5.1.

We can use the standard identities for expanding determinants to write

$$\sqrt{\det(g_{ab})} = \sqrt{\det(g^o_{ab})}\left(1 + \frac{1}{2}h^a_a + \frac{1}{8}(h^a_a)^2 - \frac{1}{4}h^{ab}h_{ab} + \cdots\right) \tag{9.5.58}$$

where

$$h^{ab} = g^{oac}g^{obd}h_{bd}. \tag{9.5.59}$$

Now using the expressions given in Section 9.5.1

$$h^a_a = \epsilon\sum_I (10ks^I)Y^I + \epsilon^2\sum_I \pi^I_{(2)}Y^I + \cdots, \tag{9.5.60}$$

where we will need only the constant harmonic term at quadratic order, $\pi^0_{(2)}$, which is given in (9.5.34). Similarly

$$h^{ab}h_{ab} = 20\epsilon^2\sum_{I,J}(k_I s^I Y^I)(k_J s^J Y^J) + \mathcal{O}(\epsilon^3) \tag{9.5.61}$$

and thus to order ϵ^2

$$\begin{aligned}\sqrt{\det(g_{ab})} \;=\; & \sqrt{\det(g^o_{ab})}\left(1 + 5\epsilon\sum_I ks^I Y^I + \frac{1}{2}\epsilon^2\pi^0_{(2)}\right. \\ & \left. +\; \frac{15}{2}\epsilon^2\sum_{I,J}k_I s^I k_J s^J Y^I Y^J + \cdots\right).\end{aligned} \tag{9.5.62}$$

Here the ellipses denote terms of ϵ^3 and higher, as well as terms at order ϵ^2 which are linear in spherical harmonics (and hence integrate to zero over the five sphere).

The non-compact components of the metric can be expressed as

$$g_{mn} = g^o_{mn} + \epsilon\sum_I h^I_{(1)mn}Y^I + \epsilon^2\sum_I h^I_{(2)mn}Y^I + \cdots \tag{9.5.63}$$

where $h^I_{(2)mn}$ is quadratic in s. The explicit form of this can be determined by the ten-dimensional supergravity equations at quadratic order in ϵ, see [24], but will not be needed here. The non-compact part of the induced metric inherits an analogous expansion in powers of ϵ

$$\gamma_{ij} = \gamma^o_{ij} + \epsilon\gamma_{(1)ij} + \epsilon^2\gamma_{(2)ij} + \cdots \tag{9.5.64}$$

where

$$\begin{aligned}
\gamma^o_{ij} &= g^o_{ij} + g^o_{xx}\partial_i x^o \partial_j x^o; \qquad (9.5.65)\\
\gamma_{(1)ij} &= \left(\sum_I (h^I_{(1)ij} + h^I_{(1)xx}(\partial_i x^o)(\partial_j x^o))Y^I\right) + g^o_{xx}(\partial_i x^o \partial_j x_{(1)} + \partial_i x_{(1)}\partial_j x^o);\\
&\equiv \sum_I \gamma^I_{(1)ij} Y^I;\\
\gamma_{(2)ij} &= \left(\sum_I (h^I_{(2)ij} + h^I_{(2)xx}(\partial_i x^o)(\partial_j x^o))Y^I\right) + g^o_{xx}(\partial_i x^o \partial_j x_{(2)} + \partial_i x_{(2)}\partial_j x^o)\\
&\quad + g^o_{xx}\partial_i x_{(1)}\partial_j x_{(1)};\\
&\equiv \sum_I \gamma^I_{(2)ij} Y^I.
\end{aligned}$$

(In the case of interest we have already shown that the embedding function depends only on the ρ coordinate but we write the above expressions more generally.)

Expanding out the induced metric determinant then gives

$$\begin{aligned}
\sqrt{\det(\gamma_{ij})} &= \sqrt{\det(\gamma^o_{ij})}\left(1 + \frac{1}{2}(\epsilon\gamma^i_{(1)i} + \epsilon^2\gamma^i_{(2)i}) \right. \qquad (9.5.66)\\
&\quad \left. + \frac{\epsilon^2}{8}(\gamma^i_{(1)i})^2 - \frac{\epsilon^2}{4}\gamma^{ij}_{(1)}\gamma_{(1)ij} + \cdots\right)
\end{aligned}$$

where

$$\gamma^{ij}_{(1)} = \gamma^{oik}\gamma^{ojl}\gamma_{(1)kl} \qquad \gamma^{ij}_{(2)} = \gamma^{oik}\gamma^{ojl}\gamma_{(2)kl}. \qquad (9.5.67)$$

Substituting (9.5.62) and (9.5.66) into (9.5.57) and integrating over the five-sphere we then obtain to linear order in ϵ

$$S = \frac{1}{4G_5}\int d^3x\sqrt{\det(\gamma^o_{ij})}\left(1 + \epsilon\gamma^{oij}\partial_i x^o\partial_j x_{(1)}\right), \qquad (9.5.68)$$

i.e. all terms linear in metric perturbations vanish since they are associated with degree $k \geq 2$ spherical harmonics which integrate to zero over the sphere. Since the five-dimensional Einstein metric is unchanged to this order, the entangling surface is also unchanged i.e. $x_{(1)} = 0$.

Dropping terms involving $x_{(1)}$, the contributions to the entanglement entropy functional at order ϵ^2 are

$$\begin{aligned}
\delta S &= \frac{\epsilon^2}{4G_5}\int d^3x\sqrt{\det(\gamma^o)}\left(\frac{5}{2}\sum_I kz(k)s^I(\gamma^{Ii}_{(1)i} + 3ks^I)\right. \qquad (9.5.69)\\
&\quad \left. + \frac{1}{8}\sum_I z(k)(\gamma^{Ii}_{(1)i})^2 - \frac{1}{4}\sum_I z(k)\gamma^{Iij}_{(1)}\gamma^I_{(1)ij} + \frac{1}{2}\gamma^{0i}_{(2)i} + \frac{1}{2}\pi^0_{(2)}\right)
\end{aligned}$$

where we define $z(k)$ as the spherical harmonic normalisation

$$\int d^5y\sqrt{\det g^o_{ab}}Y^IY^J = z(k)\delta^{IJ}V_{S^5}. \tag{9.5.70}$$

The corresponding expression for the contribution to the five-dimensional entanglement entropy at quadratic order is

$$\delta S = \frac{\epsilon^2}{4G_5}\int d^3x\sqrt{\det(\gamma^o)}\left(\frac{1}{2}H^i_{(2)i} + \frac{1}{2}H_{(2)xx}(\partial^i x^o)(\partial_i x^o) + \partial^i x^o\partial_i x_{(2)}\right) \tag{9.5.71}$$

where $H_{(2)mn}$ is the quadratic correction to the five-dimensional Einstein metric and implicitly indices are raised with γ^{oij}. Let us split $H_{(2)mn}$ as

$$H_{(2)mn} = h^0_{(2)mn} + \frac{1}{3}\pi^0_{(2)}g^o_{mn} + \sigma_{(2)mn} \tag{9.5.72}$$

where $\sigma_{(2)mn}$ defines the field redefinition and is quadratic in s, while $\pi^0_{(2)}$ is also quadratic in s.

To match (9.5.69) and (9.5.71) one requires that

$$\begin{aligned}&\sigma^i_{(2)i} + \sigma_{(2)xx}(\partial^i x^o)(\partial_i x^o) = \\ &\quad 5\sum_I kz(k)s^I(\gamma^{Ii}_{(1)i} + 3ks^I) + \frac{1}{4}\sum_I z(k)(\gamma^{Ii}_{(1)i})^2 - \frac{1}{2}\sum_I z(k)\gamma^{Iij}_{(1)}\gamma^I_{(1)ij}\end{aligned} \tag{9.5.73}$$

To interpret this relationship, it is useful to consider first the case of an infinite strip. For an infinite strip, the entangling surface in AdS is described by constant x^o and extends throughout the bulk. In this case the entangling surface extends beyond the asymptotic region in which the geometry can be expressed as a perturbation of $AdS_5\times S^5$, but nonetheless one can match the integrands for the five-dimensional and ten-dimensional entanglement entropy in the asymptotic region by setting x^o to be constant in (9.5.73).

In the case of an infinite strip x^o is constant and dropping these terms gives

$$\sigma^i_{(2)i} = \sum_I z(k)\left(5ks^I(h^{Ii}_{(1)i} + 3ks^I) + \frac{1}{4}(h^{Ii}_{(1)i})^2 - \frac{1}{2}h^{Iij}_{(1)}h^I_{(1)ij}\right), \tag{9.5.74}$$

where now indices are raised by $\gamma^{oij}\equiv g^{oij}$, i.e. the hyperbolic metric. This expression reduces to

$$\sigma^i_{(2)i} = \sum_I \frac{16z(k)}{(k+1)^2}\left(-8\rho^2(\partial_\rho s^I)^2 + k(15-k)\rho s^I\partial_\rho s^I + k^2(k-7)(s^I)^2\right) \tag{9.5.75}$$

However, using (9.5.31) in Section 9.5.1, one can show that for perturbations s^I which

depend only on the radial coordinate

$$\sigma^i_{(2)i} = \sum_I z(k)\left[(18A_I+3D_I)\rho^2(\partial_\rho s^I)^2+(8k(k-4)A_I+2B_I)\rho s^I\partial_\rho s^I\right. \quad (9.5.76)$$
$$\left.+(3E_I+k(k-4)(k(k-4)A_I+B_I))(s^I)^2\right],$$

where the coefficients (A_I, B_I, D_I, E_I) for $k = 2$ are given in (9.5.30). Taking into account an appropriate choice of diffeomorphism F_I, defined in (9.5.33), this indeed matches (9.5.75).

For general k the coefficients (A_I, B_I, D_I, E_I) were not computed in [24]. Nonetheless, it is apparent that (9.5.76) has the same structure as (9.5.75) and we can argue as follows that these expressions agree, mode by mode, even without knowing the explicit expressions for the coefficients. We have already shown that the ten-dimensional and five-dimensional entanglement entropies agree for Coulomb branch solutions which admit consistent truncations. For such solutions (9.5.75) agrees with the result that one gets from direction reduction (9.5.76). Moreover, the matching between (9.5.75) and (9.5.76) arises mode by mode, as the fields s^I associated with spherical harmonics of different rank k have different functional dependence on the radial coordinate, see (9.5.25), and cannot cancel each other.

Since the agreement between (9.5.75) and (9.5.76) holds for all consistent truncations with different symmetry groups and different profiles for the scalar fields, this implies that the coefficients of the terms $(\partial_\rho s^I)^2$, $s^I\partial_\rho s^I$ and $(s_I)^2$ must match between the left and right hand sides of (9.5.75). However, since these coefficients match for all solutions with consistent truncations, they also match for solutions which do not admit consistent truncations and therefore the matching of five-dimensional and ten-dimensional entanglement entropy holds for entangling surfaces in all Coulomb branch solutions, up to quadratic order in the expansion parameter. The same argument can be used for strip entangling regions, i.e. (9.5.73), and indeed for generic shape entangling regions.

9.5.3 Summary and Interpretation

Let us summarise what has been proven in this section. We considered solutions of ten-dimensional type IIB supergravity which respect the Poincaré invariance of the dual field theory; the Einstein frame metric in ten dimensions is therefore of the form

$$ds^2 = g_{\rho\rho}(\rho, y^a)d\rho^2 + g_{\mu\nu}(\rho, y^a)dx^\mu dx^\nu + g_{ab}(\rho, y^a)dy^a dy^b, \quad (9.5.77)$$

where we choose a gauge in which $g_{\rho a} = 0$. We also assumed that the geometry is asymptotic to $AdS_5 \times S^5$ so that as $\rho \to 0$

$$g_{\rho\rho} \to \frac{1}{\rho^2} \qquad g_{\mu\nu} \to \frac{1}{\rho^2}\eta_{\mu\nu} \qquad g_{ab} \to g^o_{ab} \quad (9.5.78)$$

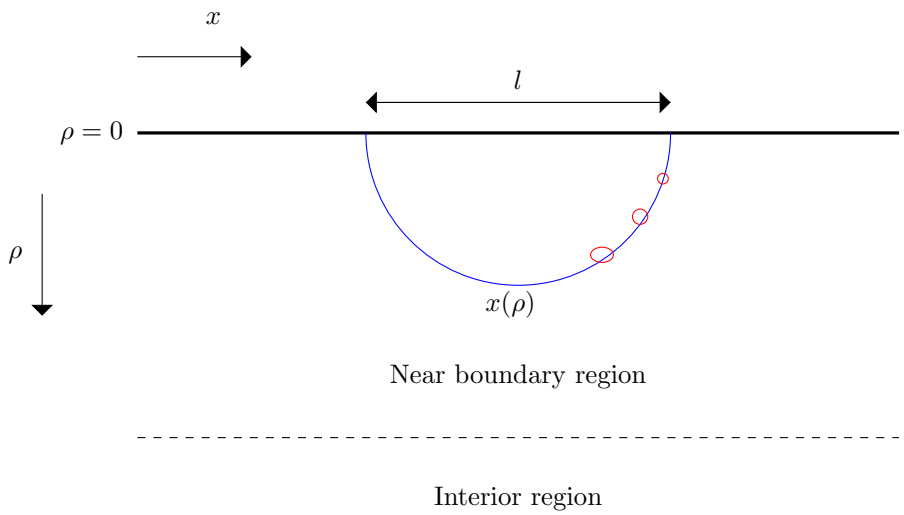

Figure 9.5.1: We consider entangling surfaces which are contained within the near boundary region where the Fefferman-Graham expansion of the metric may be used. At each point on the three-dimensional Ryu-Takayanagi minimal surface (shown in blue), there is a five-dimensional compact space (shown in red) which is topologically a five sphere.

where g^o_{ab} is the metric on the unit S^5.

We then computed the entanglement entropy for a strip region in the dual field theory by finding a codimension two minimal surface on a surface of constant time which asymptotically wraps the five sphere. Working in the region near the conformal boundary in which all metric coefficients can be expanded perturbatively in a Fefferman-Graham expansion in the basis of spherical harmonics, we showed that such an entangling surface depends only on the radial coordinate ρ to all perturbative orders, i.e. it is described by $x(\rho)$ with the width of the strip being l on the conformal boundary $\rho \to 0$.

As an immediate consequence of the minimal surface being described by $x(\rho)$, the induced metric $\gamma_{\alpha\beta}$ on the minimal surface factorises

$$\gamma_{\rho\rho} = g_{\rho\rho} + g_{xx}(x')^2 \qquad \gamma_{yy} = g_{yy} \qquad \gamma_{zz} = g_{zz} \qquad \gamma_{ab} = g_{ab}. \tag{9.5.79}$$

The eight-dimensional minimal surface is therefore topologically a product of a three-dimensional surface and a five-sphere, see Figure 9.5.1. It is nonetheless non-trivial to show that the area of this minimal surface gives the entanglement entropy computed from the five-dimensional perspective.

The induced metric depends explicitly on both the radial coordinate and the spherical coordinates, so one cannot trivially integrate over the spherical coordinates. In addition, the relationship between the five-dimensional Einstein metric g^5_{mn} occurring in the Ryu-Takayanagi formula and the ten-dimensional Einstein metric is extremely complicated,

involving derivative field redefinitions.

The induced metric on the co-dimensional two Ryu-Takayanagi surface is

$$\gamma^5_{\rho\rho} = g^5_{\rho\rho} + g^5_{xx}(x')^2 \qquad \gamma^5_{yy} = g^5_{yy} \qquad \gamma^5_{zz} = g^5_{zz}. \tag{9.5.80}$$

Working up to quadratic order in the perturbation relative to $AdS \times S^5$, i.e. to order $(h_{AB})^2$ in $g_{AB} = g^o_{AB} + h_{AB}$, we showed that the ten-dimensional entanglement entropy

$$S = \frac{1}{4G_{10}} \int d^3x d^5y \sqrt{\gamma} \tag{9.5.81}$$

indeed agrees with the five-dimensional Ryu-Takayanagi computation

$$S = \frac{1}{4G_5} \int d^3x \sqrt{\gamma^5} \tag{9.5.82}$$

when we take into account the reduction map. More precisely, the Ryu-Takayanagi integrand matches the top-down integrand once the latter is integrated over the five-sphere: the volume form of the Ryu-Takayanagi minimal surface matches the volume form of the top-down minimal surface, once the latter is integrated over the spherical coordinates.

Before leaving this section, we should mention another related test of the top-down entanglement entropy formula using Kaluza-Klein holography. Entanglement entropy for asymptotically $AdS_3 \times S^3$ geometries corresponding to 1/4 and 1/8 BPS geometries associated with black hole microstates was computed in [206]. The entanglement entropy was computed using both the top-down prescription, i.e. codimension two minimal surfaces in six dimensions, and by applying the Ryu-Takayanagi formula to the three-dimensional Einstein metric extracted using Kaluza-Klein holography. The results were in agreement, working up to quadratic order in perturbations around $AdS_3 \times S^3$, as in the asymptotically $AdS_5 \times S^5$ case analysed above.

9.6 Unquenched Flavour Solutions

Another example for studying top-down entanglement entropy is provided by unquenched flavour solutions, i.e. systems of flavour branes in which the backreaction of the branes onto the metric has been computed, working perturbatively in the ratio of flavours to colors.

The computation of the backreaction is most tractable when the branes are smeared over transverse directions. In particular, [238,274] discuss the case of the massless D3/D7 system in which probe D7 branes are smeared over the transverse S^2 space. The system is type IIB supergravity coupled to D7-brane sources, and [238, 274] takes the following

ansatz for the Einstein frame metric in the supersymmetric (zero temperature) case

$$ds_{10}^2 = h^{-\frac{1}{2}} dx_\mu dx^\mu + h^{\frac{1}{2}} \left[F^2 d\varrho^2 + S^2 ds_{KE}^2 + F^2 (d\tau + A_{KE})^2 \right] \tag{9.6.1}$$

where the functions $h(\varrho)$, $S(\varrho)$, $F(\rho)$ only depend on the radial coordinate ϱ, and the five-dimensional Sasaki-Einstein manifold X^5 is written as a $U(1)$ fibration over a 4d Kähler-Einstein base. For $X = S^5$ the KE base is CP^2.

To compute the entanglement entropy for a strip in the x-direction from 10d we follow the usual procedure. By symmetry the embedding is given by $x = x(\varrho)$ and the induced metric on the embedding surface is

$$ds_8^2 = h^{-\frac{1}{2}} \left[dy^2 + dz^2 + x'^2 d\varrho^2 \right] + h^{\frac{1}{2}} \left[F^2 d\varrho^2 + S^2 ds_{KE}^2 + F^2 (d\tau + A_{KE})^2 \right], \tag{9.6.2}$$

where $x' \equiv dx/d\varrho$. Note that the minimal surface wraps the entire internal space.

One thus finds that the entanglement entropy functional is

$$S = \frac{1}{4G_{10}} \int d^3x d^5y \sqrt{\det \gamma_8} \tag{9.6.3}$$

where

$$\sqrt{\det \gamma_8} = h^{\frac{1}{2}} F S^4 \sqrt{x'^2 + h F^2} \sqrt{\det g_{X^5}}. \tag{9.6.4}$$

Since this determinant factorises we can immediately integrate over the internal space to obtain

$$S = \frac{V_{X^5}}{4G_{10}} \int d^3x h^{\frac{1}{2}} F S^4 \sqrt{x'^2 + h F^2} \tag{9.6.5}$$

where the integration is over (ϱ, y, z) and we define

$$V_{X^5} = \int d^5y \sqrt{\det g_{X^5}}. \tag{9.6.6}$$

Explicit expressions for the metric functions were calculated in [238, 274] working perturbatively in the number of flavours,

$$\begin{aligned} S &= \alpha'^{\frac{1}{2}} e^{\varrho} \left(1 + \epsilon_* \left(1/6 + \varrho_* - \varrho\right)\right)^{\frac{1}{6}}; \\ F &= \alpha'^{\frac{1}{2}} e^{\varrho} \left(1 + \epsilon_* (\varrho_* - \varrho)\right)^{\frac{1}{2}} \left(1 + \epsilon_* \left(1/6 + \varrho_* - \varrho\right)\right)^{-\frac{1}{3}}; \\ \frac{dh}{d\varrho} &= -Q_c \alpha'^{-2} e^{-4\varrho} \left(1 + \epsilon_* \left(1/6 + \varrho_* - \varrho\right)\right)^{-\frac{2}{3}}. \end{aligned} \tag{9.6.7}$$

Here ϱ_* is a scale that is introduced for convenience; Q_c is proportional to the number of colors and $\epsilon_* \equiv Q_f e^{\Phi_*}$ is the small expansion parameter: Q_f is proportional to the number of flavours and Φ_* is the value of the dilaton at ϱ_*.

The equation for $dh/d\varrho$ can be integrated up to express $h(\varrho)$ in terms of incomplete gamma functions, with integration constant being determined by the requirement that

the metric is asymptotically anti-de Sitter. Using the explicit expressions above and expanding in ϵ_* one finds

$$h^{\frac{5}{4}}S^4F = \frac{Q_c^{\frac{5}{4}}}{4\sqrt{2}} + \frac{Q_c^{\frac{5}{4}}}{32\sqrt{2}}\epsilon_* + \frac{Q_c^{\frac{5}{4}}(19+48\varrho-48\varrho_*)}{1536\sqrt{2}}\epsilon_*^2 + \mathcal{O}(\epsilon_*^3) \tag{9.6.8}$$

Note that to order ϵ_* this expression is independent of the radial coordinate.

Now let us turn to the calculation of the entanglement entropy from the five-dimensional perspective. Let us first note that it is clear that the five-dimensional Einstein metric cannot be identified as just the non-compact part of the above metric, i.e.

$$ds_5^2 = h^{-\frac{1}{2}}dx_\mu dx^\mu + h^{\frac{1}{2}}F^2 d\varrho^2. \tag{9.6.9}$$

Using the latter metric the computation of the entanglement entropy from five dimensions would be

$$S = \frac{1}{4G_5}\int d^3x\sqrt{\det\gamma_3} \tag{9.6.10}$$

where

$$\sqrt{\det\gamma_3} = h^{-\frac{3}{4}}\sqrt{x'^2 + hF^2}. \tag{9.6.11}$$

This does not agree with the ten-dimensional result; the latter contains also an additional factor $h^{\frac{5}{4}}S^4F$ which as we showed above depends on the radial coordinate ϱ.

9.6.1 Linear Order

To extract the correct five-dimensional Einstein metric we can again use Kaluza-Klein holography. Working to zeroth order in ϵ^* the metric is

$$ds_{10}^2 = \frac{2\alpha'}{\sqrt{Q_c}}e^{2\varrho}dx_\mu dx^\mu + \frac{\sqrt{Q_c}}{2}d\varrho^2 + \frac{\sqrt{Q_c}}{2}\left[ds_{KE}^2 + (d\tau + A_{KE})^2\right]. \tag{9.6.12}$$

By rescaling the coordinates one can pull out an overall factor as

$$ds_{10}^2 = \frac{\sqrt{Q_c}}{2}\left[e^{2\varrho}d\tilde{x}_\mu d\tilde{x}^\mu + d\varrho^2 + ds_{KE}^2 + (d\tau + A_{KE})^2\right] \tag{9.6.13}$$

where

$$\tilde{x}_\mu = \frac{2\sqrt{\alpha'}}{\sqrt{Q_c}}x_\mu \tag{9.6.14}$$

For computational convenience, and to match the conventions of earlier sections, we will set $\sqrt{Q_c}/2 = \sqrt{\alpha'} = 1$; these factors can be reinstated if required. The leading order metric is therefore the produce of AdS_5 (in domain wall coordinates) with the Sasaki-Einstein space.

Now let

$$S = S^o(1+\delta S); \qquad F = F^o(1+\delta F); \qquad h = h^o(1+\delta h), \tag{9.6.15}$$

where the superscript refers to the value in the $AdS_5 \times S^5$ background and the perturbations are expressed as power series in the parameter ϵ_*. The explicit forms for the perturbations are

$$\begin{aligned} \delta S &= \epsilon_* \left(\frac{1}{36} + \frac{1}{6}(\varrho_* - \varrho) \right) + \cdots \\ \delta F &= \epsilon_* \left(-\frac{1}{18} + \frac{1}{6}(\varrho_* - \varrho) \right) + \cdots \\ \delta h &= \epsilon_* \left(\frac{1}{18} - \frac{2}{3}(\varrho_* - \varrho) \right) + \cdots \end{aligned} \tag{9.6.16}$$

The metric can as before be written as

$$g_{AB} = g^o_{AB} + h_{AB} \tag{9.6.17}$$

where

$$\begin{aligned} h_{\mu\nu} &= e^{2\varrho} \left(-\frac{1}{2}\delta h + \frac{3}{8}(\delta h)^2 + \cdots \right) \eta_{\mu\nu} \\ &= e^{2\varrho} \epsilon_* \left(-\frac{1}{36} + \frac{1}{3}(\varrho_* - \varrho) \right) \eta_{\mu\nu} + \cdots \end{aligned} \tag{9.6.18}$$

$$\begin{aligned} h_{\varrho\varrho} = &= 2\delta F + \frac{1}{2}\delta h + \delta F^2 - \frac{1}{8}\delta h^2 + \delta h \delta F \\ &= -\frac{1}{12}\epsilon_* + \cdots \end{aligned} \tag{9.6.19}$$

while along the compact space

$$h_{ab} dy^a dy^b = h_{KE} ds^2_{KE} + h_{\tau\tau}(d\tau + A_{KE})^2 \tag{9.6.20}$$

with

$$h_{KE} = 2\delta S + \frac{1}{2}\delta h + \delta S^2 - \frac{1}{8}\delta h^2 + \delta h \delta S = \frac{1}{12}\epsilon_* + \cdots \tag{9.6.21}$$

and $h_{\tau\tau} = h_{\varrho\varrho}$. Here the ellipses denote terms of order ϵ_*^2 and higher.

As in previous sections, the metric perturbations can be expressed in the complete basis of harmonics. For the metric perturbations in the non-compact directions, this expansion involves only the constant harmonic, i.e.

$$h_{mn} \equiv h^0_{mn}. \tag{9.6.22}$$

since (9.6.18)-(9.6.19) are independent of the compact space coordinates. Now consider

the perturbations along the compact space. The trace of the metric perturbation

$$h^a_a = g^{oab} h_{ab} = 4h_{KE} + h_{\tau\tau} \tag{9.6.23}$$

is independent of the compact space coordinates, and therefore the expansion of the trace in harmonics involves only the constant harmonic

$$h^a_a \equiv \pi^0 = \frac{1}{4}\epsilon_* + \cdots \tag{9.6.24}$$

We will discuss the decomposition of the traceless part into harmonics below.

To linear order in the metric perturbations the correction to the five-dimensional Einstein metric is

$$H_{mn} = h^0_{mn} + \frac{1}{3}\pi^0 g^o_{mn} \tag{9.6.25}$$

and therefore to linear order in ϵ_*

$$H_{\mu\nu} = \epsilon_* \left(\frac{1}{18} + \frac{1}{3}(\varrho_* - \varrho) \right) e^{2\varrho} \eta_{\mu\nu} + \cdots \qquad H_{\varrho\varrho} = \mathcal{O}(\epsilon_*^2) \tag{9.6.26}$$

This defines the five-dimensional Einstein metric to linear order.

We already showed that the entanglement entropy for a strip computed in the ten-dimensional metric $g_{AB} = g^o_{AB} + h_{AB}$ is always equivalent, to linear order in the perturbations, to the entanglement entropy computed using the five-dimensional Einstein metric $g^5_{mn} = g^o_{mn} + H_{mn}$. This general result implies that (9.6.5) is indeed equivalent to

$$S = \frac{1}{4G_5} \int d^3x \sqrt{g^5_{yy} g^5_{zz}} \sqrt{g^5_{\rho\rho} + g^5_{xx}(x')^2} \tag{9.6.27}$$

at linear order in the perturbations. One can show the equivalence directly using the identifications

$$g^5_{\mu\nu} = h^{\frac{1}{3}} F^{\frac{2}{3}} S^{\frac{8}{3}} \eta_{\mu\nu} \qquad g^5_{\rho\rho} = h^{\frac{4}{3}} F^{\frac{8}{3}} S^{\frac{8}{3}}, \tag{9.6.28}$$

to linear order in ϵ_*.

9.6.2 Non-Linear Order

The traceless part of the metric perturbation on the compact space is

$$h_{(ab)} dy^a dy^b = \left(\frac{h_{KE}}{5} - \frac{h_{\tau\tau}}{5} \right) ds^2_{KE} + \left(\frac{4h_{\tau\tau}}{5} - \frac{4h_{KE}}{5} \right) (d\tau + A_{KE})^2 \tag{9.6.29}$$

Working to linear order in the perturbations

$$h_{(ab)} dy^a dy^b = \left(\frac{1}{30}\epsilon_* + \cdots \right) ds^2_{KE} + \left(-\frac{2}{15}\epsilon_* + \cdots \right) (d\tau + A_{KE})^2 \tag{9.6.30}$$

We can now project this onto harmonics,

$$h_{(ab)} = \sum \left(\phi^{I_t} Y^{I_t}_{(ab)} + \psi^{I_v} D_{(a} Y^{I_v}_{b)} + \chi^I D_{(a} D_{b)} Y^I \right). \tag{9.6.31}$$

For example

$$\int D^a h_{(ab)} D^b Y^I d\Omega = 4\Lambda^I \left(\frac{\Lambda^I}{5} - 1 \right) z(k) \chi^I, \tag{9.6.32}$$

where

$$\Box Y^I = \Lambda^I Y^I \tag{9.6.33}$$

and $d\Omega$ is the volume element on the Sasaki-Einstein, with $z(k)$ the harmonic normalisation. While $h_{(ab)}$ does not depend on the Sasaki-Einstein coordinates, all individual harmonics depend on the coordinates and $h_{(ab)}$ is therefore decomposed into an infinite series of harmonics, as one would have anticipated, given the smearing.

As in Section 9.5, the perturbations associated with non-trivial harmonics do not contribute to the entanglement entropy at linear order, but they do contribute at non-linear order. Unfortunately the non-linear relation between the five-dimensional Einstein metric and the ten-dimensional metric is not known for general perturbations in which ϕ^{I_t}, ψ^{I_v} and χ^I are non-zero and therefore we cannot check the equivalence of five-dimensional and ten-dimensional entanglement entropy to non-linear order.

It is interesting to note, however, that the ten-dimensional entanglement entropy (9.6.5) can be expressed in five-dimensional form (9.6.27) provided that one makes the identifications (9.6.28). This suggests that the five-dimensional Einstein metric at non-linear order is simply

$$ds^2 = h^{\frac{1}{3}} F^{\frac{2}{3}} S^{\frac{8}{3}} \left(h F^2 d\varrho^2 + \eta_{\mu\nu} dx^\mu dx^\nu \right). \tag{9.6.34}$$

One could explore whether this is indeed the correct expression for the five-dimensional Einstein metric by checking whether it gives the expected forms for e.g. one point function and higher correlation functions of the holographic stress energy tensor.

Finally, we should note that very similar analysis should be applicable to smeared solutions in other dimensions including [202]; one would need to set up Kaluza-Klein holography for ABJM to explore this case.

9.7 General Case

In this section we consider ten-dimensional asymptotically $AdS_5 \times S^5$ type IIB solutions which respect the Poincaré invariance of the dual field theory. The ten-dimensional Einstein metric therefore takes the form

$$ds^2 = g_{\rho\rho} d\rho^2 + g_{\mu\nu} dx^\mu dx^\nu + 2 g_{\rho a} d\rho dy^a + g_{ab} dy^a dy^b \tag{9.7.1}$$

where $g_{\mu\nu} \propto \eta_{\mu\nu}$ and all metric components depend on (ρ, y^a). For simplicity let us focus on the case in which the $SO(6)$ symmetry is broken to $SO(5)$, so that the metric depends only on ρ and a single angular coordinate θ (examples of such supergravity solutions would be D3-brane Coulomb branch solutions in which all branes lie along a line).

Suppose we make a coordinate redefinition $(\rho, \theta) \to (r, \vartheta)$ to bring the metric into the following form

$$ds^2 = e^{2B(r,\vartheta)}(dr^2 + e^{2A(r)}dx^\mu dx_\mu) + 2\mathcal{A}(r,\vartheta)drd\vartheta + g_{\vartheta\vartheta}(r,\vartheta)d\vartheta^2 + g_{S^4}(r,\vartheta)d\Omega_{S^4}, \quad (9.7.2)$$

with r being the radial coordinate of the five-dimensional metric in Einstein frame

$$ds_5^2 = dr^2 + e^{2A(r)}dx^\mu dx_\mu. \quad (9.7.3)$$

For consistent truncations, we know the explicit form of the map between five and ten-dimensional solutions, i.e. the explicit form of $B(r,\vartheta)$ etc. In the vicinity of the conformal boundary one can use Kaluza-Klein holography to work out the map as a power series in the radial coordinate.

Deep in the interior of a general such spacetime we do not know the explicit form of the map, but such a map must exist. Note however that the causal structures of the five-dimensional Einstein metric and the ten-dimensional Einstein metric do not necessarily agree: even in consistent truncations, the former can be singular while the latter is smooth. The choice of a specific ten-dimensional radial coordinate adapted to the five-dimensional Einstein metric corresponds to identifying the RG scale of the dual field theory. The five-dimensional Einstein metric would in general be supported by the stress energy tensor associated with the entire tower of Kaluza-Klein modes.

Next consider the simplest possible entangling surface in this geometry, corresponding to the half plane entangling region $x > 0$ in the dual field theory. On symmetry grounds, the bulk entangling surfaces are codimension two surfaces $x = 0$ at constant time. Agreement between the ten-dimensional and five-dimensional entanglement entropies requires

$$\frac{1}{4G_{10}}\int d^3x d^5y\sqrt{\gamma} = \frac{1}{4G_5}\int d^3x\sqrt{\gamma_5} \quad (9.7.4)$$

which in turn requires that

$$\int drd\vartheta e^{2B+2A}\left(e^{2B}g_{\vartheta\vartheta} - \mathcal{A}^2\right)^{\frac{1}{2}}\sqrt{\mathrm{detg_{S^4}}} = \pi^3\int dre^{2A}. \quad (9.7.5)$$

In this chapter we have effectively checked that this relation holds in all cases in which we can independently calculate the five-dimensional Einstein metric. In cases where the five-dimensional Einstein metric is not known, one may be able to deduce the five-dimensional Einstein metric by insisting that this expression hold.

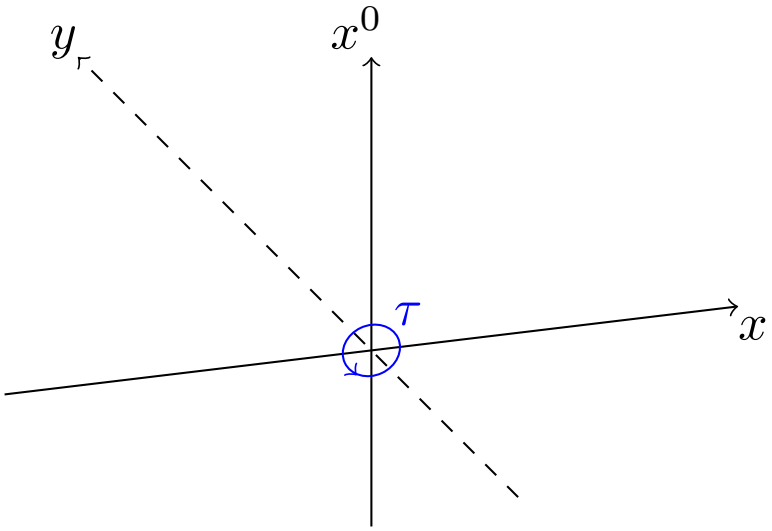

Figure 9.7.1: The half space entangling region $x \geq 0$, with boundary the y-axis. The coordinate τ is the polar coordinate in the plane of x and the Euclidean time x^0.

9.7.1 Relation to Lewkowycz-Maldacena Derivation

In this section we will explain the origin of the top-down entanglement entropy formula, using a similar approach to Lewkowycz-Maldacena in [172].

The entropy associated with a given density matrix ρ can be computed using the replica trick as

$$S = -n\partial_n \left[\log Z(n) - n \log Z(1)\right]_{n=1} \tag{9.7.6}$$

where

$$Z(n) = \mathrm{Tr}(\rho^n). \tag{9.7.7}$$

Here $Z(1)$ can be computed by considering (Euclidean) evolution on a circle, i.e.

$$\rho = \mathcal{P} \exp\left(-\int_{\tau_0}^{\tau_0+2\pi} d\tau H(\tau)\right) \tag{9.7.8}$$

where H is the Hamiltonian and the periodicity of the τ direction is 2π. $Z(n)$ is then computed by considering the evolution over a circle of n times the length of the original circle.

In the context of thermal density matrices the circle direction is Euclidean time. For entanglement entropy, the appropriate circle direction is that enclosing the boundary of the entangling region, see the example shown in Figure 9.7.1. The well-known CHM map relates certain thermal entropies to entanglement entropies in conformal field theories [187].

To compute the entanglement entropy holographically (to leading order in $1/N$), one considers a dual spacetime whose Euclidean onshell action gives minus $\log Z(1)$. The

replica holographic dual is constructed by considering a boundary theory in which the circle has period n times the length of the original circle. Then $\log Z(n)$ is minus the action $I_E(n)$ for a smooth solution of the bulk field equations in which the circle has a periodicity of n times the original periodicity. Hence we can use holography to rewrite (9.7.6) as

$$S = n\partial_n \left[I_E(n) - nI_E(1) \right]_{n=1} \tag{9.7.9}$$

The second term in (9.7.9) is associated with the solution at $n = 1$ but with the circle having periodicity of n times the original length; this solution has a conical singularity but the contribution of the conical singularity to the onshell action is not included.

In [172] the main focus was implicitly asymptotically anti-de Sitter geometries, i.e. solutions of lower-dimensional gauged supergravity theories, in which the bulk actions are Einstein gravity coupled to matter fields. However, the general arguments given in [172] apply equally to any holographic dual and therefore, in particular, apply to solutions of type IIB supergravity in ten dimensions which asymptote to $AdS_5 \times S^5$.

In cases where a consistent truncation exists, one obtains the same result for working out the onshell (Einstein frame) action from ten dimensions using the Euclidean continuation of (9.4.1)

$$I_E = -\frac{1}{16\pi G_{10}} \int d^{10}x \sqrt{g} \left[R - \frac{1}{2 \cdot 5!} F^2_{(5)} + \cdots \right] \tag{9.7.10}$$

as one does using the five-dimensional Euclidean action

$$I_E = -\frac{1}{16\pi G_5} \int d^5x \sqrt{g_5} \left[R(g_5) + \cdots \right] \tag{9.7.11}$$

where the ellipses denote the matter contributions to the consistent truncation. In cases for which no consistent truncation exists, it remains true that the onshell action computed from ten dimensions, by construction, gives the same result as the five-dimensional onshell action. However, when no consistent truncation exist, the ellipses in (9.7.11) include the complete tower of Kaluza-Klein modes.

We now need to argue that (9.7.9) localises on a minimal surface and is given by

$$S = \frac{\mathcal{A}}{4G_{10}} = \frac{A}{4G_5} \tag{9.7.12}$$

where A is the area of the Ryu-Takayanagi surface and $\mathcal{A}$ is the area of the codimension two minimal surface in ten dimensions.

Let us first give an argument following the approach of [172]. Let $\mathcal{M}_n$ be the regular bulk geometry corresponding to τ being periodic with period $2\pi n$ and let $\mathcal{M}_1$ be the geometry with a conical singularity. Note that the conical singularity extends to the conformal

boundary, in contrast to the black hole setup discussed in [172] in which it was localised in the interior of the bulk geometry.

Now the argument given in [172] goes as follows. Consider a smooth offshell configuration with geometry $\tilde{\mathcal{M}}_n$ which regularises the conical singularity of $\mathcal{M}_1$. Away from the fixed point surface the geometry of $\tilde{\mathcal{M}}_n$ agrees with that of $\mathcal{M}_1$ and $\tilde{\mathcal{M}}_n$ is chosen such that the offshell configuration differs by order $(n-1)$ from a solution of the equations of motion. Let $\tilde{I}_E(n)$ be the onshell action of the configuration with geometry $\tilde{\mathcal{M}}_n$. Since the offshell configuration can always be viewed as a first order variation of an onshell configuration (working perturbatively in the expansion parameter $(n-1)$), its action is equivalent to $I_E(n)$ up to quadratic order in $(n-1)$ and therefore we can replace $I_E(n)$ by $\tilde{I}_E(n)$ in (9.7.9),

$$S = n\partial_n \left[\tilde{I}_E(n) - nI_E(1)\right]_{n=1}. \tag{9.7.13}$$

Since the geometries only differ at the fixed point set, it is then apparent that this expression localises on the fixed point set. Moreover, the contribution is extensive in the area of the codimension two fixed point set and is proportional to the integral over the cone directions

$$\int d^2x\sqrt{g}\mathcal{R} \sim 4\pi(1-n). \tag{9.7.14}$$

Thus we can write

$$S = \frac{\mathcal{A}}{16\pi\mathcal{G}_N}\left(-n\partial_n \int d^2x\sqrt{g}\mathcal{R}\right)_{n=1} = \frac{\mathcal{A}}{4\mathcal{G}_N}, \tag{9.7.15}$$

where $\mathcal{G}_N$ is the Newton constant.

This general argument clearly does not depend on the spacetime asymptotics, and is thus equally applicable to asymptotically AdS and asymptotically $AdS \times S$ geometries. The overall constant of proportionality obtained in (9.7.15) can always be fixed by exploiting the CHM map, relating spherical region entanglement entropy to hyperbolic black hole entropy. The latter is given by the standard expression, the area of the horizon (in the Einstein frame metric) divided by $4\mathcal{G}_N$.

Starting with (9.7.13) we can give a different argument that this expression localises on fixed point sets of the vector ∂_τ using the work of Gibbons and Hawking [271]. We consider the case in which ∂_τ is a Killing vector both on the boundary and in the bulk[2]. Since τ is a circle symmetry we can always write the metric locally as

$$ds^2 = V(d\tau + \omega)^2 + V^{-1}ds_B^2 \tag{9.7.16}$$

where the scalar V and the one form ω take values on the base space B, which is the space of non-trivial orbits of the circle symmetry. The fibering is trivial if the one form

[2]Throughout this chapter we have assumed Poincaré invariance of the dual field theory. In the case of the half space entangling region shown in Figure 9.7.1 this guarantees that ∂_τ is indeed a Killing vector.

ω is globally exact; we have implicitly assumed this above. By construction the onshell Euclidean action can be expressed as an integral over B,

$$I_E = \int d\tau d^{D-1}x\sqrt{g}\mathcal{L} = \beta_\tau \int_B d^{D-1}xV^{-1}\sqrt{g_B}\mathcal{L} \tag{9.7.17}$$

where β_τ is the periodicity of τ, $\sqrt{g_B}$ is the base metric determinant and $\mathcal{L}$ is the onshell Lagrangian.

The circle symmetry $k = \partial_\tau$ has fixed points wherever $V = 0$. The action of the symmetry is generated by the antisymmetric matrix $D_{[M}K_{N]}$; such matrices have even rank, i.e. rank $(2, 4...)$ (the zero rank case would imply that the Killing vector is zero and acts trivially). When $D_{[M}K_{N]}$ has rank $2k$ the action of the symmetry leaves fixed a $(D-2k)$-dimensional submanifold. Note that when ω is globally exact the only possible fixed point sets are of dimension $(D-2)$.

Gibbons and Hawking showed in [271] that for four-dimensional Einstein gravity the onshell action (9.7.17) can be expressed as the divergence of a Noether current J^s associated with a dilation symmetry,

$$I_E = \beta_\tau \int_B d^{D-1}x\sqrt{g_B}D_sJ^s = \beta_\tau \int_{\partial B} d^{D-2}\sigma_sJ^s \tag{9.7.18}$$

and hence the action localises on the $(D-2)$-dimensional boundary ∂B of the base space.

The boundary ∂B consists of $(D-2)$-dimensional boundaries surrounding each fixed point together with the spatial boundary at infinity (if B is non-compact). When τ is the imaginary time, contributions from infinity are associated with conserved charges (mass $\mathcal{M}$ etc) while contributions from the fixed point sets give the entropy $\mathcal{S}$,

$$I_E = \beta_\tau\mathcal{M} + \cdots - \mathcal{S} \tag{9.7.19}$$

where the ellipses denote contributions from additional conserved charges.

The entropy $\mathcal{S}$ includes not only the usual area terms but additional contributions associated with a scalar potential ψ dual to the one-form ω, see [271]

$$d\psi = V^2 *_3 d\omega \tag{9.7.20}$$

where the dual is computed on the base space B. In four dimensions the fixed point sets are either two-dimensional bolts, characterised by their self-intersection Y, or zero-dimensional nuts, characterised by relatively prime integers (p, q). The entropy contri-

butions are then given by

$$\mathcal{S} = \frac{\mathcal{A}}{4G_4} + \frac{\beta_\tau^2}{16\pi G_4}\sum_{\text{bolts}}\psi Y + \frac{\beta_\tau^2}{16\pi G_4}\sum_{\text{nuts}}\frac{\psi}{pq} \tag{9.7.21}$$

where the scalar potential ψ is invariant over a bolt.

The scalar potential contributions are zero if ω is globally exact, and then the entropy reduces to the usual form

$$\mathcal{S} = \frac{\mathcal{A}}{4G_4} \tag{9.7.22}$$

with $\mathcal{A}$ the sum of the areas of $(D-2)$-dimensional fixed point sets. The expressions (9.7.18) and (9.7.19) are believed to apply to Einstein gravity coupled to matter in all dimensions although explicit expressions for the terms in the entropy depending on the one-form ω are not known in general dimensions.

In the case at hand, the circle direction is not the imaginary time but the approach of [271] can still be applied, provided that the circle direction is a symmetry. Thus the onshell action can be expressed as

$$I_E = \beta_\tau \sum_a \Phi_a Q_a - \mathcal{S} \tag{9.7.23}$$

where Φ_a and Q_a are conjugate potential and conserved charge pairs, respectively, and $\mathcal{S}$ is again associated with fixed point sets of the circle symmetry. By construction we choose $\tilde{\mathcal{M}}_n$ to be such that the charge terms cancel between the two terms in (9.7.13) leaving

$$S = [n\partial_n(n-1)]_{n=1}\mathcal{S} = \mathcal{S}, \tag{9.7.24}$$

i.e. the entanglement entropy is equal to the geometric entropy, which is given by (9.7.22) when the fibration in (9.7.16) is trivial.

Note that the derivation using (9.7.18) relies on ∂_τ being a Killing vector. While τ is periodic, it is not necessarily a symmetry direction even for generic entangling regions on flat spatial hypersurfaces of constant time. For example, consider the spherical entangling region $w = R$ in a four-dimensional quantum field theory in the flat background

$$ds^2 = (dx^0)^2 + dw^2 + w^2(d\theta^2 + \sin^2\theta d\phi^2) \tag{9.7.25}$$

where x^0 is the imaginary time. By changing coordinates as

$$w = R + \tilde{w}\cos\tau \qquad x^0 = \tilde{w}\sin\tau \tag{9.7.26}$$

to

$$ds^2 = d\tilde{w}^2 + \tilde{w}^2 d\tau^2 + (R + \tilde{w}\cos\tau)^2(d\theta^2 + \sin^2\theta d\phi^2) \tag{9.7.27}$$

we note that the boundary of the entangling region is at $\tilde{w} = 0$, with ∂_τ having a dimen-

sion two fixed point set at $\tilde{w} = 0$. Here τ is the circle direction used in the replica trick, but it is not a symmetry. In most previous discussions of holographic entanglement, the circle direction τ was trivially fibered but not necessarily a symmetry.

On the other hand, the approach of (9.7.18) raises the interesting possibility that there may in general be additional leading order contributions to the holographic entanglement entropy, beyond the area of the extremal surface. Suppose that the following metric describes the geometry near the boundary of an entangling region (in a three-dimensional field theory)

$$ds^2 = d\tilde{w}^2 + \tilde{w}^2(d\tau + a(\tilde{w})d\phi)^2 + b(\tilde{w})d\phi^2, \tag{9.7.28}$$

with $b(0) \neq 0$. Here ∂_τ is a Killing vector with a two-sphere fixed point set at $\tilde{w} = 0$, which is interpreted as the boundary of the entangling region. Note that for suitable choices of $(a(\tilde{w}), b(\tilde{w}))$ one can obtain (9.7.28) as a limit of the Euclidean Kerr-de Sitter metric.

Given the boundary metric (9.7.28) in the vicinity of the entangling region boundary, one can then reconstruct the asymptotic expansion of the 4-dimensional bulk metric

$$ds^2 = \frac{d\rho^2}{\rho^2} + \frac{1}{\rho^2} g_{st} dx^s dx^t \tag{9.7.29}$$

with

$$g_{st} dx^s dx^t = d\tilde{w}^2 + \tilde{w}^2(d\tau + a(\tilde{w})d\phi)^2 + b(\tilde{w})d\phi^2 + \mathcal{O}(\rho^2) \tag{9.7.30}$$

where terms at order ρ^2 can be computed from the curvature of the boundary metric, see [43]. Thus, the fixed point set of ∂_τ is extended to a two-dimensional surface in the bulk. Following the logic above, the associated entanglement entropy should depend not just not on the area of this surface but also on the non-trivial fibration of this circle direction over the surface. From (9.7.29) one can deduce that the potential (9.7.20) satisifes

$$d\psi = \frac{\tilde{w}^3}{\rho^2} \frac{a'}{\sqrt{b}} d\rho + \cdots \tag{9.7.31}$$

and hence the potential ψ is indeed constant on the surface defined by $\tilde{w}(\rho)$ with $\tilde{w} \to 0$ as $\rho \to 0$. Integration of this equation to find the potential and hence apply the formula (9.7.21) would however require the full bulk reconstruction and we postpone this analysis for future work.

9.8 Conclusions

In this chapter we have presented evidence that the entanglement entropy computed from top-down (9.1.2) is equivalent to that computed using the Ryu-Takanagi formula (9.1.1); we showed that the formulae agree in a wide range of examples and used general arguments based on the replica trick. Both formulae, (9.1.1) and (9.1.2), are applica-

ble to time independent situations. It would be interesting to generalise the analysis of this chapter to the covariant holographic entanglement entropy [186] and, in particular, to understand whether contributions associated with non-trivial fibration of the circle coordinate over the entangling region boundary can indeed arise.

We have emphasised that the relationship between the ten-dimensional solution and the lower-dimensional asymptotically AdS solution is in general very complicated. To calculate quantities related to the dual stress energy tensor, one needs to extract the asymptotic form of the lower-dimensional metric, which is related to the upstairs metric by derivative field redefinitions. It is computationally complex to extract the required field redefinitions. The agreement between (9.1.1) and (9.1.2) imposes constraints on the field redefinitions which can be used both to check Kaluza-Klein holography calculations and, in symmetric situations, to infer the lower-dimensional fields, without going through the entire Kaluza-Klein holography procedure.

In this chapter we have focussed primarily on backgrounds which are asymptotic to $AdS_{d+1} \times X$ but the general arguments of Section 9.8 are equally applicable to any gauge/gravity duality for which the conformal boundary is timelike and the bulk theory is described by Einstein gravity. Thus in particular the top-down entanglement entropy (9.1.2) is applicable to top-down realisations of Lifshitz and Schrödinger (with one example of the latter being given in Section 9.4). The formula (9.1.2) is also applicable to non-conformal brane dualities [21], in the regimes where supergravity is a valid description.

Our results have implications for the long standing question of how the compact part of the bulk spacetime is reconstructed from field theory data: entanglement entropy tells us about minimal surfaces in the top-down geometry. One could use these surfaces to explore how global features of the top-down geometry are reconstructed.

Part IV

Outlook

CHAPTER 10

Concluding Remarks

Gauge/gravity duality is an extremely active research area due to its capacity for providing new insight into a number of fundamental questions in physics, as well as its broad range of application. A large part of the appeal is that the framework provides novel and simpler methods for studying strongly coupled field theories (which are inaccessible via traditional perturbative methods) by translating the problem into its corresponding gravitational dual. We have seen many examples of this in the preceding pages, learning about graphene, QCD, and field theory entanglement by performing comparatively simple computations in higher-dimensional classical gravity theories. Of course, one can also utilise the correspondence in the reverse direction, and there has been considerable work along these lines to further our understanding of black holes, quantum gravity and string theory by studying the dual field theory (see for example the recent review [275] and references therein). Consequently, the development of the field has led to an increasingly cross-disciplinary approach within theoretical physics due to the discovery of these surprising connections; for example, that the theory of black holes can be used to study superconductors, creating discourse between relativists and condensed matter physicists.

Duality is not a new concept of course, and in a sense the history of theoretical physics can largely be interpreted as a series of unifications, bringing together seemingly disparate concepts under the light of a new perspective. Dualities in string theory and $\mathcal{N} = 4$ SYM, such as *S-duality* and *T-duality* (see e.g. [5]), were also known to exist before the advent of the AdS/CFT correspondence, and relate the theories to themselves under a particular transformation of parameters. The unique attribute of gauge/gravity duality is that, as well as relating significantly different physical theories to each other (theo-

ries with and without gravity, and with different numbers of spacetime dimensions), it is in fact a general idea rather than being tied to any specific equivalence - this has allowed a formal framework to be constructed that thus really applies to a whole class of equivalences, as we discussed in Chapter 3. The scope of that framework is still growing today, and similar dictionaries either have been or are being developed to incorporate other cases of holographic dualities, such as the dS/CFT correspondence [276], holographic cosmology [277], Lifshitz holography [278] (and the recent review [279]), and the fluid/gravity correspondence [280].

There is still much work to be done on the subject matters studied in this thesis. In Part II we focussed on holographic studies of flavour physics, where we stated that by this we mean systems that include matter degrees of freedom, such as quarks, in addition to gauge fields. This is thus a very broad area of research. The study of holographic graphene in Chapter 5 is itself part of a wider programme on using top-down probe brane models to study condensed matter systems - other problems that have been studied include the quantum Hall effect (e.g. [263,281]) and the Kondo effect (e.g. [282]). There has also been further research on using D5-probe brane models to study graphene (see e.g. [283,284]), but there are still many aspects and scenarios to consider, though the expectation is that such models are unlikely to ever give quantitatively correct answers as discussed in Chapter 5 - nevertheless, such models can make useful qualitative predictions about systems that can hopefully be engineered experimentally.

The Dynamic AdS/QCD model used in Chapter 6 has also found application to a range of problems within QCD as discussed previously. The model has produced predictions that are within 10% agreement to lattice or experiment, but there still remains a lot to be explored. For example, a potential avenue of research that we have begun exploring is to extend the model to describe theories that possess *asymptotic safety* rather than asymptotic freedom, with the coupling running to a non-trivial fixed point in the UV. One can use the flows in asymptotically safe theories such as those described in [285] to generate the anomalous dimensions that are used as input in the Dynamic AdS/QCD model. For example, one could explore the effect this has on the meson spectra as one increases the value of the coupling at the fixed point. Our discussion in Chapter 6 showed that furthermore there might sometimes be inherent limitations to the scope of the model; we showed for example that Regge slopes could be incorporated via soft walls, but that this comes at the cost of a peculiar running of the quark mass in the IR, and that perhaps stringy descriptions must ultimately be used to satisfyingly capture this aspect of QCD. One could envisage the same being true for other problems within QCD, and that perhaps future top-down or more sophisticated bottom-up models will be required in the attempt to construct a more complete gravity dual.

Part III then investigated the subject of holographic entanglement entropy, first studying the entanglement contribution of probe branes in Chapter 8, before naturally leading

onto a discussion of entanglement entropy in top-down models in general in Chapter 9. We presented a new method for computing the flavour contribution to the entanglement entropy for any top-down probe brane system using Kaluza-Klein holography. We demonstrated the method explicitly for the D3/D7 system at finite mass and density, but it could in principle be applied to any number of interesting systems with relevance to condensed matter physics and wider afield; top-down models of the quantum Hall effect or the Kondo effect, probe brane systems at finite temperature, ABJM theory with flavours etc. The scope for further research along these particular lines is large. The result that entanglement entropy can be computed from minimal surfaces in the top-down geometry naturally leads to the idea that entanglement might be key in understanding how the compact part of the bulk is reconstructed from field theory data; this is a future avenue of open research, as the question is not understood at present but has important implications for holography, and thus transitively for all applications of holography. This is another element in the growing chain of connections between entanglement and geometry discussed throughout Part III, which is a relatively new research programme that still requires considerable work to fully unravel the way these two concepts are related (see for example the recent review [286]). The potential consequences of this unexpected relationship are extremely far reaching however, and these questions excite physicists of all persuasions, from practical to philosophical in motivation; it thus appears highly likely that research into them will continue for some time.

Bibliography

[1] N. Evans and P. Jones, *Holographic Graphene in a Cavity*, *Phys. Rev.* **D90** (2014), no. 8 086008, [arXiv:1407.3097].

[2] P. A. R. Jones and M. Taylor, *Entanglement entropy and differential entropy for massive flavors*, *JHEP* **08** (2015) 014, [arXiv:1505.0769].

[3] N. Evans, P. Jones, and M. Scott, *Soft walls in dynamic AdS/QCD and the technidilaton*, *Phys. Rev.* **D92** (2015), no. 10 106003, [arXiv:1508.0654].

[4] P. A. R. Jones and M. Taylor, *Entanglement entropy in top-down models*, *JHEP* **08** (2016) 158, [arXiv:1602.0482].

[5] K. Becker, M. Becker, and J. Schwarz, *String Theory and M-Theory*. Cambridge University Press, 2006.

[6] M. Ammon and J. Erdmenger, *Gauge/Gravity Duality: Foundations and Applications*. Cambridge University Press, 2015.

[7] J. Polchinski, *Dirichlet Branes and Ramond-Ramond charges*, *Phys. Rev. Lett.* **75** (1995) 4724–4727, [hep-th/9510017].

[8] J. Dai, R. G. Leigh, and J. Polchinski, *New Connections Between String Theories*, *Mod. Phys. Lett.* **A4** (1989) 2073–2083.

[9] E. Bergshoeff, R. Kallosh, T. Ortin, D. Roest, and A. Van Proeyen, *New formulations of D = 10 supersymmetry and D8 - O8 domain walls*, *Class. Quant. Grav.* **18** (2001) 3359–3382, [hep-th/0103233].

[10] R. Grimm, M. Sohnius, and J. Wess, *Extended Supersymmetry and Gauge Theories*, *Nucl. Phys.* **B133** (1978) 275–284.

[11] G. 't Hooft, *A Planar Diagram Theory for Strong Interactions*, *Nucl. Phys.* **B72**

(1974) 461.

[12] G. t. Hooft, *Dimensional Reduction in Quantum Gravity*, 9310026.

[13] L. Susskind, *The world as a hologram*, *Journal of Mathematical Physics* **36** (Sept., 1995) 6377, [9409089].

[14] L. Susskind and E. Witten, *The Holographic bound in anti-de Sitter space*, hep-th/9805114.

[15] J. M. Bardeen, B. Carter, and S. W. Hawking, *The Four laws of black hole mechanics*, *Commun. Math. Phys.* **31** (1973) 161–170.

[16] J. Bekenstein, *Black Holes and Entropy*, *Physical Review D* **7** (Apr., 1973) 2333–2346.

[17] J. M. Maldacena, *The large n limit of superconformal field theories and supergravity*, hep-th/9711200.

[18] O. Aharony, O. Bergman, D. L. Jafferis, and J. Maldacena, *N=6 superconformal Chern-Simons-matter theories, M2-branes and their gravity duals*, *JHEP* **10** (2008) 091, [arXiv:0806.1218].

[19] O. Aharony, Y. Oz, and Z. Yin, *M theory on AdS(p) x S(11-p) and superconformal field theories*, *Phys. Lett.* **B430** (1998) 87–93, [hep-th/9803051].

[20] A. J. Nurmagambetov and I. Y. Park, *On the M5 and the AdS(7) / CFT(6) correspondence*, *Phys. Lett.* **B524** (2002) 185–191, [hep-th/0110192].

[21] N. Itzhaki, J. M. Maldacena, J. Sonnenschein, and S. Yankielowicz, *Supergravity and the large N limit of theories with sixteen supercharges*, *Phys. Rev.* **D58** (1998) 046004, [hep-th/9802042].

[22] H. J. Boonstra, K. Skenderis, and P. K. Townsend, *The domain wall / QFT correspondence*, *JHEP* **01** (1999) 003, [hep-th/9807137].

[23] I. Kanitscheider, K. Skenderis, and M. Taylor, *Precision holography for non-conformal branes*, arXiv:0807.3324.

[24] K. Skenderis and M. Taylor, *Kaluza-Klein holography*, *JHEP* **05** (2006) 057, [hep-th/0603016].

[25] K. Skenderis and M. Taylor, *Holographic Coulomb branch vevs*, *JHEP* **0608** (2006) 001, [hep-th/0604169].

[26] M. Pernici, K. Pilch, and P. van Nieuwenhuizen, *Gauged N=8 D=5 Supergravity*, *Nucl. Phys.* **B259** (1985) 460.

[27] M. Gunaydin, L. J. Romans, and N. P. Warner, *Compact and Noncompact Gauged Supergravity Theories in Five-Dimensions*, *Nucl. Phys.* **B272** (1986) 598–646.

[28] K. Lee, C. Strickland-Constable, and D. Waldram, *Spheres, generalised parallelisability and consistent truncations*, arXiv:1401.3360.

[29] S. S. Gubser, I. R. Klebanov, and A. M. Polyakov, *Gauge theory correlators from non-critical string theory*, *Phys. Lett.* **B428** (1998) 105–114, [hep-th/9802109].

[30] E. Witten, *Anti-de Sitter space and holography*, *Adv. Theor. Math. Phys.* **2** (1998) 253–291, [hep-th/9802150].

[31] K. Skenderis, *Lecture notes on holographic renormalization*, *Class. Quant. Grav.* **19** (2002) 5849–5876, [hep-th/0209067].

[32] D. T. Son and A. O. Starinets, *Minkowski space correlators in AdS / CFT correspondence: Recipe and applications*, *JHEP* **09** (2002) 042, [hep-th/0205051].

[33] K. Skenderis and B. C. van Rees, *Real-time gauge/gravity duality*, *Phys. Rev. Lett.* **101** (2008) 081601, [arXiv:0805.0150].

[34] K. Skenderis and B. C. van Rees, *Real-time gauge/gravity duality: Prescription, Renormalization and Examples*, arXiv:0812.2909.

[35] C. Fefferman and C. Graham, *Conformal Invariants*, *Elie Cartan et les Mathématiques d'aujourd'hui (Asterisque 95)* (1985).

[36] H. J. Kim, L. J. Romans, and P. van Nieuwenhuizen, *The Mass Spectrum of Chiral N=2 D=10 Supergravity on S**5*, *Phys. Rev.* **D32** (1985) 389.

[37] S. Lee, S. Minwalla, M. Rangamani, and N. Seiberg, *Three-point functions of chiral operators in D = 4, N = 4 SYM at large N*, *Adv. Theor. Math. Phys.* **2** (1998) 697–718, [hep-th/9806074].

[38] M. Gunaydin and N. Marcus, *The Spectrum of the s**5 Compactification of the Chiral N=2, D=10 Supergravity and the Unitary Supermultiplets of U(2, 2/4)*, *Class. Quant. Grav.* **2** (1985) L11.

[39] L. Andrianopoli and S. Ferrara, *K-K excitations on AdS(5) x S**5 as N=4 'primary' superfields*, *Phys. Lett.* **B430** (1998) 248–253, [hep-th/9803171].

[40] E. Witten, *Anti-de Sitter space, thermal phase transition, and confinement in gauge theories*, *Adv. Theor. Math. Phys.* **2** (1998) 505–532, [hep-th/9803131].

[41] P. Breitenlohner and D. Z. Freedman, *Positive Energy in anti-De Sitter Backgrounds and Gauged Extended Supergravity*, *Phys. Lett.* **B115** (1982) 197–201.

[42] P. Breitenlohner and D. Z. Freedman, *Stability in Gauged Extended Supergravity*, *Annals Phys.* **144** (1982) 249.

[43] S. de Haro, S. N. Solodukhin, and K. Skenderis, *Holographic reconstruction of spacetime and renormalization in the AdS/CFT correspondence*, *Commun. Math. Phys.* **217** (2001) 595–622, [hep-th/0002230].

[44] R. G. Leigh and M. J. Strassler, *Exactly marginal operators and duality in four-dimensional N=1 supersymmetric gauge theory*, *Nucl. Phys.* **B447** (1995) 95–136, [hep-th/9503121].

[45] D. Freedman, S. Gubser, K. Pilch, and N. Warner, *Renormalization group flows from holography supersymmetry and a c theorem*, *Adv.Theor.Math.Phys.* **3** (1999) 363–417, [hep-th/9904017].

[46] A. B. Zamolodchikov, *Irreversibility of the Flux of the Renormalization Group in a 2D Field Theory*, *JETP Lett.* **43** (1986) 730–732. [Pisma Zh. Eksp. Teor. Fiz.43,565(1986)].

[47] O. Lunin and J. M. Maldacena, *Deforming field theories with U(1) x U(1) global symmetry and their gravity duals*, *JHEP* **05** (2005) 033, [hep-th/0502086].

[48] I. R. Klebanov and M. J. Strassler, *Supergravity and a confining gauge theory: Duality cascades and chi SB resolution of naked singularities*, *JHEP* **08** (2000) 052, [hep-th/0007191].

[49] J. M. Maldacena and C. Nunez, *Towards the large N limit of pure N=1 superYang-Mills*, *Phys. Rev. Lett.* **86** (2001) 588–591, [hep-th/0008001].

[50] J. Polchinski and M. J. Strassler, *The String dual of a confining four-dimensional gauge theory*, hep-th/0003136.

[51] M. Taylor, *Anomalies, counterterms and the N=0 Polchinski-Strassler solutions*, hep-th/0103162.

[52] J. Erdmenger, N. Evans, I. Kirsch, and E. Threlfall, *Mesons in Gauge/Gravity Duals - A Review*, *Eur.Phys.J.* **A35** (2008) 81–133, [arXiv:0711.4467].

[53] A. Karch and E. Katz, *Adding flavor to AdS / CFT*, *JHEP* **0206** (2002) 043, [hep-th/0205236].

[54] M. Kruczenski, D. Mateos, R. C. Myers, and D. J. Winters, *Meson spectroscopy in AdS / CFT with flavor*, *JHEP* **07** (2003) 049, [hep-th/0304032].

[55] I. Kirsch, *Spectroscopy of fermionic operators in AdS/CFT*, *JHEP* **09** (2006) 052, [hep-th/0607205].

[56] C. Johnson, *D-branes*. Cambridge University Press, 2003.

[57] H. Hamber and G. Parisi, *Numerical estimates of hadronic masses in a pure su (3) gauge theory*, *Phys. Rev. Lett.* **47** (Dec, 1981) 1792–1795.

[58] E. Marinari, G. Parisi, and C. Rebbi, *Computer estimates of meson masses in su (2) lattice gauge theory*, *Phys. Rev. Lett.* **47** (Dec, 1981) 1795–1799.

[59] A. Karch, A. O'Bannon, and K. Skenderis, *Holographic renormalization of probe D-branes in AdS/CFT*, *JHEP* **04** (2006) 015, [hep-th/0512125].

[60] M. Peskin and D. Schroeder, *An Introduction to Quantum Field Theory*. Westview Press Inc, 1995.

[61] D. J. Gross and F. Wilczek, *Ultraviolet behavior of non-abelian gauge theories*, *Phys. Rev. Lett.* **30** (Jun, 1973) 1343–1346.

[62] H. D. Politzer, *Reliable Perturbative Results for Strong Interactions?*, *Phys. Rev. Lett.* **30** (1973) 1346–1349.

[63] J. F. Donoghue, E. Golowich, and B. R. Holstein, *Dynamics of the Standard Model*. Cambridge University Press, 1994.

[64] V. Mathieu, N. Kochelev, and V. Vento, *The Physics of Glueballs*, *Int. J. Mod. Phys.* **E18** (2009) 1–49, [arXiv:0810.4453].

[65] W. Ochs, *The Status of Glueballs*, *J. Phys.* **G40** (2013) 043001, [arXiv:1301.5183].

[66] K. G. Wilson, *Confinement of Quarks*, *Phys. Rev.* **D10** (1974) 2445–2459. [,45(1974)].

[67] J. M. Maldacena, *Wilson loops in large N field theories*, *Phys. Rev. Lett.* **80** (1998) 4859–4862, [hep-th/9803002].

[68] S. Scherer and M. R. Schindler, *A Chiral perturbation theory primer*, hep-ph/0505265.

[69] E. Witten, *Current Algebra Theorems for the U(1) Goldstone Boson*, *Nucl. Phys.* **B156** (1979) 269–283.

[70] G. 't Hooft, *How Instantons Solve the U(1) Problem*, *Phys. Rept.* **142** (1986) 357–387.

[71] Y. Nambu, *Quasi-particles and gauge invariance in the theory of superconductivity*, *Phys. Rev.* **117** (Feb, 1960) 648–663.

[72] J. Goldstone, *Field Theories with Superconductor Solutions*, *Nuovo Cim.* **19** (1961) 154–164.

[73] **Particle Data Group** Collaboration, K. A. Olive *et. al.*, *Review of Particle Physics*, *Chin. Phys.* **C38** (2014) 090001.

[74] L. Girardello, M. Petrini, M. Porrati, and A. Zaffaroni, *Novel local CFT and exact results on perturbations of N=4 superYang Mills from AdS dynamics*, *JHEP* **12** (1998) 022, [hep-th/9810126].

[75] L. Girardello, M. Petrini, M. Porrati, and A. Zaffaroni, *The Supergravity dual of N=1 superYang-Mills theory*, *Nucl. Phys.* **B569** (2000) 451–469, [hep-th/9909047].

[76] N. R. Constable and R. C. Myers, *Exotic scalar states in the AdS / CFT correspondence*, *JHEP* **11** (1999) 020, [hep-th/9905081].

[77] M. N. Chernodub, *Superconductivity of QCD vacuum in strong magnetic field*, *Phys. Rev.* **D82** (2010) 085011, [arXiv:1008.1055].

[78] T. Sakai and S. Sugimoto, *Low energy hadron physics in holographic QCD*, *Prog. Theor. Phys.* **113** (2005) 843–882, [hep-th/0412141].

[79] T. Sakai and S. Sugimoto, *More on a holographic dual of QCD*, *Prog. Theor. Phys.* **114** (2005) 1083–1118, [hep-th/0507073].

[80] J. Erlich, E. Katz, D. T. Son, and M. A. Stephanov, *QCD and a holographic model of hadrons*, *Phys. Rev. Lett.* **95** (2005) 261602, [hep-ph/0501128].

[81] L. Da Rold and A. Pomarol, *Chiral symmetry breaking from five dimensional spaces*, *Nucl. Phys.* **B721** (2005) 79–97, [hep-ph/0501218].

[82] N. Evans and K. Tuominen, *Holographic modelling of a light technidilaton*, *Phys. Rev.* **D87** (2013), no. 8 086003, [arXiv:1302.4553].

[83] T. Alho, N. Evans, and K. Tuominen, *Dynamic AdS/QCD and the Spectrum of Walking Gauge Theories*, *Phys. Rev.* **D88** (2013) 105016, [arXiv:1307.4896].

[84] N. Evans and M. Scott, *Hyper-Scaling Relations in the Conformal Window from Dynamic AdS/QCD*, *Phys. Rev.* **D90** (2014), no. 6 065025, [arXiv:1405.5373].

[85] J. Erdmenger, N. Evans, and M. Scott, *Meson spectra of asymptotically free gauge theories from holography*, *Phys. Rev.* **D91** (2015), no. 8 085004, [arXiv:1412.3165].

[86] K. S. Novoselov, A. K. Geim, S. V. Morozov, D. Jiang, M. I. Katsnelson, I. V. Grigorieva, S. V. Dubonos, and A. A. Firsov, *Two-dimensional gas of massless Dirac fermions in graphene*, *Nature* **438** (2005) 197, [cond-mat/0509330].

[87] A. Karch and L. Randall, *Open and closed string interpretation of SUSY CFT's on branes with boundaries*, *JHEP* **06** (2001) 063, [hep-th/0105132].

[88] O. DeWolfe, D. Z. Freedman, and H. Ooguri, *Holography and defect conformal field theories*, *Phys. Rev.* **D66** (2002) 025009, [hep-th/0111135].

[89] J. Erdmenger, Z. Guralnik, and I. Kirsch, *Four-dimensional superconformal theories with interacting boundaries or defects*, *Phys. Rev.* **D66** (2002) 025020, [hep-th/0203020].

[90] K. Jensen, A. Karch, D. T. Son, and E. G. Thompson, *Holographic Berezinskii-Kosterlitz-Thouless Transitions*, *Phys. Rev. Lett.* **105** (2010) 041601, [arXiv:1002.3159].

[91] N. Evans, A. Gebauer, K.-Y. Kim, and M. Magou, *Phase diagram of the D3/D5 system in a magnetic field and a BKT transition*, *Phys. Lett.* **B698** (2011) 91–95, [arXiv:1003.2694].

[92] K. Skenderis and M. Taylor, *Branes in AdS and p p wave space-times*, *JHEP* **06** (2002) 025, [hep-th/0204054].

[93] V. G. Filev, *A Quantum Critical Point from Flavours on a Compact Space*, *JHEP* **08** (2014) 105, [arXiv:1406.5498].

[94] V. G. Filev, M. Ihl, and D. Zoakos, *Holographic Bilayer/Monolayer Phase Transitions*, *JHEP* **07** (2014) 043, [arXiv:1404.3159].

[95] V. G. Filev, M. Ihl, and D. Zoakos, *A Novel (2+1)-Dimensional Model of Chiral Symmetry Breaking*, *JHEP* **12** (2013) 072, [arXiv:1310.1222].

[96] G. Grignani, N. Kim, and G. W. Semenoff, *D3–D5 holography with flux*, *Phys. Lett.* **B715** (2012) 225–229, [arXiv:1203.6162].

[97] H. Omid and G. W. Semenoff, *D3-D7 Holographic dual of a perturbed 3D CFT*, *Phys. Rev.* **D88** (2013), no. 2 026006, [arXiv:1208.5176].

[98] G. W. Semenoff, *Chiral Symmetry Breaking in Graphene*, *Phys. Scripta* **T146** (2012) 014016, [arXiv:1108.2945].

[99] E. M. Purcell, *Spontaneous emission probabilities at radio frequencies*, *Phys. Rev.* **69** (1946) 681.

[100] G. T. Horowitz and R. C. Myers, *The AdS / CFT correspondence and a new positive energy conjecture for general relativity*, *Phys. Rev.* **D59** (1998) 026005, [hep-th/9808079].

[101] M. Kruczenski, D. Mateos, R. C. Myers, and D. J. Winters, *Towards a holographic dual of large N(c) QCD*, *JHEP* **05** (2004) 041, [hep-th/0311270].

[102] V. G. Filev, C. V. Johnson, R. C. Rashkov, and K. S. Viswanathan, *Flavoured large N gauge theory in an external magnetic field*, *JHEP* **10** (2007) 019, [hep-th/0701001].

[103] J. L. Davis and N. Kim, *Flavor-symmetry Breaking with Charged Probes*, *JHEP* **06** (2012) 064, [arXiv:1109.4952].

[104] G. Grignani, N. Kim, and G. W. Semenoff, *D7-anti-D7 bilayer: holographic dynamical symmetry breaking*, *Phys. Lett.* **B722** (2013) 360–363, [arXiv:1208.0867].

[105] N. Evans and K.-Y. Kim, *Vacuum alignment and phase structure of holographic bi-layers*, *Phys. Lett.* **B728** (2014) 658–661, [arXiv:1311.0149].

[106] M. Fujita, T. Takayanagi, and E. Tonni, *Aspects of AdS/BCFT*, *JHEP* **11** (2011) 043, [arXiv:1108.5152].

[107] J. Babington, J. Erdmenger, N. J. Evans, Z. Guralnik, and I. Kirsch, *Chiral symmetry breaking and pions in nonsupersymmetric gauge / gravity duals*, *Phys. Rev.* **D69** (2004) 066007, [hep-th/0306018].

[108] E. Schreiber, *Excited mesons and quantization of string endpoints*, hep-th/0403226.

[109] M. Shifman, *Highly excited hadrons in QCD and beyond*, in *ECT* Workshop on Highly Excited Hadrons Trento, Italy, July 4-9, 2005*, pp. 171–191, 2005. hep-ph/0507246. [,171(2005)].

[110] A. Karch, E. Katz, D. T. Son, and M. A. Stephanov, *Linear confinement and AdS/QCD*, *Phys. Rev.* **D74** (2006) 015005, [hep-ph/0602229].

[111] U. Gursoy and E. Kiritsis, *Exploring improved holographic theories for QCD: Part I*, *JHEP* **02** (2008) 032, [arXiv:0707.1324].

[112] U. Gursoy, E. Kiritsis, and F. Nitti, *Exploring improved holographic theories for QCD: Part II*, *JHEP* **02** (2008) 019, [arXiv:0707.1349].

[113] M. Jarvinen and E. Kiritsis, *Holographic Models for QCD in the Veneziano Limit*, *JHEP* **03** (2012) 002, [arXiv:1112.1261].

[114] D. Arean, I. Iatrakis, M. Järvinen, and E. Kiritsis, *V-QCD: Spectra, the dilaton and the S-parameter*, *Phys. Lett.* **B720** (2013) 219–223, [arXiv:1211.6125].

[115] D. Arean, I. Iatrakis, and M. Järvinen, *The spectrum of (h)QCD in the Veneziano limit*, *PoS* **Corfu2012** (2013) 129, [arXiv:1305.6294].

[116] M. Jarvinen, *Massive holographic QCD in the Veneziano limit*, *JHEP* **07** (2015) 033, [arXiv:1501.0727].

[117] A. Ballon-Bayona, R. Carcassés Quevedo, M. S. Costa, and M. Djuri·, *Soft Pomeron in Holographic QCD*, *Phys. Rev.* **D93** (2016) 035005, [arXiv:1508.0000].

[118] D. Kutasov, J. Lin, and A. Parnachev, *Holographic Walking from Tachyon DBI*, *Nucl. Phys.* **B863** (2012) 361–397, [arXiv:1201.4123].

[119] B. Holdom, *Raising the Sideways Scale*, *Phys. Rev.* **D24** (1981) 1441.

[120] **LatKMI** Collaboration, Y. Aoki, T. Aoyama, M. Kurachi, T. Maskawa, K.-i. Nagai, H. Ohki, A. Shibata, K. Yamawaki, and T. Yamazaki, *Many flavor QCD as exploration of the walking behavior with the approximate IR fixed point*, *PoS* **LATTICE2011** (2011) 080, [arXiv:1202.4712].

[121] A. Cheng, A. Hasenfratz, G. Petropoulos, and D. Schaich, *Scale-dependent mass anomalous dimension from Dirac eigenmodes*, *JHEP* **07** (2013) 061, [arXiv:1301.1355].

[122] A. Deuzeman, M. P. Lombardo, T. Nunes da Silva, and E. Pallante, *Bulk transitions of twelve flavor QCD and $U_A(1)$ symmetry*, *PoS* **LATTICE2011** (2011) 321, [arXiv:1111.2590].

[123] T. Appelquist, G. T. Fleming, M. F. Lin, E. T. Neil, and D. A. Schaich, *Lattice Simulations and Infrared Conformality*, *Phys. Rev.* **D84** (2011) 054501, [arXiv:1106.2148].

[124] A. Hasenfratz, *Conformal or Walking? Monte Carlo renormalization group studies of SU(3) gauge models with fundamental fermions*, *Phys. Rev.* **D82** (2010) 014506, [arXiv:1004.1004].

[125] Z. Fodor, K. Holland, J. Kuti, D. Nogradi, and C. Schroeder, *Nearly conformal gauge theories in finite volume*, *Phys. Lett.* **B681** (2009) 353–361, [arXiv:0907.4562].

[126] Y. Aoki, T. Aoyama, M. Kurachi, T. Maskawa, K.-i. Nagai, H. Ohki, A. Shibata, K. Yamawaki, and T. Yamazaki, *Lattice study of conformality in twelve-flavor QCD*, *Phys. Rev.* **D86** (2012) 054506, [arXiv:1207.3060].

[127] T. Appelquist, G. T. Fleming, and E. T. Neil, *Lattice Study of Conformal Behavior in SU(3) Yang-Mills Theories*, *Phys. Rev.* **D79** (2009) 076010, [arXiv:0901.3766].

[128] A. Deuzeman, M. P. Lombardo, and E. Pallante, *Evidence for a conformal phase in SU(N) gauge theories*, *Phys. Rev.* **D82** (2010) 074503, [arXiv:0904.4662].

[129] Y. Shamir, B. Svetitsky, and T. DeGrand, *Zero of the discrete beta function in SU(3) lattice gauge theory with color sextet fermions*, *Phys. Rev.* **D78** (2008) 031502, [arXiv:0803.1707].

[130] Y. Iwasaki, K. Kanaya, S. Kaya, S. Sakai, and T. Yoshie, *Phase structure of lattice QCD for general number of flavors*, *Phys. Rev.* **D69** (2004) 014507, [hep-lat/0309159].

[131] R. Lawrance and M. Piai, *Holographic Technidilaton and LHC searches*, *Int. J. Mod. Phys.* **A28** (2013) 1350081, [arXiv:1207.0427].

[132] D. Elander and M. Piai, *A composite light scalar, electro-weak symmetry breaking and the recent LHC searches*, *Nucl. Phys.* **B864** (2012) 241–259, [arXiv:1112.2915].

[133] W. E. Caswell, *Asymptotic Behavior of Nonabelian Gauge Theories to Two Loop Order*, *Phys. Rev. Lett.* **33** (1974) 244.

[134] T. Banks and A. Zaks, *On the Phase Structure of Vector-Like Gauge Theories with Massless Fermions*, *Nucl. Phys.* **B196** (1982) 189–204.

[135] T. Appelquist, J. Terning, and L. C. R. Wijewardhana, *The Zero temperature chiral phase transition in SU(N) gauge theories*, *Phys. Rev. Lett.* **77** (1996) 1214–1217, [hep-ph/9602385].

[136] T. Appelquist, A. Ratnaweera, J. Terning, and L. C. R. Wijewardhana, *The Phase structure of an SU(N) gauge theory with N(f) flavors*, *Phys. Rev.* **D58** (1998) 105017, [hep-ph/9806472].

[137] T. Appelquist, K. Lane, and U. Mahanta, *Ladder approximation for spontaneous chiral-symmetry breaking*, *Phys. Rev. Lett.* **61** (Oct, 1988) 1553–1556.

[138] A. G. Cohen and H. Georgi, *Walking Beyond the Rainbow*, *Nucl. Phys.* **B314** (1989)

7–24.

[139] T. A. Ryttov and F. Sannino, *Supersymmetry inspired QCD beta function*, *Phys. Rev.* **D78** (2008) 065001, [arXiv:0711.3745].

[140] T. A. Ryttov and F. Sannino, *Conformal Windows of SU(N) Gauge Theories, Higher Dimensional Representations and The Size of The Unparticle World*, *Phys. Rev.* **D76** (2007) 105004, [arXiv:0707.3166].

[141] D. D. Dietrich and F. Sannino, *Conformal window of SU(N) gauge theories with fermions in higher dimensional representations*, *Phys. Rev.* **D75** (2007) 085018, [hep-ph/0611341].

[142] F. Sannino and J. Schechter, *Chiral phase transition for SU(N) gauge theories via an effective Lagrangian approach*, *Phys. Rev.* **D60** (1999) 056004, [hep-ph/9903359].

[143] A. Armoni, *The Conformal Window from the Worldline Formalism*, *Nucl. Phys.* **B826** (2010) 328–336, [arXiv:0907.4091].

[144] H. Gies and J. Jaeckel, *Chiral phase structure of QCD with many flavors*, *Eur. Phys. J.* **C46** (2006) 433–438, [hep-ph/0507171].

[145] R. Alvares, N. Evans, and K.-Y. Kim, *Holography of the Conformal Window*, *Phys. Rev.* **D86** (2012) 026008, [arXiv:1204.2474].

[146] V. A. Miransky and K. Yamawaki, *Conformal phase transition in gauge theories*, *Phys. Rev.* **D55** (1997) 5051–5066, [hep-th/9611142]. [Erratum: Phys. Rev.D56,3768(1997)].

[147] D. B. Kaplan, J.-W. Lee, D. T. Son, and M. A. Stephanov, *Conformality Lost*, *Phys. Rev.* **D80** (2009) 125005, [arXiv:0905.4752].

[148] R. Sundrum and S. D. Hsu, *Walking technicolor and electroweak radiative corrections*, *Nuclear Physics B* **391** (1993), no. 1 127 – 146.

[149] T. Appelquist and F. Sannino, *The Physical spectrum of conformal SU(N) gauge theories*, *Phys. Rev.* **D59** (1999) 067702, [hep-ph/9806409].

[150] K. Yamawaki, M. Bando, and K.-i. Matumoto, *Scale-invariant hypercolor model and a dilaton*, *Phys. Rev. Lett.* **56** (Mar, 1986) 1335–1338.

[151] M. Bando, K. iti Matumoto, and K. Yamawaki, *Technidilaton*, *Physics Letters B* **178** (1986), no. 2 308 – 312.

[152] D. K. Hong, S. D. H. Hsu, and F. Sannino, *Composite Higgs from higher representations*, *Phys. Lett.* **B597** (2004) 89–93, [hep-ph/0406200].

[153] D. D. Dietrich, F. Sannino, and K. Tuominen, *Light composite Higgs from higher representations versus electroweak precision measurements: Predictions for*

CERN LHC, *Phys. Rev.* **D72** (2005) 055001, [hep-ph/0505059].

[154] A. Einstein, B. Podolsky, and N. Rosen, *Can quantum-mechanical description of physical reality be considered complete?*, *Phys. Rev.* **47** (May, 1935) 777–780.

[155] J. S. Bell, *On the Einstein-Podolsky-Rosen paradox*, *Physics* **1** (1964) 195–200.

[156] J. S. Bell, *On the Problem of Hidden Variables in Quantum Mechanics*, *Rev. Mod. Phys.* **38** (1966) 447–452.

[157] A. Kitaev and J. Preskill, *Topological entanglement entropy*, *Phys. Rev. Lett.* **96** (2006) 110404, [hep-th/0510092].

[158] M. Levin and X.-G. Wen, *Detecting topological order in a ground state wave function*, *Phys. Rev. Lett.* **96** (Mar, 2006) 110405.

[159] B. Swingle, *Entanglement renormalization and holography*, *Phys. Rev. D* **86** (Sep, 2012) 065007.

[160] M. Van Raamsdonk, *Comments on quantum gravity and entanglement*, arXiv:0907.2939.

[161] M. Van Raamsdonk, *Building up spacetime with quantum entanglement*, *Gen. Rel. Grav.* **42** (2010) 2323–2329, [arXiv:1005.3035]. [Int. J. Mod. Phys.D19,2429(2010)].

[162] J. M. Maldacena, *Eternal black holes in Anti-de-Sitter*, *JHEP* **04** (2003) 021, [hep-th/0106112].

[163] J. Maldacena and L. Susskind, *Cool horizons for entangled black holes*, *Fortsch.Phys.* **61** (2013) 781–811, [arXiv:1306.0533].

[164] M. Nielsen and I. Chuang, *Quantum Computation and Quantum Information*. Cambridge University Press, 2010.

[165] P. V. Buividovich and M. I. Polikarpov, *Entanglement entropy in gauge theories and the holographic principle for electric strings*, *Phys. Lett.* **B670** (2008) 141–145, [arXiv:0806.3376].

[166] W. Donnelly, *Decomposition of entanglement entropy in lattice gauge theory*, *Phys. Rev.* **D85** (2012) 085004, [arXiv:1109.0036].

[167] H. Casini, M. Huerta, and J. A. Rosabal, *Remarks on entanglement entropy for gauge fields*, *Phys. Rev.* **D89** (2014), no. 8 085012, [arXiv:1312.1183].

[168] W. Donnelly, *Entanglement entropy and nonabelian gauge symmetry*, *Class. Quant. Grav.* **31** (2014), no. 21 214003, [arXiv:1406.7304].

[169] S. Ghosh, R. M. Soni, and S. P. Trivedi, *On The Entanglement Entropy For Gauge Theories*, *JHEP* **09** (2015) 069, [arXiv:1501.0259].

[170] P. Calabrese and J. Cardy, *Entanglement entropy and conformal field theory*, arXiv:0905.4013.

[171] A. Rényi, *On measures of entropy and information*, in *Proceedings of the Fourth Berkeley Symposium on Mathematical Statistics and Probability, Volume 1: Contributions to the Theory of Statistics*, (Berkeley, Calif.), pp. 547–561, University of California Press, 1961.

[172] A. Lewkowycz and J. Maldacena, *Generalized gravitational entropy*, *JHEP* **1308** (2013) 090, [arXiv:1304.4926].

[173] L. Bombelli, R. K. Koul, J. Lee, and R. D. Sorkin, *A Quantum Source of Entropy for Black Holes*, *Phys. Rev.* **D34** (1986) 373–383.

[174] M. Srednicki, *Entropy and area*, *Phys.Rev.Lett.* **71** (1993) 666–669, [hep-th/9303048].

[175] H. Araki and E. H. Lieb, *Entropy inequalities*, *Comm. Math. Phys.* **18** (1970), no. 2 160–170.

[176] E. H. Lieb and M. B. Ruskai, *A fundamental property of quantum-mechanical entropy*, *Phys. Rev. Lett.* **30** (Mar, 1973) 434–436.

[177] E. H. Lieb and M. B. Ruskai, *Proof of the strong subadditivity of quantum-mechanical entropy*, *J. Math. Phys.* **14** (1973) 1938–1941.

[178] A. Wehrl, *General properties of entropy*, *Rev. Mod. Phys.* **50** (1978) 221–260.

[179] D. D. Blanco, H. Casini, L.-Y. Hung, and R. C. Myers, *Relative Entropy and Holography*, *JHEP* **1308** (2013) 060, [arXiv:1305.3182].

[180] N. Lashkari, M. B. McDermott, and M. Van Raamsdonk, *Gravitational dynamics from entanglement 'thermodynamics'*, *JHEP* **04** (2014) 195, [arXiv:1308.3716].

[181] T. Faulkner, M. Guica, T. Hartman, R. C. Myers, and M. Van Raamsdonk, *Gravitation from Entanglement in Holographic CFTs*, *JHEP* **03** (2014) 051, [arXiv:1312.7856].

[182] B. Swingle and M. Van Raamsdonk, *Universality of Gravity from Entanglement*, arXiv:1405.2933.

[183] S. Ryu and T. Takayanagi, *Holographic derivation of entanglement entropy from AdS/CFT*, *Phys.Rev.Lett.* **96** (2006) 181602, [hep-th/0603001].

[184] R. Bousso, *A Covariant entropy conjecture*, *JHEP* **07** (1999) 004, [hep-th/9905177].

[185] R. Bousso, *Holography in general space-times*, *JHEP* **06** (1999) 028, [hep-th/9906022].

[186] V. E. Hubeny, M. Rangamani, and T. Takayanagi, *A Covariant holographic*

entanglement entropy proposal, *JHEP* **07** (2007) 062, [arXiv:0705.0016].

[187] H. Casini, M. Huerta, and R. C. Myers, *Towards a derivation of holographic entanglement entropy*, *JHEP* **1105** (2011) 036, [arXiv:1102.0440].

[188] C. R. Graham and E. Witten, *Conformal anomaly of submanifold observables in AdS / CFT correspondence*, hep-th/9901021.

[189] S. de Haro, S. N. Solodukhin, and K. Skenderis, *Holographic reconstruction of space-time and renormalization in the AdS / CFT correspondence*, hep-th/0002230.

[190] C. Fefferman and C. R. Graham, *The ambient metric*, arXiv:0710.0919.

[191] C. R. Graham and A. Karch, *Minimal area submanifolds in AdS x compact*, *JHEP* **04** (2014) 168, [arXiv:1401.7692].

[192] M. Headrick and T. Takayanagi, *A Holographic proof of the strong subadditivity of entanglement entropy*, *Phys. Rev.* **D76** (2007) 106013, [arXiv:0704.3719].

[193] T. Nishioka and T. Takayanagi, *AdS Bubbles, Entropy and Closed String Tachyons*, *JHEP* **01** (2007) 090, [hep-th/0611035].

[194] I. R. Klebanov, D. Kutasov, and A. Murugan, *Entanglement as a probe of confinement*, *Nucl.Phys.* **B796** (2008) 274–293, [arXiv:0709.2140].

[195] I. Bah, A. Faraggi, L. A. Pando Zayas, and C. A. Terrero-Escalante, *Holographic entanglement entropy and phase transitions at finite temperature*, *Int. J. Mod. Phys.* **A24** (2009) 2703–2728, [arXiv:0710.5483].

[196] D. Arean, P. Merlatti, C. Nunez, and A. V. Ramallo, *String duals of two-dimensional (4,4) supersymmetric gauge theories*, *JHEP* **12** (2008) 054, [arXiv:0810.1053].

[197] A. V. Ramallo, J. P. Shock, and D. Zoakos, *Holographic flavor in N=4 gauge theories in 3d from wrapped branes*, *JHEP* **02** (2009) 001, [arXiv:0812.1975].

[198] F. Bigazzi, A. L. Cotrone, A. Paredes, and A. V. Ramallo, *The Klebanov-Strassler model with massive dynamical flavors*, *JHEP* **03** (2009) 153, [arXiv:0812.3399].

[199] S. Bennett, E. Caceres, C. Nunez, D. Schofield, and S. Young, *The Non-SUSY Baryonic Branch: Soft Supersymmetry Breaking of N=1 Gauge Theories*, *JHEP* **05** (2012) 031, [arXiv:1111.1727].

[200] P. Dey and S. Roy, *Holographic entanglement entropy of the near horizon 1/4 BPS F-Dp bound states*, *Phys. Rev.* **D87** (2013), no. 6 066001, [arXiv:1208.1820].

[201] K. Kontoudi and G. Policastro, *Flavor corrections to the entanglement entropy*, *JHEP* **1401** (2014) 043, [arXiv:1310.4549].

[202] Y. Bea, E. Conde, N. Jokela, and A. V. Ramallo, *Unquenched massive flavors and*

flows in Chern-Simons matter theories, *JHEP* **1312** (2013) 033, [arXiv:1309.4453].

[203] F. Aprile and V. Niarchos, *Large-N transitions of the connectivity index*, *JHEP* **1502** (2015) 083, [arXiv:1410.7773].

[204] K. K. Kim, O.-K. Kwon, C. Park, and H. Shin, *Renormalized Entanglement Entropy Flow in Mass-deformed ABJM Theory*, *Phys.Rev.* **D90** (2014), no. 4 046006, [arXiv:1404.1044].

[205] Y. Bea, J. D. Edelstein, G. Itsios, K. S. Kooner, C. Nunez, D. Schofield, and J. A. Sierra-Garcia, *Compactifications of the Klebanov-Witten CFT and new AdS_3 backgrounds*, *JHEP* **05** (2015) 062, [arXiv:1503.0752].

[206] S. Giusto, E. Moscato, and R. Russo, *AdS_3 holography for 1/4 and 1/8 BPS geometries*, *JHEP* **11** (2015) 004, [arXiv:1507.0094].

[207] A. Mollabashi, N. Shiba, and T. Takayanagi, *Entanglement between Two Interacting CFTs and Generalized Holographic Entanglement Entropy*, *JHEP* **1404** (2014) 185, [arXiv:1403.1393].

[208] M. Taylor, *Generalized entanglement entropy*, arXiv:1507.0641.

[209] L. Huijse, S. Sachdev, and B. Swingle, *Hidden Fermi surfaces in compressible states of gauge-gravity duality*, *Phys.Rev.* **B85** (2012) 035121, [arXiv:1112.0573].

[210] D. L. Jafferis, I. R. Klebanov, S. S. Pufu, and B. R. Safdi, *Towards the F-Theorem: N=2 Field Theories on the Three-Sphere*, *JHEP* **06** (2011) 102, [arXiv:1103.1181].

[211] M. Taylor and W. Woodhead, *Renormalized entanglement entropy*, arXiv:1604.0680.

[212] K. Jensen and A. O'Bannon, *Holography, Entanglement Entropy, and Conformal Field Theories with Boundaries or Defects*, *Phys.Rev.* **D88** (2013), no. 10 106006, [arXiv:1309.4523].

[213] H.-C. Chang and A. Karch, *Entanglement Entropy for Probe Branes*, *JHEP* **1401** (2014) 180, [arXiv:1307.5325].

[214] A. Karch and C. F. Uhlemann, *Generalized gravitational entropy of probe branes: flavor entanglement holographically*, *JHEP* **1405** (2014) 017, [arXiv:1402.4497].

[215] J. Estes, K. Jensen, A. O'Bannon, E. Tsatis, and T. Wrase, *On Holographic Defect Entropy*, *JHEP* **1405** (2014) 084, [arXiv:1403.6475].

[216] H.-C. Chang, A. Karch, and C. F. Uhlemann, *Flavored $\mathcal{N} = 4$ SYM - a highly entangled quantum liquid*, *JHEP* **1409** (2014) 110, [arXiv:1406.2705].

[217] I. R. Klebanov, T. Nishioka, S. S. Pufu, and B. R. Safdi, *On Shape Dependence and RG Flow of Entanglement Entropy*, *JHEP* **1207** (2012) 001, [arXiv:1204.4160].

[218] T. Nishioka, *Relevant Perturbation of Entanglement Entropy and Stationarity*, *Phys.Rev.* **D90** (2014), no. 4 045006, [arXiv:1405.3650].

[219] J. Lee, A. Lewkowycz, E. Perlmutter, and B. R. Safdi, *Renyi entropy, stationarity, and entanglement of the conformal scalar*, *JHEP* **1503** (2015) 075, [arXiv:1407.7816].

[220] A. Allais and M. Mezei, *Some results on the shape dependence of entanglement and Renyi entropies*, *Phys.Rev.* **D91** (2015), no. 4 046002, [arXiv:1407.7249].

[221] M. Mezei, *Entanglement entropy across a deformed sphere*, *Phys.Rev.* **D91** (2015), no. 4 045038, [arXiv:1411.7011].

[222] O. Ben-Ami, D. Carmi, and M. Smolkin, *Renormalization group flow of entanglement entropy on spheres*, arXiv:1504.0091.

[223] A. Schwimmer and S. Theisen, *Entanglement Entropy, Trace Anomalies and Holography*, *Nucl.Phys.* **B801** (2008) 1–24, [arXiv:0802.1017].

[224] S. N. Solodukhin, *Entanglement entropy, conformal invariance and extrinsic geometry*, *Phys.Lett.* **B665** (2008) 305–309, [arXiv:0802.3117].

[225] V. Rosenhaus and M. Smolkin, *Entanglement Entropy Flow and the Ward Identity*, *Phys.Rev.Lett.* **113** (2014), no. 26 261602, [arXiv:1406.2716].

[226] V. Rosenhaus and M. Smolkin, *Entanglement entropy, planar surfaces, and spectral functions*, *JHEP* **1409** (2014) 119, [arXiv:1407.2891].

[227] V. Rosenhaus and M. Smolkin, *Entanglement Entropy for Relevant and Geometric Perturbations*, *JHEP* **1502** (2015) 015, [arXiv:1410.6530].

[228] S. He, J.-R. Sun, and H.-Q. Zhang, *On Holographic Entanglement Entropy with Second Order Excitations*, arXiv:1411.6213.

[229] H. Casini, F. Mazzitelli, and E. T. Lino, *Area terms in entanglement entropy*, arXiv:1412.6522.

[230] C. Park, *Logarithmic Corrections in the Entanglement Entropy*, arXiv:1505.0395.

[231] E. Bianchi and R. C. Myers, *On the Architecture of Spacetime Geometry*, *Class.Quant.Grav.* **31** (2014), no. 21 214002, [arXiv:1212.5183].

[232] V. Balasubramanian, B. Czech, B. D. Chowdhury, and J. de Boer, *The entropy of a hole in spacetime*, *JHEP* **1310** (2013) 220, [arXiv:1305.0856].

[233] V. Balasubramanian, B. D. Chowdhury, B. Czech, J. de Boer, and M. P. Heller, *Bulk curves from boundary data in holography*, *Phys.Rev.* **D89** (2014), no. 8 086004, [arXiv:1310.4204].

[234] R. C. Myers, J. Rao, and S. Sugishita, *Holographic Holes in Higher Dimensions*,

JHEP **1406** (2014) 044, [arXiv:1403.3416].

[235] V. Balasubramanian, B. D. Chowdhury, B. Czech, and J. de Boer, *Entwinement and the emergence of spacetime*, *JHEP* **1501** (2015) 048, [arXiv:1406.5859].

[236] B. Czech, X. Dong, and J. Sully, *Holographic Reconstruction of General Bulk Surfaces*, *JHEP* **1411** (2014) 015, [arXiv:1406.4889].

[237] M. Headrick, R. C. Myers, and J. Wien, *Holographic Holes and Differential Entropy*, *JHEP* **1410** (2014) 149, [arXiv:1408.4770].

[238] F. Bigazzi, A. L. Cotrone, J. Mas, A. Paredes, A. V. Ramallo, *et. al.*, *D3-D7 Quark-Gluon Plasmas*, *JHEP* **0911** (2009) 117, [arXiv:0909.2865].

[239] F. Bigazzi, A. L. Cotrone, J. Mas, D. Mayerson, and J. Tarrio, *D3-D7 Quark-Gluon Plasmas at Finite Baryon Density*, *JHEP* **1104** (2011) 060, [arXiv:1101.3560].

[240] F. Bigazzi, A. L. Cotrone, J. Mas, D. Mayerson, and J. Tarrio, *Holographic Duals of Quark Gluon Plasmas with Unquenched Flavors*, *Commun.Theor.Phys.* **57** (2012) 364–386, [arXiv:1110.1744].

[241] D. Mateos, R. C. Myers, and R. M. Thomson, *Holographic phase transitions with fundamental matter*, *Phys.Rev.Lett.* **97** (2006) 091601, [hep-th/0605046].

[242] S. Kobayashi, D. Mateos, S. Matsuura, R. C. Myers, and R. M. Thomson, *Holographic phase transitions at finite baryon density*, *JHEP* **0702** (2007) 016, [hep-th/0611099].

[243] M. P. Hertzberg and F. Wilczek, *Some Calculable Contributions to Entanglement Entropy*, *Phys.Rev.Lett.* **106** (2011) 050404, [arXiv:1007.0993].

[244] M. P. Hertzberg, *Entanglement Entropy in Scalar Field Theory*, *J.Phys.* **A46** (2013) 015402, [arXiv:1209.4646].

[245] H. Casini and M. Huerta, *A Finite entanglement entropy and the c-theorem*, *Phys.Lett.* **B600** (2004) 142–150, [hep-th/0405111].

[246] H. Casini, C. Fosco, and M. Huerta, *Entanglement and alpha entropies for a massive Dirac field in two dimensions*, *J.Stat.Mech.* **0507** (2005) P07007, [cond-mat/0505563].

[247] H. Casini and M. Huerta, *Entanglement and alpha entropies for a massive scalar field in two dimensions*, *J.Stat.Mech.* **0512** (2005) P12012, [cond-mat/0511014].

[248] H. Casini and M. Huerta, *Entanglement entropy in free quantum field theory*, *J.Phys.* **A42** (2009) 504007, [arXiv:0905.2562].

[249] H. Liu and M. Mezei, *A Refinement of entanglement entropy and the number of degrees of freedom*, *JHEP* **1304** (2013) 162, [arXiv:1202.2070].

[250] H. Liu and M. Mezei, *Probing renormalization group flows using entanglement entropy*, *JHEP* **1401** (2014) 098, [arXiv:1309.6935].

[251] M. Duff, R. R. Khuri, and J. Lu, *String solitons*, *Phys.Rept.* **259** (1995) 213–326, [hep-th/9412184].

[252] M. M. Wolf, *Violation of the entropic area law for Fermions*, *Phys.Rev.Lett.* **96** (2006) 010404, [quant-ph/0503219].

[253] D. Gioev and I. Klich, *Entanglement Entropy of Fermions in Any Dimension and the Widom Conjecture*, *Phys.Rev.Lett.* **96** (2006) 100503.

[254] M. Cramer, J. Eisert, and M. Plenio, *Statistics dependence of the entanglement entropy*, *Phys.Rev.Lett.* **98** (2007) 220603, [quant-ph/0611264].

[255] N. Evans, A. Gebauer, K.-Y. Kim, and M. Magou, *Holographic Description of the Phase Diagram of a Chiral Symmetry Breaking Gauge Theory*, *JHEP* **1003** (2010) 132, [arXiv:1002.1885].

[256] K. Jensen, A. Karch, and E. G. Thompson, *A Holographic Quantum Critical Point at Finite Magnetic Field and Finite Density*, *JHEP* **1005** (2010) 015, [arXiv:1002.2447].

[257] S. Banerjee, *Trace Anomaly Matching and Exact Results For Entanglement Entropy*, arXiv:1405.4876.

[258] S. Banerjee, *Note On The Dilaton Effective Action And Entanglement Entropy*, arXiv:1406.3038.

[259] L.-Y. Hung, R. C. Myers, and M. Smolkin, *Some Calculable Contributions to Holographic Entanglement Entropy*, *JHEP* **1108** (2011) 039, [arXiv:1105.6055].

[260] D. Z. Freedman, S. D. Mathur, A. Matusis, and L. Rastelli, *Correlation functions in the CFT(d) / AdS(d+1) correspondence*, *Nucl.Phys.* **B546** (1999) 96–118, [hep-th/9804058].

[261] D. Freedman, S. Gubser, K. Pilch, and N. Warner, *Continuous distributions of D3-branes and gauged supergravity*, *JHEP* **0007** (2000) 038, [hep-th/9906194].

[262] O. Bergman, N. Jokela, G. Lifschytz, and M. Lippert, *Quantum Hall Effect in a Holographic Model*, *JHEP* **1010** (2010) 063, [arXiv:1003.4965].

[263] C. Kristjansen and G. W. Semenoff, *Giant D5 Brane Holographic Hall State*, *JHEP* **1306** (2013) 048, [arXiv:1212.5609].

[264] J. Erdmenger, C. Hoyos, A. O'Bannon, and J. Wu, *A Holographic Model of the Kondo Effect*, *JHEP* **1312** (2013) 086, [arXiv:1310.3271].

[265] J. Cardy and C. P. Herzog, *Universal Thermal Corrections to Single Interval Entanglement Entropy for Two Dimensional Conformal Field Theories*,

Phys.Rev.Lett. **112** (2014), no. 17 171603, [arXiv:1403.0578].

[266] C. P. Herzog, *Universal Thermal Corrections to Entanglement Entropy for Conformal Field Theories on Spheres*, *JHEP* **1410** (2014) 28, [arXiv:1407.1358].

[267] S. Datta, J. R. David, M. Ferlaino, and S. P. Kumar, *Higher spin entanglement entropy from CFT*, *JHEP* **1406** (2014) 096, [arXiv:1402.0007].

[268] S. Datta, J. R. David, M. Ferlaino, and S. P. Kumar, *Universal correction to higher spin entanglement entropy*, *Phys.Rev.* **D90** (2014), no. 4 041903, [arXiv:1405.0015].

[269] S. Datta, J. R. David, and S. P. Kumar, *Conformal perturbation theory and higher spin entanglement entropy on the torus*, *JHEP* **1504** (2015) 041, [arXiv:1412.3946].

[270] H. Lin, O. Lunin, and J. M. Maldacena, *Bubbling AdS space and 1/2 BPS geometries*, *JHEP* **10** (2004) 025, [hep-th/0409174].

[271] G. W. Gibbons and S. W. Hawking, *Classification of Gravitational Instanton Symmetries*, *Commun. Math. Phys.* **66** (1979) 291–310.

[272] D. M. Hofman and J. Maldacena, *Conformal collider physics: Energy and charge correlations*, *JHEP* **05** (2008) 012, [arXiv:0803.1467].

[273] J. Maldacena, D. Martelli, and Y. Tachikawa, *Comments on string theory backgrounds with non- relativistic conformal symmetry*, *JHEP* **10** (2008) 072, [arXiv:0807.1100].

[274] C. Nunez, A. Paredes, and A. V. Ramallo, *Unquenched Flavor in the Gauge/Gravity Correspondence*, *Adv. High Energy Phys.* **2010** (2010) 196714, [arXiv:1002.1088].

[275] V. E. Hubeny, *The AdS/CFT Correspondence*, *Class. Quant. Grav.* **32** (2015), no. 12 124010, [arXiv:1501.0000].

[276] A. Strominger, *The dS / CFT correspondence*, *JHEP* **10** (2001) 034, [hep-th/0106113].

[277] P. McFadden and K. Skenderis, *The Holographic Universe*, *J. Phys. Conf. Ser.* **222** (2010) 012007, [arXiv:1001.2007].

[278] S. Kachru, X. Liu, and M. Mulligan, *Gravity duals of Lifshitz-like fixed points*, *Phys. Rev.* **D78** (2008) 106005, [arXiv:0808.1725].

[279] M. Taylor, *Lifshitz holography*, arXiv:1512.0355.

[280] S. Bhattacharyya, V. E. Hubeny, S. Minwalla, and M. Rangamani, *Nonlinear Fluid Dynamics from Gravity*, *JHEP* **02** (2008) 045, [arXiv:0712.2456].

[281] M. Fujita, W. Li, S. Ryu, and T. Takayanagi, *Fractional Quantum Hall Effect via*

Holography: Chern-Simons, Edge States, and Hierarchy, *JHEP* **06** (2009) 066, [arXiv:0901.0924].

[282] P. Benincasa and A. V. Ramallo, *Holographic Kondo Model in Various Dimensions*, *JHEP* **06** (2012) 133, [arXiv:1204.6290].

[283] G. Grignani, N. Kim, A. Marini, and G. W. Semenoff, *Holographic D3-probe-D5 Model of a Double Layer Dirac Semimetal*, *JHEP* **12** (2014) 091, [arXiv:1410.4911].

[284] G. Grignani, A. Marini, A.-C. Pigna, and G. W. Semenoff, *Phase structure of a holographic double monolayer Dirac semimetal*, *JHEP* **06** (2016) 141, [arXiv:1603.0258].

[285] D. F. Litim and F. Sannino, *Asymptotic safety guaranteed*, *JHEP* **12** (2014) 178, [arXiv:1406.2337].

[286] M. Rangamani and T. Takayanagi, *Holographic Entanglement Entropy*, *Lect. Notes Phys.* **931** (2017) [arXiv:1609.0128].